

**INVESTIGATING THE EFFECTS OF
PHARMACOLOGICAL UPREGULATION OF THE
HEAT SHOCK RESPONSE IN MODELS OF
INCLUSION BODY MYOSITIS**

Charlotte Jayne Spicer

UCL Institute of Neurology

&

MRC Centre for Neuromuscular Diseases

PhD supervisors:

Professor Linda Greensmith (Primary)

Professor Michael Hanna (Secondary)

A Thesis submitted for the degree of Doctor of Philosophy

University College London

2018

Declaration

I, Charlotte Spicer, confirm that the work presented in this Thesis is my own. Where information has been derived from other sources, I confirm that this has been indicated in the Thesis.

Signed:

Abstract

Inclusion body myositis (IBM) is the most common acquired muscle disease affecting adults over the age of 50 and is characterised by a combination of inflammatory and degenerative features. Although the precise cause of IBM is unknown, previous therapeutic trials have targeted only the inflammatory component of IBM, but all have been unsuccessful and as a result, IBM remains untreatable.

The characteristic degenerative features of IBM include the accumulation and aggregation of a number of proteins, most likely as a result of disturbances in protein homeostasis. It is therefore possible that targeting protein mishandling may be an effective therapeutic strategy for IBM. Indeed, recent results from our laboratory have demonstrated that upregulation of the cytoprotective heat shock response (HSR) with Arimoclomol, a novel co-inducer of the HSR, ameliorates IBM-like pathology in cultured primary rat muscle cells, by improving protein handling.

In this study, these results were taken forward into an *in vivo* pre-clinical trial, using a transgenic mouse model of multisystem proteinopathy (MSP), caused by a mutation in the valosin-containing protein (*VCP*) gene. This model recapitulates many key features of IBM in muscle. Treatment with Arimoclomol was found to significantly attenuate IBM-like characteristics in the muscle of 14-month old mutant *VCP* mice and importantly, also improved muscle strength.

To establish whether these pathological findings are reproduced in a more clinically relevant, human model of IBM, dermal fibroblasts were obtained from sporadic IBM patients or MSP patients expressing mutant *VCP*, presenting with an inclusion body myopathy. These fibroblasts recapitulated the IBM disease phenotype, which was ameliorated following treatment with Arimoclomol.

The results presented in this Thesis show that Arimoclomol reduces characteristic pathological features of IBM both *in vivo*, in a mutant *VCP* mouse model and *in vitro*, in patient-derived dermal fibroblasts. These findings build upon our previous *in vitro* data and together provide strong evidence to suggest that Arimoclomol may be a potential therapeutic agent for the treatment of IBM.

Impact statement

Inclusion body myositis (IBM) is an acquired muscle disease that typically affects adults over the age of 50 and results in the progressive muscle weakness and wasting. The disease can lead to severe disability within several years of onset.

The work presented in this Thesis demonstrates that this disease can be modelled *in vivo*, in transgenic mice that express mutant forms of human VCP and *in vitro*, in fibroblasts derived from patients with sporadic IBM or patients with multisystem proteinopathy, expressing mutant VCP.

Using these models of IBM, I found that Arimoclomol, a novel drug that targets an endogenous cytoprotective mechanism known as the heat shock response, may be a potential beneficial treatment for IBM. My results show that Arimoclomol reduces key disease features of IBM both *in vivo*, in mutant VCP mice and *in vitro*, in IBM patient-derived dermal fibroblasts. We observed significant improvements in signs of both inflammation and degeneration, the two main components of IBM, in mice and patient fibroblasts treated with Arimoclomol. This research is highly significant for the field as currently there is no effective treatment for IBM.

As a result of these positive findings in experimental models of IBM, a 20-month, multi-centre efficacy trial in 150 IBM patients has now commenced. This is jointly led by the MRC Centre for Neuromuscular Diseases at Queen Square and the University of Kansas. An investigator-led, randomised, double-blind, placebo-controlled, proof of concept pilot study of Arimoclomol in 24 sporadic IBM patients has already demonstrated that Arimoclomol is safe and well-tolerated and may slow the decline in muscle strength and physical function in patients.

As well as this clinical impact, the work described in this Thesis will also have important benefits for preclinical IBM research. A significant challenge in IBM research is the lack of preclinical models which replicate all aspects of the disease phenotype. Well-established and relevant models of disease are vital for examining the efficacy of novel therapeutic compounds and for the

translation of successful preclinical research into human trials. The characterisation of the *in vitro* and *in vivo* models described in this Thesis means these will be valuable tools in which other drugs for the treatment of IBM can be assessed, using Arimoclomol as a standard.

The research presented in this Thesis will therefore have a beneficial impact on both preclinical and clinical IBM research.

Acknowledgements

This Thesis would not have been possible without a number of people, to whom I express my sincerest gratitude. I would firstly like to thank my primary supervisor, Prof Linda Greensmith, for her invaluable mentorship. I have thoroughly enjoyed completing this PhD and I cannot express how grateful I am to have been given this opportunity. I would also like to thank Dr Mhoriam Ahmed, for her fundamental contribution to the work presented in this Thesis, as well as for the training and guidance she has given me throughout the course of my PhD. I'm so glad to have been a part of 'Team IBM'.

I also need to thank all the other members of the Greensmith lab, past and present, as well as the Schiavo and Fratta labs, for sharing their skills, knowledge and time and most importantly, for making the last few years so enjoyable. I feel incredibly lucky to have made so many great friendships during my time at the Institute of Neurology.

I am especially grateful to our lab manager James Dick for his advice, technical assistance and his continual moral support. Also to my PhD buddy, Dr(!) Emma Wilson, who shared the ups and downs of this PhD journey with me from the beginning and bought me an endless supply of treats whenever my experiments weren't going quite as planned! This Thesis would also not have been possible without other members of the Sobell Department, particularly Kully, Debbie, Ligia and Chris. I am also grateful to Alex, Ben, Ione and Verna for giving up their time to proofread chapters of this Thesis!

I would additionally like to thank Prof Mike Hanna, Prof Mary Reilly and everyone else at the MRC Centre for Neuromuscular Diseases, for providing the funding which allowed me to undertake this translational research project and for giving me many opportunities to present my work.

Finally, I would like to thank my family and friends for all their support and encouragement and for helping me to achieve this PhD.

Table of Contents

TITLE PAGE	1
DECLARATION	2
ABSTRACT	3
IMPACT STATEMENT	4
ACKNOWLEDGEMENTS	6
LIST OF FIGURES	14
LIST OF TABLES	17
LIST OF ABBREVIATIONS	18
CHAPTER 1 GENERAL INTRODUCTION	21
1.1. Inclusion body myositis (IBM)	22
1.1.1. Clinical features	22
1.1.2. Disease prevalence	24
1.1.3. Histopathology and diagnosis	26
1.1.4. Genetic susceptibility	28
1.1.5. Therapeutic strategies	31
1.1.5.1. Exercise	31
1.1.5.2. Immunosuppressants	32
1.1.5.3. Tumour necrosis factor-blocking agents	32
1.1.5.4. T-cell depletion	33
1.1.5.5. Rapamycin	34
1.1.5.6. Myostatin antagonists	34
1.2. Pathomechanisms of IBM	35
1.2.1. Inflammatory mechanisms in IBM	36
1.2.2. Degenerative mechanisms in IBM	37
1.3. Protein homeostasis	39
1.3.1. Stress granule formation	41
1.3.2. Chaperones and the heat shock response (HSR)	41
1.3.3. The unfolded protein response	42
1.3.4. The ubiquitin-proteasome system	43
1.3.5. Autophagy	44
1.3.6. The mitochondrial unfolded protein response	45
1.4. Protein homeostasis and ageing	47
1.5. Protein homeostasis in IBM	50
1.6. Upregulation of the HSR with Arimoclomol	52

1.7. The effects of Arimoclomol in <i>in vitro</i> models of IBM	52
1.8. Examining the effects of Arimoclomol in additional models of IBM	53
1.9. Aims of this Thesis	56
CHAPTER 2 MATERIALS AND METHODS	57
2.1. Breeding and maintenance of mice	58
2.2. PCR genotyping	58
2.3. Arimoclomol treatment regime	60
2.4. Longitudinal assessment of grip strength and body weight	60
2.5. <i>In vivo</i> analysis of isometric muscle force	60
2.6. Removal and storage of mouse hindlimb muscles	61
2.7. Histochemistry and immunostaining	61
2.8. Muscle fibre area measurements	62
2.9. Analysis of centralised nuclei	63
2.10. Western blots (mouse tissue)	63
2.11. Electron microscopy (EM)	64
2.12. Establishment of human fibroblast cultures	65
2.13. Arimoclomol treatment	66
2.14. Immunocytochemistry	66
2.15. Western blots (cell lysates)	67
2.16. Disrupted nuclei counts	68
2.17. TUNEL assay	68
2.18. Statistical analysis	68
CHAPTER 3 TARGETING THE HEAT SHOCK RESPONSE IN A TRANSGENIC MOUSE MODEL OF MULTISYSTEM PROTEINOPATHY	69
3.1. Introduction	70
3.1.1. Clinical features of multisystem proteinopathy (MSP)	70
3.1.2. Histopathological features of MSP	71
3.1.3. Valosin-containing protein (VCP)	72
3.1.3.1. VCP structure	72
3.1.3.2. VCP function	72
3.1.3.3. MSP-associated VCP mutations	74
3.1.4. Additional MSP-causing mutations	76

3.2. Aims of this Chapter	77
3.3. Materials and methods	78
3.3.1. Breeding and maintenance of mutant VCP mice	78
3.3.2. Arimoclomol treatment regime	78
3.3.3. Grip strength analysis	78
3.3.4. <i>In vivo</i> analysis of isometric muscle force	78
3.3.5. Histochemistry and immunostaining	79
3.3.6. Muscle fibre area measurements	79
3.3.7. Analysis of centralised nuclei	79
3.3.8. Western blot	79
3.3.9. Electron microscopy (EM)	79
3.3.10. Statistical analysis	79
3.4. Results	81
3.4.1. Muscles of mutant VCP mice show pathological hallmarks of IBM which are attenuated following treatment with Arimoclomol	81
3.4.2. Mutant VCP mice have hypertrophic muscles which are attenuated following treatment with Arimoclomol	83
3.4.3. Mutant VCP mice have an increased incidence of centralised nuclei within myofibres which is further increased by Arimoclomol treatment	83
3.4.4. Muscles of mutant VCP mice show cytoplasmic mislocalisation of TDP-43 which is prevented by treatment with Arimoclomol	86
3.4.5. Muscles of mutant VCP mice show ubiquitin-positive inclusions which are prevented by treatment with Arimoclomol	86
3.4.6. Muscles of mutant VCP mice show p62 aggregates which are prevented by treatment with Arimoclomol	89
3.4.7. Muscles of mutant VCP mice have increased inflammatory cell infiltration which is reduced following treatment with Arimoclomol	89

3.4.8. Muscles of mutant VCP mice have disrupted mitochondrial morphology and an increased number of vacuoles which are prevented by treatment with Arimoclomol	92
3.4.9. Mutant VCP mice have a decrease in muscle force which is prevented by treatment with Arimoclomol	95
3.5. Discussion	97
3.5.1. Muscles of mutant VCP mice display an IBM-like pathology	97
3.5.2. The effects of Arimoclomol <i>in vivo</i>	98
3.5.3. Arimoclomol is a co-inducer of the heat shock response	100
3.5.4. Pathomechanisms of IBM	102
3.6. Conclusion	105
 CHAPTER 4 TARGETING THE HEAT SHOCK RESPONSE TO REDUCE THE PATHOLOGICAL FEATURES OF SPORADIC IBM IN PATIENT-DERIVED FIBROBLASTS	 106
4.1. Introduction	107
4.1.1. Advantages of fibroblasts as a cellular model of disease	107
4.1.2. Fibroblasts as a model of human disease	108
4.1.3. Fibroblasts as a model of IBM	109
4.2. Aims of this Chapter	109
4.3. Materials and methods	111
4.3.1. Fibroblasts lines	111
4.3.2. Immunocytochemistry	114
4.3.3. Western blot	114
4.3.4. Disrupted nuclei counts	114
4.3.5. TUNEL assay	114
4.3.6. Arimoclomol treatment	114
4.3.7. Statistical analysis	114
4.4. Results	115
4.4.1. Sporadic IBM patient fibroblasts display aggregation of key IBM proteins under basal culture conditions	115

4.4.2. Sporadic IBM patient fibroblasts show no evidence of stress granule-like aggregates	118
4.4.3. Sporadic IBM patient fibroblasts display evidence of mitochondrial disruption	118
4.4.4. Sporadic IBM patient fibroblasts have abnormal nuclear morphology	122
4.4.5. Abnormal nuclei in sporadic IBM patient fibroblasts are associated with a disrupted actin cytoskeleton	122
4.4.6. Sporadic IBM patient fibroblasts display predominantly normal localisation of nuclear envelope markers	125
4.4.7. Pharmacological upregulation of the heat shock response reduces the number of disrupted nuclei in sporadic IBM patient fibroblasts	127
4.4.8. HSP70 expression in sporadic IBM fibroblasts following Arimoclomol treatment	127
4.5. Discussion	130
4.5.1. Patient fibroblasts exhibit characteristic pathological features of sporadic IBM	130
4.5.1.1. TDP-43 pathology in sporadic IBM fibroblasts	130
4.5.1.2. Stress granule formation in sporadic IBM	132
4.5.1.3. Nuclear disruption in sporadic IBM patient fibroblasts	132
4.5.2. Investigating pathomechanisms in sporadic IBM patient fibroblasts: proteasome activity, autophagy and mitochondrial function	135
4.5.3. Upregulation of the heat shock response in sporadic IBM patient fibroblasts: the effect of Arimoclomol on IBM pathology	136
4.5.4. Differences between sporadic IBM patient fibroblast lines	138
4.5.5. Degenerative and inflammatory changes in sporadic IBM patient fibroblasts	139
4.6. Conclusion	140

CHAPTER 5 UPREGULATING THE HEAT SHOCK RESPONSE IN VCP PATIENT FIBROBLASTS	141
5.1. Introduction	142
5.1.1. VCP patient fibroblasts	142
5.1.2. Alternative <i>in vitro</i> VCP models	143
5.2. Aims of this Chapter	145
5.3. Materials and methods	146
5.3.1. Fibroblast cell lines	146
5.3.2. Immunocytochemistry	146
5.3.3. Western blots	146
5.3.4. Disrupted nuclei counts	146
5.3.5. TUNEL assay	149
5.3.6. Arimoclomol treatment	149
5.3.7. Heat shock treatment	149
5.3.8. Statistical analysis	149
5.4. Results	150
5.4.1. VCP patient fibroblasts display pathological abnormalities under basal culture conditions	150
5.4.2. VCP patient fibroblasts have an abnormal nuclear morphology	153
5.4.3. Arimoclomol reduces the number of disrupted nuclei in VCP patient fibroblasts	157
5.4.4. HSP70 expression in VCP patient fibroblasts following Arimoclomol treatment	157
5.4.5. Establishing a model of heat shock for human fibroblasts	160
5.4.6. Effects of heat shock on VCP patient fibroblasts	160
5.5. Discussion	166
5.5.1. IBM-relevant pathological features in VCP patient fibroblasts	166
5.5.1.1. Aggregation of IBM-associated proteins	166
5.5.1.2. Mitochondrial morphology in VCP patient fibroblasts	168
5.5.1.3. Disrupted nuclei in VCP patient fibroblasts	170

5.5.2. Comparison of different VCP mutations on pathological features in patient fibroblasts	171
5.5.3. Effect of Arimoclomol on pathological characteristics in VCP patient fibroblasts	172
5.5.4. VCP mutations and the implications of upregulating the heat shock response	173
5.5.5. Effects of heat stress in VCP patient fibroblasts	174
5.6. Conclusion	176
CHAPTER 6 GENERAL DISCUSSION	178
6.1. Replicating the cellular stress response in models of IBM	180
6.2. Cellular chaperones as therapeutic targets	182
6.3. Implications of findings for IBM research	183
6.3.1. Characterisation of <i>in vivo</i> and <i>in vitro</i> models of IBM	183
6.3.2. Clinical trial of Arimoclomol in sporadic IBM patients	185
6.4. Limitations of this investigation	186
6.5. Future work	188
6.6. Concluding remarks	191
REFERENCES	192

List of Figures

Figure 1.1. Clinical features of IBM	23
Figure 1.2. Pathological changes in muscle of IBM patients	27
Figure 1.3. Cellular proteostasis	40
Figure 1.4. Arimoclomol treatment ameliorates IBM-like pathology <i>in vitro</i> in primary rat myocyte cultures overexpressing β -APP or exposed to inflammatory mediators	54
Figure 2. Timeline of mouse <i>in vivo</i> studies and Arimoclomol treatment	59
Figure 3.1. MSP-related <i>VCP</i> mutations	75
Figure 3.2. Arimoclomol treatment improves IBM-like pathology in tibialis anterior (TA) muscles of mutant <i>VCP</i> mice	82
Figure 3.3. Muscle fibre hypertrophy in mutant <i>VCP</i> mice is reduced by treatment with Arimoclomol	84
Figure 3.4. Arimoclomol increases the percentage of myofibres with centralised nuclei in TA muscles of mutant <i>VCP</i> mice, suggestive of past regeneration of muscle fibres	85
Figure 3.5. Cytoplasmic TDP-43 mislocalisation in TA muscles of mutant <i>VCP</i> mice is prevented by treatment with Arimoclomol	87
Figure 3.6. The formation of ubiquitin-positive inclusions in TA muscles of mutant <i>VCP</i> mice is reduced following treatment with Arimoclomol	88
Figure 3.7. Increased expression of p62 in TA muscles of mutant <i>VCP</i> mice is reduced following treatment with Arimoclomol	90
Figure 3.8. Increased expression of inflammatory markers in TA muscles of mutant <i>VCP</i> mice is reduced following treatment with Arimoclomol	91
Figure 3.9. Macrophage infiltration in TA muscles of mutant <i>VCP</i> mice is prevented by treatment with Arimoclomol	93
Figure 3.10. Arimoclomol improves mitochondrial morphology and reduces the number of vacuoles in TA muscles of mutant <i>VCP</i> mice	94

Figure 3.11. Arimoclomol reduces the decline in grip strength and improves the maximum tetanic force of extensor digitorum longus (EDL) muscles in mutant VCP mice	96
Figure 4.1. TDP-43 is mislocalised from the nucleus to the cytoplasm and shows evidence of nuclear depletion in sporadic IBM fibroblasts under basal culture conditions	116
Figure 4.2. Sporadic IBM fibroblasts display ubiquitin-positive aggregates	117
Figure 4.3. Sporadic IBM fibroblasts display p62-positive aggregates and rimmed vacuoles	119
Figure 4.4. Sporadic IBM patient fibroblasts show no evidence of stress granule-like aggregates	120
Figure 4.5. Sporadic IBM fibroblasts display alterations in mitochondrial morphology	121
Figure 4.6. Sporadic IBM patient fibroblasts have abnormal nuclear morphology but show no evidence of apoptosis	123
Figure 4.7. Abnormal nuclei in sporadic IBM patient fibroblasts are associated with a disrupted cytoskeleton	124
Figure 4.8. Sporadic IBM patient fibroblasts display predominantly normal localisation of nuclear envelope markers	126
Figure 4.9. Arimoclomol reduces the number of disrupted nuclei in sporadic IBM patient fibroblasts	128
Figure 4.10. HSP70 expression in Arimoclomol-treated sporadic IBM patient fibroblasts	129
Figure 5.1. TDP-43 is mislocalised and forms cytoplasmic aggregates in VCP patient fibroblasts under basal culture conditions	151
Figure 5.2. VCP patient fibroblasts form ubiquitin-positive aggregates under basal culture conditions	152
Figure 5.3. VCP patient fibroblasts form ubiquitin- and p62-positive vacuoles	154
Figure 5.4. Mitochondrial morphology in VCP patient fibroblasts	155

Figure 5.5. VCP patient fibroblasts have an increased number of abnormal nuclei but show no evidence of apoptosis	156
Figure 5.6. Arimoclomol reduces the number of disrupted nuclei in VCP patient fibroblasts	158
Figure 5.7. HSP70 expression in Arimoclomol-treated VCP patient fibroblasts	159
Figure 5.8. HSP70 expression is increased in control and VCP patient fibroblasts in response to heat shock	161
Figure 5.9. Cellular pathology in VCP patient fibroblasts following heat shock	162
Figure 5.10. Heat shock increases the number of abnormal nuclei in control fibroblasts but has no effect on VCP patient fibroblasts	164
Figure 5.11. VCP patient fibroblasts with severely disrupted nuclei do not express HSP70 after heat shock	165

List of Tables

Table 1. Summary of studies on the prevalence of IBM in different populations	25
Table 2. Primary antibodies used in Chapter 3 for the study of mutant VCP mouse muscle	80
Table 3. Sporadic IBM patient fibroblasts	112
Table 4. Primary antibodies used in Chapter 4 for the study of sporadic IBM fibroblasts	113
Table 5. VCP patient fibroblasts	147
Table 6. Primary antibodies used in Chapter 5 for the study of VCP patient fibroblasts	148

List of Abbreviations

6MWD	6 minute walking distance
A β	Amyloid-beta
ActRII	Activin II receptor
AD	Alzheimer's disease
ADP	Adenosine diphosphate
ALS	Amyotrophic lateral sclerosis
ALSFRS	Amyotrophic lateral sclerosis functional rating scale
AMP	Adenosine monophosphate
ANOVA	Analysis of variance
ATF6	Activating transcription factor 6
ATP	Adenosine triphosphate
β -APP	Beta-amyloid precursor protein
BiP	Binding immunoglobulin protein
BMD	Becker muscular dystrophy
CNMD	Centre for Neuromuscular Diseases
CHOP	CCAAT/enhancer-binding protein homologous protein
CMA	Chaperone-mediated autophagy
cN1A	Cytosolic 5'nucleotidase 1A
COX	Cytochrome C oxidase
CTL	Chymotrypsin-like
DAPI	4, 6-diamidino-2-phenylindole
DM	Dermatomyositis
DMD	Duchenne muscular dystrophy
DMEM	Dulbecco's Modified Eagle Medium
DNA	Deoxyribonucleic acid
DNase	Deoxyribonuclease
EDL	Extensor digitorum longus
EDTA	Ethylenediaminetetraacetic acid
EGTA	Ethylene glycol tetraacetic acid
eIF	Eukaryotic translation initiation factor
EM	Electron microscopy
ENMC	European Neuromuscular Centre
ER	Endoplasmic reticulum
ERAD	Endoplasmic reticulum associated degradation

FBS	Fetal bovine serum
fIBM	Familial inclusion body myositis
FTD	Frontotemporal dementia
GAPDH	Glyceraldehyde-3-phosphate dehydrogenase
G3BP	GTPase-activating protein-binding protein
H&E	Haematoxylin and eosin
HD	Huntington's disease
HEK	Human embryonic kidney
HERP	Homocysteine-induced endoplasmic reticulum protein
hIBM	Hereditary inclusion body myositis
HLA	Human leukocyte antigen
hnRNP	Heterogeneous nuclear ribonucleoprotein
HS	Heat shock
HSC	Heat shock cognate
HSE	Heat shock element
HSF	Heat shock factor
HSP	Heat shock protein
HSR	Heat shock response
IBM	Inclusion body myositis
IBMFRS	Inclusion body myositis functional rating scale
IBMPFD	Inclusion body myopathy with Paget's disease of bone and frontotemporal dementia
IFN	Interferon
I κ B α	NF- κ B inhibitor alpha
IL-1	Interleukin-1
IRE1	Inositol-requiring transmembrane kinase/endonuclease 1
iPSC	Induced pluripotent stem cell
IVIG	Intravenous immunoglobulin
JNK	c-Jun N-terminal kinase
LAMP	Lysosome-associated membrane protein
LC3	Microtubule-associated protein 1A/1B-light chain 3
LDH	Lactate dehydrogenase
MHC	Major histocompatibility complex
MRI	Magnetic resonance imaging
mRNA	Messenger RNA

MSP	Multisystem proteinopathy
NF-kB	Nuclear factor-kappa B
PBS	Phosphate buffer saline
PCR	Polymerase chain reaction
PD	Parkinson's disease
PDB	Paget's disease of bone
PERK	Pancreatic ER kinase
PFA	Paraformaldehyde
PM	Polymyositis
PrLD	Prion-like domain
ROS	Reactive oxygen species
RNA	Ribonucleic acid
SBF SEM	Serial block face scanning electron microscopy
SBMA	Spinal and bulbar muscular atrophy
SDH	Succinate dehydrogenase
SDS	Sodium dodecyl sulphate
SEM	Standard error of the mean
SOD	Superoxide dismutase
SMA	Spinal muscular atrophy
SQSTM1	Sequestosome 1
TA	Tibialis anterior
TBE	Tris-Borate-EDTA
TBS	Tris-buffered saline
TDP-43	Transactive response DNA-binding protein-43
TEM	Transmission electron microscopy
Th1	T-helper type 1
TIA1	T-cell intracellular antigen 1
TL	Trypsin-like
TNF	Tumour necrosis factor
TOMM	Translocase of Outer Mitochondrial Membrane
TUNEL	Terminal deoxynucleotidyl transferase dUTP nick end labeling
UPR	Unfolded protein response
UPS	Ubiquitin-proteasome system
VCP	Valosin-containing protein
WT	Wild-type

Chapter 1

General Introduction

1.1. Inclusion body myositis (IBM)

Sporadic inclusion body myositis (IBM) is the most common acquired myopathy among adults over the age of 50. The disease is characterised by gradual progressive muscle weakness and atrophy of the upper and lower limbs, eventually leading to severe disability and wheelchair dependency within several years of onset (Peng et al. 2000). First described in the 1960s, IBM is considered a rare disease, affecting 1-71 people per million and is often initially misdiagnosed (Dabby et al. 2001; Lavian et al. 2016; Mammen 2017). The cause of the disease remains enigmatic and there is a great unmet need for new therapeutic treatments. To date, there is no effective treatment to slow or prevent the progression of IBM.

1.1.1. Clinical features

IBM typically presents as progressive proximal and distal muscle atrophy, which is often asymmetric in nature (Lotz et al. 1989; Amato et al. 1996; Phillips et al. 2001; Dalakas 2015; Albayda et al. 2018). Early weakness tends to be apparent in the quadriceps and deep finger flexors, so that patients report frequent falls, difficulty standing up and climbing stairs, loss of finger dexterity and difficulty gripping objects as some of the most common initial signs of the disease (**Fig. 1.1**; Badrising et al. 2005; Needham et al. 2008; de Camargo et al. 2018; Tsukita et al. 2018). As the disease progresses, other muscles including the hip flexors, elbow flexors, knee flexors, neck flexors and the ankle dorsiflexors may be affected, leading to eventual loss of ambulation and wheelchair dependency within several years of onset (Sekul & Dalakas 1993; Cox et al. 2011; Lloyd et al. 2014). Dysphagia, caused by dysfunction of the pharyngeal and oesophageal muscles, is also experienced by approximately 40-80% of patients (Houser et al. 1998; Oh et al. 2008; Cox et al. 2009; Cox et al. 2011; Mulcahy et al. 2012; Dobloug et al. 2015).



Figure 1.1. Clinical features of IBM

Typical example of atrophy of the quadriceps femoris **(A)** and muscle wasting of the forearm flexor compartment and finger flexor weakness **(B)** in a patient with IBM. Photos provided by Dr Pedro Machado (MRC Centre for Neuromuscular Diseases, UCL) with patient's consent.

Due to the slow progression and late age of onset of IBM, early signs of the disease are often attributed to ageing. Symptoms tend to therefore be present for up to 5 years before disease diagnosis (Phillips et al. 2000; Needham et al. 2008; Benveniste et al. 2011; Dobloug et al. 2015; Paltiel et al. 2015). Loss of ambulation can occur between 7-14 years from diagnosis, whilst a later onset of IBM has been linked to a more rapid decline in function (Benveniste et al. 2011; Lindberg & Oldfors 2012; Cortese et al. 2014). Although IBM is not considered to directly impact lifespan, the disease may contribute to premature mortality due to secondary complications, such as injurious falls and pneumonia linked to the dysfunction of the pharyngeal and oesophageal muscles (Price et al. 2016).

1.1.2. Disease prevalence

IBM preferentially affects men, with a male-to-female ratio of 3:1. There is considerable variation in prevalence between different populations and ethnic groups, although to date there have been relatively few studies examining this (**Table 1**; Lotz et al. 1989; Dimachkie & Barohn 2012; Tan et al. 2013; Meyer et al. 2015; Callan et al. 2017). When age-adjusted, the reported prevalence of 1-71 per million, rises to 139 per million in people over the age of 50. Northern European, North American Caucasian and Australian populations typically have the highest incidence of IBM, whilst the disease is rare in African Americans and non-Caucasian population. The variation among these reported figures is likely due to an underestimation of cases due to incomplete diagnosis or differences in inclusion criteria, highlighting the need more precise diagnostic criteria (Badrising et al. 2000; Brady et al. 2013). Indeed, more recent studies suggest that prevalence of IBM may be higher than previously reported due to an increasing clinical awareness of the disease over the last few decades and more reliable diagnostic markers (Aoife et al. 2016; Lefter et al. 2017).

Country	Author	Year of publication	Prevalence (per million)
Netherlands	Badrising et al.	2000	4.9 ≥50 years; 16
Western Australia	Phillips et al.	2000	9.3 ≥50 years; 35.3
USA; Connecticut	Felice & North	2001	10.7 ≥45 years; 28.9
USA; Minnesota (Olmsted County)	Wilson et al.	2008	70.6
Western Australia	Needham et al.	2008	14.9 ≥50 years; 51.3
Turkey; Istanbul	Oflazer et al.	2011	1.06 ≥50 years; 5.96
Japan	Suzuki et al.	2012	9.83
South Australia	Tan et al.	2013	50.5 ≥50 years; 139.3
South-East Norway	Dobloug et al.	2015	33
Republic of Ireland	Lefter et al.	2017	≥50 years; 117

Table 1. Summary of studies on the prevalence of IBM in different populations

1.1.3. Histopathology and diagnosis

IBM is distinguished by a distinct set of histological features which can be identified from patient muscle biopsies and which are essential for diagnosis (**Fig. 1.2**). Traditionally, the disease has been considered an immune-mediated inflammatory myopathy, categorised alongside polymyositis (PM) and dermatomyositis (DM). Inflammation in IBM is characterised by the clonal expansion of infiltrating cytotoxic CD8⁺ T-cells and ubiquitous overexpression of major histocompatibility complex class I (MHC-I) antigens (Arahata & Engel 1984; Karpati et al. 1988; de Camargo et al. 2018). The MHC is a set of cell surface proteins that bind peptide fragments from intracellular antigens and display them for recognition by cytotoxic T cells. In normal, healthy skeletal muscle fibres, MHC-I antigens are not constitutively expressed but in IBM patient muscle, there is an increase in MHC-I-expressing fibres (Karpati et al. 1988). In addition, proinflammatory cytokines, chemokines and adhesion molecules are upregulated in IBM muscle (Tews & Goebel 1996; De Bleecker et al. 2002; Figarella-Branger et al. 2003; Raju et al. 2003; Badrising et al. 2017).

In contrast to PM and DM, myofibres of IBM patients have a number of distinct myodegenerative features, which likely contribute to IBM pathology. These include rimmed vacuoles and inclusion bodies, containing a wide range of proteins such as beta-amyloid precursor protein (β -APP) and amyloid-beta ($A\beta$), tau, ubiquitin, p62 and heat shock proteins (Askanas et al. 1991; Askanas & Engel 2008; Askanas et al. 2009; Nogalska et al. 2009; Vattermi et al. 2009; Dubourg et al. 2011; Cacciottolo et al. 2013; de Camargo et al. 2018). In addition, cytoplasmic mislocalisation of the nuclear protein transactive response DNA-binding protein 43 (TDP-43) is observed in IBM muscle, distinguishing the disease from the other inflammatory myopathies (Weihl et al. 2008).

Morphological changes associated with mitochondrial abnormalities have also been observed in muscle biopsies from IBM patients. Cytochrome c oxidase (COX)-negative fibres and succinate dehydrogenase (SDH)-positive fibres and ragged red fibres are frequently observed (Müller-Höcker 1990; Oldfors et al. 1995; Rifai et al. 1995; Dahlbom et al. 2002). Although common in normal aged muscle, in IBM these are greater in number compared to age-matched controls, suggesting an accelerated occurrence of these mitochondrial abnormalities.

Image removed due to copyright

Figure 1.2. Pathological changes in muscle of IBM patients

Histopathological changes in muscle tissue sections of IBM patients include **(A)** muscle fibres containing rimmed vacuoles, as shown with haematoxylin and eosin (H&E) stain, **(B)** increased amyloid (red), as shown using Congo red stain and **(C)** the presence of tubulofilaments, observed using electron microscopy **(D)** MHC-I upregulation in the sarcolemma and sarcoplasm, **(E)** fibres containing sarcoplasmic p62 and **(F)** TDP-43 immunoreactive aggregates with loss of normal myonuclear TDP-43 staining. Scale bar represents 50 μm (A, B, D and F); 25 μm (E); and 0.7 μm (C). **(G)** MRI images of the thighs of IBM patients showing fatty infiltration (white areas), predominantly of the anterior muscles. Images used with permission from Machado et al. (2013).

The diagnosis of IBM is classically based on the Griggs Criteria, proposed in the 1990s (Griggs et al. 1995). These criteria allow a definitive diagnosis of IBM based on three key pathological features; inflammatory infiltrates with partial invasion, rimmed vacuoles and either amyloid deposits or 15- to 18-nm tubulofilaments. However, as these measures do not take into account the clinical features of the disease, new criteria have since been developed. These include the European Neuromuscular Centre (ENMC) Criteria (Rose & ENMC IBM Working Group 2013) and the MRC Centre for Neuromuscular Diseases (CNMD) Criteria (Benveniste & Hilton-Jones 2010; Hilton-Jones et al. 2010). These criteria aim to aid diagnosis in less straightforward cases, such as early on in the disease course when there may be an absence of the key histopathological features in muscle biopsies as defined by the Griggs criteria (Calabrese et al. 1987; van der Meulen et al. 1998; Dahlbom et al. 2002). Further work investigating additional markers of IBM is still required to advance the understanding of disease progression and enhance diagnosis of IBM.

Magnetic resonance imaging (MRI) is emerging as a complementary tool for aiding diagnosis of IBM, although it is not yet part of the standard diagnostic process. Currently, MRI is used to guide the optimal site for muscle biopsies. However, the technique has potential for use in clinical diagnosis in neuromuscular disorders, particularly in diseases with highly selective muscle involvement, such as IBM. Research suggests that fatty infiltration in muscle is more prominent than inflammation in IBM, with the vastus intermedius and medialis thigh muscles characteristically affected to a greater extent than other thigh muscles (Phillips et al. 2001; Dion et al. 2002; Cox, Reijnierse, et al. 2011; Machado et al. 2014; Tasca et al. 2015; Morrow et al. 2016; Guimaraes et al. 2017). Furthermore, MRI could be a useful tool for monitoring disease progression.

1.1.4. Genetic susceptibility

The varying prevalence between different populations suggests a potential link between the susceptibility of developing IBM and a complex interplay of genetic and environmental factors (Needham et al. 2007). Despite IBM being considered a sporadic disease, candidate gene studies have pointed to certain susceptibility genes which may affect the development and progression of IBM

(Gang et al. 2014; Rothwell, Lilleker & Lamb 2017; Britson et al. 2018). Candidate gene studies have focused mainly on the MHC, with the human leukocyte antigen (HLA) region repeatedly shown to contain the strongest risk alleles for the development of IBM (Garlepp et al. 1994; Rojana-udomsart et al. 2012; Johari et al. 2017; Rothwell, Cooper et al. 2017). The HLA locus contains genes that encode MHC- I (HLA-A, HLA-B and HLA-C) and MHC-II (HLA-DR, HLA-DQ, HLA-DP, HLA-DOA, HLA-DOB and HLA-DM). Allelic variations in both MHC-I (HLA-A) and MHC-II (HLA-DRA and HLA-DRB) have been associated with the susceptibility of developing IBM. In particular, there is a strong association with the HLA-DRB1*0301 allele (and its equivalent serological specificity DR3) and other allelic components of the 8.1 MHC ancestral haplotype (HLA-A1, B8) in Caucasian populations. HLA-DRB1*0301 carriers have been reported to have more severe muscle weakness, a more rapid rate of disease progression and a higher risk of developing IBM (Garlepp et al. 1994; Koffman et al. 1998; Lampe et al. 2003; Price et al. 2004; Needham et al. 2008; Rojana-udomsart et al. 2012). This increased susceptibility has been estimated as being up to ten times greater in a Western Australian population (Mastaglia 2009). Conversely, populations and countries with a low incidence of IBM, such as African-American and Australian aboriginal populations and countries such as Turkey and Thailand, have much lower HLA-DR3 frequencies (Mastaglia 2009). Furthermore, HLA-DRB loci DRB4 and DRB5 have been reported to have protective effects (Rojana-udomsart et al. 2013).

Although genetic studies of IBM are challenging due to the rarity of the disease and thus the small sample sizes available, the Myositis Genetics Consortium (MYOGEN) have recently conducted the largest genetic association study to date in 252 Caucasian IBM patients and 1008 ethnically-matched controls from 11 countries (Rothwell, Cooper et al. 2017). This study confirmed the involvement of the HLA-DRB1 loci in the risk of developing IBM and identified novel amino acid associations within the HLA-DRB1 binding pocket that may explain the risk in this locus. In contrast to previous studies, no HLA alleles were found to modify disease onset. The MHC contains a number of different genes, not all of which influence immune function. In addition, these genes may have varying expression patterns, with some expressed solely in muscle or

others more ubiquitously. Further characterisation of these genes in the MHC will therefore be a vital aid for unravelling the pathogenesis of IBM.

Aside from the risk factor associated with the MHC, more recently, areas outside of HLA loci have been suggested to be associated with IBM. Possible pathogenic variants have been found in genes encoding proteins commonly found within inclusions bodies in IBM, including the valosin-containing protein (*VCP*) gene and the sequestosome 1 (*SQSTM1*) gene, encoding p62 (Gang et al. 2015; Weihl et al. 2015; Gang et al. 2016).

IBM is usually associated with a large number of cytochrome c oxidase (COX)-deficient muscle fibres with increased mitochondrial DNA (mtDNA) deletions compared to COX-normal fibres (Lindgren et al. 2015; Rygiel et al. 2015; Rygiel et al. 2016). The proportion of COX-deficient fibres correlates with the amount of T-lymphocyte infiltration and muscle fibre atrophy (Rygiel et al. 2015). The mtDNA rearrangements in IBM are complex, with a recent study having reported 20% of COX-deficient cells harbouring two or more mtDNA deletions (Rygiel et al. 2016). Variants in nuclear genes involved in mtDNA maintenance have been investigated but the study concluded that they are unlikely to be the sole cause of the mtDNA deletions and COX deficiency found in IBM (Lindgren et al. 2015). Further investigation involving a broader spectrum of genes is therefore required to examine the triggers of mtDNA rearrangements in IBM.

Finally, a polymorphism in the translocase of outer mitochondrial membrane 40 (*TOMM40*) gene has been reported to be associated with a later onset of symptoms in IBM patients (Mastaglia et al. 2013; Gang et al. 2015). However, the results of these studies are conflicting as to whether polymorphisms in the *TOMM40* gene have a disease-modifying effect, so further studies are needed to confirm these findings.

Interestingly, there have been reports of siblings affected by IBM (Sivakumar et al. 1997; Amato & Shebert 1998; Tateyama et al. 2003; Ranque-Francois et al. 2005). These cases are termed familial inclusion body myositis (fIBM). Patients with fIBM have histological similarities and the same clinical phenotype to sporadic cases, as well as similar genetic markers. This familial occurrence is

extremely rare but genetic studies of these cases are important for increasing our understanding of IBM and may reveal pathways or risk factors involved in the disease and allow the identification of potential therapeutic targets.

Likewise, investigations into the hereditary inclusion body myopathies (hIBM) may be useful for uncovering similar mechanisms that may be linked to the pathogenesis of IBM. IBM is frequently confused with hIBM, which encompasses several autosomal-recessive and autosomal-dominant muscle disorders (Griggs et al. 1995). Although somewhat similar to IBM, these disorders are distinct to the sporadic condition. Muscle biopsies from these patients display rimmed vacuoles, protein accumulations and intracytoplasmic and intranuclear inclusions but unlike sporadic cases, these patients typically have negative MHC-I expression, a lack of inflammation, and an earlier age of onset of the disease (Askanas & Engel 1993; Askanas & Engel 2002).

1.1.5. Therapeutic strategies

Despite numerous clinical trials, there remains no effective disease-modifying treatment to slow or prevent disease progression in IBM. Clinical studies may be hampered by the fact that IBM is typically not diagnosed until many years after disease onset, by which time damage to muscle may have progressed too far for any notable benefit and there is often low patient recruitment due to the rare nature of the disease.

1.1.5.1. Exercise

Recent studies have highlighted the benefit of exercise as part of the treatment strategies for patients with IBM. It was previously thought that overworking muscles might lead to more rapid breakdown. However, several small, short-term studies have shown that low-moderate resistance programs can improve or at least maintain muscle strength and function (Spector et al. 1997; Arnardottir et al. 2003; Johnson et al. 2007; L.G. Johnson et al. 2009; Alexanderson 2012; Alexanderson & Lundberg 2012; Jørgensen et al. 2018). Although these studies have only examined a small cohort of patients, they do indicate that exercise strategies are safe and may temporarily reduce progression of IBM. Further investigation is still required in order to establish an

effective protocol for IBM patients but exercise remains an important non-pharmacological strategy in a disease with limited restorative treatment.

1.1.5.2. Immunosuppressants

The presence of inflammation in muscle biopsies from IBM patients has led to specific attention on targeting the immune component of IBM. However, various forms of immunotherapy have failed to show a clear long-term benefit in IBM patients. These have included a combination of corticosteroids, such as prednisolone and immunosuppressive agents such as methotrexate, cyclosporine, azathioprine, prednisone and mycophenolate mofetil (Leff et al. 1993; Lindberg et al. 1994; Mowzoon et al. 2001; Badrising et al. 2002; Rose et al. 2015; Saltychev et al. 2016). It is possible that particular subgroups of IBM patients, such as those with existing co-morbidities such as Sjögren's syndrome, may be more responsive to this type of treatment but this has not yet been assessed.

The efficacy of intravenous immunoglobulin (IVIG) has also been examined, although its use remains controversial. Some minor gain in muscle strength has been reported but no long-term sustainable improvements in muscle strength or function have been observed in clinical trials (Dalakas 1998; Walter et al. 2000; Dalakas et al. 2001; Dobloug et al. 2012; Patwa et al. 2012; Recher et al. 2012; Foreman et al. 2017). Moreover, some immunosuppressant drug therapy has been linked to an exacerbation of disease progression (Benveniste et al. 2011). Improvements have however been noted in the dysphagia experienced by IBM patients, suggesting that the pharyngeal muscles may be more responsive to IVIG treatment than limb muscles (Cherin et al. 2002; Pars et al. 2013).

1.1.5.3. Tumour necrosis factor-blocking agents

As T-helper type I (Th1)-related cytokines, including tumour necrosis factor (TNF)- α and interferon (IFN)- γ , are strongly expressed in IBM muscle, the effect of cytokine-targeted therapies have been investigated. These include TNF- α inhibitors such as etanercept and infliximab, as well as interleukin-1 (IL-1) receptor antagonists such as anakinra.

In a small study of nine IBM patients, twice weekly treatment with etanercept for an average of 17 months had no improvement on grip strength after six months and only a small, statistically significant increase in grip strength was reported at 12 months (Barohn et al. 2006). Likewise, in a separate study, only one patient out of four showed a clinical response to treatment with the TNF- α antagonist infliximab and no changes were observed in inflammatory markers in muscle tissue from any of these patients (Dastmalchi et al. 2008).

A pilot study examining the effects of the IL-1 β receptor blocker, anakinra, on IBM has also been undertaken. Four patients with IBM were given a subcutaneous daily dose of the compound but no improvement in muscle or grip strength was shown in any of the patients over a 5-12 month period (Kosmidis et al. 2013). In a separate study, assessing the effects of a daily self-administered injection of anakinra in patients with refractory myositis, only one out of five IBM patients showed improvement in muscle strength after three months. Three patients had no improvement in symptoms, whilst one withdrew due to a worsening of symptoms (Zong et al. 2014).

1.1.5.4. T-cell depletion

An alternative approach to controlling the inflammatory component of IBM is the use of T-cell depletion. Particular attention has been focused on the monoclonal antibody alemtuzumab, targeted against CD52, a glycoprotein expressed on mature T-cells which causes a depletion of peripheral lymphocytes. A pilot study of 13 IBM patients receiving a single course of alemtuzumab treatment over four days reported a reduction in disease progression for up to six months and four of these patients had an improvement in muscle strength (Dalakas et al. 2009). However, it is important to take into account the fact that this study was unblinded and it has been noted that the rate of disease progression over a 12-month period was higher compared to natural history studies (Greenberg 2010; Carstens & Schmidt 2014). Post-hoc analysis of muscle biopsies from the subset of IBM patients who had a transient improvement in muscle strength showed a trend towards downregulated expression of inflammatory molecules, however, no effect was seen on several typical markers of degeneration such as ubiquitin and β -amyloid (Schmidt et al. 2016). Further analysis with a larger, controlled trial of this drug is therefore required.

1.1.5.5. Rapamycin

Another promising agent, currently under investigation in a phase II clinical trial, is rapamycin (www.clinicaltrials.gov; No. NCT02481453). Rapamycin not only targets inflammatory processes by preventing the translation of mRNA for key cytokines involved in T-cell signalling but also induces autophagic clearance and therefore has a role in accelerating the clearance of abnormal protein aggregates. In a mouse model of IBM, rapamycin was found to improve muscle performance and pathology within the quadriceps (Nalbandian, Llewellyn, Nguyen et al. 2015). However, a separate study investigating the effects of rapamycin on an different mouse model of IBM found that rapamycin in fact accelerated muscle weakness and disease pathology (Ching & Weihl 2013). Whether this drug will be effective in improving IBM pathology in patients therefore remains to be determined, with the completion of an ongoing clinical trial expected in 2018.

1.1.5.6. Myostatin antagonists

Until recently, Bimagrumab (BYM338) was thought to hold much promise for IBM. Bimagrumab is a human monoclonal antibody that binds to activin II receptors (ActRII), outcompeting and thus blocking the effects of the natural inhibitory ligands activin and myostatin on muscle growth, thereby inducing skeletal muscle hypertrophy. When administered subcutaneously over four weeks, Bimagrumab has been shown to dramatically increase skeletal muscle mass and increase muscle fibre diameter in mice with glucocorticoid-induced skeletal muscle atrophy and weakness (Lach-Trifilieff et al. 2014).

In the clinic, an initial proof of concept trial in which 11 IBM patients received a single high dose of Bimagrumab, indicated that the compound was well tolerated and after eight weeks, improvements were observed in thigh muscle volume and lean body mass when compared to three IBM patients who received a placebo (Amato et al. 2014). Furthermore, patients receiving Bimagrumab had increased muscle strength and 6 min walking distance (6MWD) measurements at a 16-week follow-up. In spite of these positive findings, a more recent international, multicentre phase IIb/III trial in 251 IBM patients resulted in the failure of Bimagrumab to reach its primary endpoint.

This study examined the effects of monthly doses of Bimagrumab versus placebo over a 48-week period. No improvement was observed in either the 6MWD or in muscle strength (Amato et al. 2016).

An alternative myostatin antagonist currently under investigation is follistatin (FS334). Follistatin is a naturally occurring, ubiquitously expressed glycoprotein and a powerful inhibitor of myostatin. Previous studies *in vivo* have shown that follistatin promotes skeletal muscle hypertrophy in healthy rodents and primates and improves muscle pathology in models of Duchenne muscular dystrophy (DMD), Becker muscular dystrophy (BMD) and spinal muscular atrophy (SMA) (Nakatani et al. 2007; Benabdallah et al. 2008; Kota et al. 2009; Rose et al. 2009; Winbanks et al. 2012; Chen et al. 2014). Recently, follistatin gene therapy has been found to improve the 6MWD after one year, in four out of six IBM patients with mild to moderate ambulatory symptoms (Mendell et al. 2017). The effect of this treatment on patients with more advanced disease progression is yet to be determined. Importantly, patients in this trial were also undertaking an exercise regime. However, a number of issues with regard to the study design have been raised, including the lack of a control group and the addition of a number of other combined interventions (Greenberg 2017).

Currently, a safety trial is underway in nine IBM patients, in which the effects of intramuscular follistatin gene transfer at three different doses is being investigated. Although the primary outcome of this trial is safety and tolerability, secondary outcome measures will include muscle strength, physical function, thigh circumference, MRI assessment and muscle histopathology. To date, three patients have received low-dose injections in the quadriceps of a single limb and have displayed transient improvements in the 6MWT (Al-Zaidy et al. 2015). The study has now advanced to treatment of patients with the high-dose, bilateral injection but these results are yet to be reported.

1.2. Pathomechanisms of IBM

The failure of these numerous clinical trials to have a significant therapeutic impact highlights the difficulty in developing new therapeutic strategies for IBM. One major hindrance is the fact that, despite intensive research, the primary pathogenic mechanism of IBM is still unknown (Greenberg 2012). The

relationship between the inflammatory and myodegenerative features in IBM is complex. It therefore remains unclear whether this disease is primarily an immune-mediated disease, with muscle degeneration occurring as a secondary consequence or whether degeneration-associated molecules are responsible for triggering an inflammatory response.

1.2.1. Inflammatory mechanisms in IBM

As reflected in the clinical trials undertaken to date, research into the pathogenesis of IBM has focused predominantly on the inflammatory component of IBM pathology, as these changes tend to be more prominent in muscle biopsies from patients at earlier stages of disease progression (Mastaglia 2009). It has been speculated that viral or inflammatory triggers cause the clonal expansion of CD8+ T cells and T cell-mediated cytotoxicity of non-necrotic fibres. Proinflammatory cytokines drive ubiquitous overexpression of MHC-I on the surface of muscle fibres, which induces endoplasmic reticulum (ER) stress. This leads to the upregulation of NF- κ B and additional cytokine release, further enhancing MHC-I expression and triggering the recruitment of activated T-cells to the muscle (Nagaraju et al. 2005; Dalakas 2008). This mechanism thereby triggers a self-sustaining T-cell response and could ultimately be responsible for the muscle degeneration occurring in IBM (Dalakas 2006a; Dalakas 2006b). NF- κ B and proinflammatory cytokines can trigger β -amyloid production (Schmidt et al. 2008). Likewise, TNF- α has been shown to induce macroautophagy in muscle cells, resulting in β -amyloid accumulation (Keller et al. 2011; Keller et al. 2013). This β -amyloid accumulation could disrupt the function of protein handling pathways and give rise to protein accumulation and ER stress, providing a potential link between inflammation and degeneration in IBM.

In further support of the immune-mediated hypothesis, IBM has frequently been associated with autoimmune diseases including Sjögren's syndrome (Gutmann et al. 1985; Khraishi et al. 1992; Rojana-udomsart et al. 2011; Misterska-Skóra et al. 2013), retroviral infections such as HIV (Cupler et al. 1996; Dalakas et al. 2007; Hiniker et al. 2016; Couture et al. 2018) and rheumatoid arthritis (Soden et al. 1994; Vordenbäumen et al. 2010; Clerici et al. 2013). Moreover, recent studies have identified autoantibodies against cytosolic 5'-nucleotidase 1A

(cN1A) as highly specific and sensitive for IBM, further pointing towards an immune pathogenesis (Salajegheh et al. 2011; Larman et al. 2013; Pluk et al. 2013; Greenberg 2014; Eura et al. 2016; Tawara et al. 2017). CN1A is a muscle-specific enzyme which catalyses the conversion of adenosine monophosphate (AMP) into adenosine and phosphate and is highly expressed in skeletal muscle (Hunsucker et al. 2001). Immunohistochemistry has revealed that cN1A accumulates in perinuclear regions and rimmed vacuoles in IBM muscle biopsies (Larman et al. 2013) and cN1A seropositivity has been associated with an increased risk of mortality in IBM patients (Lilleker et al. 2016). However, false positive and false negative results have been reported. The presence of cN1A has been detected in the serum of patients with other forms of myositis as well as autoimmune diseases including Sjögren's syndrome and systemic lupus erythematosus (Larman et al. 2013; Pluk et al. 2013; Rietveld et al. 2018). In addition, in these studies, less than half of IBM patients were reported as cN1A-positive, suggesting that this autoantibody may be restricted to a subset of IBM patients. Nonetheless, further investigation is needed in order to determine whether cN1A seropositivity is disease relevant.

1.2.2. Degenerative mechanisms in IBM

Unlike other inflammatory myopathies, attempts to treat IBM with anti-inflammatory, immunosuppressant and immunomodulatory therapies, as discussed above (section 1.1.6), have had little, if any, success (Amato et al. 1994; Dalakas et al. 2001; Amato & Barohn 2009). This lack of significant clinical effect suggests that inflammation may in fact occur as a secondary response to degenerative processes. Furthermore, IBM-like degenerative changes observed in muscle from hIBM patients, occur without inflammation (Askanas & Engel 1998). For this reason, attention has more recently shifted towards examining the role of cellular mechanisms of myofibre degeneration and non-immune mechanisms in IBM.

The characteristic accumulation of ubiquitinated, multi-protein aggregates in muscle fibres of IBM patients points to disruption of protein homeostasis. It has been suggested that the formation of inclusion bodies is an attempt by the cell to sequester excessive, damaged or useless proteins (Gispert-Sanchez & Auburger 2006). Although it is still unclear as to what extent these protein

aggregates contribute to IBM pathology, they are considered to be a major source of toxicity and are often colocalised with degenerative features such as vacuoles (Kopito & Ron 2000; Querfurth et al. 2001; Ferreira et al. 2007; Nogalska, D'Agostino, Engel et al. 2010; Olzscha et al. 2011; Kriegenburg 2012; Askanas et al. 2015).

The majority of rimmed vacuoles within the muscle of IBM patients contain nuclear membrane proteins, suggesting disintegration of nuclear surface structures in the myonuclei. Proteins that have been reported within the rimmed vacuoles include the nuclear membrane proteins lamin A/C and emerin, the histone variant H2AX and DNA repair regulatory components such as DNA-dependent protein kinase, Hu70, and Hu80 (Greenberg et al. 2006; Nakano et al. 2008; Nishii et al. 2011). More recent findings have shown that the lengths of nuclear surface structures, including the outer nuclear membrane, inner nuclear membrane and nuclear fibrous lamina containing nuclear lamins A, B and C, are severely decreased in myonuclei of muscle biopsies taken from patients with early stages of muscle fibre degeneration (Matsubara et al. 2016), providing further evidence that the integrity of myonuclear surface structures are disrupted in IBM.

Another characteristic pathological hallmark of IBM muscle is the mislocalisation of the RNA-binding protein TDP-43 (Weihl et al. 2008; Salajegheh et al. 2009). Although TDP-43 shuttles between the nucleus and cytoplasm (Ayala et al. 2008), it is predominantly a nuclear ribonucleoprotein, with roles in RNA metabolism, including transcription, splicing, mRNA transport and microRNA biosynthesis (Buratti & Baralle 2010). When TDP-43 is cleaved by caspase-3, a pro-apoptotic protein, carboxyl-terminal fragments are generated that translocate from the nucleus to the cytoplasm, as is the case in muscle of IBM patients. This mislocalisation further implies that protein handling pathways are disrupted in IBM. Abnormal TDP-43 accumulation is a common feature in a number of neurodegenerative diseases, including Alzheimer's disease, Parkinson's disease and amyotrophic lateral sclerosis (ALS; Baloh 2011).

Cytoplasmic accumulations of TDP-43 are typically accompanied by nuclear depletion of the protein, suggesting that loss of normal nuclear TDP-43 function

could result in the muscle degeneration observed in IBM (Xu 2012). On the other hand, overexpression of TDP-43 *in vitro* and *in vivo*, suggests that TDP-43 is toxic in a dose-dependent manner (Winton et al. 2008; Zhang et al. 2009; Barmada et al. 2010; Kabashi et al. 2010; Baloh 2011; Gendron et al. 2013). In addition, mice expressing a mutant form of human TDP-43 develop a progressive and fatal neurodegenerative disease, without displaying cytoplasmic TDP-43 aggregates, suggesting that TDP-43 has toxic properties in the absence of aggregation (Wegorzewska et al. 2009). It is possible that pathological cytoplasmic TDP-43 and depletion of nuclear TDP-43 both contribute to the pathogenesis of IBM and similar neurodegenerative diseases.

The parallels between aberrant protein aggregates in IBM muscle fibres and accumulated proteins in other neurodegenerative diseases, such as in brain tissue from ALS, Alzheimer's and Parkinson's disease patients, suggest that similar pathogenic pathways may be involved (Askanas & Engel 2001; Askanas & Engel 2008). Impaired handling and degradation of unfolded or misfolded proteins may therefore be an important contributor to the aetiology and pathogenesis of IBM. This could in theory trigger the accompanying inflammation and thus be a potential therapeutic target. Thus, understanding the complex interactions of the proteostasis network is of great importance.

1.3. Protein homeostasis

Proteins are essential molecules, responsible for nearly all the biochemical processes taking place in cells. Maintaining protein homeostasis (proteostasis) and proteome integrity is fundamental for cellular health and function. Cells have developed a highly complex quality-control network to ensure proteome stability and to regulate the expression and degradation of proteins. As the specific biological functions of proteins are largely dependent on their correct folding into stable, three-dimensional conformations, this proteostasis network ensures that correct protein folding, processing and assembly/disassembly is maintained and any damaged or misfolded proteins are repaired or removed (Wolff et al. 2014). The proteostasis network is comprised of chaperone proteins, the heat shock response (HSR), the unfolded protein response (UPR) in the ER, the ubiquitin-proteasome system (UPS), the autophagy system and the mitochondrial UPR (**Fig. 1.3**; Chen et al. 2011; Kalmar & Greensmith 2017).

Image removed due to copyright

Figure 1.3. Cellular proteostasis

The diagram summarises the main cellular processes initiated by protein misfolding which include **(A)** chaperone-assisted protein refolding, **(B)** the unfolded protein response (UPR) in the endoplasmic reticulum (ER), **(C)** protein degradation via the ubiquitin-proteasome system (UPS) and autophagy-lysosome system, **(D)** mitophagy and the mitochondrial UPR (mtUPR) and **(E)** stress granule formation. Protein misfolding may occur as a result of exposure to various kinds of stress, including environmental factors, disease-causing mutations or ageing. Image used with permission from Kalmar & Greensmith (2017).

1.3.1. Stress granule formation

Stress granule formation is considered an early hallmark of stress. Upon exposure to stress, cells actively limit synthesis of non-essential “housekeeping” proteins in order to conserve energy and divert cellular resources toward survival and recovery. Non-translating mRNAs, translation initiation components and associated RNA-binding proteins are rapidly assembled into aggregate-like structures known as stress granules (Anderson & Kedersha 2002; Anderson & Kedersha 2006; Kedersha & Anderson 2007; Buchan & Parker 2009). This allows for the preferential synthesis of specific stress response proteins required to prevent the deleterious effects of the stress. Once the cellular stress condition has been resolved, cells can promptly resume protein synthesis and stress granules eventually disappear.

1.3.2. Chaperones and the heat shock response (HSR)

One of the key components of the protein quality control network, required for maintaining a functional proteome, are molecular chaperones. Molecular chaperones are a ubiquitous class of proteins which have a variety of important roles. These include stabilising and assisting folding of nascent polypeptide chains into native three-dimensional functional conformations, as well as facilitating intracellular protein transport, disaggregation and refolding of denatured or non-native proteins. Furthermore, chaperones aid proteolytic degradation via disassembly and unfolding of proteins (Young et al. 2004; Hartl & Hayer-Hartl 2009).

The expression of chaperone proteins is actively regulated in order to meet the demands of the cell. As proteins must retain conformational flexibility in order to function, conditions of cellular stress such as heat/cold shock, osmolality changes and pH fluctuation, can cause a disturbance of protein homeostasis. In this instance, molecular chaperones are transcriptionally upregulated in a process known as the heat shock response (HSR), an endogenous cytoprotective mechanism acting as a first line of defence to prevent protein aggregation under stressful conditions. These chaperones are known as heat shock proteins (HSPs) and are typically classified according to their molecular

weight, for example HSP40, HSP60, HSP70, HSP90, HSP100 and the small HSPs which have molecular masses of 12-43 kDa (Jee 2016).

The main component of the HSR is the transcription factor heat shock factor 1 (HSF1). Under normal non-stressful conditions, HSF1 exists in an inactive form in the cytosol, interacting with two major chaperone proteins, HSP70 and HSP90, which suppress the transcriptional activity. Upon exposure to stress, these HSPs bind to denatured proteins, releasing HSF1 from the chaperone complex. HSF1 translocates into the nucleus, where it trimerises and binds to the conserved promoter sequence of the 5' flanking region of HSP genes, the heat shock element (HSE). This activates transcription of HSPs that promote correct protein folding and degradation (Toko et al. 2008). The HSR therefore acts to prevent protein aggregation under stressful conditions and ameliorates the deleterious effects of cell stress (Brown 2007).

1.3.3. The unfolded protein response

The endoplasmic reticulum (ER) is a multifunctional organelle that has important roles in protein synthesis, namely of secretory and transmembrane proteins, lipid synthesis and additionally serves as a major store of intracellular calcium (Schwarz & Blower 2016). Roughly one-third of protein synthesis takes place in ER-associated ribosomes. These proteins are either embedded into the ER membrane or co-translationally transported to the ER lumen, where protein folding and post-translational modification takes place. Protein chaperones and folding enzymes facilitate this process and correctly assembled proteins are transported to the Golgi apparatus and then on to their final destinations. Proteins that fail to acquire a native conformation, either being incompletely folded or misfolded, are retained within the ER and eventually undergo ER-associated degradation (ERAD). ERAD is a tightly controlled process whereby these proteins are retrogradely translocated from the ER lumen to the cytosol for degradation by the 26S proteasome (Ruggiano et al. 2014).

It is vital for the ER to maintain the balance between protein load and folding capacity. Any disruption to protein homeostasis within the ER, including inactivation of ERAD, can result in an accumulation of misfolded and unfolded proteins in the ER lumen and membrane, leading to ER stress. This disruption

may be a consequence of any number of changes to the environment, including increased protein synthesis, expression of mutant proteins, environmental toxins, pathogens and viral infections, inflammatory stimuli and altered Ca^{2+} levels.

In an attempt to re-establish ER homeostasis under conditions of ER stress, the ER has its own stress response known as the unfolded protein response (UPR). The UPR is a collection of three parallel signalling pathways, mediated by inositol-requiring transmembrane kinase/endonuclease 1 (IRE1), pancreatic ER kinase (PERK) and activating transcription factor 6 (ATF6). Under normal conditions, the ER chaperone immunoglobulin heavy-chain binding protein (BiP), a member of the HSP70 family, negatively regulates IRE1, PERK and ATF6. However, upon binding of unfolded or misfolded proteins to BiP, these transducers are released, initiating a complex downstream intracellular signalling pathway that helps restore normal function to the ER. This is by means of a transient inhibition of protein translation, increased degradation of misfolded proteins via ERAD and upregulation of ER chaperone proteins to facilitate the protein folding capacity (Kaufman 1999; Mori 2000; Travers et al. 2000). Under conditions of excessive and prolonged ER stress due to the failure of the UPR to re-establish homeostasis, the UPR initiates apoptosis, namely mediated by CCAAT/enhancer binding protein homologous protein (CHOP) and c-Jun N-terminal Kinase (JNK) (Wu & Kaufman 2006; Tabas & Ron 2011). In addition, apoptosis may also be mediated via a mitochondrial-dependent pathway caused by Ca^{2+} efflux from the ER (Nutt et al. 2002; Scorrano et al. 2003). ER stress has also been shown to initiate the activation of NF- κ B and TNF- α and an associated inflammatory response (Zhang & Kaufman 2008).

1.3.4. The ubiquitin-proteasome system (UPS)

In order to maintain the balance of protein homeostasis, it is important that damaged or misfolded proteins are removed and recycled. There are two distinct pathways which mediate protein degradation, the ubiquitin-proteasome system (UPS) and the autophagy-lysosomal system.

The UPS is responsible for the removal of short-lived, damaged and misfolded proteins, as well as proteins exported from the ER. This system is a multistep process in which proteins are first tagged by ubiquitin proteins and then targeted to a large proteolytic complex, called the proteasome, for degradation. Ubiquitin is a small globular protein (8.5 kDa) which covalently attaches to substrate proteins in a rapid, precise and reversible manner. Not all proteins require ubiquitination in order to be degraded by the proteasome, however. Proteins can be tagged with varying lengths of ubiquitin chains, or may even be monoubiquitinated with a single ubiquitin tag.

Once tagged, substrate proteins are targeted to the 26S proteasome. The 26S proteasome is a large, highly conserved ATP-dependent multisubunit protease complex, composed of a 19S regulatory subunit and a 20S catalytic core. The 19S particle is responsible for recognising, binding and unfolding polyubiquitinated proteins and contains deubiquitinating enzymes that mediate the disassembly of ubiquitin chains from substrate proteins. This allows free ubiquitin to be recycled and maintains a sufficient pool of free ubiquitin in cells. The polypeptide chains are translocated to the 20S particle, which contains six active proteolytic sites, where they are cleaved into shorter peptides (Kisselev et al. 1999; Bhattacharyya et al. 2014). These peptides are released from the proteasome and are rapidly processed into amino acids by cytosolic endopeptidases and aminopeptidases and recycled for synthesis of new proteins (Reits et al. 2003).

1.3.5. Autophagy

Autophagy is the process of 'self-eating' in which cells digest and recycle their own cytoplasmic components within lysosomes. Whilst chaperone proteins and the UPS typically handle abnormal soluble proteins, autophagy is mainly responsible for the degradation of longer-lived, structural proteins and obsolescent cellular organelles. Damaged or misfolded proteins and small aggregates that have not been degraded by the UPS are also degraded via autophagy.

There are three main subtypes of autophagy; macroautophagy, microautophagy, and chaperone-mediated autophagy (Boya et al. 2013; Nikolettou et al. 2015). Macroautophagy involves the formation of a membrane, known as a phagophore that surrounds and sequesters cytosolic substrates to form a double-membrane autophagosome. The autophagosome fuses with lysosomes, forming an autolysosome, in which proteolytic breakdown of the isolated materials occurs (Yang & Klionsky 2010). In microautophagy, cytosolic proteins are engulfed by invaginations of the lysosome membrane itself. These vesicles pinch off into the lumen of the lysosome where they are degraded. This type of autophagy has been described in yeast, but has not yet been well characterised in mammalian cells (Li et al. 2012). In chaperone-mediated autophagy, the chaperone protein heat shock cognate 70 (HSC70) forms a complex with a specific subset of cytosolic proteins by a recognition motif in their amino acid sequences and targets them to the lysosome. The substrate-chaperone complex is targeted to the lysosome, where it binds to the lysosome-associated membrane protein (LAMP)-2A receptor on the lysosomal membrane. The substrate proteins are unfolded and subsequently undergo translocation into the lumen of the lysosome for degradation by a lysosomal form of HSC70 (Bandyopadhyay & Cuervo 2008; Cuervo & Wong 2014).

1.3.6. The mitochondrial unfolded protein response

The maintenance of mitochondrial integrity is also a key aspect in ensuring the viability of cells. Mitochondria have their own protein quality control machinery, present within each sub-compartment. This ensures the balance between folding load and chaperone abundance is controlled and protects the mitochondrial proteome against protein misfolding and other stress conditions within the mitochondrial matrix, such as oxidative stress.

Although human mitochondria have their own genome (mtDNA), it encodes only 13 proteins of the total mitochondrial proteome. These 13 proteins are all core components of oxidative phosphorylation. The majority of the mitochondrial proteome (~1500 proteins) is encoded by nuclear genes and is synthesised in the cytosol (Calvo & Mootha 2010; Bragoszewski et al. 2017). Mitochondria thus have sophisticated mechanisms to efficiently import these unfolded nuclear-encoded mitochondrial proteins into the organelle and rely on members

of the heat shock family, HSP70 and HSP90, to guide them to the outer mitochondrial membrane. An additional set of chaperones, namely HSP60 associated with HSP10, as well as the mitochondrial HSP70 and the mitochondrial HSP90 analogue TRAP1, are involved in the final folding phase of these proteins (Chacinska et al. 2009).

In order to cope with increased unfolded protein load under stress conditions, mitochondria have evolved a mitochondrial unfolded protein response (mtUPR) which aims to re-establish protein homeostasis within the mitochondria. This is regulated by the transcription factor CHOP and results in a signal transduction pathway between mitochondria and the nucleus and the induction of mitochondrial protective genes, including mitochondrial molecular chaperones and proteases. The mtUPR also leads to transcriptional repression of a number of nuclear genes, in order to reduce the load of protein misfolding (Münch & Harper 2016).

High levels of unfolded proteins in the mitochondrial matrix can also lead to the accumulation of the PINK1 kinase on the outer mitochondrial membrane, resulting in the selective degradation of mitochondria by autophagy, termed mitophagy (Pellegrino & Haynes 2015). Normally, PINK1 is imported into mitochondria where it is processed and ultimately degraded by mitochondrial and cytosolic proteases and thus PINK1 levels remain very low or undetectable. However, during mitochondrial stress when there is an overexpression of misfolded mitochondrial proteins or depletion of the mitochondrial inner membrane potential, PINK1 fails to cross the inner membrane. PINK1 accumulates on the outer membrane, where it recruits PARK2 specifically to the damaged mitochondrion, leading to the induction of PARK2/Parkin-mediated clearance by the autophagy-lysosomal pathway.

Interestingly, a recent study has demonstrated that non-mitochondrial related, disease-causing, aggregation-prone proteins are actively sequestered within mitochondria in yeast, which suggests that mitochondria may also play a role in the maintenance of cytoplasmic proteostasis (Ruan et al. 2017). The import of aggregated proteins was found in both the inter-membrane space and the mitochondrial matrix. This has been proposed to be a compensatory

mechanism for a defective protein chaperone system, as impairment of HSP70 levels lead to an increase in the uptake of misfolded proteins to mitochondria. The study also showed that unstable aggregation-prone cytosolic proteins are imported into mitochondria in human cells, although how misfolded proteins are transported from the cytoplasm into the mitochondria remains unclear.

1.4. Protein homeostasis and ageing

The fate of proteins over their lifetime can be influenced by a number of adverse extrinsic factors, including exposure to stress, or unique metabolic challenges such as ageing. As non-native proteins are prone to aggregation due to hydrophobic residues exposed on their surfaces, any impairment or overloading of protein quality control mechanisms within the proteostasis network can lead to the accumulation of misfolded proteins and cellular dysfunction (Stirling et al. 2003). Proteostasis is thought to decline over time in most tissues and as a result, cells are at a greater risk of protein misfolding and aggregation with increasing age (Cuervo & Dice 2000; Balch et al. 2008).

Disruption of proteostasis is implicated in a number of neurodegenerative diseases, including ALS, Alzheimer's, Parkinson's and Huntington's disease, which are all characterised by the accumulation of specific misfolded proteins (Chiti & Dobson 2006; Douglas & Dillin 2010; Yerbury et al. 2016; Webster et al. 2017; Reisz et al. 2018). Like IBM, these diseases are typically considered late-onset diseases, highlighting ageing as a common risk factor. Indeed, in IBM, it has been proposed that ageing may have a significant influence on the accumulation of protein aggregates and on muscle fibre damage (Askanas et al. 2015). However, the mechanisms behind the age-associated decline in protein homeostasis are still unclear. A reduction in components of the proteostasis network or defects within the various processes could be responsible. On the other hand, the physical properties of the proteins themselves may undergo changes which could, for example, reduce their solubility and make them more prone to aggregation (David et al. 2010). Understanding the reasons for the gradual failure of the proteostasis network in ageing and disease is of great importance if the cause of IBM and similar protein misfolding diseases is to be established and new, beneficial therapeutics are to be developed.

Emerging evidence from various aged animal models suggests that the HSR declines with age, with impaired activation of HSF1 and a diminished HSP induction evident in cells and tissues (Fagnoli et al. 1990; Blake et al. 1991; Heydari et al. 1993; Locke & Tanguay 1996; Rao et al. 1999; Hall et al. 2000; Heydari et al. 2000; Rea et al. 2001; Singh et al. 2006). As this system is responsible for maintaining a functional proteome under stressful conditions, any disruption of other quality control pathways within the proteostasis network could be further exacerbated by the reduced ability of cells to mount a robust HSR. However, contrasting data have shown that HSF1 activation and HSP72 accumulation does not differ between fast and slow skeletal muscle from adult and aged rats, after whole-animal heat shock (Locke 2000). In addition, an increase in muscle-specific small HSPs has been observed in the gastrocnemius muscles of aged rats (Doran et al. 2007). It is possible that the ability of cells to mount a HSR may be tissue-specific and further investigation is therefore required to elucidate the relationship between the chaperone network and ageing.

As with the HSR, research points to an age-associated decline in ER stress response mechanisms and a change in the balance between the adaptive and apoptotic responses (Ben-Zvi et al. 2009; Brown & Naidoo 2012). Studies in rodents have shown that the expression and efficacy of BiP and other chaperones declines with age in a number of tissues, including brain, lung, liver, kidney, heart and spleen (Rabek et al. 2003; Erickson et al. 2006; Paz Gavilán et al. 2006; Hussain & Ramaiah 2007; Naidoo et al. 2008). However, little is known on the effect of ageing on ER stress and the UPR in skeletal muscle.

Skeletal muscle has an extensive network of specialised ER, known as the sarcoplasmic reticulum (SR), which has an important role in regulating calcium release and reuptake required for myofibrillar contraction. Impaired function of the SR is thought to be implicated in ageing and is associated with increased ER stress (Russ et al. 2012; Russ et al. 2014). For example, expression of CHOP in both the soleus and tibialis anterior (TA) muscles of old rats at 29 months has been shown to be higher compared to adult rats at 9 months (Baehr et al. 2016). Research suggests that UPR activation due to ER stress within muscle may have opposing effects. Low levels of ER stress play a role in

regulating skeletal muscle growth, regeneration and adaptation to external physiological changes (Bohnert et al. 2017). However, chronic ER stress and UPR-mediated cell death is thought to be a factor in a number of degenerative diseases, including IBM, myasthenia gravis, DMD, Alzheimer's and Parkinson's disease (Iwasa et al. 2014; Ogen-Shtern et al. 2016). As the UPS is also responsible for degrading proteins retrotranslocated from the ER, disruption to this system can also cause ER stress.

There is conflicting evidence as to what impact ageing has on the functioning of the UPS. A decrease in proteasome activity in ageing has been reported in a number of different models, including yeast, *Drosophila*, rodents and human fibroblasts (Hayashi & Goto 1998; Keller et al. 2000; Chen et al. 2004; Hwang et al. 2007; Vernace et al. 2007; Dasuri et al. 2009), as well as in a variety of cell types, including skeletal muscle (Radák et al. 2002; Husom et al. 2004; Ferrington et al. 2005; Selsby et al. 2005). In mice, knock-down of proteasome activity decreases lifespan (Zetterberg et al. 2007; Tomaru et al. 2012; Li et al. 2013), whilst activating the UPS using genetic or chemical manipulation extends the lifespan of yeast, *C. elegans* and *Drosophila* (Chen et al. 2006; Tonoki et al. 2009; Kruegel et al. 2011; Vilchez et al. 2012; Chondrogianni et al. 2015). Moreover, restoring proteasome function in fibroblasts obtained from elderly donors has been shown to delay senescence (Hwang et al. 2007). Fibroblast cultures from healthy centenarians also appear to have a more active proteasome, comparable to younger control fibroblasts (Chondrogianni et al. 2000). In rats, ageing has been associated with an increase of 26S proteasomes in skeletal muscle (Altun et al. 2010). In further support of these data, increased 20S proteasomal activity has been observed in fibroblasts obtained from primates of longer-lived species compared to shorter-lived species (Pickering et al. 2015). However, in the same study, 26S proteasome activity was not linked to lifespan. Furthermore, in skeletal muscle from healthy male individuals age is not associated with proteasome activity (Bossola et al. 2008). The reasons for such differences between these studies may relate to tissue-specific differences, as well as lack of distinction between activity of the 20S and 26S proteasomes.

An increase in misfolded and accumulated proteins, either due to a decline in proteasome function or due to other stressors, leads to a greater need for autophagic degradation. Impairment of autophagy and lysosome function has been reported to play a role in the pathogenesis of a number of late-onset neurodegenerative diseases (Sridhar et al. 2012; Nixon 2013; Nah et al. 2015). Reports of an age-related decline in lysosome function and autophagy are abundant, with reduced levels of autophagy markers reported in human and mouse brain tissue from elderly subjects, as well as senescent human fibroblasts (Lipinski et al. 2010; Rubinsztein et al. 2011; Yang et al. 2014; Ott et al. 2016). A decrease of the autophagy-related (ATG) protein ATG7 has been observed in both aged mice and in muscle biopsies from elderly subjects (Carnio et al. 2014). Moreover, mutations in ATG genes, core regulators of autophagy, lead to reduced lifespan in a number of *in vivo* models, including *C. elegans*, *Drosophila* and mice (Meléndez et al. 2003; Hara et al. 2006; Juhász et al. 2007). ATG5 mutant *Drosophila* and ATG7 mutant mice additionally develop cytoplasmic inclusions, accompanied by neurodegeneration (Hara et al. 2006; Juhász et al. 2007). ATG7-deficient mice additionally display degeneration of neuromuscular junctions (NMJ) and reduced muscle function and have a shortened lifespan. Rescuing ATG7 and autophagy improves NMJ morphology and leads to increased muscle mass (Carnio et al. 2014). A number of other studies also suggest that activating or restoring autophagy can restore function in various organs, including the heart, liver and muscle and promote longevity (Zhang & Cuervo 2008; Demontis & Perrimon 2010; Pyo et al. 2013; Shirakabe et al. 2016).

1.5. Protein homeostasis in IBM

It is clear that disruption of proteostasis pathways and the gradual accumulation of proteome damage is implicated in the pathogenesis of a number of age-related neurodegenerative diseases (Ross et al. 2015). There is also evidence to suggest that impaired protein homeostasis plays a role in IBM aetiology.

One of the key hallmarks of IBM is the presence of ubiquitinated inclusions within muscle fibres, which suggests that protein activity is compromised in the muscle of IBM patients. The accumulation of the shuttle proteins p62 and neighbour of BRCA1 gene 1 (NBR1), which are responsible for transporting

poly-ubiquitinated proteins for degradation, in IBM muscle fibres is evidence of inhibited proteasome or lysosome function (Nogalska et al. 2009; D'Agostino et al. 2011). Indeed, significant proteasomal abnormalities have been reported in IBM, including abnormal proteasomal accumulations within muscle that colocalise with proteins such as A β , p-tau, ubiquitin, HSP70 and other abnormal protein aggregates, increased expression of 26S proteasome subunits and reduced activities of the three major proteasomal proteolytic enzymes, trypsin-like (TL), chymotrypsin-like (CTL), and peptidyl-glutamyl-peptide hydrolytic (PGPH) enzymes (Ferrer et al. 2004; Fratta et al. 2005). On the other hand, the accumulation and aggregation of damaged and misfolded proteins can itself directly impair proteasome function (Bence et al. 2001).

In addition to these findings, there is increasing evidence of a link between A β PP/A β and impaired proteasomal activity (Ferrer et al. 2004). *In vitro*, A β PP/A β causes proteasome inhibition and the induction of aggresome formation in APP-overexpressing cultured human muscle fibres (Fratta et al. 2005; Oddo 2008). In addition, a significant decrease in proteasome activity has been found in rodent myotube cultures overexpressing human β -APP, an *in vitro* model of IBM (Ahmed et al. 2016). Other factors which have been proposed to be responsible for inhibition of proteasome function in IBM include oxidative stress and the accumulation of reactive oxygen species (ROS) alongside ageing, which could potentially impair the structure of proteins and the quality of the proteome (Askanas et al. 2012, 2015).

In IBM skeletal muscle biopsies, as well as increased expression of HSP70 and HSP90 in aggregates (De Paepe et al. 2009), there is an increase in the three main UPR transcription factors activated in response to ER-stress. An increase in ATF4 protein and spliced XBP1, as well as increased cleavage of ATF6 have been reported (Nogalska et al. 2015). Additionally, increased eIF2 α phosphorylation has been observed in IBM muscle samples, in addition to elevated levels of ER stress-inducible proteins, such as calnexin, calreticulin, BiP, GRP94, ERp72, HERP and CHOP which colocalise with A β protein in muscle fibres (Vattemi et al. 2004; Nogalska et al. 2006; Amici et al. 2017). Although further investigation is required into the effect of prolonged ER stress on myofibre viability, the UPR is a potential contributor to IBM pathogenesis.

Relatively few studies have investigated the involvement of autophagy in the pathogenesis of IBM. The presence of rimmed vacuoles containing various proteins including A β , α -syn, BACE1 and tau in IBM muscle is thought to be linked to an impaired autophagy, caused by failure of lysosomes to clear accumulated substrates (Suzuki et al. 2002; Nogalska, D'Agostino, Engel et al. 2010; Lee et al. 2012). Increased expression of lysosome-related proteins, at the mRNA and protein levels, have been reported in skeletal muscle of IBM patients (Kumamoto et al. 2004). However, although the major lysosomal enzymes cathepsin D and B are increased, the activity of these enzymes has been reported to be reduced by as much as 40-60% (Nogalska D'Agostino, Terracciano & Engel 2010). In addition, LC3-II, an autophagosome marker, is upregulated in IBM muscle, indicating increased autophagosome formation and maturation (Nogalska, D'Agostino, Terracciano & Engel 2010). Components of the chaperone-mediated autophagy pathway have also been reported to be increased in IBM muscle (Cacciottolo et al. 2013). However, despite these observations pointing to impairment of the lysosomal degradation pathway, relatively little is known about how autophagy may contribute to protein aggregation in IBM muscle fibres and further work is required to address this.

1.6. Upregulation of the HSR with Arimoclomol

The pathogenesis of IBM is complex and there are numerous unanswered questions relating to the failure of protein homeostasis pathways to degrade or remove misfolded or damaged proteins which accumulate in IBM, the interaction between these pathways and the potential toxicity of accumulated proteins. However, there is strong evidence to suggest a role of disrupted protein handling in the disease progression. Maintaining the balance of proteostasis is fundamental for ensuring cellular function and survival. Restoring the balance of protein homeostasis, by reducing protein overload and the subsequent accumulation and aggregation of misfolded proteins, could therefore be a potential therapeutic strategy for IBM.

Previous work from the Greensmith lab has investigated the effects of a novel compound called Arimoclomol. Arimoclomol is a hydroxylamine derivative that co-induces the HSR in the presence of stressful stimuli, by prolonging the activation of HSF1, thus augmenting upregulation of HSPs. Importantly, under

unstressed conditions, Arimoclomol does not induce HSP expression and is therefore considered to be a co-inducer of the HSR (Hargitai et al. 2003). Arimoclomol has been shown to have potential therapeutic benefit in several mouse models of neurodegeneration. In the SOD^{G93A} mouse model of ALS, Arimoclomol prolongs lifespan and improves motor neuron survival, when given both pre-symptomatically and after symptom onset (Kieran et al. 2004; Kalmar et al. 2008). Arimoclomol has also been shown to delay disease progression in a transgenic mouse model of spinal and bulbar muscular atrophy (SBMA), in which protein aggregation is also a key characteristic (Malik et al. 2013).

A number of early clinical trials have since been conducted testing Arimoclomol in ALS (Cudkowicz et al. 2008; Lanka et al. 2009) and the therapeutic potential of this drug is currently under investigation. A recent Phase II trial for ALS patients with $SOD1$ mutations has reported that Arimoclomol is safe and well-tolerated, with preliminary evidence to suggest potential efficacy (Benatar et al. 2018). It is therefore possible that upregulating the HSR with Arimoclomol may also be beneficial in IBM, by working to reduce protein mishandling and aggregation.

1.7. The effects of Arimoclomol in *in vitro* models of IBM

In order to assess the effects of upregulating the HSR with Arimoclomol in IBM, Dr Mhoriam Ahmed and Dr Adrian Miller from the Greensmith lab developed *in vitro* models of the disease (Ahmed et al. 2016). Primary rat myoblast cultures were transfected with β -APP or exposed to inflammatory mediators (IL-1 β or TNF α), thus modelling the two major aspects of IBM, degeneration and inflammation. Both approaches resulted in the development of IBM-like pathological characteristics in the muscle cells, including TDP-43 mislocalisation, MHC-I upregulation and cell death. Arimoclomol treatment significantly improved cell survival and attenuated cellular pathology in these models (**Fig. 1.4**). In addition, both these models induced NF- κ B activation, indicated by nuclear translocation of the NF- κ B subunit p65. This effect was inhibited by Arimoclomol. Arimoclomol also reduced the level of ER stress induced in both the β -APP and inflammatory cell models, by restoring ER calcium ion homeostasis. These findings therefore established a beneficial effect of Arimoclomol in *in vitro* models of IBM.

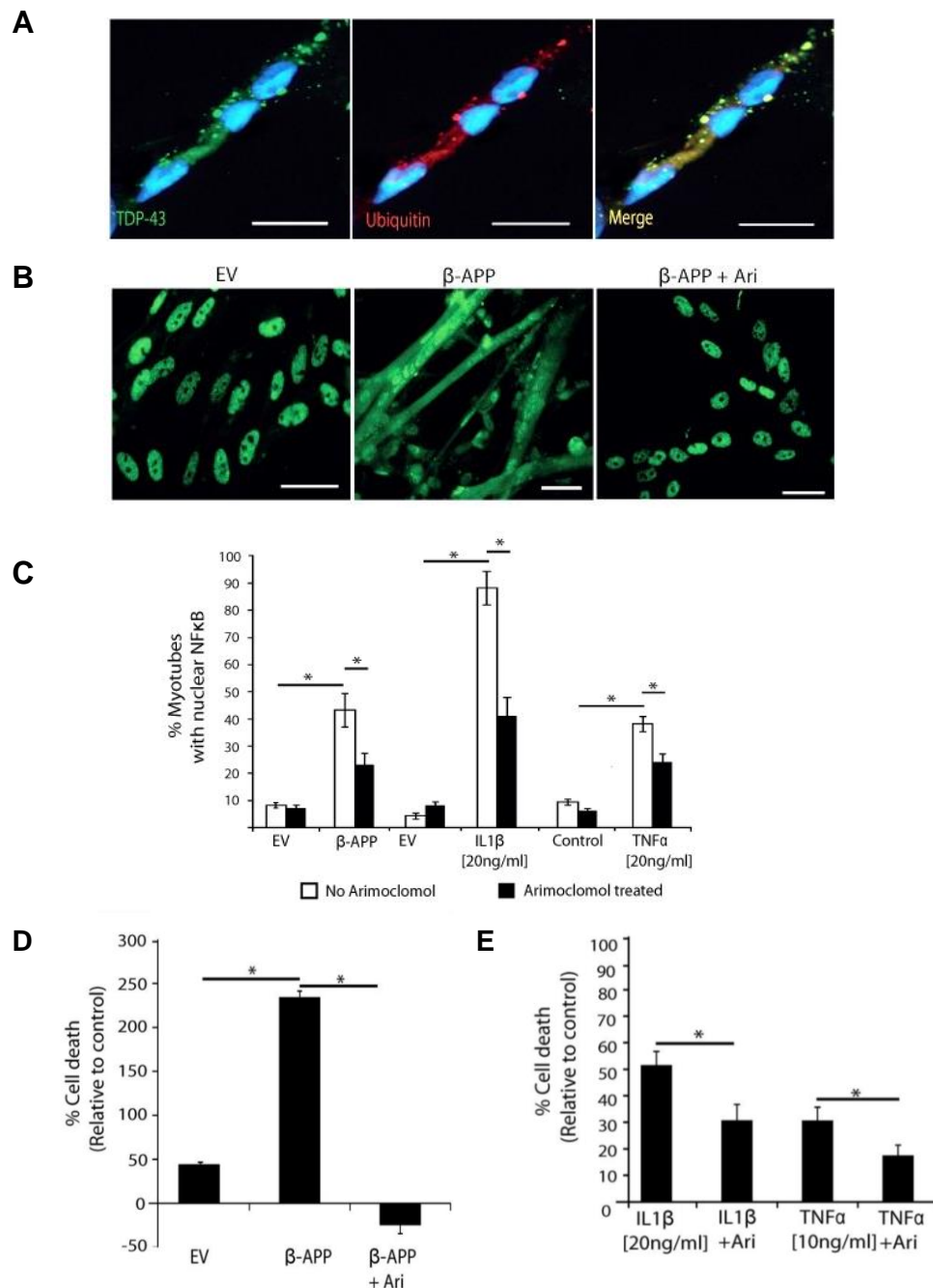


Figure 1.4. Arimoclomol treatment ameliorates IBM-like pathology *in vitro* in primary rat myocyte cultures overexpressing β -APP or exposed to inflammatory mediators

(A) Representative images of rat myocytes transfected with full-length human β -APP showing the formation of cytoplasmic inclusion bodies immunopositive for TDP-43 (green) and ubiquitin (red), costained with the nuclear marker DAPI (blue). Arimoclomol treatment attenuates TDP-43 mislocalisation (B), significantly reduces the percentage of rat myocytes with nuclear NF- κ B subunit p65 (C) and reduces cell death, as demonstrated in a LDH cell-survival assay in rat myocytes transfected with β -APP (D) or exposed to inflammatory mediators (E). Scale bars represent 20 μ m. * $p < 0.05$; one-way ANOVA, $n = 3$. Adapted from Ahmed et al. (2016). Reprinted with permission from AAAS.

1.8. Examining the effects of Arimoclomol in additional models of IBM

Since data from these *in vitro* studies showed that Arimoclomol ameliorates key pathological markers in cellular models of IBM, one of the main aims of this Thesis was to investigate whether these findings could be replicated *in vivo*, in a more physiologically relevant model. Since IBM is a sporadic condition however, with no genetic cause, it is not possible to directly model this condition in mice. For this reason, we obtained a mouse model of the degenerative disorder multisystem proteinopathy (MSP) which is caused by mutations in the *VCP* gene. This is a dominantly inherited disorder with a phenotype that includes inclusion body myopathy, Paget's disease of bone and frontotemporal dementia, therefore also known as IBMPFD (Custer et al. 2010; Taylor 2015). *VCP* belongs to the type II AAA+ (ATPases associated with diverse cellular activities) family of proteins and has an important role in regulating protein degradation via the proteasome and autophagy-mediated pathways (Ju & Weihl 2010; Nalbandian et al. 2011). Transgenic mice overexpressing a mutant form of the human *VCP* (amino acid changes of A232E) have been reported to display many aspects of the human disease (Custer et al. 2010). This mouse model, described in greater detail in Chapter 3, is an important tool in advancing the understanding of the pathology and molecular pathomechanisms of IBM, as well as enabling us to examine the effects of upregulating the HSR with Arimoclomol *in vivo*.

In addition, to establish whether these pathological findings are reproduced in a more clinically relevant, human model of IBM, dermal fibroblasts were obtained from patients with sporadic IBM or MSP patients expressing mutant *VCP*, presenting with an inclusion body myopathy. These findings are described in detail in Chapters 4 and 5 of this Thesis.

1.9. Aims of this Thesis

The experiments presented in this Thesis were undertaken in order to test the hypothesis that targeting of the degenerative features of IBM would ameliorate disease pathology. Specifically, the effects of upregulation of the HSR, a cytoprotective protein chaperone response, were examined both *in vivo*, in mutant VCP mice and *in vitro*, in patient-derived fibroblasts, in order to assess whether this may be an effective therapeutic strategy for the treatment of IBM.

The specific aims of this Thesis were:

- (1) To characterise the histopathological features of muscle in a transgenic mutant VCP mouse model of MSP and examine the effects of Arimoclomol on muscle histopathology, in a preclinical trial for IBM.
- (2) To characterise the inherent cellular pathology in fibroblasts from sporadic IBM patients and examine the effects of Arimoclomol treatment.
- (3) To characterise the inherent pathology in fibroblasts from MSP patients carrying pathogenic VCP mutations and examine the effects of Arimoclomol treatment.

Chapter 2

Materials and methods

2.1. Breeding and maintenance of mice

All experimental work was carried out by Charlotte Spicer and Dr Mhoriam Ahmed (UCL Institute of Neurology, UK) under licence from the UK Home Office (Scientific Procedures Act 1986) and was approved by the Animal Welfare and Ethical Review Board of UCL Institute of Neurology. Transgenic mice overexpressing the wild-type or mutant (A232E) human VCP gene under the cytomegalovirus (CMV)-enhanced chicken beta-actin were obtained from Dr J. Paul Taylor (St Jude Children's Research Hospital, Memphis, TN, USA; Custer et al. 2010). Transgenic female mice carrying the wild-type or mutant gene were mated with wild-type C57BL/6J males to generate transgenic and non-transgenic littermates. Only male offspring were used in this study to prevent gender differences. All mice, including controls, were littermates and were housed in a temperature and humidity controlled environment maintained on a 12-h light/dark cycle. Food and water were provided *ad libitum*. Wild-type VCP (WT-VCP) mice were used as a transgenic control for mutant VCP mice. A timeline of the analyses described below is given in **Fig. 2**.

2.2. PCR genotyping

Offspring were genotyped to identify transgenic and wild-type mice by polymerase chain reaction (PCR) amplification of DNA extracted from ear biopsies, vortexed in 50 μ L of rapid digest buffer (10 mM Tris-HCl pH 8.3, 50 mM KCl, 0.1 mg/ml Gelatin, 0.45 % NP40, 0.45% Tween-20) and 2 μ L of proteinase K (20 mg/ml, Invitrogen) and digested at 55 °C (5 mins) and then at 95°C (10 mins). Digested samples were centrifuged at 15996 x g for 2 minutes. PCR amplification was achieved using forward (CAACGTGCTGGTTGTTGTG) and reverse (AAGGACGATGCAAACAGCTT) primers. Each PCR reaction mix was made up of 11.5 μ l of sterile water, 2.5 μ l of 10X PCR buffer (Invitrogen), 0.75 μ l of 50 mM MgCl₂ (Invitrogen), 0.7 μ l of 10mM dNTP mix (Promega), 1 μ l of each primer pair, 5 μ l of 5M betaine solution (Sigma-Aldrich), 0.5 μ l of recombinant Taq polymerase (Invitrogen) and 2.5 μ l of genomic DNA. Cycling conditions were as follows: 94°C (5 mins); 94°C (30 secs), 55°C (45 secs), 72°C (30 secs) for 35 cycles; 72°C (7 mins). BlueJuice™ Gel Loading Buffer (Invitrogen) was added and PCR products run on a 2% agarose gel in Tris-Borate-EDTA (TBE) buffer for 25 minutes at 65 V. Bands were visualised using GelRed™ nucleic acid stain (Biotium) and GeneSnap software (Syngene).



Figure 2. Timeline of mouse *in vivo* studies and Arimoclomol treatment

Mice were genotyped and split into appropriate treatment groups at time of weaning (WT, WT-VCP, mutant VCP, mutant VCP+Ari; 15 animals per group). Mice were treated with Arimoclomol continually from 4 months of age. Body weight and grip strength (longitudinal analysis) of all mice were measured fortnightly from 4-14 months of age. *In vivo* assessment of muscle function (terminal analysis) was performed in all mice at 14 months of age, after which mice were culled. Both hindlimb TA muscles were snap frozen for immunohistochemical studies and western blot analysis.

2.3. Arimoclomol treatment regime

The Arimoclomol used in this study was provided as a gift to Prof Greensmith by Biorex R&D or as part of a Research Agreement by Orphazyme Aps. Wild-type and mutant VCP mice were treated with either Arimoclomol or vehicle (water). Following genotyping, mice were randomly divided into the following treatment groups: (i) Non-transgenic wild-type mice treated with water alone (WT) (ii) Transgenic wild-type mice treated with water alone (WT-VCP) (iii) A232E mutant VCP mice with water alone (mutant VCP) (iv) A232E mutant mice treated with 120mg/kg/day Arimoclomol (mutant VCP + Ari). Arimoclomol was diluted in drinking water and mice were treated from 4 months of age (start of symptomatic stage) to time of examination. The body weight of all mice was recorded fortnightly and Arimoclomol dose adjusted accordingly. Mice were followed to 14 months of age, as the end stage of these mice has previously been reported to be 15 months (Custer et al. 2010). All experiments were undertaken blinded to genotype and treatment.

2.4. Longitudinal assessment of grip strength and body weight

Grip strength analysis was carried out by Dr Mhoriam Ahmed. Mice were monitored for signs of muscle weakness by analysis of hindlimb grip-strength. Grip strength was measured fortnightly from 4-14 months of age in all mice, along with body mass. Briefly, mice were placed on a horizontal metal grid and then pulled by the tail. The peak amount of force required to make a mouse release its grip was measured using an automated grip strength meter (Bioseb Grip strength meter). The ratio of grip strength:body mass was determined for individual animals and pooled by each genotype.

2.5. *In vivo* analysis of isometric muscle force

In vivo assessment of muscle function was carried out by Dr Mhoriam Ahmed. Mice were deeply anaesthetised with 1.5-2.0% isoflurane in oxygen delivered through a Fortec vapouriser (Vet Tech Solutions Ltd.). The distal tendons of the tibialis anterior (TA) and the extensor digitorum longus (EDL) muscles in both hindlimbs were exposed and dissected free of other tendons before being attached by silk thread to isometric force transducers (Dynamometer UFI Devices). The sciatic nerve was exposed and sectioned, and all branches were

cut except for the deep peroneal nerve that innervates the TA and EDL muscles. Muscle length was adjusted for maximum twitch tension and muscles and nerves were kept moist with saline throughout the recordings. All experiments were carried out at room temperature (23°C). Isometric contractions were elicited by stimulating the nerve to the TA and EDL muscles using square-wave pulses of 0.02-ms duration at supramaximal intensity, using silver wire electrodes. Contractions were elicited by trains of stimuli at frequencies of 40, 80, and 100 Hz for 450 ms. The maximum twitch and tetanic tension were measured using force transducers connected to a PicoScope 3423 oscilloscope (Pico Technology) and subsequently analysed using PicoScope software v5.16.2 (Pico Technology).

2.6. Removal and storage of mouse hindlimb muscles

Mice were culled at 14 months of age using terminal anaesthesia (pentobarbitone or isoflurane). One TA muscle was removed per animal and embedded in OCT, before being frozen in isopentane chilled in liquid nitrogen and stored at -80°C before use. Transverse muscle sections were cut at 12 µm thickness using a Bright OTF refrigerated cryostat (Bright Instruments) and mounted onto Polysine™ glass slides (VWR), before being stored at -20°C for future histochemical and immunofluorescence analysis. Contralateral TA muscles were removed and snap-frozen in liquid nitrogen and stored at -80°C for use in western blot experiments.

2.7. Histochemistry and immunostaining

Transverse cryosections were obtained from TA muscles as described in section 2.6. Haematoxylin and Eosin (H&E) staining was performed using routine methods. Briefly, slides were immersed in Harris Haematoxylin (2 mins), washed with distilled water, immersed in Eosin (2 mins) and washed again in distilled water. Slides were then dehydrated with alcohol and cleared in histoclear (1 min). Slides were mounted with DPX mounting medium.

For immunofluorescent labelling, slide-mounted sections were incubated for 1 hour at room temperature in blocking buffer containing 1X phosphate buffer saline (PBS; Thermo Fisher Scientific), 0.1% Triton X-100 (Sigma-Aldrich) and

10% normal goat serum (Vector Laboratories, Inc.). Sections were washed with PBS and then incubated for 1 hour at room temperature with the appropriate primary antibodies. The specific antibodies used are detailed in the methods section of Chapter 3. Sections were washed in PBS and incubated for 2 hours at room temperature with the appropriate fluorescently labelled secondary antibodies (goat anti-rabbit/mouse Alexa568 or goat anti-rabbit/mouse Alexa488; 1:500; Invitrogen) and 4', 6-diamidino-2-phenylindole (DAPI; 1:1000; 1 mg/ml stock solution; Sigma-Aldrich) to label nuclei. For mouse antibodies, biotinylated goat anti-mouse IgG secondary antibody (1:200; Vector Laboratories) was used followed by Texas Red® Avidin D (1:200; Vector Laboratories) and (DAPI; 1:2000). Sections were washed again and then mounted onto glass slides with fluorescence mounting medium (Dako). Appropriate negative controls were also carried out in parallel for all experiments, in which primary antibodies were omitted to check specificity of binding of the secondary antibody.

All sections were visualised under a Leica DMR microscope and analysed using Leica Application Suite software (Leica Microsystems). Images were captured at 20x (approximately 50-125 fibres per image) and 40x magnifications.

2.8. Muscle fibre area measurements

Muscle fibre area measurements were undertaken by Dr Mhoriam Ahmed. Transverse cryosections were obtained from TA muscles as described in section 2.6. One section per mouse, from the centre of one TA muscle, was stained for succinate dehydrogenase activity (SDH) according to published protocol (Kieran & Greensmith 2004), in 3 animals per experimental group. A single image of the entire TA muscle was taken per mouse at 2.5x magnification (approximately 2000-2500 fibres). Using a Wacom graphics tablet and pen, the perimeter of every fibre in the muscle was measured. ImageJ software (National Institutes of Health) was used to record and analyse the data.

2.9. Analysis of centralised nuclei

Transverse cryosections were obtained from TA muscles as described in section 2.6. One section per mouse, from the centre of one TA muscle, was stained with DAPI (1:1000; 1 mg/ml stock solution), in 3 animals per group. Five images of randomly selected areas were taken at 20x magnification (approximately 50-125 fibres per image), using a Leica Microscope. For each image, the percentage of fibres with centralised nuclei was manually quantified. Cells were excluded from the counts if less than 75% of the cell area was visible in the image being analysed. An average was then taken for each animal and each experimental group. In all cases, cell counts were performed blind to the treatment condition of the animal from which the muscle had been obtained.

2.10. Western blots (mouse tissue)

Western blot analysis was carried out on one TA muscle from 3 animals per experimental group, as a minimum of 3 repeats was required for scientific significance. Tissue homogenates from isolated TA muscles were obtained by homogenisation in a 1:5 ratio of RIPA buffer (2% SDS, 2 mM EDTA, 2 mM EGTA in 5mM Tris, pH 6.8) containing Halt protease and phosphatase inhibitor cocktail (Thermo Fisher Scientific). Samples were spun at 15996 x g for 15 minutes and supernatant collected.

Protein concentration was determined using a Bio-Rad DC (detergent-compatible) protein assay system (Bio-Rad Laboratories). Protein standards were made by serially diluting 2 mg/ml Bovine Serum Albumin (BSA; Sigma-Aldrich) in homogenising buffer to obtain final concentrations of 1, 0.5, 0.25, 0.125 mg/ml and 0 mg/ml. 10 µL of BSA standards and homogenised samples were added to a 96-well plate and reagents A, B and S were added according to the manufacturer's instructions. Plates were incubated for 15 minutes at room temperature before absorbance was measured at 750 nm on a spectrophotometer.

Homogenised samples were diluted in a 1:1 ratio with 2x Laemmli sample buffer (Bio-Rad Laboratories) containing 5% 2-mercaptoethanol and denatured by heating for 5 minutes at 95°C. Equal amounts of protein from each sample were

loaded on acrylamide gels alongside a molecular weight marker (Bio-Rad Laboratories). Gels were run at 160 V for 1 hour. Proteins were transferred onto a nitrocellulose membrane (Amersham) by running at 100V for 1 hour.

Blots were blocked in PBS + 0.1% Tween 20 + 5% milk protein or TBS + 0.1% Tween + 5% BSA for 1 hour at room temperature before incubating overnight at 4°C with the appropriate primary antibodies. The specific antibodies used are detailed in the methods section of Chapter 3. GAPDH (1:5000; Abcam; ab9385) was used as a loading control. Membranes were washed in either PBS + 0.1% Tween or TBS + 0.1% Tween and then incubated in HRP-conjugated secondary antibodies (1:500; Thermo Fisher Scientific) for 2 hours at room temperature. StrepTactin (Bio-Rad Laboratories; 1:10,000) was also added for visualisation of the protein ladder. Blots were visualised using Supersignal chemiluminescent HRP substrate (Thermo Fisher Scientific) and developed on Kodak film. Densitometry was analysed using ImageJ software (National Institutes of Health, Bethesda, MD, USA). Densities for the samples were normalised against densities of the loading control in each blot.

2.11. Electron microscopy (EM)

EM experiments on TA muscle samples (one muscle from 3 animals per group) were carried out in collaboration with Dr Mhoriam Ahmed, Prof Giampietro Schiavo (UCL Institute of Neurology, UK), Dr Anne Weston (The Francis Crick Institute, UK) and Dr Lucy Collinson (The Francis Crick Institute, UK). Muscles were fixed in glutaraldehyde and cut into approximately 1mm³ blocks. The blocks were further fixed in 2.5% glutaraldehyde and 4% formaldehyde in 0.1 M phosphate buffer (pH 7.4) for 1 hour and then processed for transmission electron microscopy (TEM). All samples were prepared using the National Centre for Microscopy and Imaging Research (NCMIR) method (Deerinck T, Bushong E, Thor A 2010).

For TEM, 70 nm sections were cut using a UCT ultramicrotome (Leica Microsystems) and collected on formvar-coated slot grids. No post-staining was required due to the density of metal deposited using the NCMIR protocol. Images were acquired using a 120 kv Tecnai G2 Spirit TEM (FEI Company) and an Orius CCD camera (Gatan Inc.).

2.12. Establishment of human fibroblast cultures

Fibroblasts were obtained from four sporadic IBM patients, four patients with *VCP* mutations and four age-matched controls. All cells used for experiments were used at passages 2-6. Specific details are provided in the 'Materials and Methods' section of the relevant Chapters.

Fibroblasts were grown in 25 cm² (T25) or 75 cm² (T75) tissue culture flasks in fibroblast media, in a humidified incubator at 37 °C with 5% CO₂. Fibroblast media contained Dulbecco's Modified Eagle Medium (DMEM) + GlutaMAX-I (4.5g/L D-Glucose, Pyruvate), with the serum and antibiotics added from stock concentrates to obtain final concentrations of 10% fetal bovine serum (FBS; Gibco™, Thermo Fisher) and 2% penstrep (200 U/mL Penicillin and 200 µg/mL Streptomycin; Gibco™, Thermo Fisher). Fibroblast media was changed every 2-3 days. Cells were subcultured or frozen down upon reaching 90% confluence.

For subculture, excess medium was removed and flasks washed with PBS. Cells were detached from culture flasks by coating the bottom of the flasks with 0.05% trypsin/EDTA solution and placing in a shaking incubator at 37 °C for 8 minutes. When all cells had detached, fibroblast media was added to inactivate the trypsin and cells transferred into a falcon tube. The cell suspensions were spun down at 400 x g for 5 minutes and the media carefully aspirated off. The cell pellet was gently resuspended in fibroblast media and divided into new flasks with fibroblast media (approximately 3-7x10⁵ cells per T75 flask) or seeded onto 13 mm coverslips in 24 well plates at an appropriate density (approximately 3000-7000 cells per well).

For storage, the collected cell pellet was resuspended in freezing media containing FBS and 10% dimethyl sulphoxide (DMSO) and divided and transferred into two cryovials per T75 flask. Cryovials were stored at -80 °C in a Nalgene Mr Frosty™ cryogenic freezing container for 24 hours before being transferred into liquid nitrogen.

2.13. Arimoclomol treatment

When cells reached ~60% confluency in 24-well plates, cultures were treated with Arimoclomol for 24 hours, by adding a single dose to wells containing 500 μ L of fibroblast media. Various concentrations of Arimoclomol (10-400 μ M) were assessed. Control cells were left untreated.

2.14. Immunocytochemistry

Fibroblasts were cultured and plated on 13 mm glass cover slips in 24-well plates containing 500 μ L of fibroblast media (approximately 3000-7000 cells per well). Upon reaching ~70% confluence, cells were rinsed once with PBS before being fixed with 4% paraformaldehyde (PFA) for 12 minutes at room temperature. PFA was prepared from one ampule of 16% stock formaldehyde solution (Agar Scientific) added to 3 equal parts of Dulbecco's PBS (pH 7.1-7.5, Sigma). Cells were then washed again with PBS for 5 mins, a total of 3 times. Following fixation, cultured cells were incubated for 1 hour at room temperature with 10% normal goat/donkey serum in 0.1% PBS-Triton-X100 to block non-specific binding sites. Blocking solution was then removed and the cells washed once in PBS. Cells were incubated overnight at 4°C with the relevant primary antibodies and where appropriate Alexa Fluor™ 488 Phalloidin (1:400; Thermo Fisher) to label the actin cytoskeleton. The specific antibodies used are detailed in the methods section of the relevant Chapters. Following incubation in primary antibody, the cells were washed in PBS (3 x 5 mins) and incubated for 2 hours at room temperature with the fluorescently labelled secondary antibodies (goat/donkey anti-rabbit/ mouse Alexa568 or goat/donkey anti-rabbit/mouse Alexa488; 1:500; Invitrogen). Cells were washed once with PBS and incubated with the nuclear marker DAPI (1:2000; 1 mg/ml stock solution) for 15 mins. Cells were washed again (3 x 5 mins) and mounted onto glass slides with Mowiol mounting medium or Citifluor glycerol PBS solution (Agar Scientific). Negative controls omitting primary antibodies were carried out in parallel for all experiments, to check the specificity of binding of the secondary antibody.

Fluorescent images were visualised under a Leica DMR microscope and analysed using Leica Application Suite software (Leica Microsystems, Germany). Images were captured at 20x, 40x and 63x magnifications and processed using Adobe Photoshop.

2.15. Western blots (cell lysates)

When fibroblasts reached ~90% confluency in tissue culture flasks, pellets were collected according to subculturing protocol described above (section 2.12). Cell suspensions were rinsed in PBS and spun again at 400 x g for 5 minutes. PBS was carefully removed by aspiration and RIPA buffer (2% SDS, 2 mM EDTA, 2 mM EGTA in 5mM Tris, pH 6.8) containing Halt protease and phosphatase inhibitor cocktail (Thermo Fisher Scientific) was added (225 μ L per T75 flask). 1 μ g/ml Deoxyribonuclease I (DNase; Sigma-Aldrich) was also added to each sample. Samples were left on ice for 30 minutes, before being spun at 15996 x g for 15 minutes and supernatant collected.

Protein concentration was determined using a Bio-Rad DC (detergent-compatible) protein assay system as described above (section 2.10). Homogenised samples were diluted in a 1:3 ratio with 4x Laemmli sample buffer (containing 5% 2-mercaptoethanol) and denatured by heating for 5 minutes at 95°C. Equal amounts of protein from each sample were loaded on 4-20% Mini-PROTEAN TGX precast gradient gels (Bio-Rad Laboratories) alongside a molecular weight marker (Bio-Rad Laboratories). Gels were run at 160 V for 1 hour. Proteins were transferred onto a nitrocellulose membrane (Amersham) by running at 100V for 1 hour.

Blots were blocked in TBS+ 0.1% Tween + 5% milk protein / 5% BSA for 1 hour at room temperature before incubating overnight at 4°C with the appropriate primary antibodies. The specific antibodies used are detailed in the methods section of the relevant Chapters. Membranes were washed in TBS + 0.1% Tween and then incubated in HRP-conjugated secondary antibodies (1:500; Thermo Scientific) for 2 hours at room temperature. Blots were developed using Luminata™ Crescendo Western HRP Substrate (Merck Millipore) and visualised using a ChemiDoc Touch Imaging System (Bio-Rad). Primary antibody incubation and subsequent steps were repeated using β -actin (1:2500; Abcam; ab6276) as a loading control. Band densities were analysed using ImageJ software or Image Lab software (Bio-Rad Laboratories). Densities for the samples were normalised against densities of the loading control in each blot.

2.16. Disrupted nuclei counts

To assess the percentage of cells with morphological nuclear abnormalities, fibroblasts were stained with DAPI to outline the nuclear region of fibroblasts. A series of ten images were taken at 20x magnification, from one coverslip for each control or patient cell line, using a Leica DMR microscope. The number of cells with nuclear abnormalities were manually counted blind using ImageJ and the percentage of the total number of cell nuclei calculated.

2.17. TUNEL assay

Fibroblasts were cultured and fixed on glass coverslips as described above (section 2.12). Fibroblasts were then labelled for apoptosis using the TACS 2 TdT/DAB kit (Trevigen), according to the manufacturer's instructions. A positive control sample in every experiment was generated, using TACS-Nuclease.

2.18. Statistical analysis

All data are presented as mean \pm SEM. Analyses were performed using IBM SPSS Statistics 20 or GraphPad Prism to determine the presence of statistically significant differences ($p < 0.05$). The specific statistical tests used are detailed in the methods section of the relevant Chapters.

Chapter 3

Targeting the heat shock response in a transgenic mouse model of multisystem proteinopathy

3.1. Introduction

Well-established and relevant models of diseases are vital for examining the efficacy of novel therapeutic compounds and for the translation of successful preclinical research into human trials. Since the Greensmith group have shown that Arimoclomol ameliorates key pathological features of IBM *in vitro*, the aim of this Chapter was to investigate whether these findings could be replicated *in vivo*. Since IBM is a sporadic condition, with no known genetic cause, it is not possible to directly model this condition in mice. For this reason, the effects of Arimoclomol were examined in a model of the degenerative disorder, multisystem proteinopathy (MSP), in which muscle pathology mimics key features of IBM.

3.1.1. Clinical features of multisystem proteinopathy (MSP)

MSP is a rare autosomal dominant disorder, predominantly associated with three distinct disease phenotypes, inclusion body myopathy, Paget's disease of bone (PDB) and frontotemporal dementia (FTD) and is therefore also known as IBMPFD. The disorder has a variable clinical phenotype, with an adult-onset typically between 20-40 years.

Skeletal muscle weakness tends to be the earliest and most common sign of pathology in MSP, affecting around 90% of MSP patients. Progressive atrophy of both proximal and distal muscles occurs, particularly affecting the pelvic and shoulder girdle muscles (Kimonis, Fulchiero et al. 2008; Weihl et al. 2009). Loss of ambulation occurs approximately 13 ± 7 years after disease onset and both cardiac and respiratory function may also become impaired as the disease progresses, leading to premature mortality in some cases (Evangelista et al. 2016). PDB occurs in just under half of MSP patients and typically affects the spine, pelvis, scapulae and skull. It is characterised by elevated turnover of bone tissue, leading to abnormal bone formation, skeletal deformities such as localised bone enlargement and bone pain (Watts et al. 2004; Kimonis et al. 2011). One-third of MSP patients develop FTD. Degeneration of the frontal and anterior temporal lobes of the brain impairs reasoning ability and judgement, personality, speech and language, movement and social interpersonal conduct. However, visuospatial ability and memory are relatively spared (Kimonis,

Fulchiero et al. 2008; Weihl 2011). It has been suggested that FTD may correlate with the severity of the disease, as patients with dementia have been shown to have a more rapid disease progression and a shorter lifespan (Figueroa-Bonaparte et al. 2016).

The phenotypic variability of MSP is extensive, even within families and among those with the same disease mutation (Abrahao et al. 2016; Al-Obeidi et al. 2018). More recently, it has been recognised that the clinical phenotype of the disease is much broader than previously thought, extending beyond myopathy, PDB and FTD to include amyotrophic lateral sclerosis (ALS), Parkinson's disease, cardiomyopathy, cerebral ataxia, spastic paraplegia, Charcot-Marie-Tooth disease (CMT) and autonomic disturbance (Miller et al. 2009; Johnson et al. 2010; de Bot et al. 2012; Chan et al. 2012; Majounie et al. 2012; Shi et al. 2012; Benatar et al. 2013; Mehta et al. 2013; Spina et al. 2013; Gonzalez et al. 2014; Figueroa-Bonaparte et al. 2016; Regensburger et al. 2017).

3.1.2. Histopathological features of MSP

Patients with MSP display a muscle pathology that resembles that seen in sporadic IBM patients. The inclusion body myopathy is accompanied by the presence of rimmed vacuoles within muscle and ubiquitin-positive cytoplasmic and nuclear inclusions, containing proteins such as TDP-43, p62 and VCP (Hübbers et al. 2007; Weihl et al. 2009; Evangelista et al. 2016). In addition, muscle biopsies show evidence of other degenerative changes, including atrophic and hypertrophic fibres, variable fibre size, increased connective tissue and marked fatty replacement of muscle fibres (Kimonis et al. 2011). In contrast to sporadic inclusion body 'myositis', muscle biopsies from MSP patients reportedly lack the presence of inflammatory infiltrates, although some biopsies have shown MHC-1 upregulation and small inflammatory infiltrates (Kovach et al. 2001; Evangelista et al. 2016).

As with muscle pathology, the brain and osteoclasts of MSP patients contain inclusions. Brain pathology in MSP is characterised by the presence of ubiquitinated and TDP-43-positive intranuclear inclusions and dystrophic neurites. Pathology is particularly abundant in the neocortex and less apparent in the limbic and subcortical areas and completely absent in the dentate gyrus

(Schröder et al. 2005; Forman et al. 2006; Neumann et al. 2007; Weihl et al. 2009). This pathology is distinct from sporadic and familial FTD cases (Kimonis, Fulchiero et al. 2008). Bone from patients with MSP demonstrates nuclear and cytoplasmic tubulofilamentous inclusions, structurally similar to inclusions seen in muscle tissue (Watts et al. 2004; Kimonis, Fulchiero et al. 2008).

3.1.3. Valosin-containing protein (VCP)

MSP is predominantly caused by mutations in the valosin-containing protein (*VCP*) gene, situated on chromosome 9p13.3. *VCP* is a highly conserved protein and belongs to the type II AAA+ (ATPases associated with diverse cellular activities) family of proteins. It is one of the most abundant cytosolic proteins, ubiquitously expressed in all tissues and is considered an essential protein, with homozygous null *VCP* mutations causing early embryonic lethality in mice (Müller et al. 2007).

3.1.3.1. VCP structure

VCP exists as a hexameric double-ring structure, comprised of 4 domains (DeLaBarre & Brunger 2003; Meyer et al. 2012). The D1 and D2 domains are ATPase domains that bind and hydrolyse ATP and form two stacked rings with a central channel. The N-domain, located at the periphery of the D1 ring plays a role in the recognition and binding of a diverse array of interacting proteins and cofactors. The C-terminal tail domain also binds a small minority of cofactors and interacting proteins, although the structure and importance of this domain is relatively unknown (Buchberger et al. 2015). Upon binding of these domains with their cofactors, ATP hydrolysis in the ATPase domains triggers distinct conformational changes that permit interaction with substrate proteins (Beuron et al. 2006).

3.1.3.2. VCP function

The tightly-controlled association of *VCP* with its numerous and diverse array of cofactors enables a broad range of cellular activities, by directing substrate specificity and subcellular localisation (Buchberger et al. 2015; Xia et al. 2016). To date, over 40 different cofactors/adaptor proteins have been identified as being responsible for regulating *VCP*-mediated processes (Schuberth &

Buchberger 2008; Yeung et al. 2008; Meyer et al. 2012; Yeo & Yu 2016). VCP is important for signal transduction and cell cycle control, nuclear envelope reconstruction, DNA repair and genome stability and Golgi reassembly. Moreover, VCP has a central role in protein homeostasis, being an essential component in the regulation of protein degradation via the proteasome, autophagy-mediated pathways and ERAD (Ju & Wehl 2010; Nalbandian et al. 2011; Meyer & Wehl 2014).

It is thought that many functions of VCP are linked to its ability to bind to ubiquitinated substrates either directly, or indirectly via its cofactors (Wang et al. 2004; Ye 2006; Meyer & Wehl 2014). In the ER, VCP is recruited to the membrane via an integral membrane protein adaptor, where it subsequently binds ubiquitinated substrates from the site of retrotranslocation, extracting them from the membrane so that they can be degraded via the proteasome. VCP may either directly shuttle ubiquitinated proteins into the proteolytic compartment of the 20S proteasome, or use a set of shuttling factors (Clemen et al. 2015). In addition, VCP can also release certain membrane-bound transcription factors, allowing them to translocate into the nucleus to influence gene expression (Xia et al. 2016).

Moreover, studies in yeast have also shown that VCP can extract aberrant ubiquitinated proteins from ribosomes in a process termed ribosome-associated degradation. The release of defective translation products from stalled ribosomes allows them to be degraded by the proteasome (Defenouillere et al. 2013; Verma et al. 2013).

VCP is also capable of extracting and degrading proteins, such as the mitofusins, from the outer mitochondrial membrane and is essential for the clearance of damaged mitochondria via the PINK1/Parkin mitochondrial quality control pathway and the regulation of mitochondrial fusion (Heo et al. 2010; Tanaka et al. 2010; Xu et al. 2011; N.C. Kim, et al. 2013; Hemion et al. 2014; Zhang et al. 2017).

3.1.3.3. MSP-associated VCP mutations

To date, more than 40 missense mutations in the *VCP* gene have been identified, with almost 30 of these leading to MSP or an inclusion body myopathy phenotype in patients (Evangelista et al. 2016; Al-Tahan et al. 2018). The majority of these mutations occur in the N-terminal domain or the D1 ATPase domain, with a small minority residing within the N-D1 linker domain (**Fig. 3.1**; Tang & Xia 2016). The R155H mutation is the most common mutation, thought to account for more than half of families with MSP.

Generally, genotype-phenotype correlations are difficult to discern in MSP due to the marked variation in clinical presentation. However, the A232E mutation, residing in the D1 domain, presents as the most severe clinical manifestation, characterised by an earlier onset of PDB and a more severe myopathy (Kimonis et al. 2011). The R155C mutation is associated with an earlier age of onset of inclusion body myopathy, while patients with the R155H mutation typically have a later onset of PDB (Watts et al. 2007).

It is not yet clear how these mutations affect the functioning of the VCP protein or the reason for the late-onset and selective vulnerability of brain, muscle and bone. Altered communication between the N-domain and the D1 domain, due to mutations at their interface, is thought to reduce affinity for ADP and enhance basal ATP hydrolysis (Tang et al. 2010). Elevated ATPase activity has been reported as up to three times higher in A232E mutant VCP compared to the wild-type protein, despite seemingly normal cellular expression (Halawani et al. 2009; Manno et al. 2010; Niwa et al. 2012). However, there are also reports that ATPase activity is normal in VCP mutants so it may be that specific mutants hydrolyse ATP at different rates (Weihl et al. 2006; Fernández-Sáiz & Buchberger 2010).

There have also been reports of altered binding of certain cofactors linked to mutations in VCP, which may impair a distinct subset of VCP functions (Fernández-Sáiz & Buchberger 2010; Manno et al. 2010; Ritz et al. 2011; Bug & Meyer 2012; Erzurumlu et al. 2013; Zhang et al. 2015). For example, reduced binding of mutant VCP to UBXD1 has been linked to impaired VCP-mediated endosomal sorting and trafficking (Ritz et al. 2011).

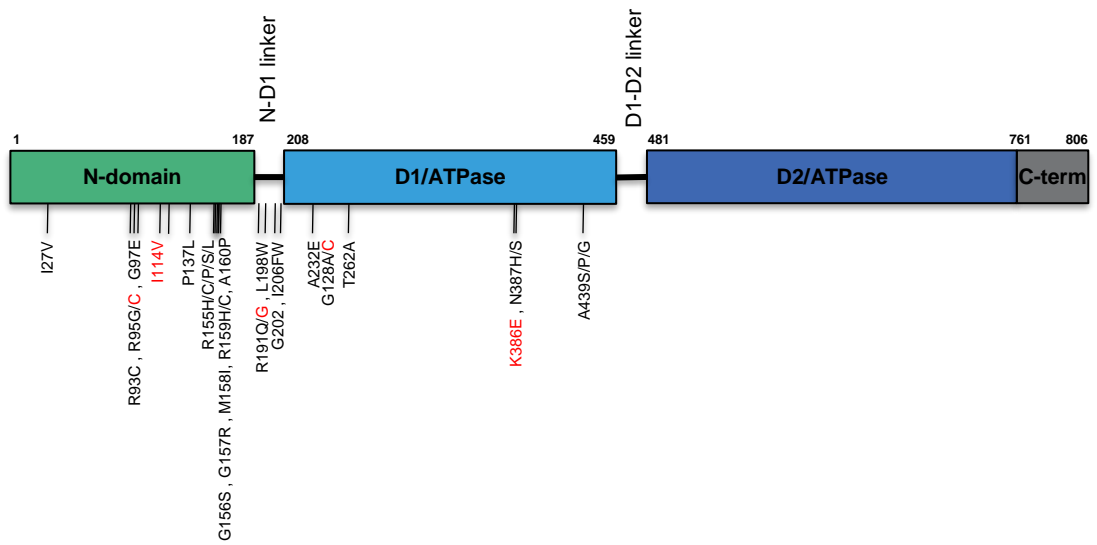


Figure 3.1. MSP-related VCP mutations

Location of disease-associated VCP mutations. The majority of mutations associated with either MSP (black) or inclusion body myopathy (red) are located within the N-terminal domain or the D1 ATPase domain.

Expression of mutant proteins leads to an increase in ubiquitinated proteins, susceptibility to proteasome inhibition and reduced aggresome formation (Kitami et al. 2006; Ju et al. 2008). VCP mutants have also been shown to cause disruption to the ERAD pathway, causing altered cofactor binding and impaired degradation of ERAD substrates (Weihl et al. 2006; Erzurumlu et al. 2013). Furthermore, expression of disease-associated VCP mutants *in vitro* and *in vivo* has been shown to impair autophagy. In human embryonic kidney (HEK) cells and human osteosarcoma (U2OS) cells, mutant VCP stimulates both autophagosome and autolysosome formation and can interfere with autophagic vesicle maturation and lysosomal fusion, leading to the accumulation of immature autophagic vesicles and disturbance of autophagic flux (Ju et al. 2009; Bayraktar et al. 2016). Large vacuoles positive for lysosome-associated membrane protein (LAMP)-1 and LAMP-2 have also been observed in myoblasts derived from MSP patients, as well as accumulation of LC3-II and immature autophagic vesicles (Tresse et al. 2010). Further investigation into the effect of VCP mutations on protein function and its precise interaction with cofactors is still required in order to understand the underlying molecular mechanism relating to disease pathology.

3.1.4. Additional MSP-causing mutations

Although mutations in VCP appear to be the main cause of MSP, recent studies have identified disease-causing mutations in other genes. Mutations within the *hnRNPA2B1* and *hnRNPA1* genes represent novel genetic causes of MSP (H.J. Kim et al. 2013). These genes encode the ubiquitously expressed heterogeneous nuclear ribonucleoproteins, RNA-binding proteins which play an important role in RNA metabolism. These proteins have glycine-rich C-terminal regions that are 'prion-like' in nature. These conserved prion-like domains (PrLDs) are essential for activity and mediate interaction with other RNA-binding proteins, including TDP-43 and the ALS-associated aggregate-prone protein FUS, which also contain conserved PrLDs (Buratti et al. 2005). The PrLDs contain "steric zipper" motifs that encourage protein-protein binding, meaning *hnRNPA2B1* and *hnRNPA1* are intrinsically fibrillisation-prone, underlying their assembly into cytoplasmic RNA granules (Benatar et al. 2013). Disease-linked mutations in *hnRNPA2B1* and *hnRNPA1* are typically found at the centre of the PrLD and facilitate enhanced fibrillisation and excess assembly of cytoplasmic

RNA granules, promoting the formation of pathological cytoplasmic inclusions (H.J. Kim et al. 2013; Shorter & Taylor 2013). Expression of mutant forms of human hnRNPA2 or hnRNPA1 in *Drosophila* or in mouse tibialis anterior (TA) muscle leads to the formation of cytoplasmic inclusions containing the mutant proteins (H.J. Kim et al. 2013). Cytoplasmic inclusions containing TDP-43, hnRNPA2B1, and hnRNPA1 have also been observed in MSP muscle biopsies (H.J. Kim et al. 2013).

Mutations in the *SQSTM1* gene, encoding p62, have also recently been identified as causing a rimmed vacuolar myopathy, PDB, ALS and FTD (Le Ber et al. 2014; Bucelli et al. 2015). Mutations in *SQSTM1* are thought to affect the binding of p62 to ubiquitinated proteins, thereby disrupting the degradation of proteins (Ciani et al. 2003; Garner et al. 2011; Bucelli et al. 2015). Inclusions containing p62 amongst other proteins, such as TDP-43, have been reported in MSP patients with these mutations (Bucelli et al. 2015).

3.2. Aims of this Chapter

MSP recapitulates many features of IBM in muscle and although the exact pathomechanisms of MSP and sporadic IBM are unknown, both are thought to involve disruption of protein quality control pathways. To date, no single animal model has been shown to recapitulate the clinical and pathologic features of IBM. Transgenic mice overexpressing a mutant form of human VCP, carrying the most severe A232E disease-associated mutation, recapitulate the MSP phenotype, displaying pathological hallmarks characteristic of IBM and developing progressive muscle weakness (Custer et al. 2010). Therefore, the aim of this Chapter was to further characterise this previously described mouse model of MSP, in order to examine the effects of upregulation of the HSR with Arimoclomol *in vivo*.

The specific aims of this Chapter were:

- (1) To characterise the histopathological features of muscle in a mutant VCP transgenic mouse model of MSP.
- (2) To examine the effects of Arimoclomol on muscle histopathology in mutant VCP mice, in a preclinical trial for IBM.

3.3. Materials and methods

A full description of the materials and methods used in this Chapter are presented in Chapter 2, and include the following:-

3.3.1. Breeding and maintenance of mutant VCP mice

All experimental work was carried out by Charlotte Spicer and Dr Mhoriam Ahmed (UCL Institute of Neurology UK) under licence from the UK Home Office (Scientific Procedures Act 1986) and was approved by the Animal Welfare and Ethical Review Board of UCL Institute of Neurology. A full description of the transgenic mice and genotyping protocols used in this study is given in Chapter 2 (section 2.1-2.2).

3.3.2. Arimoclomol treatment regime

Wild-type and mutant VCP mice were treated with Arimoclomol from 4 months of age to the time of examination at 14 months, using the protocol described in Chapter 2 (section 2.3). Mice were randomly divided into the following treatment groups: (i) Non-transgenic wild-type mice treated with water alone (WT) (ii) Transgenic wild-type mice treated with water alone (WT-VCP) (iii) A232E mutant VCP mice with water alone (mVCP) (iv) A232E mutant mice treated with 120mg/kg/day Arimoclomol (mVCP+Ari).

3.3.3. Grip strength analysis

Grip strength analysis was carried out by Dr Mhoriam Ahmed, according to the protocol described in Chapter 2 (section 2.4).

3.3.4. *In vivo* analysis of isometric muscle force

In vivo assessment of muscle function was carried out by Dr Mhoriam Ahmed, according to the protocol described in Chapter 2 (section 2.5).

3.3.5. Histochemistry and immunostaining

Transverse cryosections of mouse tibialis anterior (TA) muscle were stained using the protocol described in Chapter 2 (section 2.7). Three sections from the central region of one TA muscle per mouse were examined (minimum of 3 animals per group) for each analysis. The antibodies used for immunofluorescence examination are detailed in **Table 2**. All sections were co-stained with the nuclear marker DAPI (1:1000; Sigma-Aldrich).

3.3.6. Muscle fibre area measurements

Analysis of muscle fibre area from transverse cryosections of TA muscle was carried out following the protocol described in Chapter 2 (section 2.8)

3.3.7. Analysis of centralised nuclei

The percentage of fibres with centralised nuclei was manually quantified following the protocol described in Chapter 2 (section 2.9).

3.3.8. Western blot

Western blot was performed to determine protein levels as described in Chapter 2 (section 2.10). Membranes were incubated with the primary antibodies indicated in **Table 2**.

3.3.9. Electron microscopy (EM)

EM experiments on muscle samples were carried out in collaboration with Dr Mhoriam Ahmed and Prof Giampietro Schiavo (UCL Institute of Neurology, UK), and Dr Anne Weston and Dr Lucy Collinson (The Francis Crick Institute, UK). A detailed protocol is described in Chapter 2 (section 2.11).

3.3.10. Statistical analysis

Analyses were performed as described in Chapter 2 (section 2.18). For analysis of centralised nuclei, muscle fibre area counts, grip strength and isometric muscle force experimental groups were compared using a one-way analysis of variance (ANOVA) with Tukey's all pairwise multiple comparisons *post hoc* analysis. All data analysis was performed blind to experimental conditions of each animal. All data are presented as mean \pm SEM.

Primary antibody	Application	Dilution	Source	Supplier
TDP-43 (C-terminal epitope)	IF	1:500	Rabbit polyclonal	ProteinTech 12892-1-AP
Ubiquitin	IF	1:500	Mouse monoclonal	GeneTex GTX78236
p62	IF, WB	1:100	Mouse monoclonal	Abcam ab56416
LC3	IF	1:500	Rabbit polyclonal	Novus NB600-1384
MHC-I	WB	1:750	Mouse monoclonal	Santa Cruz sc-53723
Phospho-I κ B α	WB	1:1000	Mouse monoclonal	Cell Signalling Technology #9246
GAPDH (Loading control)	WB	1:5000	Rabbit polyclonal	Abcam Ab9385
F4/80 (macrophage marker)	IF	1:500	Mouse	AbD Serotec

Table 2. Primary antibodies used in Chapter 3 for the study of mutant VCP mouse muscle

Description of primary antibodies used within this Chapter. IF = immunofluorescence; WB = western blot.

3.4. Results

3.4.1. Muscles of mutant VCP mice show pathological hallmarks of IBM which are attenuated following treatment with Arimoclomol

Haematoxylin and Eosin (H&E) staining was performed on TA muscle of 14-month old mutant VCP mice in order to examine the integrity of the muscle tissue. Histological analysis showed that mutant VCP mice displayed characteristic hallmarks of pathology in muscle, whilst muscle from wildtype mice appeared normal (**Fig. 3.2 A-B**). Muscle sections from mutant VCP mice showed evidence of necrotic and atrophied fibres, degenerating fibres and increased endomysial connective tissue (**Fig. 3.2 A-B**). Furthermore, there was evidence of split fibres and inflammatory cell infiltration. These features were dispersed across all sections examined in the mutant VCP mice. Noticeable variations in fibre size were also observed, with groups of small angular fibres interspersed with hypertrophic fibres. Myofibres also had uneven irregular edges in contrast to the smooth round edges displayed by healthy fibres. This pathology was not observed in muscle from aged-matched wildtype animals (**Fig. 3.2 A**).

Since Arimoclomol ameliorates key pathological markers of IBM *in vitro*, muscles from 14-month old Arimoclomol-treated mutant VCP mice were examined to investigate whether Arimoclomol was effective in ameliorating IBM-like pathology *in vivo*. Treatment with Arimoclomol attenuated all the key IBM pathologies observed in muscle of mutant VCP mice (**Fig. 3.2 C**); myofibres had a more uniform size and shape and were separated by only a thin layer of connective tissue. In addition, there were fewer inflammatory infiltrates and necrotic and atrophied cells. Arimoclomol had no effect on muscle of WT-VCP mice.

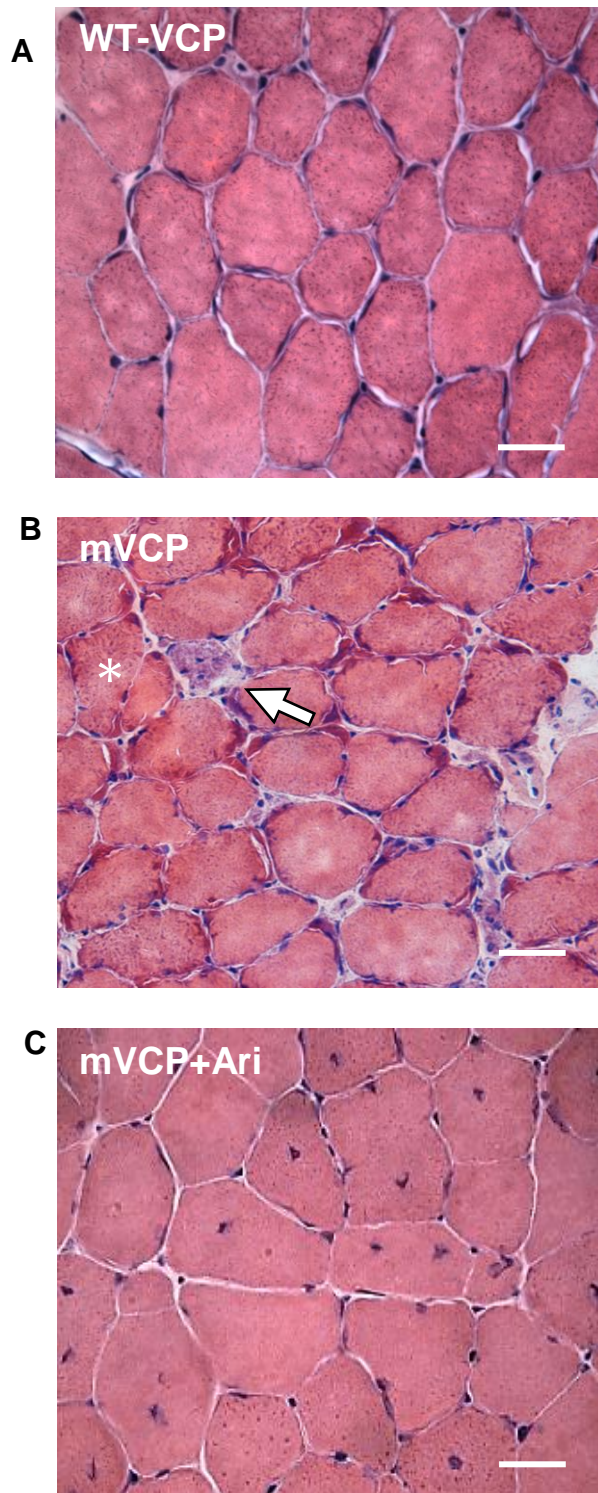


Figure 3.2. Arimoclomol treatment improves IBM-like pathology in tibialis anterior (TA) muscles of mutant VCP mice

Haematoxylin and Eosin (H&E) HE staining of tibialis anterior (TA) muscle from 14-month old **(A)** wild-type VCP (WT-VCP) mice, **(B)** mutant VCP (mVCP) mice demonstrating necrotic (arrow) and split fibres (asterisk) and **(C)** Arimoclomol-treated mutant (mVCP+Ari) mice. Scale bars represent 25 μ m.

3.4.2. Mutant VCP mice have hypertrophic muscles which are attenuated following treatment with Arimoclomol

Since hypertrophic fibres were observed in muscles of mutant VCP mice, the average myofibre area in TA muscles was measured, in order to quantify the extent of hypertrophy. There was a significant increase in the average myofibre area in muscles from mutant VCP mice compared to muscles from WT-VCP mice, indicative of muscle hypertrophy ($p < 0.0001$; one-way ANOVA; **Fig. 3.3**). Arimoclomol treatment reduced the level of hypertrophy, so that the average muscle fibre area in TA muscle from Arimoclomol-treated mutant VCP mice was less than the average muscle fibre diameter of TA muscle from untreated mutant VCP mice ($p < 0.0001$; one-way ANOVA; **Fig. 3.3**) and not significantly different from fibre area of WT-VCP mice.

3.4.3. Mutant VCP mice have an increased incidence of centralised nuclei within myofibres which is further increased by Arimoclomol treatment

In normal muscle, multiple nuclei are located just beneath the sarcolemma of the myocyte. Centralised nuclei within myofibres (**Fig. 3.4 A**) are an indicator of muscle that has undergone past regeneration, where muscle precursor cells add to the myonuclei population. Only around 1-3% of nuclei located within the interior of the cell in normal muscle, as was observed in the muscle of WT-VCP mice (**Fig. 3.4 B**). The incidence of centralised nuclei was significantly increased in TA muscle from mutant VCP mice compared to TA muscle from WT-VCP mice ($18.7 \pm 3.4\%$ vs $3.1 \pm 0.5\%$ respectively; $p < 0.001$; one-way ANOVA; **Fig. 3.4 B**). However, an even greater increase in the percentage of myofibres with centralised nuclei was observed in TA muscles of mutant VCP mice treated with Arimoclomol ($18.7 \pm 3.4\%$ vs $35.3 \pm 4.5\%$ respectively; $p < 0.05$; one-way ANOVA; **Fig 3.4 B**).

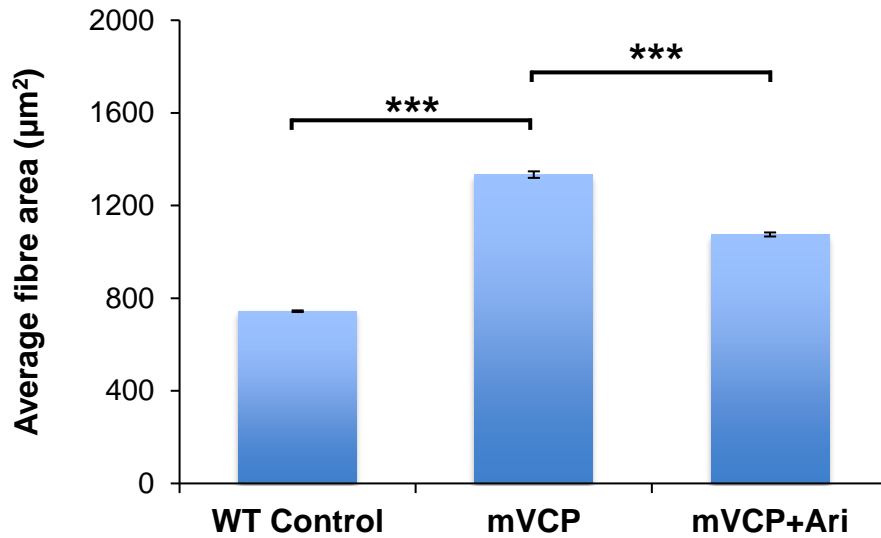


Figure 3.3. Muscle fibre hypertrophy in mutant VCP mice is reduced by treatment with Arimoclomol

The bar chart shows the average fibre area in TA muscle at 14 months from wild-type and wild-type VCP (WT control), mutant VCP (mVCP) and Arimoclomol-treated mutant VCP mice (mVCP+Ari). Error bars = SEM. N=3 per group (approximately 2000-2500 individual fibres per animal); ***p<0.0001; one-way ANOVA. Measurements analysed by Dr Mhoriam Ahmed. Adapted from Ahmed et al. (2016). Reprinted with permission from AAAS.

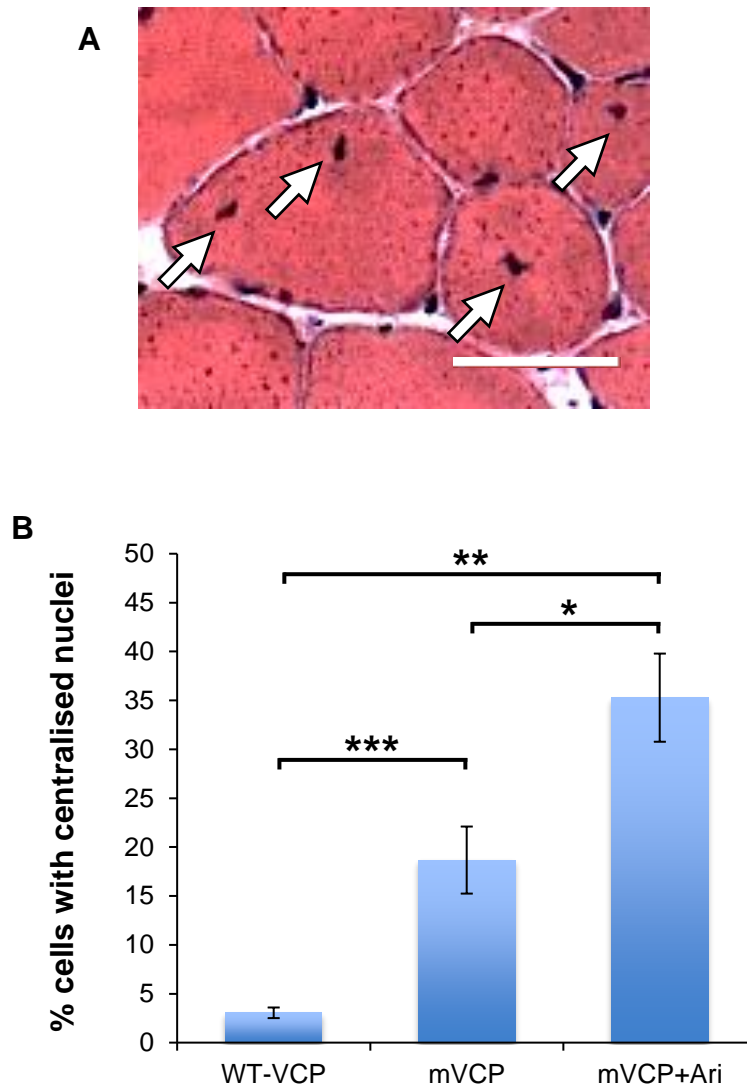


Figure 3.4. Arimoclomol increases the percentage of myofibres with centralised nuclei in TA muscles of mutant VCP mice, suggestive of past regeneration of muscle fibres

(A) H&E staining showing centralised nuclei (arrows) within myofibres in a TA muscle of a 14-month old mutant VCP mouse. Scale bar represents 25 μm . **(B)** The bar chart shows the average percentage of myofibres with centralised nuclei in TA muscle at 14 months from wild-type-VCP (WT-VCP), mutant VCP (mVCP) and Arimoclomol-treated mutant VCP mice (mVCP+Ari). Error bars = SEM. N= 5 per group (approximately 300-500 individual fibres examined per animal); * $p < 0.05$, ** $p < 0.01$, *** $p < 0.001$; one-way ANOVA.

3.4.4. Muscles of mutant VCP mice show cytoplasmic mislocalisation of TDP-43 which is prevented by treatment with Arimoclomol

Mislocalisation of TDP-43 from the nucleus to the cytoplasm in muscle fibres is a characteristic hallmark of IBM (Weihl et al. 2008). Within the TA muscle of 14-month old WT-VCP mice, TDP-43 was restricted to peripheral nuclei (**Fig. 3.5 A(i), B**) which as well as myonuclei may be nuclei of satellite cells, stromal cells or blood vessels. This could be determined by staining for laminin, which is abundant in the extracellular matrix (ECM) of muscle fibres, to determine whether these peripheral nuclei are inside or outside the basal lamina. In muscle of mutant VCP mice, however, cytoplasmic accumulations of TDP-43 were present and TDP-43 was depleted from the nuclei (**Fig. 3.5 A(ii), B**). This cytoplasmic accumulation was observed in numerous fibres across all muscle sections examined in the mutant VCP mice. Treatment with Arimoclomol prevented TDP-43 mislocalisation in muscles of mutant VCP mice (**Fig. 3.5 A(iii), B**).

3.4.5. Muscles of mutant VCP mice show ubiquitin-positive inclusions which are prevented by treatment with Arimoclomol

Ubiquitinated inclusions are considered a key feature in the pathogenesis of IBM. Ubiquitin has a well-documented role in the degradation of misfolded proteins via the ubiquitin-proteasome system (UPS) and is thus important for maintaining protein homeostasis in cells. Immunohistochemistry of TA muscle of 14-month old mice showed evidence of numerous ubiquitin-positive inclusions throughout all muscle sections examined from the mutant VCP mice. Ubiquitin-positive inclusions were not observed in wildtype mice (**Fig. 3.6 A-B**). However, treatment with Arimoclomol prevented this formation of ubiquitinated inclusions in mutant VCP mice (**Fig. 3.6 C**).

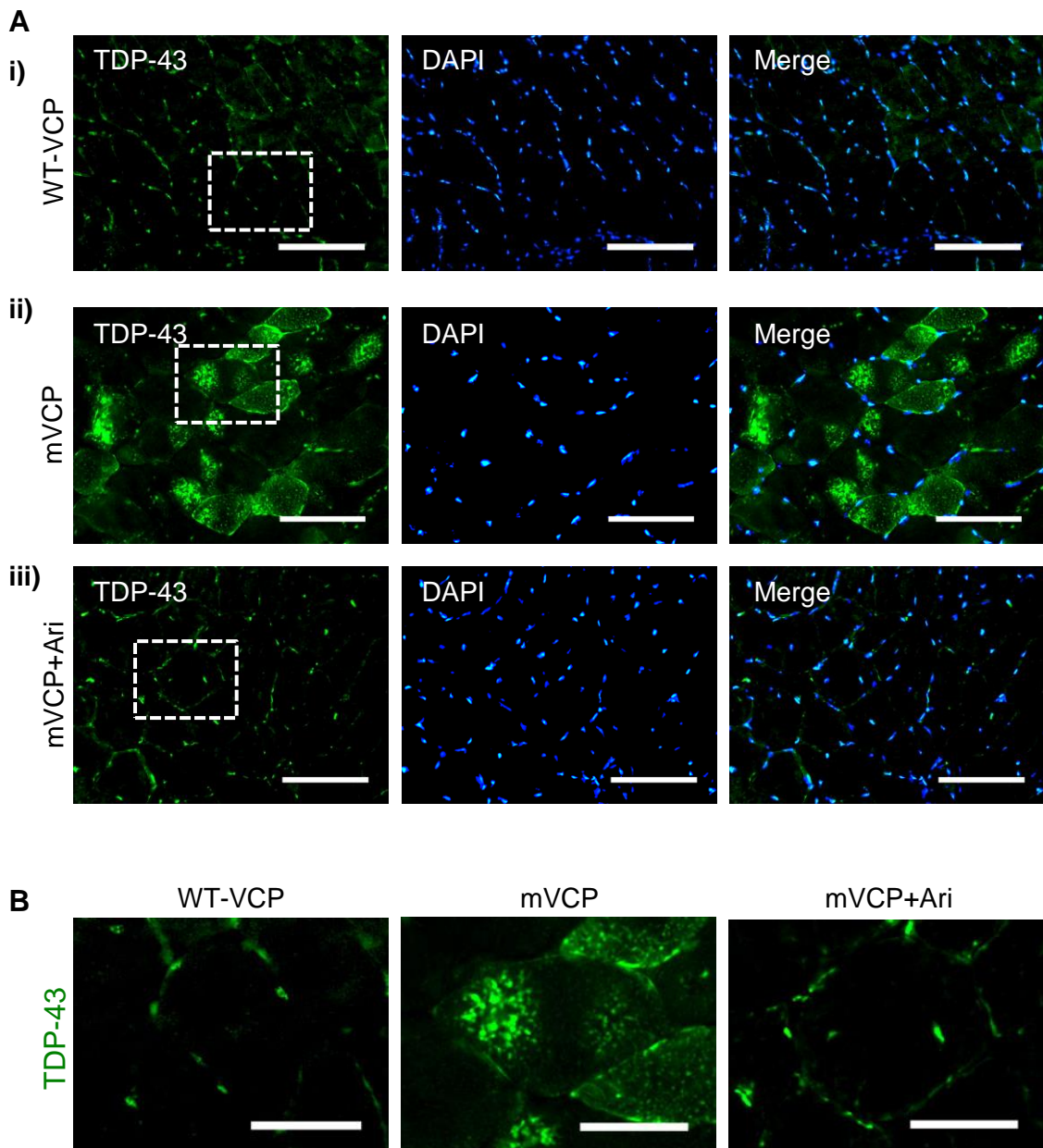


Figure 3.5. Cytoplasmic TDP-43 mislocalisation in TA muscles of mutant VCP mice is prevented by treatment with Arimoclomol

(A) Immunostaining for TDP-43 (green) in sections of TA muscles of wild-type VCP mice (WT-VCP; i), mutant VCP mice (mVCP; ii) and Arimoclomol-treated mutant mice (mVCP+Ari; iii) at 14 months. The sections were co-stained for the nuclear marker DAPI (blue). Scale bar represents 50 μ m. The areas in the dotted boxes are shown at higher magnification in (B). Scale bar represents 20 μ m. Adapted from Ahmed et al. (2016). Reprinted with permission from AAAS.

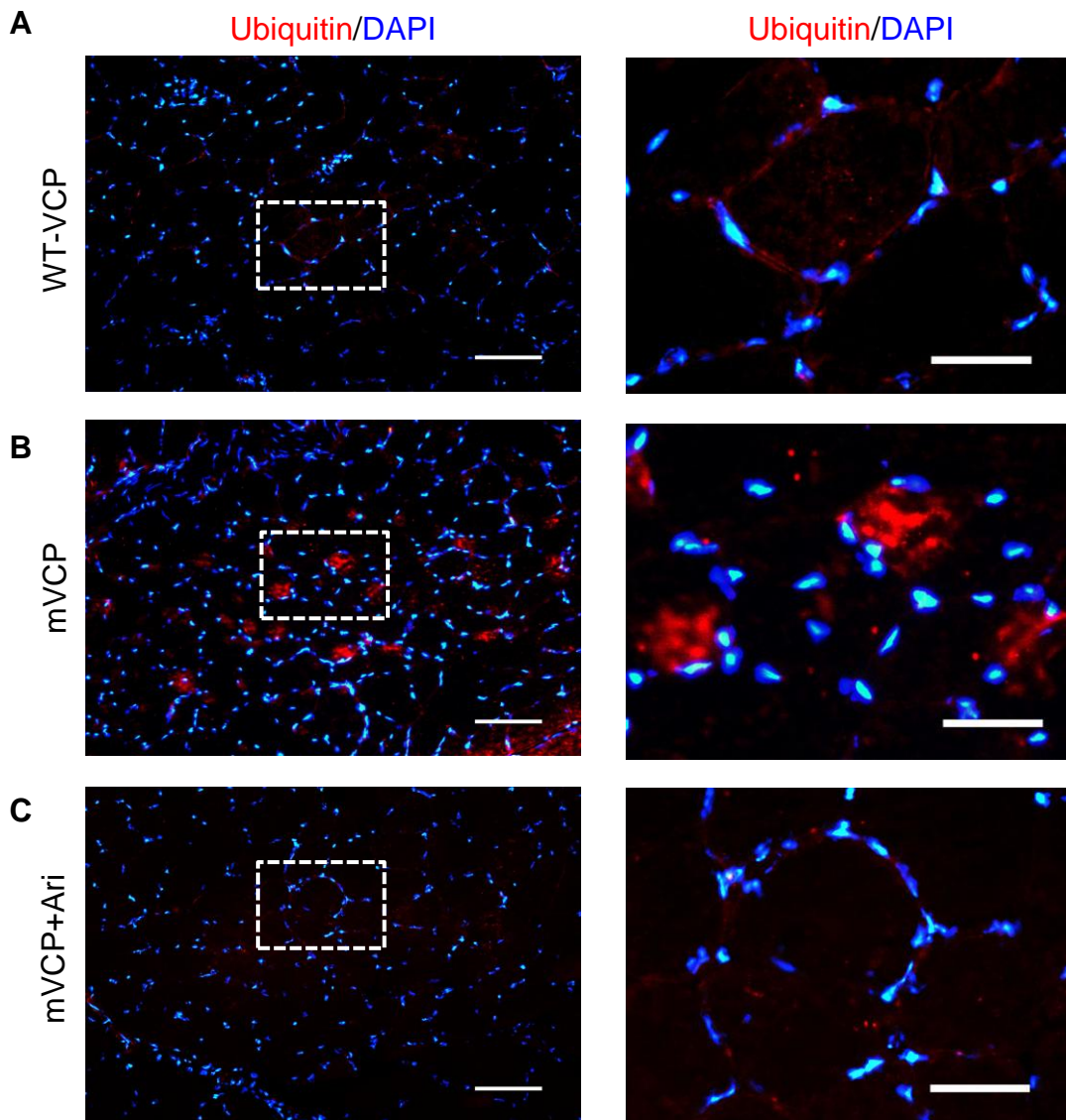


Figure 3.6. The formation of ubiquitin-positive inclusions in TA muscles of mutant VCP mice is reduced following treatment with Arimoclomol

Immunostaining for ubiquitin (red) in sections of TA muscles of **(A)** wild-type VCP mice (WT-VCP), **(B)** mutant VCP mice (mVCP) and **(C)** Arimoclomol-treated mutant mice (mVCP+Ari) at 14 months. The sections were co-stained for the nuclear marker DAPI (blue). Scale bar represents 50 µm. Muscle fibres in the highlighted boxes are shown at higher magnification (right). Scale bar represents 20 µm. Adapted from Ahmed et al. (2016). Reprinted with permission from AAAS.

3.4.6. Muscles of mutant VCP mice show p62 aggregates which are prevented by treatment with Arimoclomol

Two other key proteins involved in protein clearance via the UPS and autophagy-lysosome pathways are p62 and LC3. These proteins are found in protein aggregates in IBM (Hiniker et al. 2013). P62 is a shuttle protein that targets ubiquitinated proteins for degradation, whilst LC3 binds p62 for lysosomal degradation and is selectively degraded via autophagy. In TA muscle sections examined from mutant VCP mice, numerous cytoplasmic aggregates of p62 were observed, as well as a number of LC3-positive muscle fibres (**Fig. 3.7 A**). Furthermore, in mutant VCP mice there was evidence of vacuoles lined with both p62 and LC3, which were not observed in WT-VCP mice (**Fig. 3.7 B**). Western blot analysis confirmed that there was an increase in p62 expression in mutant VCP mouse muscle relative to muscle from WT-VCP mice (**Fig. 3.7 C**). However, treatment with Arimoclomol reduced the expression of p62 in muscle of mutant VCP mice (**Fig. 3.7 B**).

3.4.7. Muscles of mutant VCP mice have increased inflammatory cell infiltration which is reduced following treatment with Arimoclomol

Inflammation in muscle is a key characteristic of IBM. Inflammatory cell infiltration was observed in H&E stained muscle fibres of mutant VCP mice (**Fig. 3.8 A**). Using western blot analysis, the expression levels of the inflammatory markers MHC-I and the phosphorylated form of the NF- κ B (nuclear factor-kappa B) substrate, inhibitor of NF- κ B alpha (phospho-I κ B α), were determined. In TA muscle of mutant VCP mice, there was a clear upregulation in the expression of MHC-I (**Fig. 3.8 B**) and phospho-I κ B α (**Fig. 3.8 C**) when compared to the expression in TA muscle of WT-VCP mice. Arimoclomol treatment reduced the expression of both MHC-I and phospho-I κ B α in mutant VCP mice. These results did not reach levels of statistical significance, however, this is likely due to the small sample size.

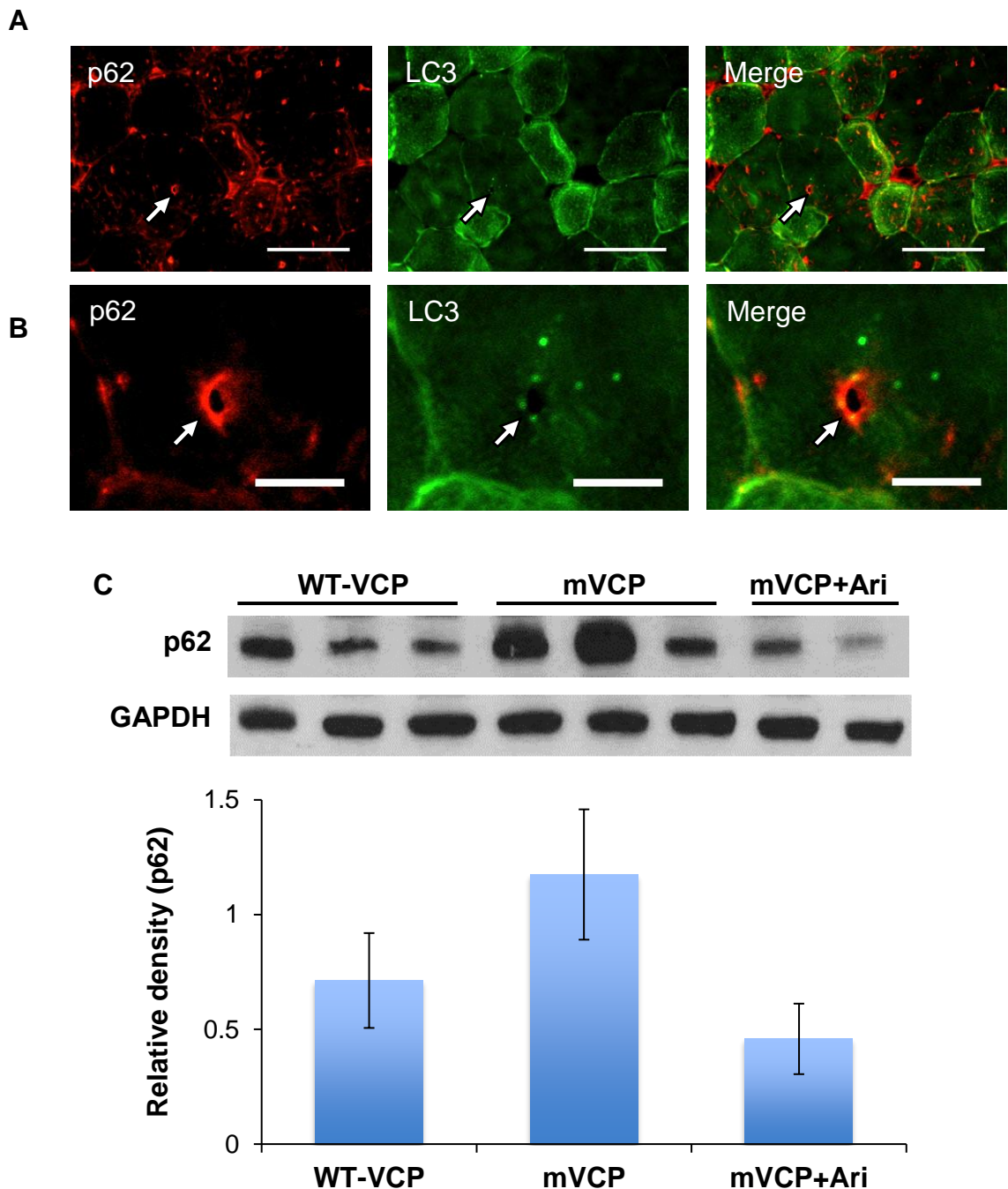


Figure 3.7. Increased expression of p62 in TA muscles of mutant VCP mice is reduced following treatment with Arimoclomol

(A) Immunostaining for p62 (red) and LC3 (green) in a section of TA muscle from a 14-month old mutant VCP mouse. Arrows indicate evidence of a vacuole lined with p62 and LC3. Scale bar represents 50 μ m. **(B)** A 'rimmed vacuole' is shown at higher magnification. Scale bar represents 10 μ m. **(C)** Western blot analysis of p62 expression in TA muscles of mice at 14 months from each experimental group. The bar chart shows the mean relative optical density of the bands in the western blot, normalised to the loading control (GAPDH). Error bars= SEM. N=3 (WT-VCP); 3 (mVCP); 2 (mVCP+Ari).

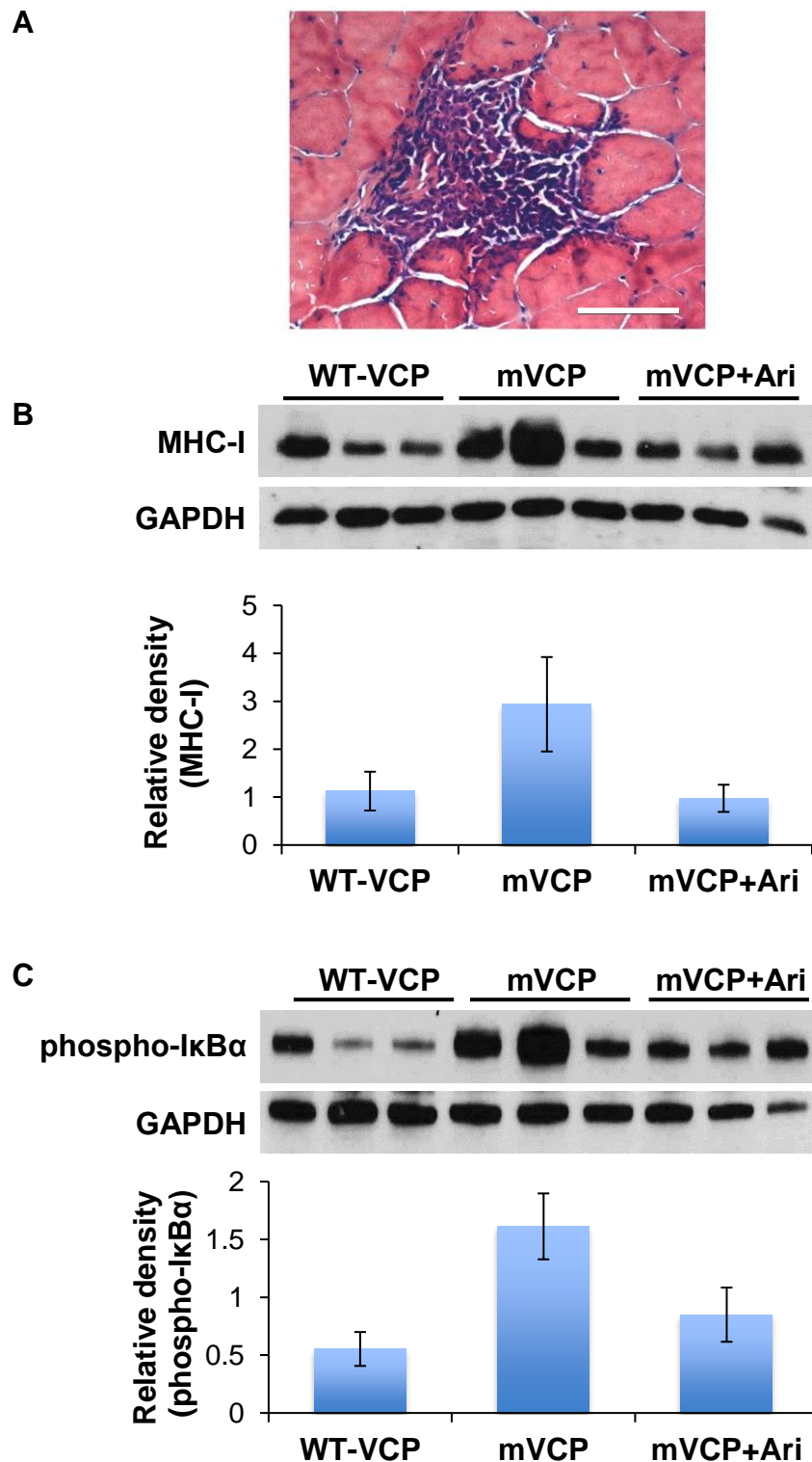


Figure 3.8. Increased expression of inflammatory markers in TA muscles of mutant VCP mice is reduced following treatment with Arimoclomol

(A) H&E staining showing an example of severe inflammatory cell infiltration in a TA muscle section from a 14-month old mutant VCP mouse. Scale bar represents 50 μ m. Western blot of (B) MHC-I and (C) phospho-I κ B α in TA muscles of mice from each experimental group. The bar chart shows the mean relative optical density of the bands in the western blot, normalised to the loading control (GAPDH). Error bars = SEM. N=3 per group. Adapted from Ahmed et al. (2016). Reprinted with permission from AAAS.

In addition, macrophage infiltration in TA muscle was examined using an antibody which recognises the mouse F4/80 antigen, a 160kD glycoprotein expressed by murine macrophages. Macrophages, a hallmark of inflammation, are important for engulfing debris around necrotic fibres and surround and invade necrotic and non-necrotic muscle fibres in IBM patients (Engel & Arahata 1984; Scola et al. 1998). There was greater macrophage infiltration in muscle from mutant VCP mice compared to WT-VCP mice, which had virtually no areas or minimal areas of macrophage infiltration in TA muscle (**Fig. 3.9 A(i-ii), B**). Arimoclomol treatment prevented macrophage infiltration in TA muscle of mutant VCP mice (**Fig. 3.9 A(iii)**). Together, these results show that Arimoclomol reduces inflammation in the muscles of mutant VCP mice.

3.4.8. Muscles of mutant VCP mice have disrupted mitochondrial morphology and an increased number of vacuoles which are prevented by treatment with Arimoclomol

Transmission electron microscopy (TEM) was used to provide higher resolution images of the TA muscle from WT-VCP and mutant VCP mice. TEM revealed extensive mitochondrial damage and sarcoplasmic reticulum swelling in the TA muscle of all mutant VCP mice (**Fig. 3.10 A**). Treatment with Arimoclomol, however, dramatically improved mitochondrial morphology and reduced sarcoplasmic reticulum swelling and vacuole number in mutant VCP mouse muscle fibres compared to untreated mutant mice (**Fig. 3.10 B**).

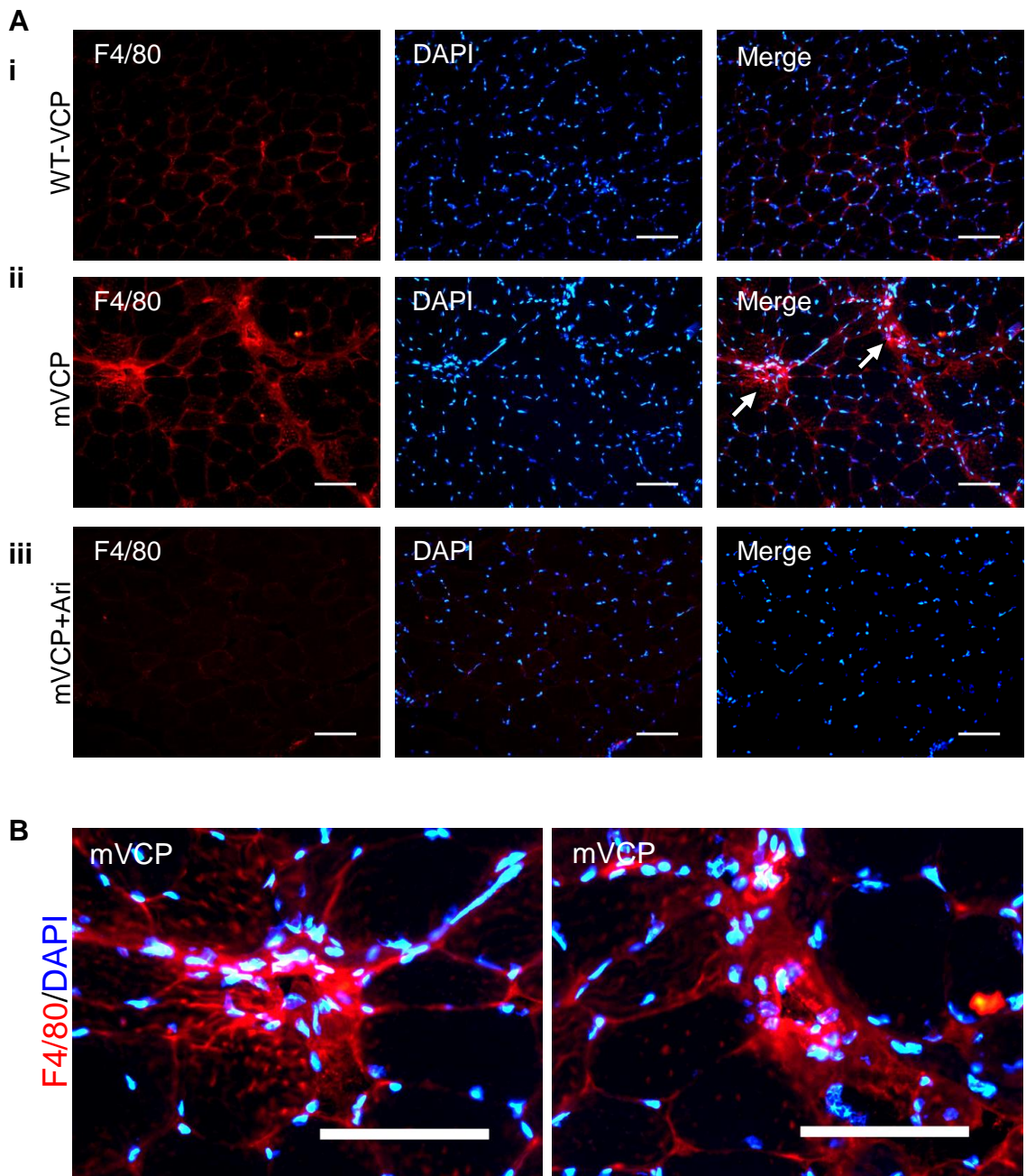


Figure 3.9. Macrophage infiltration in TA muscles of mutant VCP mice is prevented by treatment with Arimoclomol

Immunostaining for the macrophage marker F4/80 (red) in sections of TA muscles from **(A)** wild-type VCP mice (WT-VCP; i), mutant VCP mice (mVCP; ii) demonstrating macrophage infiltration (arrows) and Arimoclomol-treated mutant VCP mice (mVCP+Ari; iii) at 14 months old. Sections were co-stained for the nuclear marker DAPI (blue). **(B)** Areas indicated by arrows are shown at higher magnification. Scale bar represents 50 μm .

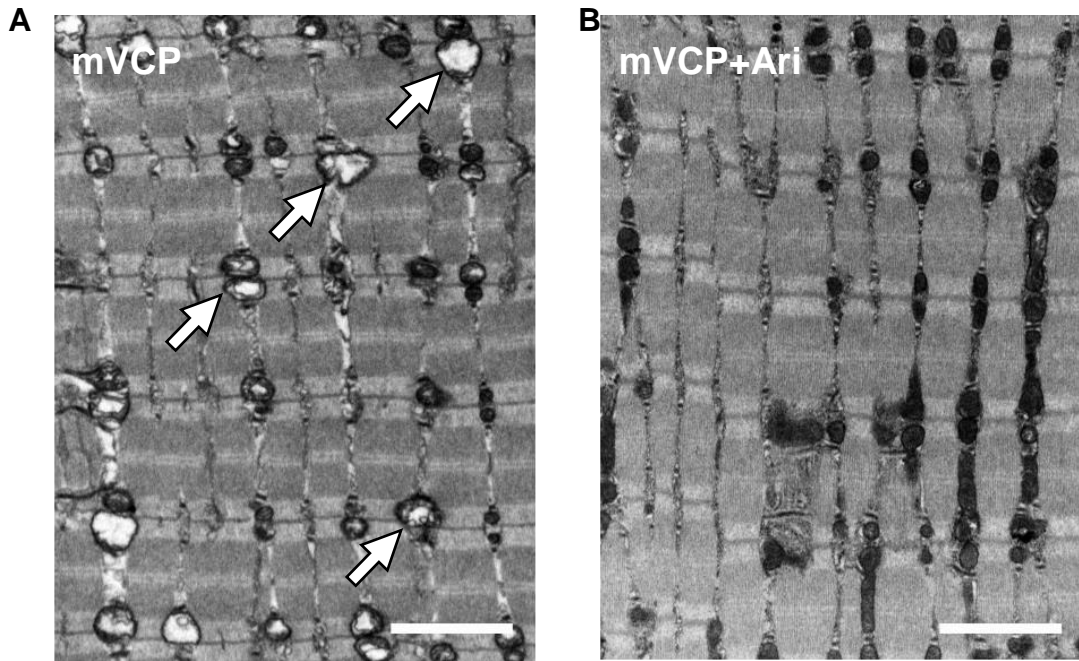


Figure 3.10. Arimoclomol improves mitochondrial morphology and reduces the number of vacuoles in TA muscles of mutant VCP mice

Transmission electron microscopy (TEM) of TA muscles from **(A)** mutant VCP mice and **(B)** Arimoclomol-treated mutant VCP mice at 14 months old. Arrows indicate enlarged/vacuolated mitochondria. Scale bars represent 2 μm . Experiments undertaken in collaboration with Dr Mhoriam Ahmed, Dr Giampietro Schiavo, Dr Anne Weston and Dr Lucy Collinson. From Ahmed et al. (2016). Reprinted with permission from AAAS.

3.4.9. Mutant VCP mice have a decrease in muscle force which is prevented by treatment with Arimoclomol

The changes in muscle histopathology in mutant VCP mice correlated with a decline in muscle function, as assessed by longitudinal analysis of grip strength, as well as acute *in vivo* physiological assessment of isometric muscle force. By 14 months, mutant VCP mice showed a significant reduction in muscle strength compared to grip strength at 4 months ($p < 0.001$; one-way ANOVA; **Fig. 3.11 A**). Arimoclomol treated mutant VCP mice, on the other hand, showed no difference in grip strength at 14 months compared to 4 months and had significantly greater grip strength at 14 months compared to untreated mutant VCP mice ($p < 0.05$, one-way ANOVA; **Fig. 3.11 A**). Furthermore, the mean maximum tetanic force of extensor digitorum longus muscles of mutant VCP mice was significantly lower compared to WT-VCP mice at 14 months ($p < 0.05$; one-way ANOVA; **Fig. 3.11 C**). Again, this loss of muscle force was prevented by treatment with Arimoclomol ($p < 0.05$; one-way ANOVA; **Fig. 3.11 B-C**).

Taken together, these findings demonstrate that that both histopathological features of IBM alongside functional deficits are recapitulated in the VCP-A232E transgenic mouse model and are attenuated with Arimoclomol treatment.

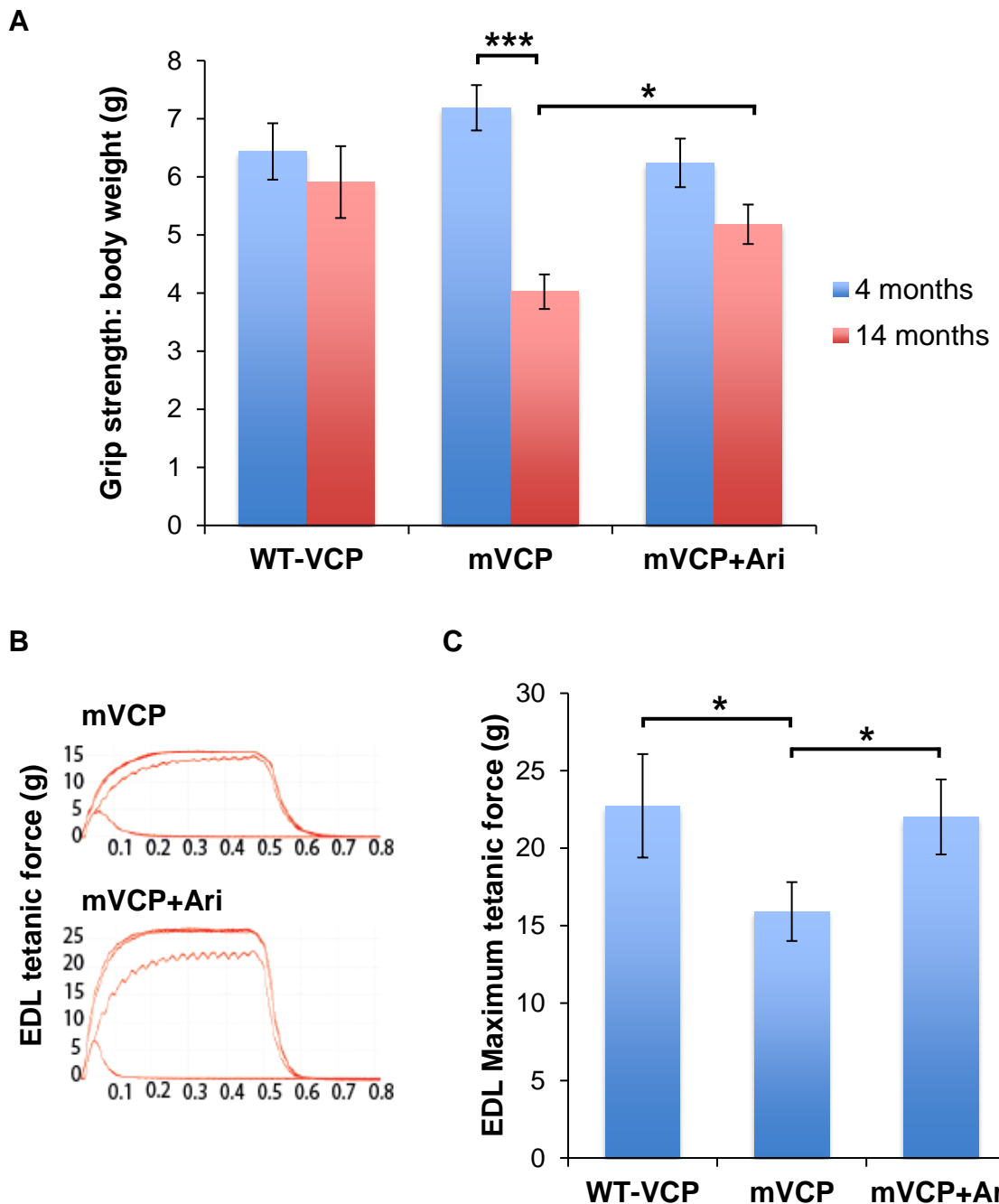


Figure 3.11. Arimocloamol reduces the decline in grip strength and improves the maximum tetanic force of extensor digitorum longus (EDL) muscles in mutant VCP mice

(A) Analysis of grip strength: body weight ratio of wild-type VCP mice (WT-VCP), mutant VCP mice (mVCP) and Arimocloamol-treated mutant VCP mice (mVCP+Ari) at 4 and 14 months. Error bars= SEM. N=10 per group. * $p < 0.05$, *** $p < 0.001$, one-way ANOVA. **(B)** Typical traces of muscle twitch and maximum tetanic force of extensor digitorum longus (EDL) muscles in untreated and Arimocloamol-treated mutant VCP mice. **(C)** Mean maximum force of EDL muscles of WT-VCP, mutant VCP, and Arimocloamol-treated mutant VCP mice. N=10; * $p < 0.05$, one-way ANOVA. Experiments completed and analysed by Dr Mhoriam Ahmed. Adapted from Ahmed et al. (2016). Reprinted with permission from AAAS.

3.5. Discussion

The varied pathological findings and complex aetiology of IBM pose many challenges for the development of effective treatments. The failure of therapies targeting the immune response in clinical trials (Amato et al. 1994; Dalakas et al. 2001; Amato & Barohn 2009), alongside the parallels between aberrant protein aggregates in IBM muscle fibres and accumulated proteins in other neurodegenerative diseases (Askanas & Engel 2001; Askanas & Engel 2008), suggests that therapeutic approaches targeting the degenerative components of IBM and impaired proteostasis may be successful. Since the heat shock response (HSR) declines with age, boosting this cytoprotective mechanism and improving protein handling may be a potential therapy for IBM and similar protein misfolding diseases. The Greensmith lab have shown that upregulation of the HSR with Arimoclomol can reduce pathology in *in vitro* models of IBM (Ahmed et al. 2016). In this Chapter, the effects of pharmacological upregulation of the HSR with Arimoclomol on IBM pathology were investigated *in vivo*, using the A232E-VCP transgenic mouse model of MSP, which recapitulates many features of sporadic IBM in muscle.

3.5.1. Muscles of mutant VCP mice display an IBM-like pathology

It has previously been established that mutant VCP mice develop muscle weakness and display cytoplasmic TDP-43 and ubiquitin-positive pathology within muscle (Custer et al. 2010). This study aimed to further characterise this model, in order to determine whether mutant VCP mice represent a relevant model and useful tool for examining the effects of upregulation of the HSR. The results of this Chapter demonstrate that these mice recapitulate both the inflammatory and degenerative components of IBM in muscle, reminiscent of the pathology seen in patients. Evidence of muscle degeneration included TDP-43 mislocalisation, ubiquitinated inclusion formation, the formation of p62- and LC3-positive rimmed vacuoles, fibre hypertrophy and damaged mitochondria. Inflammatory cells surrounding and infiltrating muscle fibres in H&E stained muscle fibres, increased macrophage infiltration and upregulated expression of the inflammatory markers MHC-I and phospho-I κ B α were evidence of an inflammatory response within the mutant VCP mice. In addition to the representative myodegenerative and inflammatory features observed in the

mutant VCP mouse model, a loss of muscle strength was also observed, consistent with the muscle weakness that occurs in IBM patients.

The presence of inflammatory markers in the muscle of mutant VCP mice was an interesting observation since, in contrast to sporadic IBM patient muscle biopsies, muscle biopsies from patients with MSP are not typically reported to display inflammatory cell infiltrates. These patients have a more 'myopathy' phenotype rather than the 'myositis' phenotype observed in sporadic IBM patients. However, there are a few published cases of MSP patients with inflammatory infiltrates and upregulated MHC-1 expression in muscle (Peyer et al. 2013; Evangelista et al. 2016). Furthermore, in one study, tumour necrosis factor alpha (TNF α), a proinflammatory cytokine upstream of NF- κ B, was found to be elevated in plasma of MSP patients and it has been suggested that inflammation in MSP may correlate with specific points in the disease course (Dec, Rana, et al. 2014). A trend for the upregulation of MHC-I and MHC-II genes in patients with VCP mutations has also been reported (Gang et al. 2016). Finally, *in vitro*, C2C12 myoblast cell lines transfected with mutant VCP constructs have been reported to display increased NF- κ B (Custer et al. 2010), whilst inhibition of VCP has been shown to increase I κ B α , causing a decrease in NF- κ B activity (Liu et al. 2012). It is therefore possible that, as speculated in IBM, disruption of protein homeostasis due to VCP mutations, may lead to an immune response that is associated with muscle wasting. As no single animal model has previously been reported to fully recapitulate the clinical and pathologic features of IBM, the observation of both degenerative and inflammatory features in the muscle of mutant VCP mice is an important finding. The VCP mutant mouse model could therefore be used to examine the effects of upregulation of the HSR *in vivo*.

3.5.2. The effects of Arimoclomol *in vivo*

Previous studies have shown that Arimoclomol has therapeutic potential in mouse models of protein misfolding and neurodegenerative diseases, including ALS and spinal and bulbar muscular atrophy (SBMA; Kalmar et al. 2008; Malik et al. 2013), as well as in *in vitro* models of IBM (Ahmed et al. 2016). Likewise, this study has demonstrated that Arimoclomol is beneficial in ameliorating key IBM-like pathology in the mutant VCP mouse at 14 months. Arimoclomol

treatment ameliorated TDP-43 mislocalisation, the formation of ubiquitinated inclusions, fibre hypertrophy and inflammation in muscle and improved mitochondrial morphology. Furthermore, these improvements in muscle pathology were accompanied by a functional recovery. Arimoclomol prevented the loss of muscle strength that was seen in untreated mutant VCP mice and led to increased maximum tetanic force of extensor digitorum longus (EDL) muscles (Ahmed et al. 2016). Arimoclomol had no effect on muscle of WT-VCP mice, most likely as Arimoclomol is a co-inducer of the HSR and thus only acts on cells already under cellular stress.

Interestingly, Arimoclomol treatment also resulted in a greater increase in the percentage of centralised nuclei in the muscle of mutant VCP mice. Typically in muscle, multiple nuclei are evenly distributed at the periphery of the myofibre, below the plasma membrane, with only approximately, 1-3% of nuclei located within the interior of the cell, as was observed in the muscle of WT-VCP mice in this study, although this may increase somewhat with age (Sakuma et al. 2008; Joyce et al. 2012; Peverelli et al. 2015). Although central nucleation may be considered a pathological feature, as nuclear positioning is thought to be essential to muscle function, in this study the occurrence of centralised nuclei in muscle fibres is likely indicative of cellular damage and subsequent regeneration (Folker & Baylies 2013). Upon damage to muscle, compensatory skeletal muscle regeneration occurs. Myoregeneration involves the activation, proliferation and differentiation of satellite cells and other cells with myogenic potential, to repair or replace the damaged or dead muscle fibres (Chargé & Rudnicki 2004; Sirabella et al. 2013). This highly coordinated myogenic pathway is controlled by myogenic regulatory nuclear transcription factors Myf5, Mrf4, MyoD, and myogenin (Tajbakhsh 2009). After activation, muscle stem cells become myoblasts. These newly recruited mononucleated myoblasts either fuse with damaged myofibres or fuse with one another to form multinucleated muscle fibres. Upon fusion, each newly incorporated nucleus is actively moved to the centre of the immature myotube. Myogenic regulatory factors subsequently help to migrate the nuclei toward the periphery and following many fusion events, the myotube will form a mature myofibre (Cadot et al. 2012; Folker & Baylies 2013; Roman & Gomes 2017). Thus, centralised nuclei are considered markers of regenerating myofibres.

Muscle fibres with prominent centralised nuclei have been observed in muscle biopsies from IBM patients (de Camargo et al. 2018) and other muscle disorders such as Duchenne muscular dystrophy (DMD; Takayama et al. 1969; Duddy et al. 2015). Furthermore, the occurrence of centralised nuclei in muscle of aged transgenic mice overexpressing β APP in skeletal muscle has been reported (Sugarman et al. 2002). TA Muscle of mutant VCP mice demonstrated an increase in the percentage of myofibres with central nuclei suggesting increased muscle fibre turnover due to fibre loss. The observation that Arimoclomol treatment resulted in a further increase in the percentage of centralised nuclei in the muscle of mutant VCP mice would suggest that there is an increase in myofibre repair. It is also possible therefore that tissue renewal is impaired in IBM and improved with Arimoclomol. Although there is evidence to suggest that regenerative processes are activated in fibres of IBM patients (Winter & Bornemann 1999; Arnardottir et al. 2004; Hollemann et al. 2008; Wanschitz et al. 2013), some studies have found that maintenance and repair of muscle is disrupted in IBM patient muscle resulting in the progressive loss of muscle fibres. Studies *in vitro* have shown that myoblasts derived from IBM patient muscle have a reduced proliferation rate compared to age-matched controls due to an insufficient expression of the differentiation molecule MyoD and insufficient muscle regeneration (Morosetti et al. 2006; Morosetti et al. 2010). Furthermore, in IBM patient muscle biopsies, expression of the transcription factor nuclear factor of activated T-cells 5 (NFAT5), a core protein to myogenesis, is reduced (Herbelet et al. 2018). Alterations in expression of myogenic regulatory factors involved in satellite cell activation and differentiation leading to disturbance of muscle repair may therefore contribute to the muscle weakness that occurs with IBM.

3.5.3. Arimoclomol is a co-inducer of the heat shock response

Arimoclomol acts as an amplifier of the cytoprotective HSR in cells under stress. As Arimoclomol only acts in cells where HSF1 is already activated (Hargitai et al. 2003), it reduces the likelihood of off-target side effects that would be caused by widespread activation of the cytoprotective mechanism. Indeed, Arimoclomol had no effect on the control mice in this study. Although Arimoclomol may have several mechanisms of action (Page et al. 2006; Crul et al. 2013), the improvements described in the overall pathology of muscle from the mutant

VCP mice are likely to be a result of the drug's ability to amplify the HSR via HSF1 activation, thus augmenting protein handling and degradation pathways (Kieran & Greensmith 2004; Kalmar et al. 2008; Kalmar & Greensmith 2009).

Treatment with Arimoclomol resulted in a significant increase in HSP70 expression in mutant VCP mouse muscle, indicating that the HSR had been upregulated (Ahmed et al. 2016). Enhanced HSP expression improves protein handling by assisting the refolding of proteins to their native state and sequestering misfolded proteins to prevent aberrant interactions with other neighbouring, non-native proteins. Hence, the requirement for ubiquitin and p62, to target and shuttle misfolded proteins for degradation is lessened. Furthermore, reducing the level of aberrant protein handling may prevent the dysfunction of protein homeostasis pathways and make the degradation of any unwanted proteins more efficient. This would thereby promote the processing of ubiquitinated proteins, preventing the accumulation of ubiquitin and p62.

The underlying mechanisms and resulting consequences of TDP-43 mislocalisation in IBM and other diseases are still unknown. However, improving protein handling via Arimoclomol treatment appears to reduce the stressful and pathological conditions under which TDP-43 translocation occurs. Indeed previous studies in *in vitro* models of IBM have shown that Arimoclomol prevents TDP-43 mislocalisation and this correlates with an increase in cell survival (Ahmed et al. 2016). We have likewise observed this *in vivo*, indicating that upregulation of the HSR with Arimoclomol ameliorates this pathological feature of IBM. Interestingly, a previous study has shown that activation of the HSR by expression of dominant active HSF1 or overexpression of HSPs in a cellular model of the TDP-43 proteinopathy can reduce the development of toxic cytoplasmic TDP-43 aggregates (Chen et al. 2016). Furthermore, the attenuation of other interrelated key pathologies observed in the muscle of mutant VCP mice, such as mitochondrial dysfunction, inflammation, macrophage infiltration and necrosis are likely a result of Arimoclomol facilitating the refolding and removal of toxic proteins and reducing inclusion body formation. Pharmacological upregulation of the HSR with Arimoclomol is therefore beneficial for ameliorating key degenerative and inflammatory features of IBM *in vivo*.

3.5.4. Pathomechanisms of IBM

The results of this *in vivo* study suggest that the degenerative components of IBM and impaired proteostasis contribute to the pathology of the disease. However, the primary cause of IBM is still yet to be elucidated. The varied pathological findings in IBM have led to a number of proposed hypotheses, including viral infections and autoimmune processes, mitochondrial changes, accumulation of misfolded proteins such as β -APP, endoplasmic reticulum (ER) stress, oxidative stress, calcium dyshomeostasis, impaired proteasomal function and autophagic pathways associated with ageing (Koffman et al. 1998; Badrising et al. 2004; Dalakas 2006a; Askanas et al. 2012; Askanas et al. 2015; Rygiel et al. 2015).

One of the main uncertainties in IBM is the role of TDP-43 in disease pathogenesis. The mislocalisation of TDP-43 is a key characteristic pathological hallmark of both IBM and MSP and a major sign of protein mishandling within muscle in patients (Weihl et al. 2008; Salajegheh et al. 2009). TDP-43 mislocalisation was also a clear characteristic feature in the muscle of mutant VCP mice. TDP-43-positive inclusions are also common to other neurodegenerative diseases, including ALS and FTD. TDP-43 is a RNA/DNA binding protein that structurally resembles a heterogeneous ribonuclear protein (hnRNP), comprising of two RNA recognition motifs and a glycine-rich C-terminal domain. The RNA recognition motifs mediate RNA recognition, as well as protein-protein interactions. Although TDP-43 is predominantly a nuclear protein, *in vitro* studies have shown that TDP-43 shuttles between the nucleus and cytoplasm, similar to many other hnRNPs (Ayala et al. 2008). However, the effect of TDP-43 inclusions on disease progression remains unclear.

TDP-43 is highly aggregation-prone, with the C-terminal domain critical for spontaneous aggregation and has been identified as a component of stress granules, which form in response to cellular stress (Johnson, B.S. et al. 2009). TDP-43 degradation is thought to be generated by caspase activation, upon induction of apoptosis, resulting in 35 kDa and 25 kDa toxic C-terminal cleavage products (Rutherford et al. 2008; Dormann et al. 2009; Zhang et al. 2009). As well as TDP-43, other novel hnRNPs, including hnRNPA1 and hnRNPA2B1, have been shown to be depleted from IBM myonuclei and accumulate in the

cytoplasm of IBM muscle (H.J. Kim, et al. 2013; Pinkus et al. 2014). Furthermore, transcriptomic analysis of frozen muscle biopsies from IBM patients has revealed widespread disruption in RNA metabolism (Cortese et al. 2014). Together, these results suggest that one aspect of IBM pathophysiology may involve misregulated RNA metabolism.

TDP-43 disruption has also been linked to impaired mitochondrial function. There have been suggestions that both wild-type and mutant TDP-43 can impair ER–mitochondria contacts in ALS and FTD (Stoica et al. 2014; Paillusson et al. 2016). In addition, other studies have found that mutant TDP-43 accumulates at the inner mitochondrial membrane, where it interacts with mitochondrial RNAs and results in disruption of mitochondrial bioenergetics (Wang et al. 2013; Wang et al. 2016; Wang et al. 2017). This may provide a link between the TDP-43 mislocalisation and mitochondrial damage in the muscle of the mutant VCP mice.

The marked mitochondrial damage and sarcoplasmic reticulum swelling within the muscle of the mutant VCP mice, as observed using TEM, as well as 3D imaging using serial block-face scanning electron microscopy (SBF SEM; Ahmed et al. 2016), was an interesting finding. A number of mitochondrial abnormalities and dysregulated mitochondrial dynamics have been reported in IBM biopsies, including ragged red fibres, cytochrome C oxidase (COX)-deficient fibres and increased succinate dehydrogenase (SDH) activity (Oldfors et al. 1993; Oldfors et al. 1995; Oldfors et al. 2006; Catalan-García et al. 2016). The mechanisms causing these activities are not yet clear, but abnormal mitophagy has been linked to ageing. Therefore it is possible that age is an important contributor to the pathogenesis of IBM (Palikaras & Tavernarakis 2012). In addition, a polymorphism in the “translocase of outer mitochondrial membrane 40” (TOMM40) gene, encoding the mitochondrial pore protein TOMM40, which is involved in the transport of A β and other proteins into mitochondria, has been shown to influence IBM disease risk and age of onset (Mastaglia et al. 2013; Gang, Conceicao Bettencourt, et al. 2015). This is further evidence suggesting a possible link between mitochondria and IBM pathogenesis.

Although EM can play an important role in differentiating normal and pathological muscle, due to the higher resolution images which can be obtained, the technique has some downfalls. In particular, artefacts may be induced during preparation of the tissue. There are numerous steps which samples undergo prior to examination and thus non-pathological alterations in muscle structure can easily occur (Sewry 2002). Although quantification of the number of disrupted mitochondria was not undertaken in this study, distinguishing between pathological features and changes caused by the fixation and embedding processes could be challenging. Furthermore, mitochondria are dynamic structures, continuously undergoing fission and fusion processes. Since these images were taken at a fixed, single time point, there may be great deal of variation among muscle tissue from different animals. Additional analysis of mitochondrial function of isolated mitochondrial from muscle may therefore be beneficial.

Finally, the accumulation of protein aggregates within the muscle of the mutant VCP mice suggests an interruption of protein handling networks. Ubiquitin targets substrates for degradation and p62 directly interacts with ubiquitin and LC3 to act as a shuttle protein, transporting ubiquitinated proteins into the autophagosome or lysosome (Pankiv et al. 2007; Ichimura et al. 2008; Kirkin et al. 2009; Komatsu & Ichimura 2010). An increase in expression of these proteins suggests that there is a disturbance in proteostasis, namely an increase in abnormal misfolded or damaged proteins or disruption to the clearance of protein aggregates. Impairment of autophagy has been proposed to underlie IBM pathogenesis as autophagic, lysosomal, and endosomal protein markers have been identified within and surrounding characteristic rimmed vacuoles, which are present in the muscle of IBM patients (Askanas & Engel 2005; Weihl & Pestronk 2010; Güttsches et al. 2016). Furthermore, as VCP plays an essential role in autophagy, it is not surprising that muscle of MSP patients also accumulates autophagosome-associated proteins including LC3 and p62, which localise to rimmed vacuoles (Evangelista et al. 2016; Papadopoulos et al. 2017; Yeo & Yu 2016). P62- and LC3-positive rimmed vacuoles were also present within the muscle of mutant VCP mice. In this study, an antibody which recognises both LC3-I and LC3-II was used. LC3-I, is found in the cytoplasm and is converted to LC3-II, which is membrane-bound, to

initiate formation and maturation of the autophagosome (Tanida et al. 2008). As LC3-II and p62 are sequestered into autophagosomes and degraded in the autolysosome, increased expression of these proteins may indeed indicate an inhibition of autophagy. Furthermore, other studies investigating VCP mutations in mice have found stimulated autophagic vesicle accumulation and abnormalities of autophagosome maturation (Ju et al. 2009; Tresse et al. 2010; Bayraktar et al. 2016). Disrupted autophagy may therefore represent a common pathomechanism between IBM and MSP.

Gaining a greater understanding of the complex pathomechanisms of IBM is vital for aiding the discovery of novel treatment strategies. Our established *in vitro* and *in vivo* models will provide useful tools for further investigating the underlying mechanisms related to the observed pathology in IBM.

3.6 Conclusion

Together with previous findings from our lab demonstrating that Arimoclomol reduces pathology in cellular models of IBM, the results of this Chapter show that Arimoclomol also ameliorates key IBM-like degenerative and inflammatory features *in vivo*, in a mutant VCP mouse model of MSP.

As IBM is a sporadic condition, it is not possible to directly model the disease *in vivo*. However MSP, caused by mutations within the VCP gene, displays muscle pathology similar to that seen in IBM patients. Despite the pathomechanisms of both IBM and MSP being unclear, the overlap between the two diseases suggests that disrupted protein handling plays a key role in the development of both diseases. Thus, the VCP mutant mouse model represents a relevant model and useful tool for examining the effects of HSR upregulation, in order to restore the balance of protein homeostasis in IBM.

The combined series of experiments *in vitro* and *in vivo*, demonstrates that Arimoclomol targets both of the major components of IBM and supports further investigation of Arimoclomol for the treatment of IBM. Our established preclinical models of IBM will now be instrumental in gaining a greater understanding of the complex pathomechanisms involved in IBM and will have a vital role for aiding the discovery of other novel therapeutic agents.

Chapter 4

Targeting the heat shock response to reduce the pathological features of sporadic IBM in patient-derived fibroblasts

4.1. Introduction

Upregulating the heat shock response (HSR) with Arimoclomol ameliorates pathology in both rat *in vitro* models of IBM (Ahmed et al. 2016) and in an *in vivo* mouse model of MSP (discussed in Chapter 3 of this Thesis), by improving protein mishandling. In order to further investigate the pathomechanisms underlying IBM in a more translatable model and to be able to screen novel therapeutic compounds, a relevant human model would be beneficial. For this reason, the inherent cellular changes in fibroblasts derived from sporadic IBM patients were examined next, to (i) confirm whether these patient-derived cells develop a disease relevant phenotype and (ii) confirm whether the beneficial effects of Arimoclomol were recapitulated in these human cells obtained from sporadic IBM patients.

4.1.1. Advantages of fibroblasts as a cellular model of disease

Human dermal fibroblasts are essential components of skin, responsible for synthesising and organising collagen and other proteins of the extracellular matrix. They also play a role in regulating skin physiology by communicating with each other and other cell types (Pieraggi et al. 1985). Fibroblasts can easily be grown as a monolayer culture on plastic substrates, whilst retaining many of their phenotypic characteristics. This makes them an excellent system in which to model many aspects of cellular and molecular physiology. In particular, fibroblasts are a useful tool for dissecting the pathological mechanisms of complex diseases and investigating new therapies.

There are many advantages to using patient-derived fibroblasts over other models of disease (Auburger et al. 2012). In contrast to muscle biopsies, from which myoblasts and mesoangioblasts (capable of differentiating into skeletal muscle) are obtained (McFerrin et al. 1999; Broccolini et al. 2006; Morosetti et al. 2006; Morosetti et al. 2010), skin punch biopsies from which dermal fibroblasts can be easily isolated, are a minimally invasive and routine procedure for patients, meaning fewer ethical concerns than alternative models. Fibroblasts can thus be obtained repeatedly with ease if required. As well as being readily obtainable, fibroblasts are simple to maintain and associated costs are relatively low. They can be rapidly expanded to large quantities due to their

comparatively fast proliferation rates and thus provide a sufficient source of cells in which the study of normal and pathological states in a controlled environment can be examined. Furthermore, the rapid generation of results that can be obtained is advantageous in terms of screening novel therapeutic compounds. Finally, the robustness and durability of fibroblasts means they are amenable to a variety of manipulations, such as genetic alterations and the induction of cellular stress. However, as patient-derived fibroblasts possess the native genetic background of the patient, they express any disease-causing mutations at physiological levels, unlike over-expression models, and so they do not typically require any further genetic manipulation, making them a desirable cellular model.

4.1.2. Fibroblasts as a model of human disease

Fibroblasts have been used extensively in a wide range of cellular and molecular studies. Several studies have used patient fibroblasts as a model to investigate the mechanisms of neurodegenerative diseases, including Huntington's disease (del Hoyo et al. 2006; Fernandez-Estevez et al. 2014; Marchina et al. 2014; Al-Ramahi et al. 2017), familial and sporadic forms of Alzheimer's disease (Area-Gomez et al. 2012; Pérez et al. 2017) and Parkinson's disease (Musanti et al. 1993; Mytilineou et al. 1994; Wiedemann et al. 1999; del Hoyo et al. 2010; Ambrosi et al. 2014; Teves et al. 2017).

Fibroblasts have also been shown to mimic classic pathological features in the neurodegenerative disease amyotrophic lateral sclerosis (ALS). Fibroblasts derived from ALS patients carrying mutations in *SOD1*, *TARDBP*, *FUS* and *C9ORF72* amongst others have been shown to display TDP-43 mislocalisation and aggregation, increased expression of *FUS* and ubiquitin, and mitochondrial dysfunction, both under normal conditions and under induced stress (Solski et al. 2012; Williams et al. 2012; Prause et al. 2013; Allen et al. 2014; Schwartz et al. 2014; Sabatelli et al. 2015; Yang et al. 2015; Liu et al. 2016; Konrad et al. 2017; Straub et al. 2018).

As dermal fibroblasts are a long-lived cell population which accumulate cellular damage over time, it is also possible to investigate ageing processes manifesting in dermal fibroblasts, including the loss of proteostasis that occurs

with age (Tigges et al. 2014; Waldera-Lupa et al. 2014). Many of these studies involve dermal fibroblasts subjected to ageing in culture, as opposed to primary dermal fibroblasts derived from elderly donors. However, it is hoped that such studies may help to differentiate the processes underlying normal ageing from age-related diseases, such as IBM.

4.1.3. Fibroblasts as a model of IBM

Despite fibroblasts being a desirable model due to their unique advantages as already discussed, thus far, it has not been investigated whether fibroblasts derived from patients with sporadic IBM display characteristic pathological features.

Fibroblasts derived from patients with multisystem proteinopathy (MSP), presenting with an inclusion body myopathy, have been shown to display IBM-like pathological features, including TDP-43 mislocalisation, mitochondrial abnormalities and increased expression of ubiquitin, LC3 and p62 (Nalbandian, Llewellyn, Gomez et al. 2015; discussed in more detail in Chapter 5). It is therefore possible that functional and pathological abnormalities may also be present in fibroblasts obtained from patients with sporadic IBM.

4.2. Aims of this Chapter

Patient-derived fibroblasts may represent a powerful and minimally invasive tool to investigate the pathogenic mechanisms of IBM and assess the effects of novel therapeutic compounds. To date, the cellular health and pathology in fibroblasts from sporadic IBM patients has not been investigated. However, as patient-derived fibroblasts have been shown to recapitulate hallmarks of a number of neurodegenerative diseases, it is possible that IBM-related cellular changes may be reproduced in fibroblasts derived from sporadic IBM patients. These cells may therefore represent a useful model to complement our previous *in vitro* and *in vivo* studies in mice, described previously in this Thesis. Thus, the overall objectives of this Chapter were to investigate if sporadic IBM patient fibroblasts display phenotypic changes of IBM, thereby providing a more clinically relevant human model in which to investigate the effects of pharmacologically upregulating the HSR with Arimocloamol.

The specific aims of this Chapter were:

- (1) To examine whether fibroblasts derived sporadic IBM patients exhibit key pathological features of IBM.
- (2) To investigate the effects of co-inducing the HSR with Arimoclomol on sporadic IBM patient-derived fibroblasts.

4.3. Materials and methods

A full description of the materials and methods used in this Chapter are presented in Chapter 2, and include the following:-

4.3.1. Fibroblasts lines

Sporadic IBM patient fibroblasts were received from Dr Josep Maria Grau Junyent (University of Barcelona, Spain). Skin biopsies were obtained from individuals above 50 years old who had attended the Internal Medicine Department of the Hospital Clinic of Barcelona and were diagnosed with sporadic IBM according to the criteria of the European Neuromuscular Centre. All individuals were informed, and signed written consent was obtained for inclusion in this study, which was approved by the Ethical Committee of the hospital, following the Declaration of Helsinki.

Control fibroblasts were obtained from Professor Hanns Lochmüller at the MRC Centre Neuromuscular Biobank (Newcastle University). Collection of samples from patients and their use in research have been ethically approved by the 'Newcastle and North Tyneside 1 Research Ethics Committee' with REC reference number 08/HO906/28 + 5, with signed written consent obtained from patients.

Fibroblast lines were established following the protocol in Chapter 2 (section 2.12). The specific human fibroblast cells lines are detailed in **Table 3**. All sporadic IBM patients answered the Inclusion Body Myositis Functional Rating Scale (IBMFRS) test, which is a validated, disease-specific test to assess disease severity. A higher score, maximum 40, indicates greater functional status of the patient.

4.3.2. Immunocytochemistry

Human dermal fibroblasts were immunostained using the protocol described in Chapter 2 (section 2.14). The antibodies used are detailed in **Table 4**. Fibroblasts were co-stained with the nuclear marker DAPI and/or F-actin-binding Alexa Fluor 488 Phalloidin.

	Gender	Age at biopsy	IBMFRS
Control 1	F	45	-
Control 2	F	47	-
Control 3	M	47	-
Control 4	F	66	-
IBM patient 1	F	67	16
IBM patient 2	M	51	16
IBM patient 3	M	67	24
IBM patient 4	M	77	28

Table 3. Sporadic IBM patient fibroblasts

Details of the patient fibroblasts used in this study, including gender age at biopsy and Inclusion Body Myositis Functional Rating Scale (IBMFRS) scores, indicating disease severity.

Primary antibody	Application	Dilution	Source	Supplier
TDP-43 (C-terminal epitope)	IF	1:500	Rabbit polyclonal	ProteinTech 12892-1-AP
Ubiquitin	IF	1:500	Mouse monoclonal	GeneTex GTX78236
Ubiquitin	WB	1:500	Rabbit polyclonal	Dako Z0458
p62	IF	1:100	Mouse monoclonal	Abcam ab56416
G3BP	IF	1:200	Mouse monoclonal	Abcam ab56574
TOMM20	IF, WB	1:400, 1:900	Rabbit polyclonal	Abcam ab78547
Lamin A/C	IF	1:50	Mouse monoclonal	Santa Cruz sc-376248
Emerin	IF	1:50	Mouse monoclonal	Santa Cruz sc-376248
HSP70	IF	1:100	Mouse monoclonal	Santa Cruz sc24

Table 4. Primary antibodies used in Chapter 4 for the study of sporadic IBM fibroblasts

Description of primary antibodies used within this Chapter. IF = immunofluorescence; WB = western blot.

4.3.3. Western blot

Western blot was performed to determine protein levels as described in Chapter 2 (section 2.15). Membranes were incubated with the primary antibodies indicated in **Table 4**.

4.3.4. Disrupted nuclei counts

The percentage of cells with morphological nuclear abnormalities was assessed according to the protocol described in Chapter 2 (section 2.16). Counts in approximately 400-800 cells were undertaken in each of the 4 control and 4 patient cell lines.

4.3.5. TUNEL assay

For detection of apoptosis cells were labelled with the TACS 2 TdT DAB (diaminobenzidine) Kit. Full details are given in Chapter 2 (section 2.17).

4.3.6. Arimoclomol treatment

Fibroblasts were treated with Arimoclomol following the protocol described in Chapter 2 (section 2.13). Fibroblasts were treated with the following concentrations of Arimoclomol; 10 μ M, 50 μ M, 100 μ M, 400 μ M.

4.3.7. Statistical analysis

Analyses were performed as described in Chapter 2 (section 2.18). For analysis of disrupted nuclei, experimental groups were compared using a one-way or two-way analysis of variance (ANOVA) with Tukey's all pairwise multiple comparisons *post hoc* analysis. All data analysis was performed blind. All data are presented as mean \pm SEM.

4.4. Results

In order to assess the effects of upregulating the HSR in a human model of IBM, it first had to be established whether dermal fibroblasts derived from IBM patients display disease-relevant pathologies *in vitro*. To achieve this, immunofluorescent staining was performed to examine the distribution of IBM-associated proteins in patient fibroblasts and age-matched control human fibroblasts under basal culture conditions.

4.4.1. Sporadic IBM patient fibroblasts display aggregation of key IBM proteins under basal culture conditions

One of the characteristic hallmarks of IBM, which was recapitulated in the *in vivo* mutant VCP mouse model of MSP, is the mislocalisation of TDP-43 from the nucleus to the cytoplasm and the formation of TDP-43 immunoreactive cytoplasmic inclusions in muscle fibres. Using an antibody that recognises the TDP-43 C-terminal cleavage product, in addition to phosphorylated and native forms, TDP-43 distribution was investigated in all fibroblast cell lines. In age-matched control fibroblasts under basal conditions, TDP-43 was almost exclusively localised to the nucleus, with nuclei displaying intense TDP-43 immunoreactivity. In contrast, in sporadic IBM patient fibroblasts, TDP-43 was mislocalised to the cytoplasm, displaying a diffuse cytoplasmic distribution (**Fig. 4.1 A-B**). Whilst some TDP-43 was still retained within the nuclei, a proportion of fibroblasts displayed evidence of nuclear depletion (**Fig. 4.1 C**). These abnormalities were observed within sporadic IBM fibroblasts of all patient cell lines.

Ubiquitin is another major component identified in abnormal protein aggregates in sporadic IBM patient muscle and is responsible for tagging proteins for degradation and facilitating protein unfolding. Whilst there was low, evenly distributed ubiquitin expression throughout the cytoplasm in a small number of control fibroblasts, ubiquitin-positive inclusions were evident in all sporadic IBM fibroblast cell lines (**Fig. 4.2 A**). Western blot analysis confirmed a significant 1.5-fold increase in ubiquitin expression in patient fibroblasts compared to age-matched controls ($p < 0.05$, unpaired t-test; **Fig. 4.2 B**).

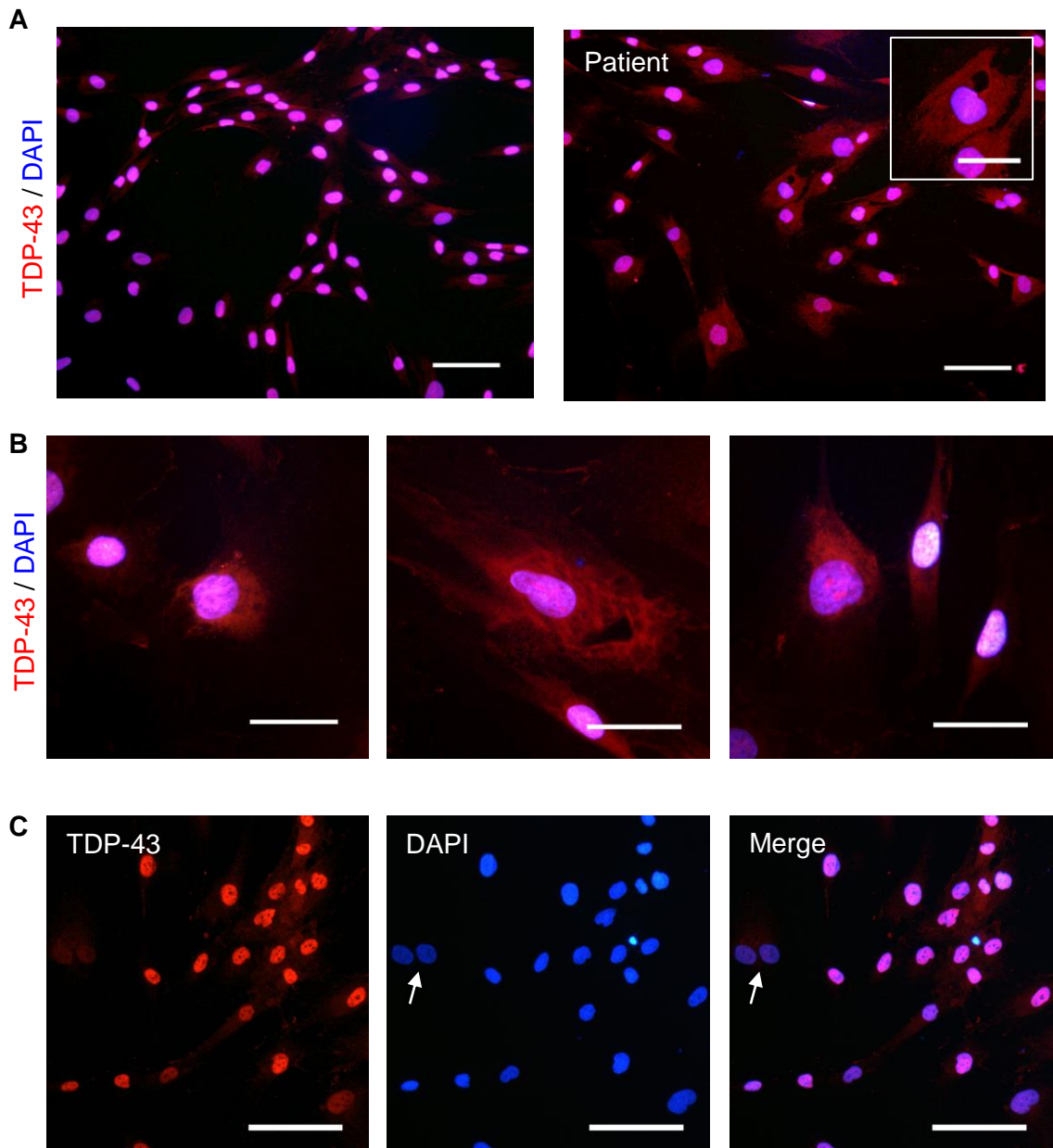


Figure 4.1. TDP-43 is mislocalised from the nucleus to the cytoplasm and shows evidence of nuclear depletion in sporadic IBM fibroblasts under basal culture conditions

(A) Immunostaining of age-matched control fibroblasts and sporadic IBM patient fibroblasts for TDP-43 (red) and co-stained with the nuclear marker DAPI (blue). Scale bars represent 50 μm. Inserts show high-power images (scale bars: 20 μm). **(B)** Representative high-power images of sporadic IBM patient fibroblasts displaying diffuse cytoplasmic distribution of TDP-43. Scale bars represent 20 μm. **(C)** Representative images of sporadic IBM patient fibroblasts demonstrating nuclear depletion of TDP-43. Scale bars represent 50 μm.

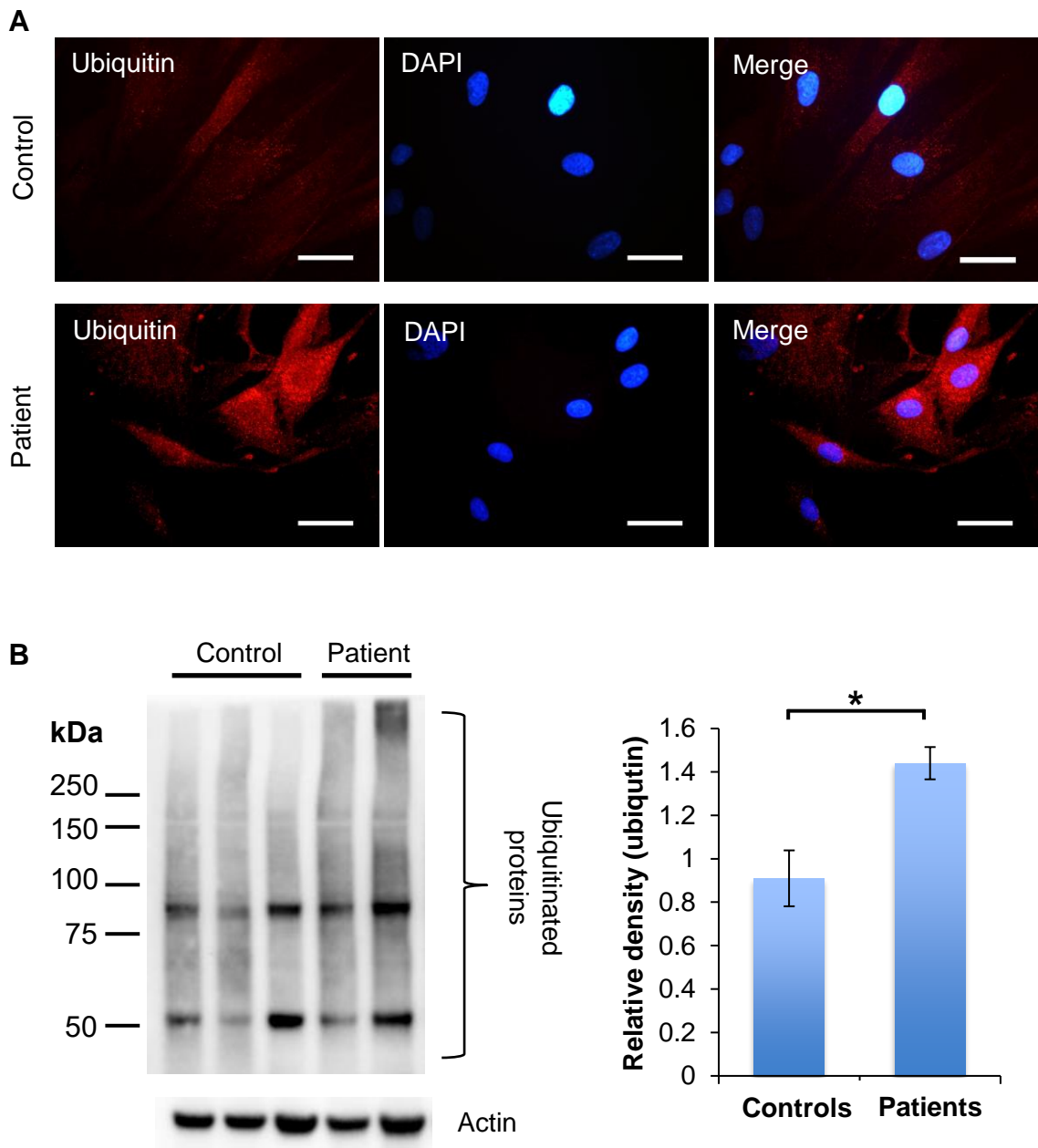


Figure 4.2. Sporadic IBM fibroblasts display ubiquitin-positive aggregates

(A) Immunostaining of age-matched control fibroblasts and sporadic IBM patient fibroblasts with ubiquitin (red) and co-stained with the nuclear marker DAPI (blue). Scale bars represent 20 μm . **(B)** Western blot of ubiquitin expression in control and sporadic IBM patient fibroblasts under basal culture conditions. The bar chart shows the mean relative optical density of the bands in the western blot, normalised to the loading control (actin). Error bars= SEM. N= 3 controls, 2 patients. * $p < 0.05$; unpaired t-test.

Since the shuttle protein p62 is important for transporting polyubiquitinated proteins for degradation and accumulates in muscle cells in IBM, the distribution of this protein was examined in patient fibroblasts. Whilst there was no evidence of p62 aggregation in control fibroblasts, fibroblasts from sporadic IBM patients showed numerous aggregates of p62, both within the cytoplasm and the nucleus (**Fig. 4.3 A-B**). P62 was also found lining large, cytoplasmic vacuoles (**Fig. 4.3 C**), characteristic of 'rimmed vacuoles' in IBM muscle.

4.4.2. Sporadic IBM patient fibroblasts show no evidence of stress granule-like aggregates

Under conditions of cellular stress, translational arrest leads to the aggregation of untranslated mRNAs and mRNA-binding proteins, into specific cytoplasmic structures known as stress granules. Stress granules accumulate in several neurodegenerative diseases and are also present in affected tissues in IBM patients. In order to examine stress granule formation in sporadic IBM patient fibroblasts, the distribution of GTPase-activating protein-binding protein 1 (G3BP), an RNA-binding protein that localises to stress granules under conditions of cellular stress, was examined. A number of patient cells had diffuse cytoplasmic microgranulation of G3BP but no G3BP-positive aggregates were observed (**Fig. 4.4**). There was minimal expression in control fibroblasts.

4.4.3. Sporadic IBM patient fibroblasts display evidence of mitochondrial disruption

Since mitochondrial dysfunction has been implicated in the pathogenesis of IBM (Rygiel et al. 2015; Catalan-García et al. 2016), the mitochondrial morphology of sporadic IBM patient fibroblasts was investigated using an antibody against the mitochondrial outer membrane marker, translocase of outer mitochondrial membrane 20 (TOMM20). Healthy control fibroblasts displayed a highly organised and interconnected tubular mitochondrial network that extended from the nuclear envelope to the plasma membrane (**Fig. 4.5 A(i)**). A typical single mitochondrion was thin and straight with frequent branching. In contrast, in sporadic IBM patient fibroblasts, mitochondria appeared smaller and more fragmented (**Fig. 4.5 A(ii), B**). However, there was no significant difference in the expression of TOMM20 between control and patient fibroblasts (**Fig. 4.5 C**).

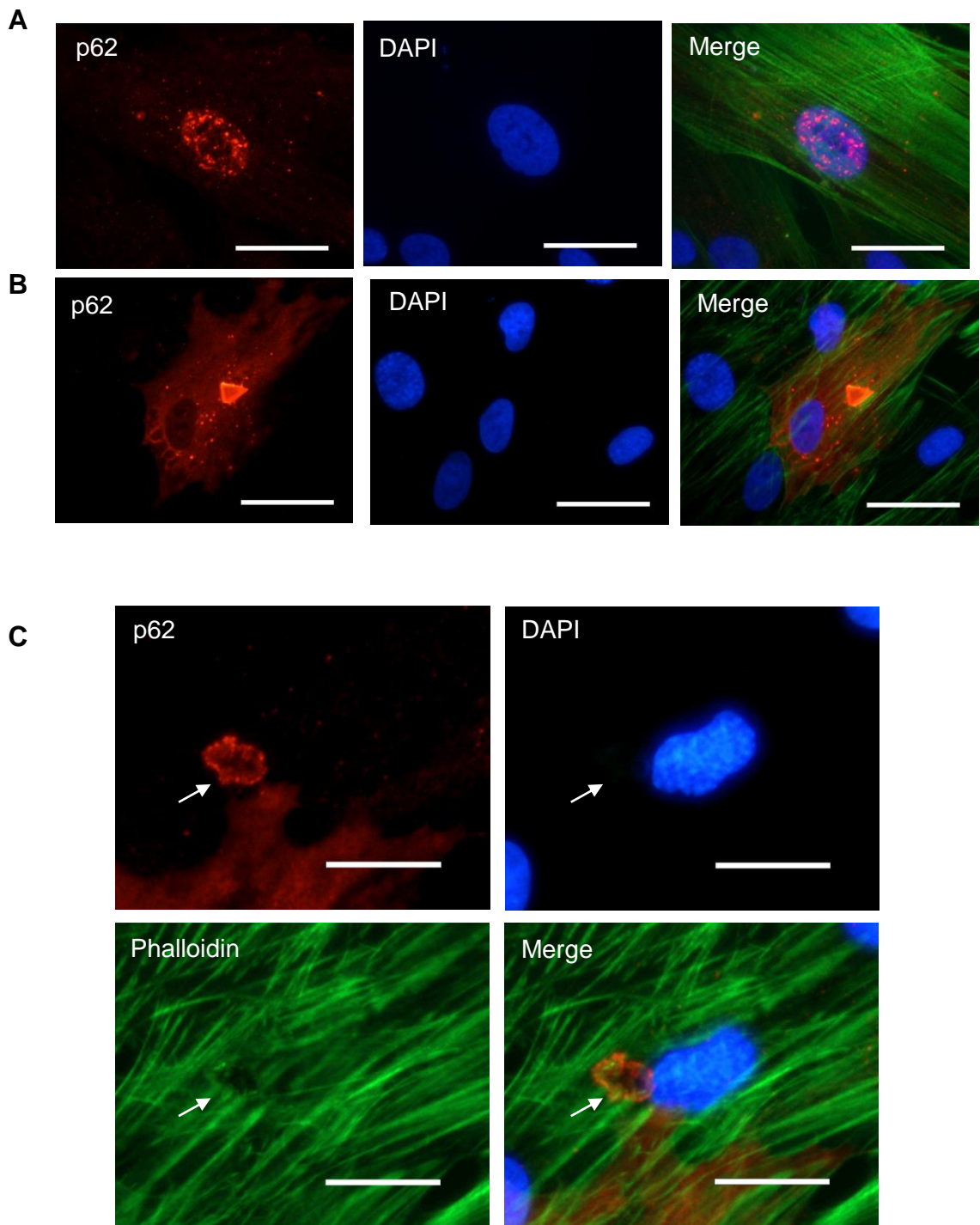


Figure 4.3. Sporadic IBM fibroblasts display p62-positive aggregates and rimmed vacuoles

Fibroblasts from sporadic IBM patient were immunostained for p62 (red) and co-stained with the nuclear marker DAPI (blue) and F-actin-binding Alexa Fluor 488 phalloidin (green). Both nuclear **(A)** and cytoplasmic **(B)** p62-positive aggregates were observed. Scale bars represent 20 μm . **(C)** Representative image of a 'rimmed vacuole', lined with p62 (arrow). Scale bars represent 10 μm .

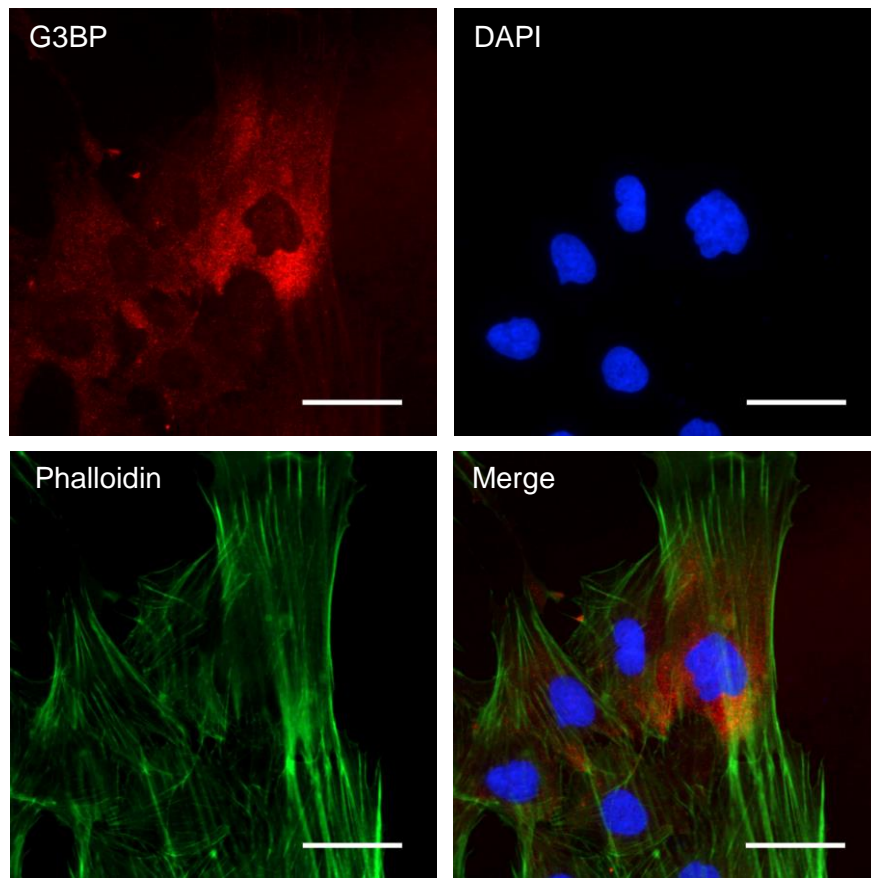


Figure 4.4 Sporadic IBM patient fibroblasts show no evidence of stress granule-like aggregates

Representative image of G3BP immunostaining (red) in sporadic IBM patient fibroblasts. The cells were co-stained with F-actin-binding Alexa Fluor 488 phalloidin (green) and DAPI (blue). Scale bars represent 20 μm .

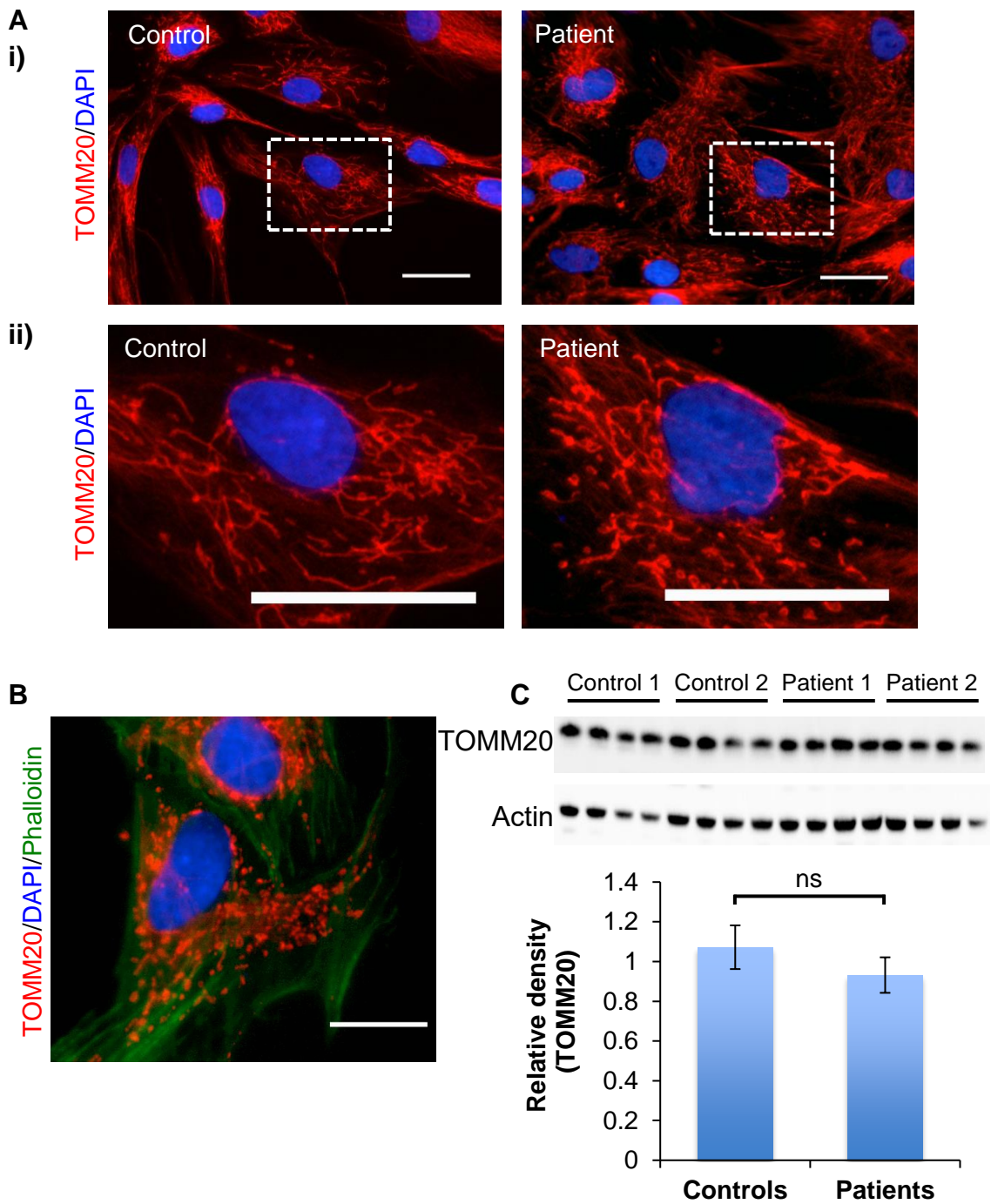


Figure 4.5. Sporadic IBM fibroblasts display alterations in mitochondrial morphology

(A) Immunostaining of age-matched control fibroblasts and sporadic IBM patient fibroblasts for **(i)** TOMM20 (red), co-stained with the nuclear marker DAPI (blue). Cells in the highlighted boxes are shown at higher magnification **(ii)**. Scale bars represent 20 μm . **(B)** Representative image of fragmentation of mitochondria in sporadic IBM patient fibroblasts co-stained with F-actin-binding Alexa Fluor 488 phalloidin (green). Scale bars represent 10 μm . **(C)** Western blot analysis of TOMM20 expression in control and IBM patient fibroblasts under basal culture conditions. The bar chart shows the mean relative optical density of the bands in the western blot, normalised to the loading control (actin). Error bars= SEM. N= 2 per group (repeated in 4 independent cultures).

4.4.4. Sporadic IBM patient fibroblasts have abnormal nuclear morphology

Morphologically abnormal myonuclei have previously been observed in muscle from sporadic IBM patients (Carpenter et al. 1978; Greenberg et al. 2006). To investigate nuclear morphology in sporadic IBM patient fibroblasts, cells were labelled with the nuclear marker DAPI and counts of approximately 400-800 cells from each of the patient and age-matched control cell lines were undertaken. In control fibroblasts the nuclei were mostly regular in size and shape, being round or oval (**Fig. 4.6 A**). Sporadic IBM patient fibroblasts on the other hand, displayed variations in nuclear shape, with a number of nuclear abnormalities observed, including protrusions of the nuclear surface, herniations and fragmentation of nuclei leading to the generation of micronuclei (**Fig. 4.6 B-D**). Whilst a small percentage of nuclei in control fibroblasts displayed some signs of minor irregularities in nuclear envelope shape, typically displaying abnormal crevices as opposed to more severe herniations and fragmentations, sporadic IBM patient fibroblasts had a significantly greater amount of disrupted nuclei ($14.1 \pm 0.4\%$ vs $22.7 \pm 2.1\%$ respectively; $p < 0.05$; unpaired t-test; **Fig. 4.6 E**). However, these fibroblasts showed no evidence of apoptosis, as assessed by a TUNEL assay (**Fig. 4.6 F**).

4.4.5. Abnormal nuclei in sporadic IBM patient fibroblasts are associated with a disrupted actin cytoskeleton

All fibroblasts were co-stained with Alexa Fluor 488 phalloidin, which selectively binds to F-actin, in order to visualise the cytoskeletal organisation of the cells. Although fibroblasts have a varied morphology, control fibroblasts were typically large, flat and elongated, with normal bundles of actin filaments and processes extending out from the ends of the cell body (**Fig. 4.7**). A large proportion of sporadic IBM patient fibroblasts also displayed this typical morphology. However, those with disrupted nuclei were found to be associated with a disrupted actin cytoskeleton, with fewer, finer and shorter actin filaments (**Fig. 4.7**).

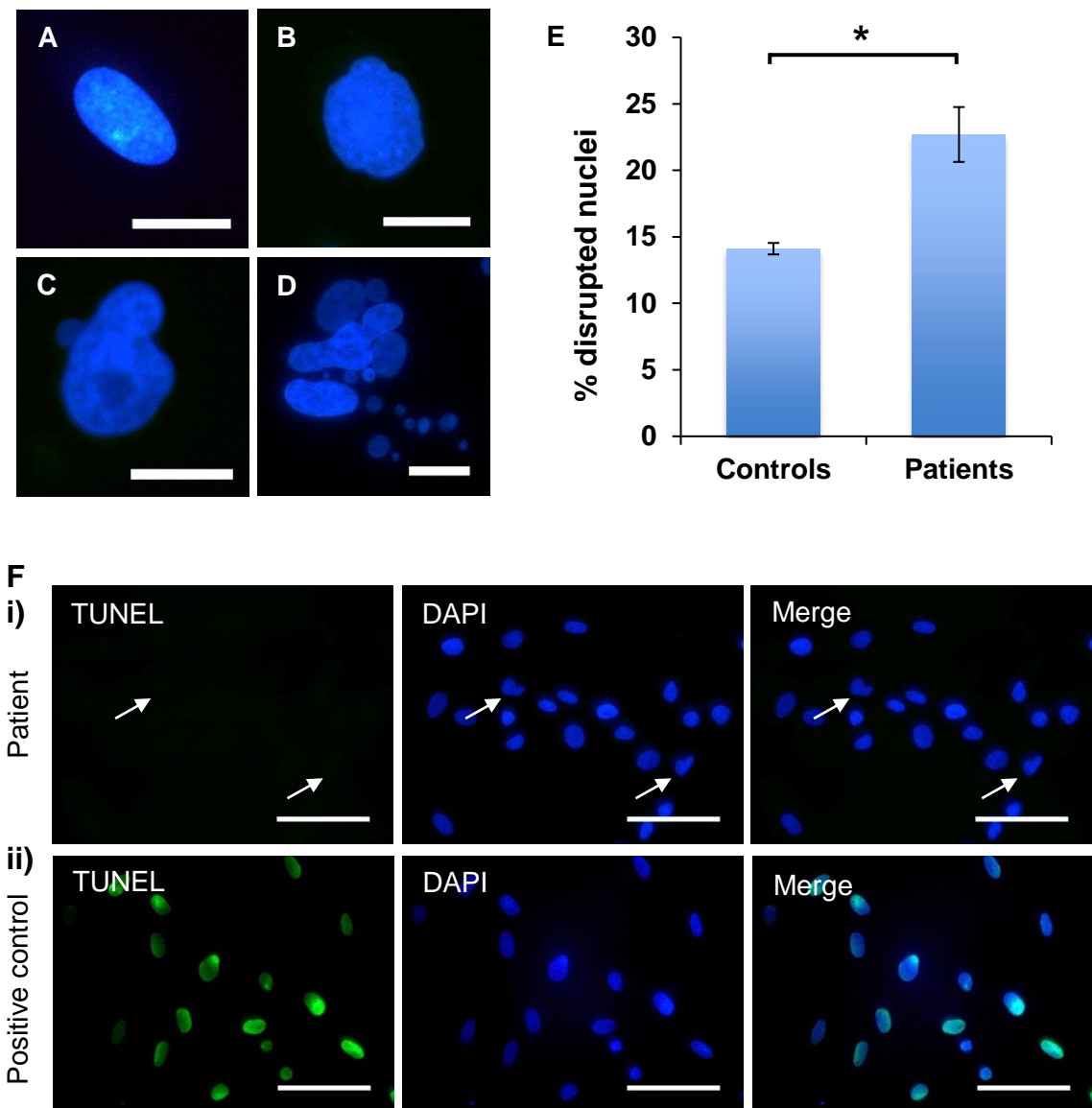


Figure 4.6. Sporadic IBM patient fibroblasts have abnormal nuclear morphology but show no evidence of apoptosis

Micrographs of nuclei from control and patient fibroblasts labelled with the nuclear marker DAPI (blue). Representative images showing (A) a nucleus from a control fibroblast with normal spheroid shape and (B-D) disrupted nuclear envelopes in sporadic IBM patient fibroblasts. The range of abnormal nuclear morphologies observed in sporadic IBM patient fibroblasts include (B) crevices in the nuclear periphery, (C) herniations and (D) fragmentation of nuclei leading to the generation of micronuclei. Scale bars represent 10 μ m. (E) The bar chart shows the average percentage of disrupted nuclei in control and IBM patient fibroblasts Error bars= SEM. N=4 per group (approximately 2000 cells per group). * $p < 0.05$; unpaired t-test. (F) TUNEL analysis (green) of sporadic IBM patient fibroblasts (i) and a TACS-Nuclease-treated positive control sample (ii). Arrows indicate disrupted nuclei that are TUNEL-negative. The cells were co-stained with DAPI (blue). Scale bars represent 50 μ m.

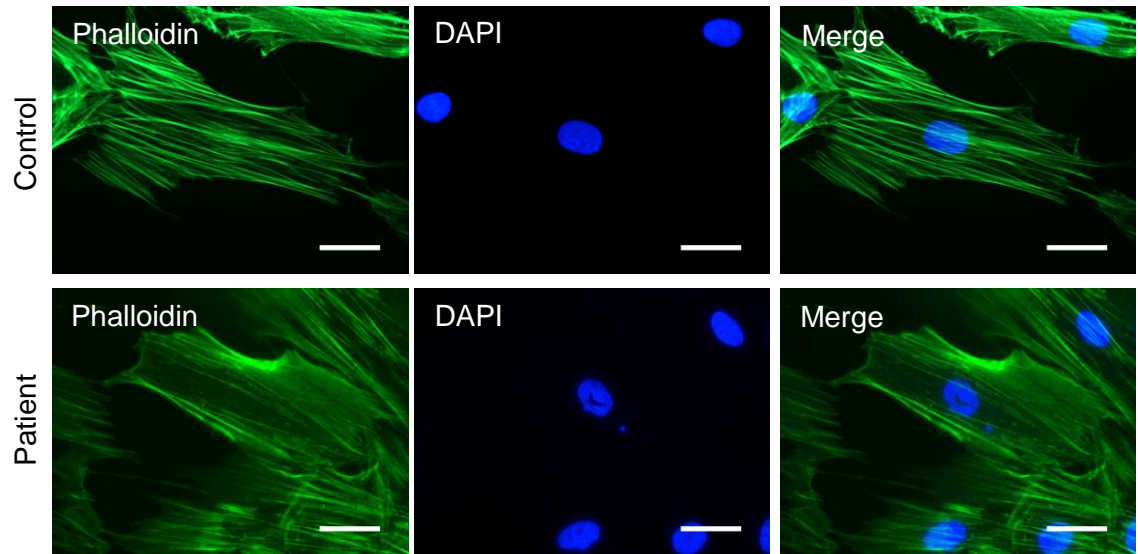


Figure 4.7. Abnormal nuclei in sporadic IBM patient fibroblasts are associated with a disrupted cytoskeleton

Representative images of F-actin-binding Alexa Fluor 488 phalloidin (green) in control and sporadic IBM patient fibroblasts. The cells were co-stained with the nuclear marker DAPI (blue). Scale bars represent 20 μm .

4.4.6. Sporadic IBM patient fibroblasts display predominantly normal localisation of nuclear envelope markers

In addition to myonuclear abnormalities, nuclear membrane proteins have been identified in rimmed vacuoles in sporadic IBM patient muscle biopsies (Nalbantoglu et al. 1994; Greenberg et al. 2006; Fidzianska et al. 2008; Nakano et al. 2008; Greenberg 2009). Fibroblasts were therefore immunostained with antibodies for the nuclear envelope markers lamin A/C and emerin. In control fibroblasts, lamin A/C and emerin were detected diffusely throughout the nuclei, with a distinct nuclear rim stain indicating its location at the nuclear envelope (**Fig. 4.8 A-B**). Fibroblasts derived from sporadic IBM patients again showed irregularly shaped nuclei and blebbing of the nuclear membrane. The majority of sporadic IBM patient fibroblasts displayed no gross abnormalities in the distribution of lamin A/C and emerin (**Fig. 4.8 A-B**), although cytoplasmic granules of lamin A/C were occasionally observed in sporadic IBM patient fibroblasts (**Fig. 4.8 C**). A small proportion of sporadic IBM patient fibroblasts also displayed folds in the nuclear envelope, which appeared as strongly stained linear and branched structures. Normal staining of the nuclear membrane was still retained, however, and there was no evidence of either of these proteins surrounding vacuoles. Co-labelling of nuclei with DAPI did not demonstrate a gross detachment between the nuclear envelope and chromatin, even in the most abnormally shaped nuclei and lamin A/C and emerin labelling were still detected in the herniated areas of nuclei (**Fig. 4.8 C**).

In summary, the following pathological features were observed in sporadic IBM patient fibroblasts: (i) cytoplasmic mislocalisation and nuclear depletion of TDP-43, (ii) ubiquitin- and p62-positive aggregates, (iii) p62-lined rimmed vacuoles, (iv) mitochondrial disruption, (v) abnormal nuclear morphology and (vi) a disrupted actin cytoskeleton. Since fibroblasts derived from sporadic IBM patients show key IBM-like pathological characteristics under basal culture conditions, the effects of upregulating the HSR were assessed using this model.

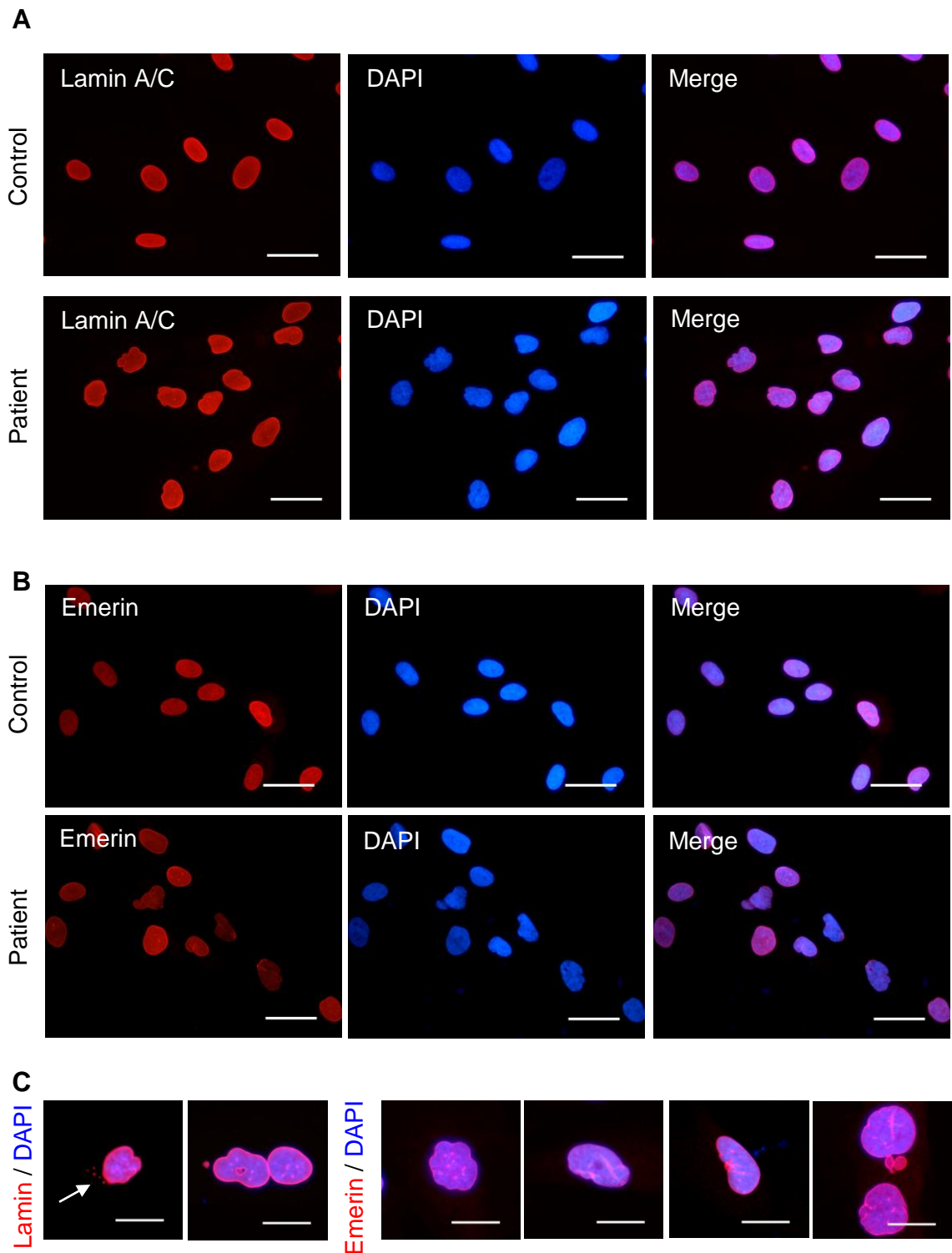


Figure 4.8. Sporadic IBM patient fibroblasts display predominantly normal localisation of nuclear envelope markers

Representative images of control and sporadic IBM patient fibroblasts labelled with **(A)** lamin A/C (red) and **(B)** emerin (red), co-stained with the nuclear marker DAPI (blue). Scale bars represent 20 μm . **(C)** Higher magnification images demonstrating disruption of lamin A/C and emerin organisation in sporadic IBM patient fibroblasts. Arrow indicates displacement of lamin A/C into the cytoplasm. Scale bars represent 10 μm .

4.4.7. Pharmacological upregulation of the heat shock response reduces the number of disrupted nuclei in sporadic IBM patient fibroblasts

In order to clarify whether the effects of Arimoclomol reported in the mouse model of MSP in Chapter 3 were recapitulated in this human model of sporadic IBM, the effect of Arimoclomol was assessed on the percentage of disrupted nuclei. As Arimoclomol has not been previously tested in human fibroblasts, four concentrations were assessed (10, 50, 100 and 400 μM). This was given as a single dose and fibroblasts fixed 24 hours later.

In sporadic IBM patient fibroblasts, treatment with all four concentrations of Arimoclomol decreased the percentage of disrupted nuclei. The greatest effect was seen with 400 μM of Arimoclomol, which significantly reduced the percentage of abnormal nuclei to almost control levels ($26.1 \pm 3.1\%$ vs $12.9 \pm 2.2\%$; $p < 0.01$; two-way ANOVA; **Fig. 4.9**). Arimoclomol had no effect on the percentage of disrupted nuclei in age-matched control fibroblasts.

4.4.8. HSP70 expression in sporadic IBM fibroblasts following Arimoclomol treatment

It has previously been shown that Arimoclomol results in activation of HSF1 and an upregulation in the expression of HSP70 (Kieran et al. 2004; Kalmar et al. 2008; Malik et al. 2013; Parfitt et al. 2014; Ahmed et al. 2016; Kirkegaard et al. 2016). In order to examine whether Arimoclomol increase HSP70 levels in patient-derived fibroblasts, immunofluorescent staining was performed. No obvious difference was observed in the expression of HSP70 between untreated control and sporadic IBM patient fibroblasts (**Fig. 4.10 A(i-ii)**). Furthermore, there was no increase in HSP70 expression in sporadic IBM patient fibroblasts, 24 hours following treatment with Arimoclomol (**Fig. 4.10 A(iii)**). This was the case with all concentrations of Arimoclomol. However, in untreated sporadic IBM patient fibroblasts, cytoplasmic aggregates of HSP70 were observed, which were not apparent in age-matched control fibroblasts or Arimoclomol-treated patient fibroblasts (**Fig. 4.10 B**).

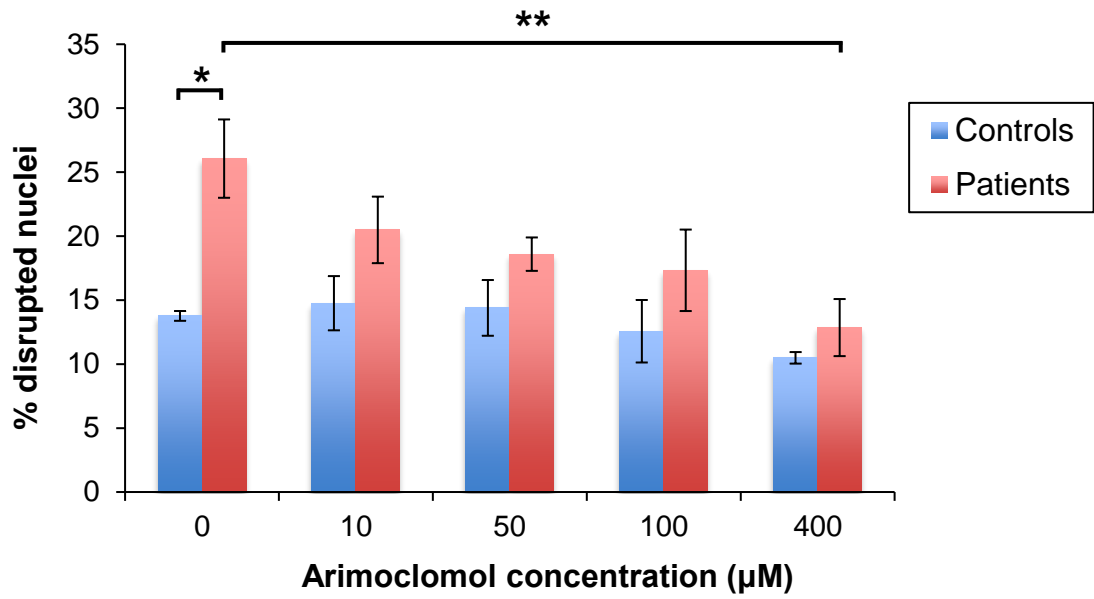


Figure 4.9. Arimoclomol reduces the number of disrupted nuclei in sporadic IBM patient fibroblasts

The bar chart shows the average percentage of disrupted nuclei in control and sporadic IBM patient fibroblasts, 24 hours after treatment with increasing concentrations of Arimoclomol. Error bars= SEM. N=4 per group (approximately 1500 cells per group). * $p < 0.05$, ** $p < 0.01$; two-way ANOVA.

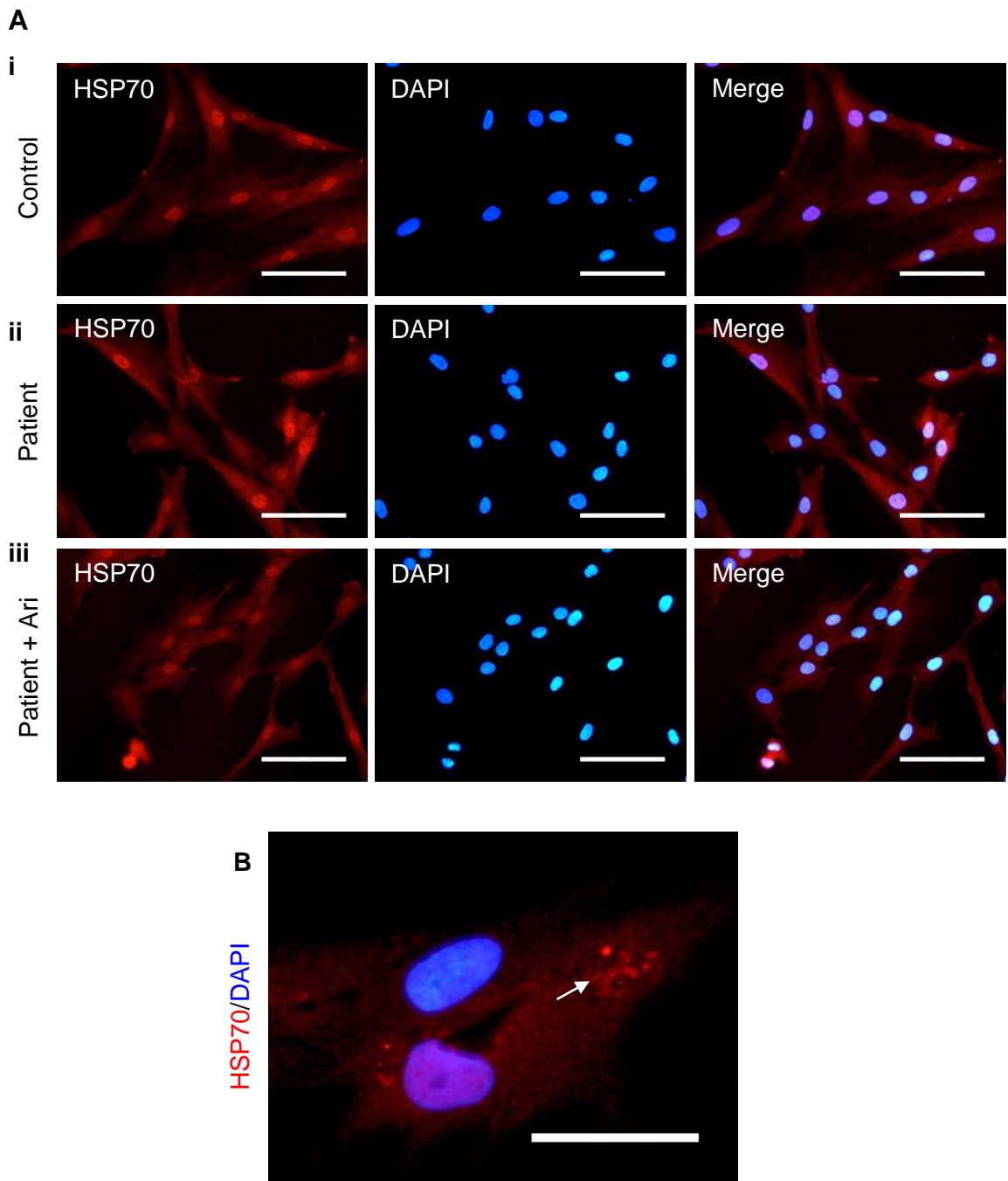


Figure 4.10. HSP70 expression in Arimoclomol-treated sporadic IBM patient fibroblasts

(A) Immunostaining for HSP70 (red) in age-matched control fibroblasts **(i)**, sporadic IBM patient fibroblasts **(ii)** and sporadic IBM patient fibroblasts treated with 10 μ M Arimoclomol **(iii)**. The cells were co-stained with the nuclear marker DAPI (blue). Scale bars represent 50 μ m. **(B)** Representative image of HSP70-positive aggregates (arrow) in an individual sporadic IBM patient fibroblast. Scale bars represent 20 μ m.

4.5. Discussion

The previously described rat *in vitro* models of IBM (Ahmed et al. 2016) and the *in vivo* mouse model of MSP, described in Chapter 3 of this Thesis allowed the investigation of the effects of upregulating the HSR with Arimoclomol in IBM. In order to further investigate the pathomechanisms underlying IBM and to be able to screen novel therapeutic compounds, the aim of this Chapter was to characterise a more clinically relevant human model of the disease, using fibroblasts derived from sporadic IBM patients.

4.5.1. Patient fibroblasts exhibit characteristic pathological features of sporadic IBM

To date, the cellular health and pathology in fibroblasts from sporadic IBM patients has not been investigated. Therefore, in order to assess the effects of Arimoclomol on these patient-derived fibroblasts, it first had to be established whether these cells display characteristic pathological abnormalities of sporadic IBM. Evaluation of fibroblasts obtained from four different sporadic IBM patients with varying degrees of disease severity, demonstrated that key IBM-like pathological features are present in these cells, even when cultured under normal basal conditions, in the absence of any additional cellular stress.

4.5.1.1. TDP-43 pathology in sporadic IBM fibroblasts

As previously discussed in this Thesis (Chapter 1, section 1.2.2), one of the characteristic pathological hallmarks of sporadic IBM is the mislocalisation of the RNA-binding protein, TDP-43. TDP-43 is widely considered to be a key protein in the pathogenesis of IBM and other neurodegenerative diseases. In this study, abnormal TDP-43 expression was found in primary fibroblast cultures from sporadic IBM patients. The localisation of this protein was observed using an antibody targeted against the C-terminus of TDP-43 that recognises the cleavage product, in addition to the native and phosphorylated forms of TDP-43. Whilst TDP-43 was exclusively retained within the nucleus of healthy control fibroblasts under basal conditions, in cultured sporadic IBM patient fibroblasts, TDP-43 was distributed throughout the cytoplasm. Nuclear depletion of TDP-43 was also observed in a proportion of cells. This pathology is consistent with findings that TDP-43 is mislocalised in muscle in sporadic IBM and represents a novel finding in this cell type.

A further interesting observation was that in patient fibroblasts, TDP-43 typically showed a diffuse cytoplasmic distribution, with a concurrent loss of nuclear TDP-43 within the same cells, rather than the formation of cytoplasmic inclusions. This pattern of intracellular protein redistribution with concurrent nuclear depletion has been reported in other cell models of disease, including FTD and ALS (Arai et al. 2006; Neumann et al. 2006; Brandmeir et al. 2007; Davidson et al. 2007; Mori et al. 2008), a primary cortical neuron model of TDP-43 proteinopathy (Barmada et al. 2010) and a human neuronal model of the neurodegenerative lysosomal storage disorder Niemann-Pick disease type C (Dardis et al. 2016). Moreover, TDP-43 has also been found to be markedly increased in the cytoplasm and reduced in the nuclei in fibroblasts derived from ALS patients (Sabatelli et al. 2015). Interestingly, in the same study, mutant fibroblasts from SOD1 ALS patients had a significant reduction of TDP-43 in the nuclei without cytoplasmic mislocalisation.

Since TDP-43 typically shuttles between the nucleus and the cytoplasm to perform its functions, the loss of nuclear TDP-43 may be a result of either a reduced inflow of TDP-43 into the nucleus, an increased outflow from the nucleus or, alternatively, suppression of TDP-43 synthesis. Interestingly, it has been suggested that the disappearance of TDP-43 from the nucleus may precede inclusion formation in the cytoplasm and that diffuse or granular cytoplasmic TDP-43 may represent a “pre-inclusion” state (Van Deerlin et al. 2008; Onodera et al. 2013). This may be what is apparent in the sporadic IBM patient fibroblasts in this study. The disappearance of TDP-43 from the nucleus may therefore be crucial in the development of disease pathology.

Recent studies have also suggested that nucleocytoplasmic transport is disrupted as a result of TDP-43 pathology in ALS and FTD and may therefore be a common disease mechanism in other TDP-43 proteinopathies (Chou et al. 2018). However, the relationship between mislocalisation of TDP-43 and nuclear transport defects remains uncertain.

Furthermore, as TDP-43 mislocalisation is a key feature of IBM in rodent *in vitro* and *in vivo* models, as well as human sporadic IBM fibroblasts, this pathological feature, also present in muscle of sporadic IBM patients, is a key disease

characteristic. As such, the novel finding that sporadic IBM patient fibroblasts have this pathology in the absence of any induced experimental stress, suggests that TDP-43 mislocalisation may be used as an outcome measure to screen for therapeutic compounds in sporadic IBM patient fibroblasts.

4.5.1.2. Stress granule formation in sporadic IBM

Stress granule formation is a highly regulated process and results from stress-induced translational arrest and the reversible aggregation of untranslated mRNAs and mRNA-binding proteins (Anderson & Kedersha 2002). Prolonged or excessive stress or pathological mutations in proteins that either increase the formation or decrease the clearance of stress granules, can lead to abnormal accumulation of stress-granule-like aggregates, which have been associated with a number of neurodegenerative diseases (Wolozin 2012; Maziuk et al. 2017; Chen & Liu 2017). TDP-43- and p62-positive aggregates colocalising with stress granule proteins have been identified in muscle biopsies from sporadic IBM patients (Nakano et al. 2005; Klar et al. 2013). TDP-43 has also been shown to colocalise with multiple protein markers of stress granules, including T-cell intracellular antigen 1 (TIA-1) and eukaryotic translation initiation factor 3 (eIF3), in affected CNS tissue from patients with ALS and frontotemporal dementia (FTD; Liu-Yesucevitz et al. 2010). TDP-43 is thought to be a transcription repressor and thus regulates the formation and dynamics of stress granules, including the expression of stress granule components such as G3BP (McDonald et al. 2011; Aulas et al. 2012). As dense aggregates of TDP-43 were not observed in the sporadic IBM patient fibroblasts examined in this study, it was not that surprising that G3BP-positive aggregates were also not observed.

4.5.1.3. Nuclear disruption in sporadic IBM patient fibroblasts

Since alterations in nuclear shape and defects in nuclear envelope structure are associated with a number of neurodegenerative disorders including Huntington's and Alzheimer's disease, as well as normal ageing, it has been suggested that impaired nuclear import may be a common mechanism of these diseases (Kim & Taylor 2017). Interestingly, abnormal nuclear morphology was one of the most obvious signs of pathology observed in the sporadic IBM patient fibroblasts studied in this Chapter.

The nuclear envelope, enclosing the nucleus, consists of a double membrane with an underlying nuclear lamina, which provides structural support and helps regulate fundamental nuclear activities, including DNA replication and cell division. In healthy cells, the nucleus maintains a smooth, round spheroid shape. Disruption of lamina proteins and the lamina organisation can lead to a weak membrane and herniation of chromatin. This membrane can undergo multiple rounds of nuclear envelope rupturing and repair, resulting in the formation of multiple micronuclei and the entrapment of cytosolic and nuclear components (Hatch & Hetzer 2014).

It is possible that nuclear damage plays a role in the pathogenesis of IBM. In this study around 25% of sporadic IBM patient-derived fibroblasts had nuclei with herniations, protrusions from the nuclear surface, folds and crevices and micronuclei. These cells were not apoptotic, but were associated with a disrupted actin cytoskeleton. There has been previous evidence of a compromised nuclear envelope in IBM. Morphologically abnormal myonuclei have been reported in muscle from sporadic IBM patients (Carpenter et al. 1978; Greenberg et al. 2006; Matsubara et al. 2016) and characteristic rimmed vacuoles in myofibres have been shown to contain nuclear components, including nuclear membrane proteins, suggesting they are derived from the breakdown of myonuclei (Nalbantoglu et al. 1994; Greenberg et al. 2006; Fidzianska et al. 2008; Nakano et al. 2008; Greenberg 2009).

The cause of this nuclear disruption and the exact link between altered nuclear shape and cellular function remains to be determined. Loss of cell membrane integrity may arise from aberrant processing and an imbalance of the various proteins that constitute the nuclear lamina, leading to fragile and mechanically unstable nuclei, ultimately resulting in double-strand breaks and impaired nuclear transport. Indeed, an increased percentage of DNA double-strand breaks has been associated with nuclear breakdown in IBM myonuclei (Nishii et al. 2011). Furthermore, it has been established that actin is present in cell nuclei and although much is still unknown about its potential mechanical role, it is thought to play a role in maintaining nuclear structure (Chen et al. 2015). Thus, disruption of actin may have a part in the abnormal nuclear morphology observed in IBM patient fibroblasts. A defect in nuclear transport may also account for the mislocalisation and subsequent aggregation of TDP-43.

On the other hand, recent studies have suggested that accumulation of cytoplasmic aggregates of TDP-43 and other misfolded proteins may themselves trigger structural defects in nuclear membrane and nuclear pore complexes, by interfering with nucleoporins and transport factors. This could lead to reduced nuclear protein import and mRNA export (Woerner et al. 2016; Chou et al. 2018).

A small percentage of control fibroblasts in this study also had nuclei with mild deviations from the typical round shape. This was not unexpected and was in line with data from other studies (Chou et al. 2018). As these cells were age-matched to the sporadic IBM patient fibroblasts, they were obtained from people at a later stage of life. Normal physiological ageing has been shown to alter nuclear morphology and this association may indeed provide a mechanistic link between ageing and neurodegenerative disease (Webster et al. 2009). Studies have reported age-related alterations in nuclear pore complexes affecting nuclear integrity (D'Angelo et al. 2009) with nucleocytoplasmic transport shown to be impaired in fibroblasts and induced neurons derived from aged donors compared with those derived from young or middle-aged donors (Mertens et al. 2015). Accumulation of misfolded proteins and aberrant protein aggregates due to the proteostasis machinery becoming compromised during ageing, could also have an indirect impact of ageing on nucleocytoplasmic transport (Taylor & Dillin 2011; Woerner et al. 2016). It would be interesting in this study to make a comparison with fibroblasts obtained from healthy controls of a younger age. This would allow the assessment of whether the abnormal nuclei seen in sporadic IBM patient fibroblasts are an exacerbation of normal ageing and whether age-associated nuclear changes, such as nuclear envelope integrity and DNA repair mechanisms, predispose the muscles of the elderly to IBM pathology.

The quantification of the percentage of fibroblasts with disrupted nuclei in this study was obtained via manual counting. Although this was undertaken under blinded conditions, this traditional method of counting is very time-consuming and the lack of standard criteria can lead to considerable variability when counts are undertaken by different people. Furthermore, the division of nuclei into two categories, normal and disrupted, does not take into consideration the

range of severities of abnormal nuclear morphologies. It would therefore be beneficial in future to use an automated method of analysis to minimise bias and subjectivity and take into account variability and the distribution of abnormalities, such as those previously described (Choi et al. 2011; Driscoll et al. 2012). These automated methods can take into account measures such as circularity, size (area and perimeter) and number of invaginations of each cell nucleus. This high throughput analysis of nuclear shapes would significantly reduce analysis time, which would be beneficial for analysing larger sample sizes and provide a more accurate quantitative endpoint.

4.5.2. Investigating pathomechanisms in sporadic IBM patient fibroblasts: proteasome activity, autophagy and mitochondrial function

As well as TDP-43 mislocalisation and nuclear integrity disruption, sporadic IBM fibroblasts also displayed an accumulation of p62-positive aggregates and increased expression of ubiquitin. Ubiquitin binds to misfolded or damaged proteins, targeting them for degradation. P62, also known as sequestosome 1, on the other hand, is an autophagosome cargo protein that targets ubiquitin-bound proteins for selective autophagy and is therefore used as a reporter of autophagic activity. An increase in expression of these proteins, which target and shuttle misfolded proteins for degradation, suggests that there is a disturbance in proteostasis in IBM, namely an increase in abnormal misfolded or damaged proteins or disruption to the clearance of protein aggregates.

Although not investigated in this study, these fibroblasts would provide an excellent model for further investigation of the mechanisms behind this pathology. In particular, it would be interesting to examine autophagic and proteasome activity in these sporadic IBM patient fibroblasts, as well-established methods have previously been described (Ambrosi et al. 2014; Onofre et al. 2016). Proteasome function could be assessed by measuring caspase-like, trypsin-like and chymotrypsin-like activities, as well as measuring proteasome content and protein expression levels of the proteasome subunits. Monitoring the levels of LC3-II, associated with autophagic vacuolar membranes, and the number of nascent double-membrane autophagosomes would provide an indication of baseline levels of autophagy.

Interestingly, p62-positive rimmed vacuoles were prominent in sporadic IBM patient fibroblasts. Other proteins may also be present in these vacuoles. In sporadic IBM patient muscles, a wide range of both sarcoplasmic and myonuclear proteins have been associated with rimmed vacuoles, including proteins associated with protein folding and autophagy, leading to the hypothesis that these vacuoles arise as a result of impaired autophagic degradation (Girolamo et al. 2013; Güttsches et al. 2016). It would also be worth investigating whether TDP43, ubiquitin and p62 were colocalised in these fibroblasts to investigate whether TDP-43 accumulation is a consequence of the autophagic build up caused a defect in autophagy. However, as TDP-43 staining was typically diffuse in nature rather than aggregated in the sporadic IBM fibroblasts, colocalisation would not necessarily be observed.

Since mitochondrial abnormalities are thought to be implicated in the pathomechanisms of IBM, mitochondrial morphology was also assessed in this study by looking at a core component of the translocase of the mitochondrial outer membrane (TOM) protein complex, TOMM20. Fibroblasts from sporadic IBM patients displayed alterations in mitochondrial distribution and morphology, appearing smaller and more fragmented than mitochondria of control fibroblasts. However, due to time restraints, it was not possible to quantify these changes, such as mitochondrial length and mitochondrial branching. These measurements, along with functional studies assessing mitochondria bioenergetics, which have been well established in fibroblasts (Bartolome et al. 2013; Nalbandian, Llewellyn, Gomez et al. 2015; Pérez et al. 2017) would provide a clearer indication of mitochondrial disruption in sporadic IBM patient fibroblasts.

4.5.3. Upregulation of the heat shock response in sporadic IBM patient fibroblasts: the effect of Arimoclomol on IBM pathology

Since fibroblasts derived from sporadic IBM patients showed characteristic features of pathology under basal culture conditions, these cells could be used to confirm the results of the previously described rat *in vitro* models of IBM and the *in vivo* mouse model of MSP, presented in Chapter 3, in which Arimoclomol was found to ameliorate key pathological characteristics of IBM. The effect of Arimoclomol was assessed on the percentage of disrupted nuclei. Arimoclomol

was found to improve nuclear morphology, with all doses having a positive effect, following a 24-hour treatment period. This beneficial effect following a short treatment period, likely reflects the doubling times of the cells and indeed such beneficial effects of Arimoclomol on IBM-like pathology have also been observed after a 24-hour treatment period in primary rat myocyte cultures overexpressing β -APP or exposed to inflammatory mediators (Ahmed et al. 2016).

The greatest reduction in the percentage of disrupted nuclei was observed at 400 μ M. As expected, Arimoclomol did not have any effect on the amount of disrupted nuclei in control fibroblasts, consistent with previous findings on the effect of the drug in control cells and wild-type mouse models. This is due to the fact that Arimoclomol only acts on cells already under stress (Hargitai et al. 2003). Importantly, no signs of cell toxicity were observed in the fibroblasts at any of the drug concentrations tested.

The results of this study suggest that treatment with Arimoclomol is beneficial in improving signs of pathology in sporadic IBM fibroblasts. As all data for the beneficial effects of Arimoclomol to date relies on results from mouse models, the confirmation of these results in patient fibroblasts strengthens the translational relevance of the finding that Arimoclomol has beneficial effects on IBM pathology.

As discussed in Chapter 3 of this Thesis, one of the main mechanisms by which Arimoclomol is acting in these cells is likely via activation of HSF1, the main HSP transcription factor which regulates stress-inducible synthesis of HSPs, thus providing cellular protection by chaperoning. As Arimoclomol is a co-inducer of the HSR, this suggests that these fibroblasts are already under conditions of cellular stress, which may involve the accumulation of damaged proteins. This could be a result of disruption to protein homeostasis pathways or an impaired ability of these cells to activate the HSR, resulting in an increased tendency for abnormal protein folding and trafficking, as well as an increased susceptibility to apoptotic insults. Subsequent elevation of HSPs due to Arimoclomol likely helps restore the normal functional folded state of proteins, resulting in a protective effect in sporadic IBM patient fibroblasts.

Surprisingly, there was no evidence of an increase in HSP70 expression in Arimoclomol-treated sporadic IBM fibroblasts. However, it is important to note that only one time point was examined, 24 hours after the addition of Arimoclomol. Therefore the time point in which an Arimoclomol-induced increase in HSP70 occurs may have been missed. It is also possible that immunocytochemistry was not sensitive enough to detect a change in HSP70 expression or that a more obvious increase in HSP70 intensity may be observed with concentrations above 10 μ M. On the other hand, it may be that the threshold for activation of the HSR in untreated patient cells has not been reached and thus, as Arimoclomol only works on cells under stress, treatment with Arimoclomol would not be expected to further increase HSP70 expression in sporadic IBM fibroblasts

Interestingly, HSP70 aggregates in sporadic IBM fibroblasts, which were not seen in control cells, were prevented with Arimoclomol treatment. It is possible that in sporadic IBM fibroblasts there is not so much of an increase in overall HSP70 levels but rather an increase in the amount of HSP70 within aggregates.

4.5.4. Differences between sporadic IBM patient fibroblast lines

The results presented in this Chapter show that IBM pathology extends beyond muscle cells in sporadic IBM patient cells. Although skin is not characteristically affected in IBM, previous studies have shown that human fibroblasts can reproduce disease-related pathological features in other neurodegenerative disorders such as ALS (Raman et al. 2015; Sabatelli et al. 2015; Konrad et al. 2017). However, an intriguing finding of this study was that there were no clear differences in the pathology observed between the four patient fibroblasts lines analysed.

The fibroblasts examined in the experiments described in this Chapter were obtained from patients with an IBM Functional Rating Scale (IBMFRS) score of between 16 and 28, with an age range of 51-77 years. The IBMFRS is a 10-point functional rating scale, modified from the ALSFRS (the ALS scale), used to measure disease severity in IBM patients (Jackson et al. 2008). The test addresses swallowing, handwriting, cutting food, handling utensils, dressing, hygiene, turning in bed, adjusting covers, sit to stand, walking and climbing

stairs and has with a maximum score of 40. The higher the score the better the functional status of the patient. This test has been shown to correlate well with isometric muscle strength and manual muscle testing.

Three of the four patients from whom fibroblasts were obtained were at a more advanced stage of disease, with a decline of 50% or greater on the IBMFRS. Despite this variation in functional rating scores, no obvious difference in pathology was observed in these fibroblast lines. Only four fibroblast lines were examined in this study, however. It is possible that by increasing the number of patients from which fibroblasts are derived and having a greater, more distinct definition between mild and severe disease states, that a difference in the extent of pathology could be observed. However, these data support a previous study investigating nuclear surface structures in muscle biopsies from seven IBM patients. Despite prominent disruption in the nuclear surface of myonuclei, the duration of illness had little influence on these changes (Matsubara et al. 2016). This suggests that other factors may be influencing the extent of pathology within these cells, rather than severity of the disease phenotype.

4.5.5. Degenerative and inflammatory changes in sporadic IBM patient fibroblasts

IBM is a complex disease, characterised by both degenerative and inflammatory changes. In this study, only aspects of the degenerative component were examined. Further investigation to establish whether pathological inflammatory features are also present in sporadic IBM patient fibroblasts would demonstrate whether this model displays all aspects of the disease phenotype. Comparisons could then be made with fibroblasts derived from patients with a primarily inflammatory disease, in which there are no vacuolated fibres or cytoplasmic inclusions, such as the autoimmune inflammatory myopathy polymyositis (Dalakas 2016). This would allow the inflammatory and degenerative components of IBM to be isolated.

4.6. Conclusion

The experiments described in this Chapter aimed to assess whether sporadic IBM patient fibroblasts recapitulate a disease phenotype and could therefore be used to confirm whether the beneficial effects of Arimoclomol, previously described in rat *in vitro* models of IBM (Ahmed et al. 2016) and in the *in vivo* mouse model of MSP (described in Chapter 3) are also observed in a more clinically relevant, human model of IBM. The results demonstrate that cultured fibroblasts derived from sporadic IBM patients display characteristic pathological features of the disease under basal culture conditions. These include morphologically abnormal nuclei, TDP-43 mislocalisation, increased ubiquitin expression, p62 aggregation and mitochondrial disruption. Importantly, the results suggest that treatment with Arimoclomol may attenuate these pathologies. This preclinical model of IBM can therefore be used to gain a greater understanding of the complex pathomechanisms involved in IBM and aid the discovery of other novel therapeutic agents.

Chapter 5

Upregulating the heat shock response in VCP patient fibroblasts

5.1. Introduction

Upregulating the heat shock response (HSR) with Arimoclomol ameliorates IBM-like pathology both *in vitro* and *in vivo*. IBM is a sporadic disease with no known genetic cause. However, the *in vivo* mouse model characterised in this Thesis (discussed in Chapter 3) was a mouse model of the degenerative disorder multisystem proteinopathy (MSP), caused by mutations in the valosin-containing protein (*VCP*) gene. MSP is also known as inclusion body myopathy with Paget's disease of bone and frontotemporal dementia (IBMPFD). The inclusion body myopathy in these patients has a similar disease phenotype to sporadic IBM, but typically lacks an inflammatory component (Evangelista et al. 2016). Since Arimoclomol was beneficial in reducing signs of pathology in the mutant *VCP* mouse model of MSP (discussed in Chapter 3), as well as in the human fibroblast model of sporadic IBM (discussed in Chapter 4), in this Chapter the aim was to investigate firstly whether cultured fibroblasts from MSP patients with mutations in *VCP* manifest disease-relevant pathology *in vitro* and if so, whether treatment with Arimoclomol would also be beneficial in ameliorating this pathology.

5.1.1. VCP patient fibroblasts

MSP, described in detail in Chapter 3 of this Thesis, is associated with a hereditary form of inclusion body myopathy, Paget's disease of bone (PDB) and frontotemporal dementia (FTD). MSP patients present with a muscle pathology that resembles the pathology seen in sporadic patients, with muscle biopsies displaying rimmed vacuoles, as well as ubiquitin-positive cytoplasmic and nuclear inclusions and other degenerative changes (Hübbers et al. 2007; Weihl et al. 2009; Kimonis et al. 2011; Evangelista et al. 2016). *VCP* has been linked to a variety of cellular functions, with an important role in protein homeostasis and the regulation of protein degradation via the proteasome and autophagy-mediated pathways and ERAD (Ju & Weihl 2010; Nalbandian et al. 2011; Meyer & Weihl 2014). However, as with sporadic IBM, the underlying molecular pathogenesis of MSP remains unclear.

It has previously been reported that fibroblasts derived from patients with pathogenic *VCP* mutations display some characteristic pathological features when grown in culture. Fibroblasts derived from patients with the most common *VCP* mutation, R155H, have shown increased expression of ubiquitin, LC3 and p62 compared to age-matched control fibroblasts, as well as evidence of TDP-43 cytoplasmic mislocalisation (Nalbandian, Llewellyn, Gomez et al. 2015). Enlarged vesicles, positive for the lysosomal membrane protein LAMP2, have also been identified in patient fibroblasts with the R155H and L198W *VCP* mutations (Ritz et al. 2011).

The strongest evidence of pathology in *VCP* patient fibroblasts is the identification of mitochondrial abnormalities. Fibroblasts from patients carrying several independent *VCP* mutations (R155H, R155C and R191Q) have been shown to have a reduced mitochondrial membrane potential, uncoupled respiration and reduced oxidative phosphorylation, as well as decreased ATP production and depletion of cellular ATP (Bartolome et al. 2013; Nalbandian Llewellyn, Gomez et al. 2015). Impairment of mitochondrial respiratory chain function and mitochondrial fusion defects have also been reported in immortalised patient fibroblasts with the R155H *VCP* mutation (Zhang et al. 2017).

5.1.2. Alternative *in vitro* *VCP* models

The current pathological findings reported in *VCP* patient fibroblasts have also been demonstrated in other *in vitro* models of MSP. For example, *VCP* patient myoblasts derived from MSP patient biopsies display features of a sporadic IBM phenotype, including enlarged vacuoles, increased apoptosis, accumulation of LC3-II and defective maturation to myotubes and impaired regenerative capacity (Vesa et al. 2009; Morosetti et al. 2010; Tresse et al. 2010). Furthermore, reduced ATP levels and mitochondrial membrane potential compared to control cell lines have been reported in *VCP* patient myoblasts (Nalbandian, Llewellyn, Gomez et al. 2015). Mitochondrial defects have also been observed in *VCP* transgenic mouse models and in an *in vivo* MSP *Drosophila* model (Custer et al. 2010; Nalbandian et al. 2012; Bartolome et al. 2013; Zhang et al. 2017), as well as in the *in vivo* mutant *VCP* mouse model described in Chapter 3 of this Thesis.

There have also been attempts to recapitulate the MSP disease phenotype in an induced pluripotent stem cell (iPSC) model system. iPSC cell lines derived from MSP patient fibroblasts have been differentiated into both cortical neurons (Dec, Ferguson, et al. 2014; Ludtmann et al. 2017) and myogenic lineages (Llewellyn et al. 2017). Differentiated neural cells display typical characteristics of MSP pathology, including increased expression of p62, LC3-I/II and TDP-43, as well as mitochondrial abnormalities. Characterisation of the differentiated VCP myogenic lineages demonstrated translocation of TDP-43 from the nucleus to the cytoplasm, along with increased expression of p62, LC3-I/II and ubiquitin compared to the control myogenic lineage.

The self-renewal capabilities and ability to differentiate into specialised cell types, including skeletal muscle, make iPSCs an attractive choice for disease modelling and drug screening. Major advances have been made in recent years in differentiating human iPSCs into skeletal muscle cells via small molecule differentiation or direct reprogramming (Abujarour & Valamehr 2015; Crist 2017; Kodaka et al. 2017; Miyagoe-Suzuki & Takeda 2017). However, despite intensive efforts, the generation of iPSCs remains a relatively long and expensive, labour-intensive process and poses many challenges (Magli & Perlingeiro 2017). The use of iPSCs has been relatively limited due to the difficulty of inducing skeletal muscle cells from human iPSCs in large enough quantities and with sufficient purity. Furthermore, inconsistent differentiation can occur among cell lines and across separate research institutions (Osafune et al. 2008). Skeletal muscle derived from human iPSCs has also been shown to display embryonic phenotypes, with reduced desmin organisation and reduced MyoD expression (Llewellyn et al. 2017). This suggests that human iPSC-derived myotubes may be more developmentally immature than primary myotubes. This is a significant disadvantage when studying age-related diseases such as MSP or sporadic IBM.

Compared to other *in vitro* cell models of disease, patient-derived dermal fibroblasts remain a desirable model. Skin biopsies are a routine procedure for patients and less invasive than muscle biopsies, from which myoblasts are obtained. The maintenance required and associated costs are also much lower than for other models, such as iPSCs, meaning results can be obtained quicker.

5.2. Aims of this Chapter

The results presented in Chapters 3 and 4 of this Thesis have demonstrated that upregulating the HSR with Arimoclomol is beneficial in reducing signs of IBM pathology in a mouse model of MSP, as well as in a fibroblast model of sporadic IBM. This Chapter therefore aimed to investigate whether Arimoclomol would also be beneficial in ameliorating pathology in cultured fibroblasts from MSP patients with mutations in the *VCP* gene. Characterisation of the fibroblasts obtained for this study was first necessary to confirm previous findings of histopathological features in *VCP* patient fibroblasts in culture. MSP patient-derived fibroblasts recapitulating phenotypic changes seen in the muscle of MSP and sporadic IBM patients would represent another model to complement the *in vitro* and *in vivo* studies described in this Thesis. Not only would it provide an additional and more clinically relevant model in which to assess the effects of co-inducing the HSR with Arimoclomol and other potential compounds, but it would also be a vital tool for comparing the pathomechanisms underlying MSP and IBM.

The specific aims of this Chapter were:

- (1) To characterise the inherent cellular pathology in fibroblasts from MSP patients carrying independent pathogenic *VCP* mutations.
- (2) To examine the effects of co-inducing the HSR with Arimoclomol on MSP patient-derived *VCP* fibroblasts.

5.3. Materials and methods

A full description of the materials and methods used in this Chapter are presented in Chapter 2. In this Chapter the following specific methods were used:-

5.3.1. Fibroblast cell lines

Control and VCP patient fibroblasts were obtained from Professor Hanns Lochmüller at the MRC Centre Neuromuscular Biobank (Newcastle University). Collection of samples from patients and their use in research have been ethically approved by the 'Newcastle and North Tyneside 1 Research Ethics Committee' with REC reference number 08/HO906/28 + 5 with signed written consent obtained from patients. Fibroblast lines were established following the protocol in Chapter 2 (section 2.12). The specific human fibroblast cell lines are detailed in **Table 5**.

5.3.2. Immunocytochemistry

Human dermal fibroblasts were immunostained using the protocol described in Chapter 2 (section 2.14). The antibodies used are detailed in **Table 6**. Fibroblasts were co-stained with the nuclear marker DAPI and/or F-actin-binding Alexa Fluor 488 Phalloidin.

5.3.3. Western blots

Western blot was performed to determine protein levels as described in Chapter 2 (section 2.15). Membranes were incubated with the primary antibodies indicated in **Table 6**.

5.3.4. Disrupted nuclei counts

The percentage of cells with morphological nuclear abnormalities was assessed according to the protocol described in Chapter 2 (section 2.16). Counts were undertaken in three independent cultures, an average of approximately 1500-2000 cells for each individual fibroblast line (3 control and 4 patient cell lines).

	Gender	Age at biopsy	Mutation	Exon	Protein	Clinical features
Control 1	F	47	-	-	-	-
Control 2	M	47	-	-	-	-
Control 3	F	66	-	-	-	-
VCP patient 1	F	57	VCP c.464G>A	5	R155H	Mild, only muscle affected
VCP patient 2	F	52	VCP c.464G>A	5	R155H	Mild, only muscle affected
VCP patient 3	F	56	VCP c.464G>A	5	R155H	Mild, only muscle affected
VCP patient 4	M	56	VCP c.277C>T	3	R93C	Severe, myopathy with dementia and Paget's

Table 5. VCP patient fibroblasts

Details of the patient fibroblasts used in this study, including gender, age at biopsy, mutation details and clinical features.

Primary antibody	Application	Dilution	Source	Supplier
TDP-43 (C-terminal epitope)	IF	1:500	Rabbit polyclonal	ProteinTech 12892-1-AP
TDP-43 (N-terminal epitope)	IF	1:200	Rabbit polyclonal	ProteinTech 10782-2-AP
Ubiquitin	IF	1:500	Mouse monoclonal	GeneTex GTX78236
p62	IF	1:100	Mouse monoclonal	Abcam Ab56416
TOMM20	IF, WB	1:400, 1:900	Rabbit polyclonal	Abcam Ab78547
HSP70	IF, WB	1:100, 1:1000	Mouse monoclonal	Santa Cruz sc24

Table 6. Primary antibodies used in Chapter 5 for the study of VCP patient fibroblasts

Description of primary antibodies used within this Chapter. IF = immunofluorescence; WB = western blot.

5.3.5. TUNEL assay

For detection of apoptosis, cells were labelled with the TACS 2 TdT DAB (diaminobenzidine) Kit. Full details are given in Chapter 2 (Section 2.17).

5.3.6. Arimoclomol treatment

Fibroblasts were treated with Arimoclomol following the protocol described in Chapter 2 (section 2.13). Fibroblasts were treated with the following concentrations of Arimoclomol: 10 μ M, 50 μ M, 150 μ M, 400 μ M.

5.3.7. Heat shock treatment

Heat shock experiments were performed by placing cells in a humidified incubator with 5% CO₂ for 1 hour at either 42°C or 44°C. Cells were then immediately transferred back to 37°C. Cells were processed following a 24-hour recovery period. For all heat shock experiments, controls were run in parallel at 37°C.

5.3.8. Statistical analysis

Analyses were performed as described in Chapter 2 (section 2.18). For analysis of disrupted nuclei, experimental groups were compared using a one-way or two-way analysis of variance (ANOVA) with Tukey's all pairwise multiple comparisons *post hoc* analysis. All data analysis was performed blind. All data are presented as mean \pm SEM.

5.4. Results

5.4.1. VCP patient fibroblasts display pathological abnormalities under basal culture conditions

In order to assess the effects of upregulating the HSR in VCP patient fibroblasts, it first had to be confirmed whether these fibroblasts displayed IBM-like cellular pathologies *in vitro*. Immunofluorescent staining was performed to examine the distribution of a number of IBM-associated proteins, including TDP-43, ubiquitin and p62, in patient fibroblasts and age-matched controls. The patient cell lines included three patients with the R155H mutation and one individual with the R93C mutation in the *VCP* gene.

Cells were first investigated under basal culture conditions. TDP-43 localisation was examined using an antibody that recognises the C-terminal cleavage product, as well as the phosphorylated and native forms, or a second antibody which recognises the N-terminus of TDP-43. Whilst in control fibroblasts TDP-43 was retained exclusively within the nuclei of cells, in all VCP patient fibroblasts lines, immunostaining for the C-terminal of TDP-43 revealed aggregates of cytoplasmic TDP-43 within a proportion of the cells (**Fig. 5.1 A**). Although TDP-43 was still retained within the nucleus, a number of nuclei showed evidence of TDP-43 nuclear depletion. Furthermore, N-terminal TDP-43 was observed only in the nuclei and strongly colocalised with micronuclei that were apparent in close proximity to the nucleus in the VCP patient fibroblasts (**Fig. 5.1 B**).

In addition to TDP-43 mislocalisation, cytoplasmic aggregates of ubiquitin were observed in VCP patient fibroblasts (**Fig. 5.2 A-C**). These aggregates were present either as large, distinct aggregates or as smaller, diffuse aggregates that were more evenly dispersed throughout the cytoplasm. This dispersed expression of ubiquitin was also noted in a small number of age-matched control fibroblasts, but there was no evidence of larger aggregates in these cells.

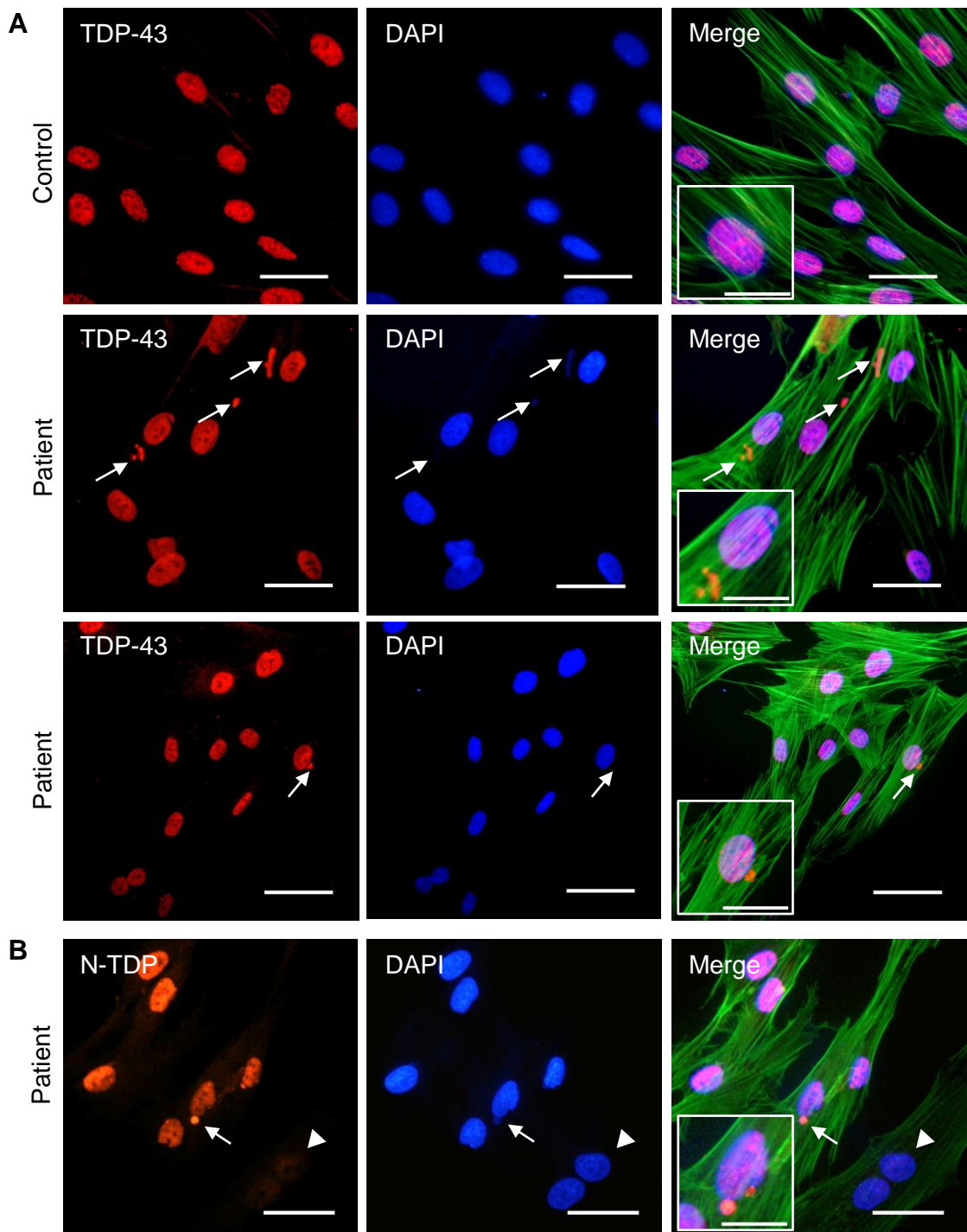


Figure 5.1. TDP-43 is mislocalised and forms cytoplasmic aggregates in VCP patient fibroblasts under basal culture conditions

(A) Immunostaining of age-matched, human control and VCP patient fibroblasts, stained for TDP-43 (C-terminal; red) and counterstained with the nuclear marker DAPI (blue). The merged images show cells co-stained with F-actin-binding Alexa Fluor 488 phalloidin (green) to visualise cell morphology. Arrows indicate TDP-43 aggregates. Scale bars represent 20 μm. Insets: higher magnification (scale bars: 10 μm). **(B)** Immunocytochemistry of VCP patient fibroblasts with TDP-43 (N-terminal; red) counterstained with DAPI (blue). Arrow indicates a micronucleus positive for TDP-43. Arrowhead indicates nuclear depletion of TDP-43. Scale bars represent 20 μm.

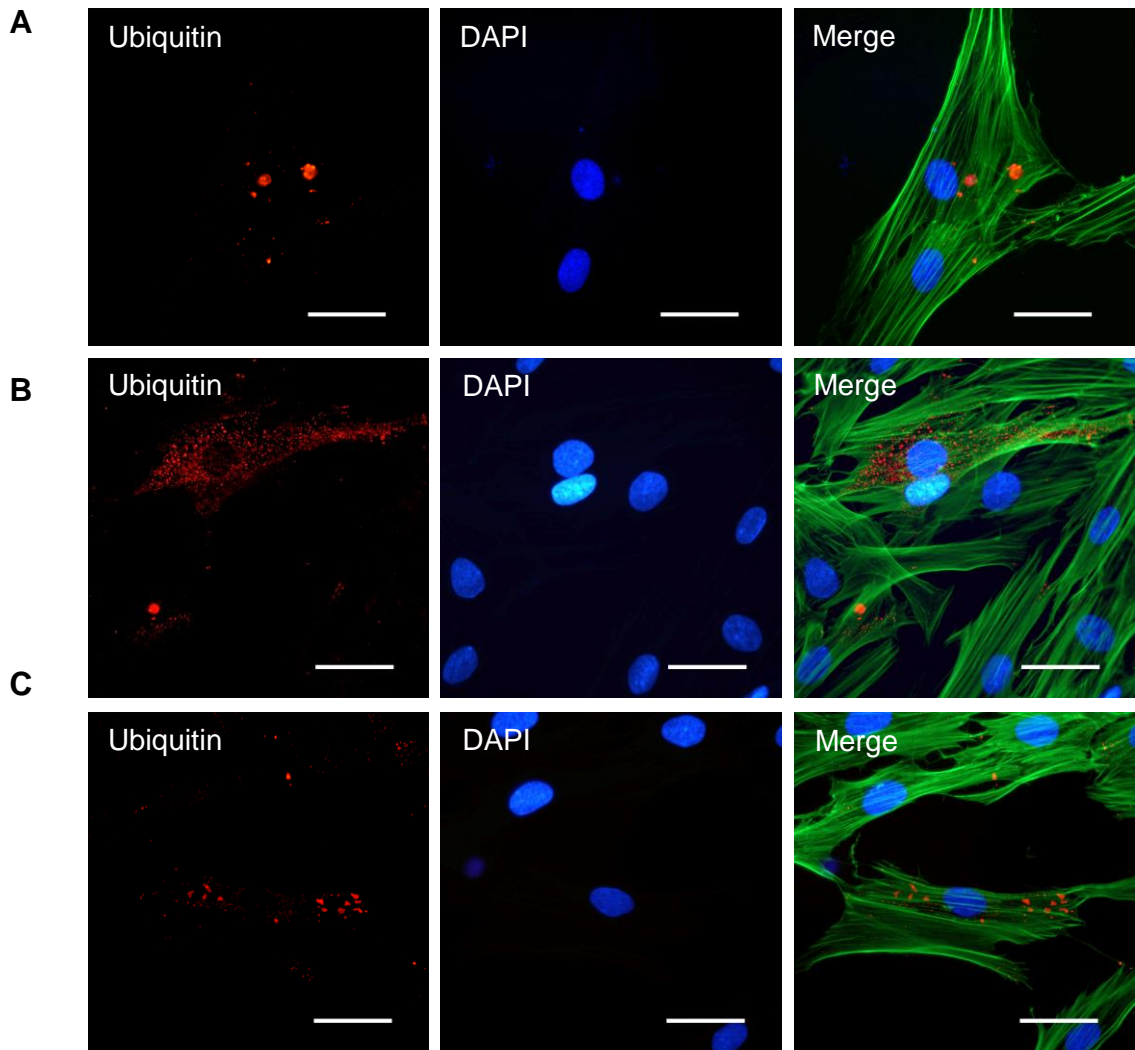


Figure 5.2. VCP patient fibroblasts form ubiquitin-positive aggregates under basal culture conditions

Immunostaining of fibroblasts from VCP patients stained for ubiquitin (red) and co-stained for the nuclear marker DAPI (blue) and F-actin-binding Alexa Fluor 488 phalloidin (green). Both large cytoplasmic aggregates (**A**) and more disperse ubiquitin aggregates (**B, C**) were observed. Scale bars represent 20 μm .

Also evident in all VCP patient fibroblast lines was the formation of rimmed vacuoles, immunopositive for ubiquitin and p62 (**Fig. 5.3 A-B**). P62-lined vacuoles were particularly prominent in VCP patient fibroblasts, with the majority of these vacuoles located adjacent to the nucleus.

Since mitochondrial disruption in VCP patient fibroblasts has been observed in previous studies (Bartolome et al. 2013; Nalbandian, Llewellyn, Gomez et al. 2015), mitochondrial morphology was examined in the VCP patient fibroblasts in this study, by immunostaining for the mitochondrial outer membrane marker translocase of outer mitochondrial membrane 20 (TOMM20). Most fibroblasts from control and VCP patients had a highly organised and interconnected tubular mitochondrial network that extended from the nuclear envelope to the plasma membrane. Some fragmentation of mitochondria in fibroblasts harbouring the R93C mutation was observed and mitochondrial density appeared to be lower (**Fig. 5.4 A**). Clustering of mitochondria around disrupted nuclei was also observed in VCP patient fibroblasts expressing both the R155H and R93C mutations (**Fig. 5.4 B**). However, there was no difference in TOMM20 expression between control and R155H patient fibroblasts, as determined by western blot analysis (**Fig. 5.4 C**).

5.4.2. VCP patient fibroblasts have an abnormal nuclear morphology

Cells with abnormal nuclear morphology have been reported in a number of neurodegenerative diseases, as well as in sporadic IBM patient fibroblasts (Carpenter et al. 1978; Greenberg et al. 2006; Mukherjee et al. 2016). To investigate nuclear morphology in the VCP patient fibroblasts, cells were labelled with the nuclear marker DAPI and a direct assessment of nuclei in approximately 2000 cells from each of the patients and age-matched control cell lines was undertaken from three independent cultures. Nuclei in the control fibroblasts appeared mostly regular in size and shape, being round or oval, with a small percentage displaying altered nuclei. In contrast, a significantly greater percentage of VCP patient fibroblasts had disrupted nuclei, with nearly 25% of patient fibroblasts demonstrating irregularities in the nuclear envelope shape ($p < 0.01$; unpaired t-test; **Fig. 5.5 A**). These irregularities included protrusions from the nuclear surface, herniations and fragmentation of nuclei leading to the generation of micronuclei. However, there was no evidence of apoptosis in these cells as assessed by TUNEL staining (**Fig. 5.5 B**).

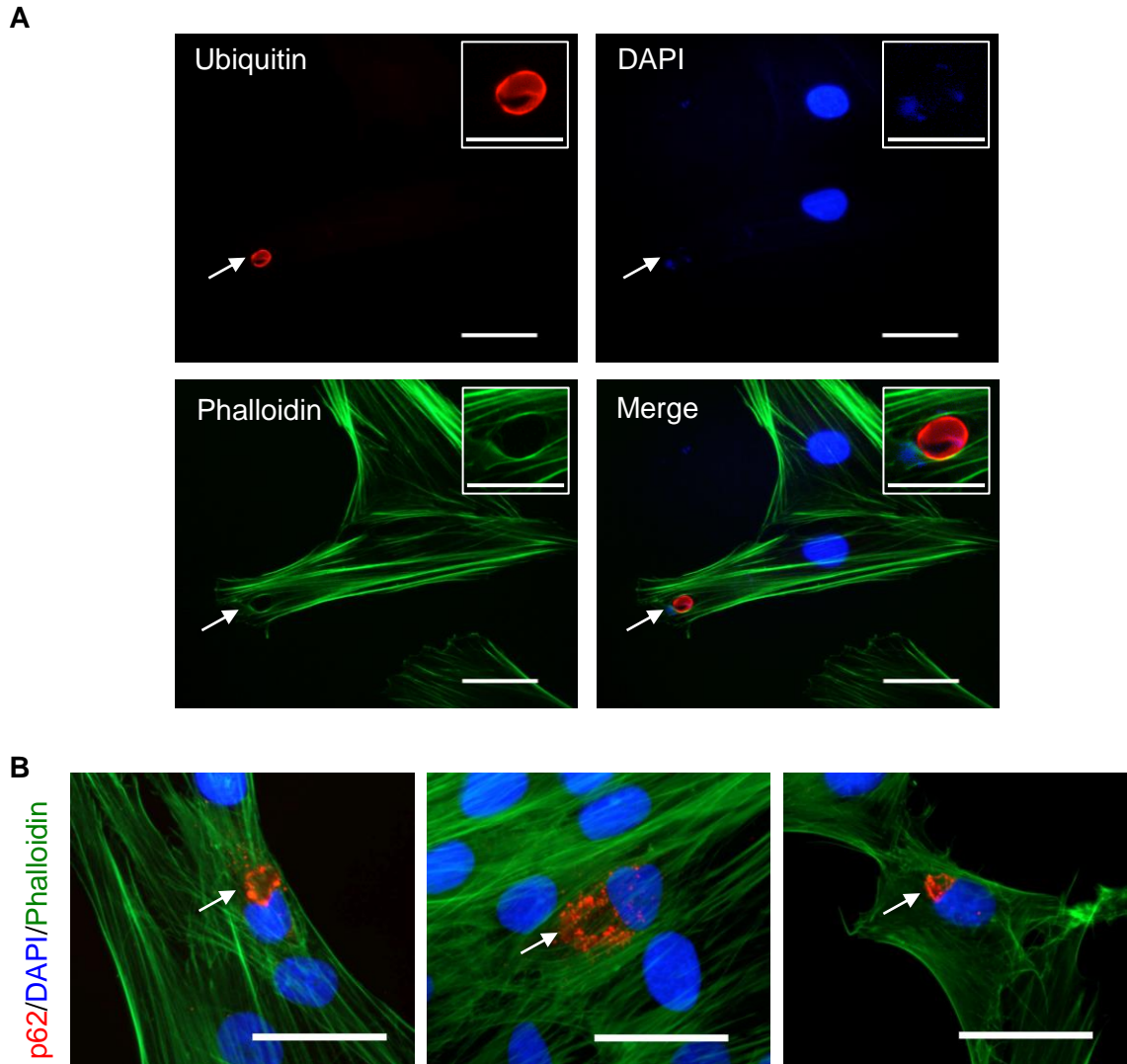


Figure 5.3. VCP patient fibroblasts form ubiquitin- and p62-positive vacuoles

(A) Immunostaining of VCP patient fibroblasts for ubiquitin (red), displaying a single ubiquitin-positive vacuole (arrow). Scale bars represent 20 μm . Insets: higher magnification (scale bar: 10 μm). **(B)** Immunostaining of VCP patient fibroblasts for p62 (red) demonstrating p62-positive rimmed vacuoles (arrows). The cells were co-stained with the nuclear marker DAPI (blue) and F-actin-binding Alexa Fluor 488 phalloidin (green). Scale bars represent 20 μm .

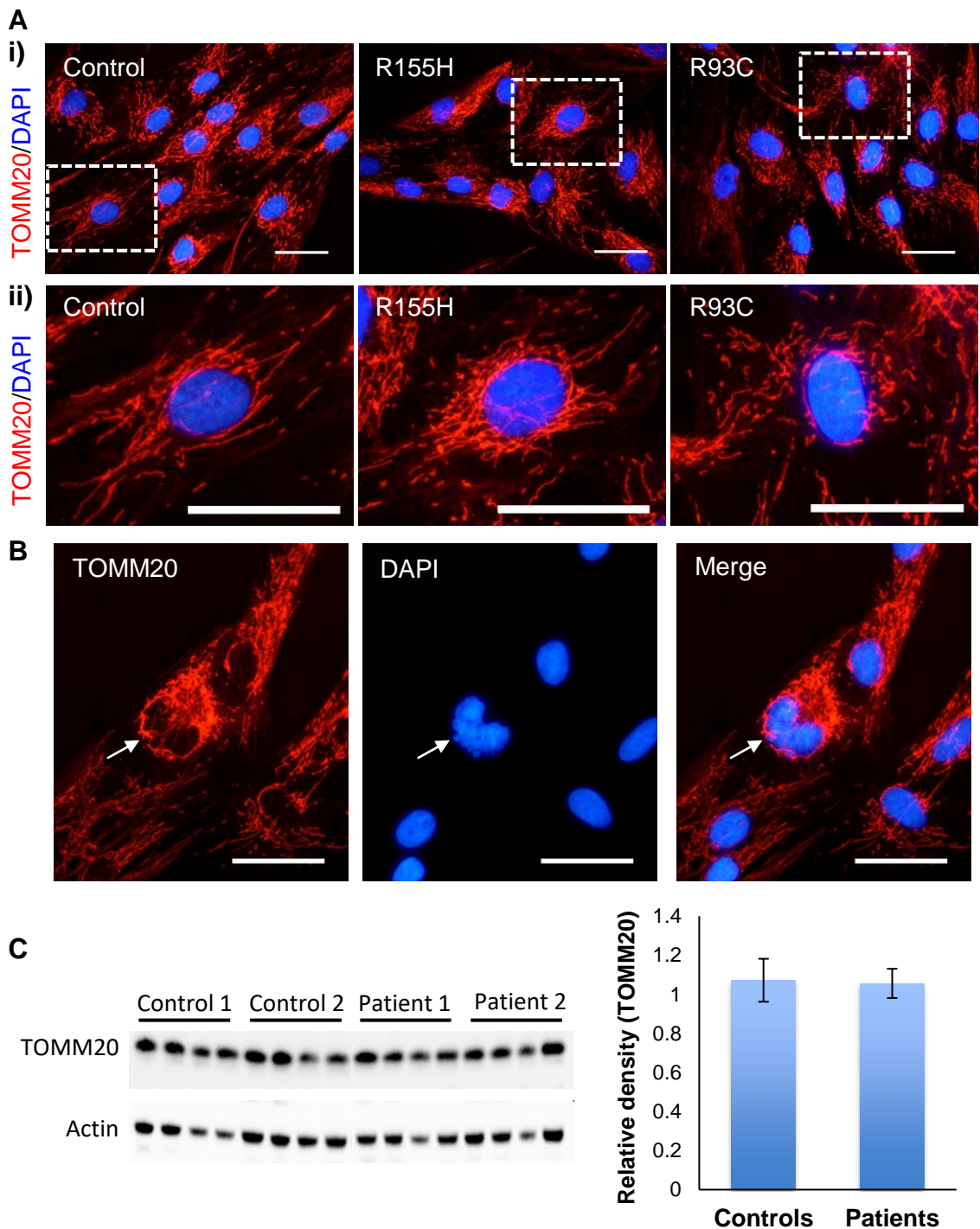


Figure 5.4. Mitochondrial morphology in VCP patient fibroblasts

(A) Immunostaining of age-matched control and VCP patient fibroblasts **(i)** for TOMM20 (red), co-stained with the nuclear marker DAPI (blue). Cells in the highlighted boxes are shown at higher magnification **(ii)**. **(B)** Immunocytochemistry with TOMM20 (red) co-stained with the nuclear marker DAPI (blue), demonstrating mitochondrial clustering around a disrupted nucleus (arrow). All scale bars represent 20 μm . **(C)** Western blot of TOMM20 expression in control and VCP patient (R155H) fibroblasts under basal culture conditions. The bar chart shows the mean relative optical density of the bands in the western blot, normalised to the loading control (actin). Error bars=SEM. N= 2 per group (repeated in 4 independent cultures).

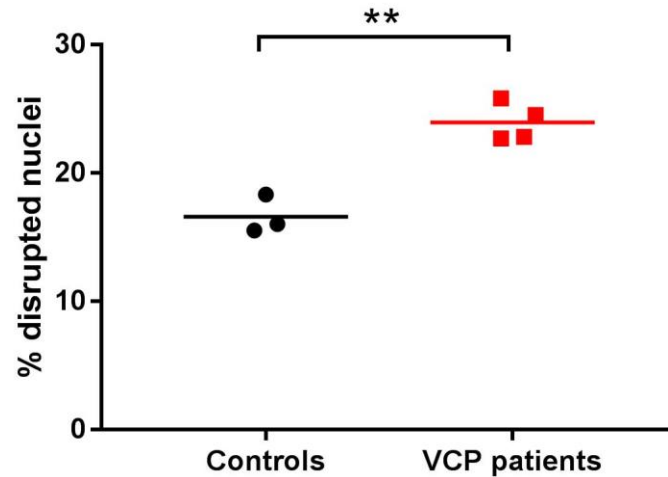
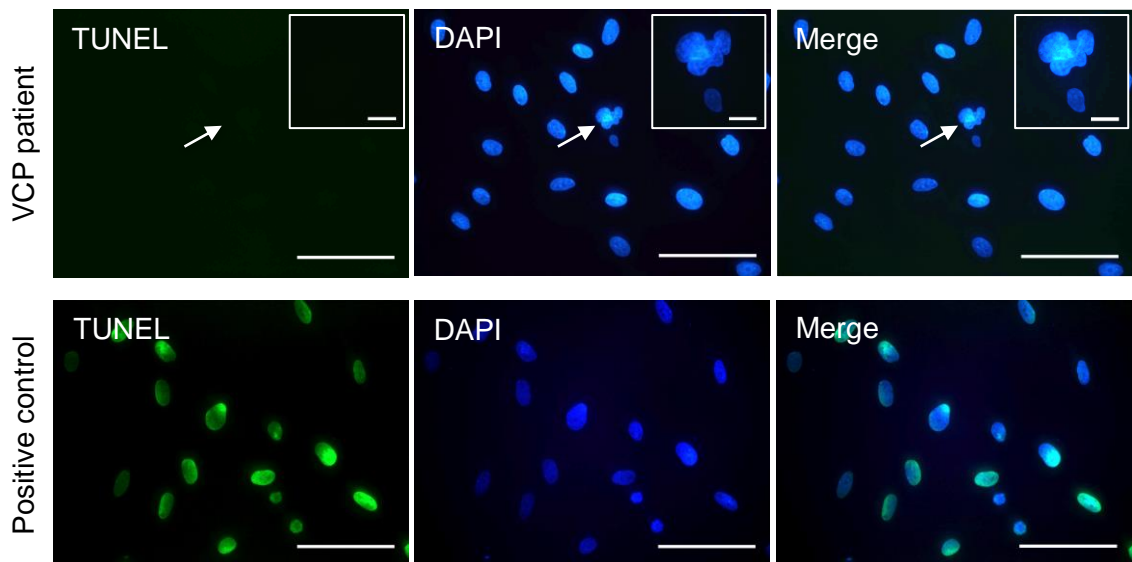
A**B**

Figure 5.5. VCP patient fibroblasts have an increased number of abnormal nuclei but show no evidence of apoptosis

(A) The graph shows the average percentage of disrupted nuclei detected in control (black dots) and VCP patient fibroblasts (red squares). Each dot represents the average of three independent cultures for each individual fibroblasts line (i.e. 3 control lines and 4 VCP patient lines; approximately 2000 cells/dot). Centre lines= mean ** $p < 0.01$; unpaired t-test. **(B)** TUNEL analysis (green) of VCP patient fibroblasts (top row) and a TACS-Nuclease-treated positive control sample (bottom row), co-stained with DAPI (blue). Arrow indicates a disrupted nucleus that is TUNEL-negative. Scale bars represent 50 μm. Insets: higher magnification (scale bar: 10 μm).

5.4.3. Arimoclomol reduces the number of disrupted nuclei in VCP patient fibroblasts

Since fibroblasts derived from patients with VCP mutations show key IBM-like pathology under basal culture conditions, it is possible to use this model to assess the effects of upregulating the HSR on the observed pathology. The effect of Arimoclomol on the percentage of disrupted nuclei from the same cell culture experiments described in Figure 5.5, was therefore investigated. Four concentrations of Arimoclomol were assessed (10, 50, 150 and 400 μM), given at a single time-point and fibroblasts fixed 24 hours later.

In VCP patient fibroblasts, treatment with all four concentrations of Arimoclomol reduced the number of disrupted nuclei. Treatment with 50 μM of Arimoclomol was sufficient to significantly reduce the percentage of abnormal nuclei in VCP patient fibroblasts ($p < 0.01$; two-way ANOVA; **Fig. 5.6**). The greatest effects of Arimoclomol were observed following treatment with 400 μM of Arimoclomol, which significantly reduced the percentage of disrupted nuclei to control levels ($p < 0.01$; two-way ANOVA; **Fig. 5.6**). Arimoclomol had no effect on the percentage of disrupted nuclei in age-matched control fibroblasts.

5.4.4. HSP70 expression in VCP patient fibroblasts following Arimoclomol treatment

It has previously been shown that Arimoclomol results in activation of heat shock factor 1 (HSF1) and an upregulation in the expression of HSP70 (Kieran et al. 2004; Kalmar et al. 2008; Malik et al. 2013; Parfitt et al. 2014; Ahmed et al. 2016; Kirkegaard et al. 2016). In order to examine whether Arimoclomol increases HSP70 levels in patient-derived fibroblasts, immunofluorescent staining was performed. No obvious difference was observed in the expression of HSP70 between untreated control and VCP patient fibroblasts (**Fig. 5.7 A-B**). Furthermore, there was no increase in HSP70 expression in sporadic IBM patient fibroblasts, 24 hours following treatment with Arimoclomol (**Fig. 5.7 C**).

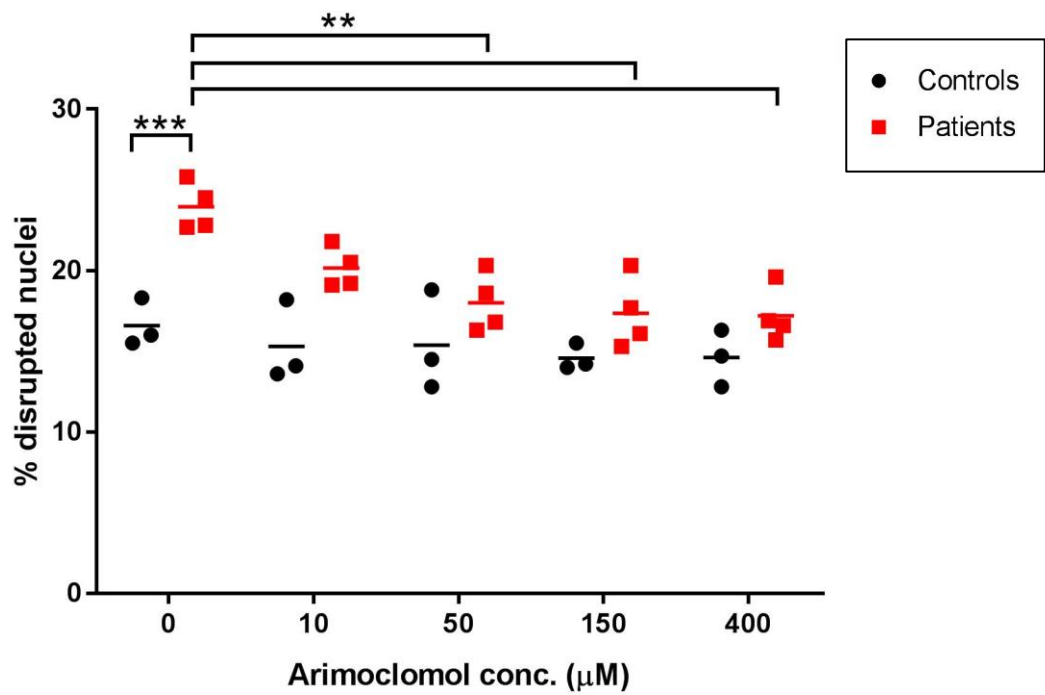


Figure 5.6. Arimoclomol reduces the number of disrupted nuclei in VCP patient fibroblasts

The graph shows the average percentage of disrupted nuclei in control (black dots) and VCP patient (red squares) fibroblasts, 24 hours after treatment with increasing concentrations of Arimoclomol. Each dot represents the average of three independent cultures for each individual fibroblasts line (i.e. 3 control lines and 4 VCP patient lines; approximately 1500 cells/dot). Non-treated cell data from Figure 5.5. Centre lines= mean. ** $p < 0.01$, *** $p < 0.001$; two-way ANOVA.

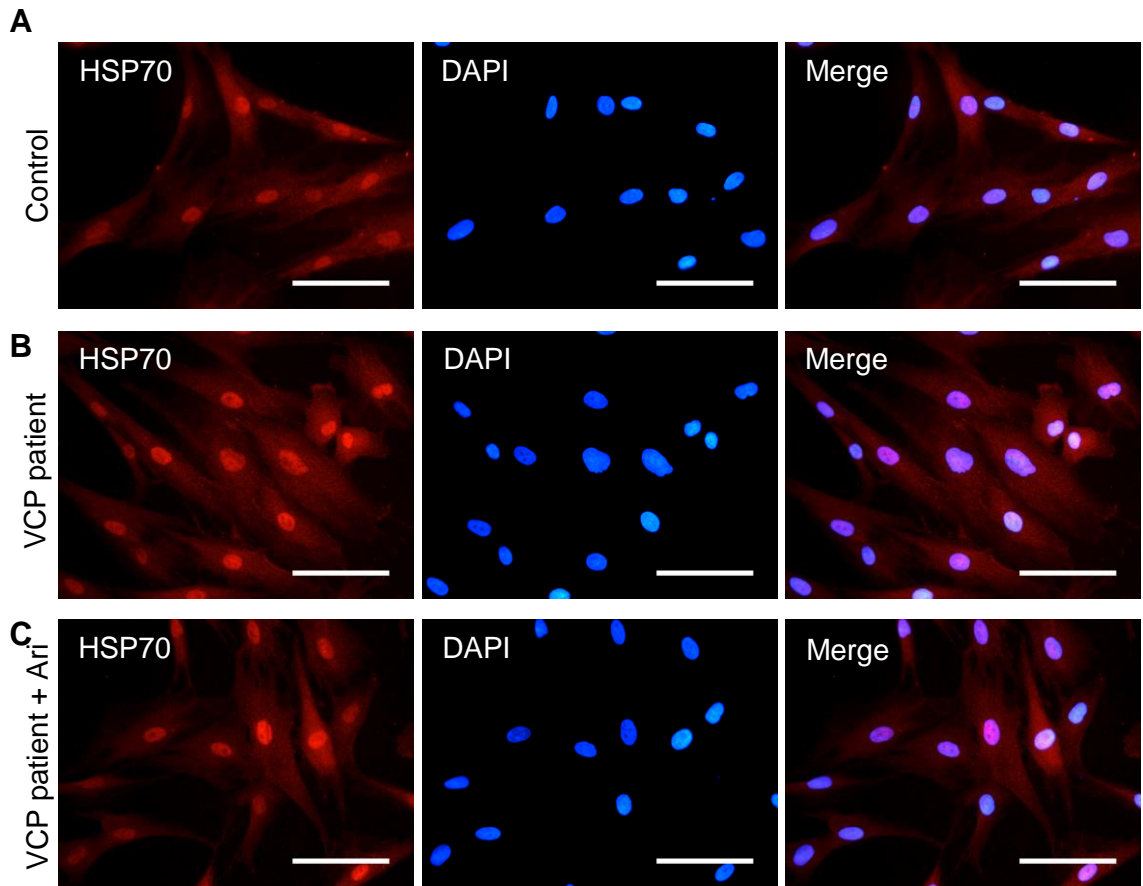


Figure 5.7. HSP70 expression in Arimoclomol-treated VCP patient fibroblasts

Immunostaining for HSP70 (red) in age-matched control fibroblasts **(A)**, VCP patient fibroblasts **(B)** and VCP patient fibroblasts treated with 10 μM Arimoclomol **(C)**. The cells were co-stained with the nuclear marker DAPI (blue). Scale bars represent 50 μm.

5.4.5. Establishing a model of heat shock for human fibroblasts

In order to examine whether cellular pathology in VCP patient fibroblasts was more pronounced under conditions of cellular stress, both control and patient cells were subjected to a short-term heat shock. As there is little data on the response of fibroblasts to heat shock, HSP70 expression was measured in control fibroblasts 24 hours after heat shock at either 42°C or 44°C for 1 hour. There was a significant increase in HSP70 levels at both 42°C and 44°C ($p < 0.05$; one-way ANOVA; **Fig. 5.8 A**). As a heat shock of 44°C for 1 hour increased HSP70 expression by approximately 3-fold, these conditions were used for the following investigations. Immunocytochemical analysis confirmed an increase of HSP70 expression in both control and patient fibroblasts 24 hours after heat shock (44°C, 1 hour; **Fig. 5.8 B**).

5.4.6. Effects of heat shock on VCP patient fibroblasts

The effect of short-term heat stress on control and VCP patient fibroblasts (44°C, 1 hour) was assessed after a 24-hour recovery period. Following heat shock, some histopathological features appeared to be more prominent in VCP patient fibroblast lines. Whilst an obvious increase in cytoplasmic TDP-43 aggregates was not observed, TDP-43 showed intense staining within a number of micronuclei which had formed (**Fig. 5.9 A-B**). No obvious increase in ubiquitin expression was observed in cells displaying multiple micronuclei (**Fig. 5.9 A**). There was, however, an increase in p62 expression, both in the cytoplasm and within the micronuclei (**Fig. 5.9 C**).

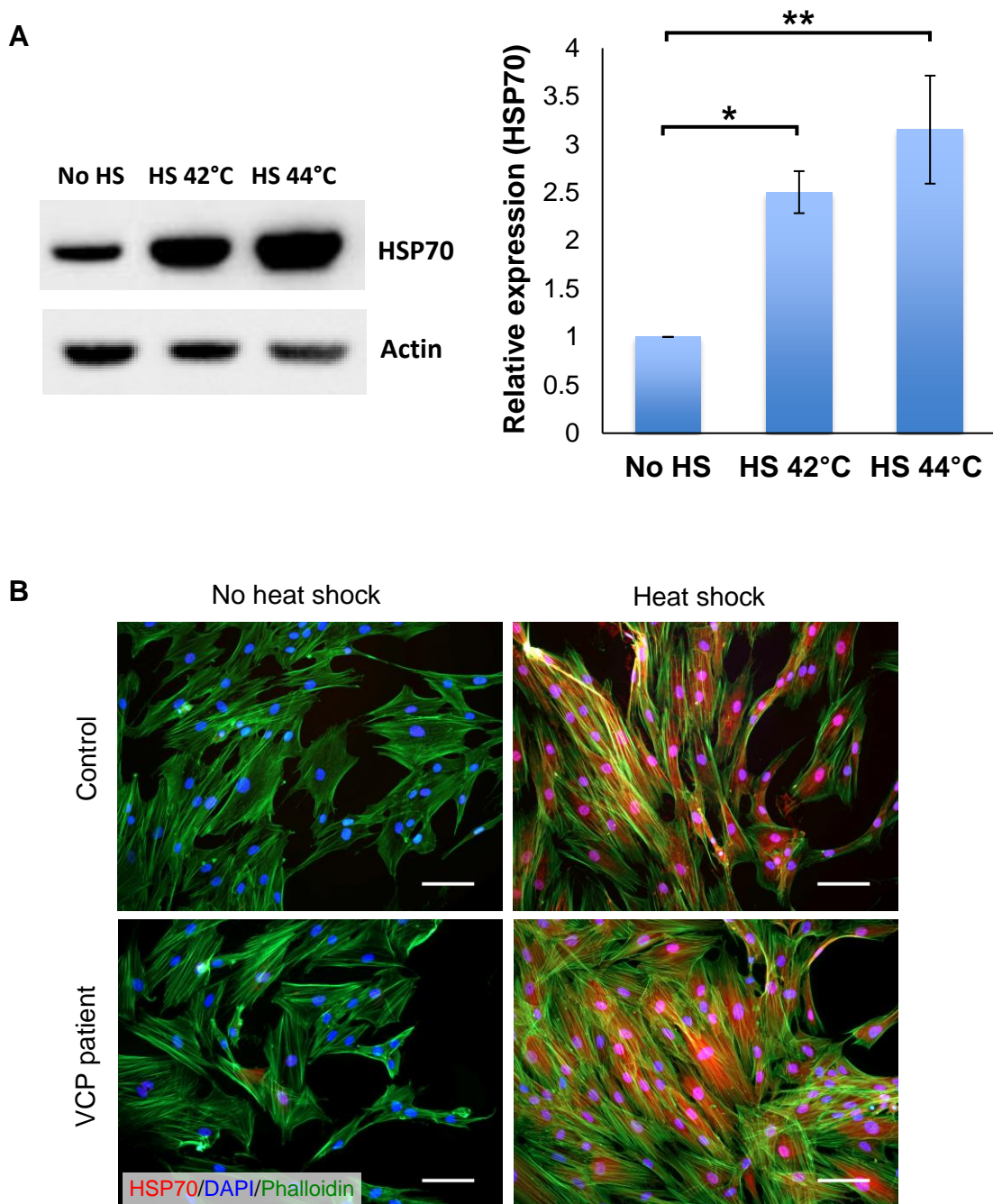


Figure 5.8. HSP70 expression is increased in control and VCP patient fibroblasts in response to heat shock

(A) Western blot of HSP70 expression in control fibroblasts under basal culture conditions and 24 hours after heat shock (HS) at 42°C or 44°C for 1 hour. The bar chart shows the mean relative optical density of the bands in the western blot, normalised to the loading control (actin). Error bars= SEM. N=4 per condition. * $p < 0.05$, ** $p < 0.01$; one-way ANOVA. **(B)** Immunostaining of control and VCP patient fibroblasts under basal culture conditions and following exposure to heat shock at 44°C for 1 hour, for HSP70 (red) co-stained with the nuclear marker DAPI (blue) and F-actin-binding Alexa Fluor 488 phalloidin (green). Scale bars represent 50 μm .

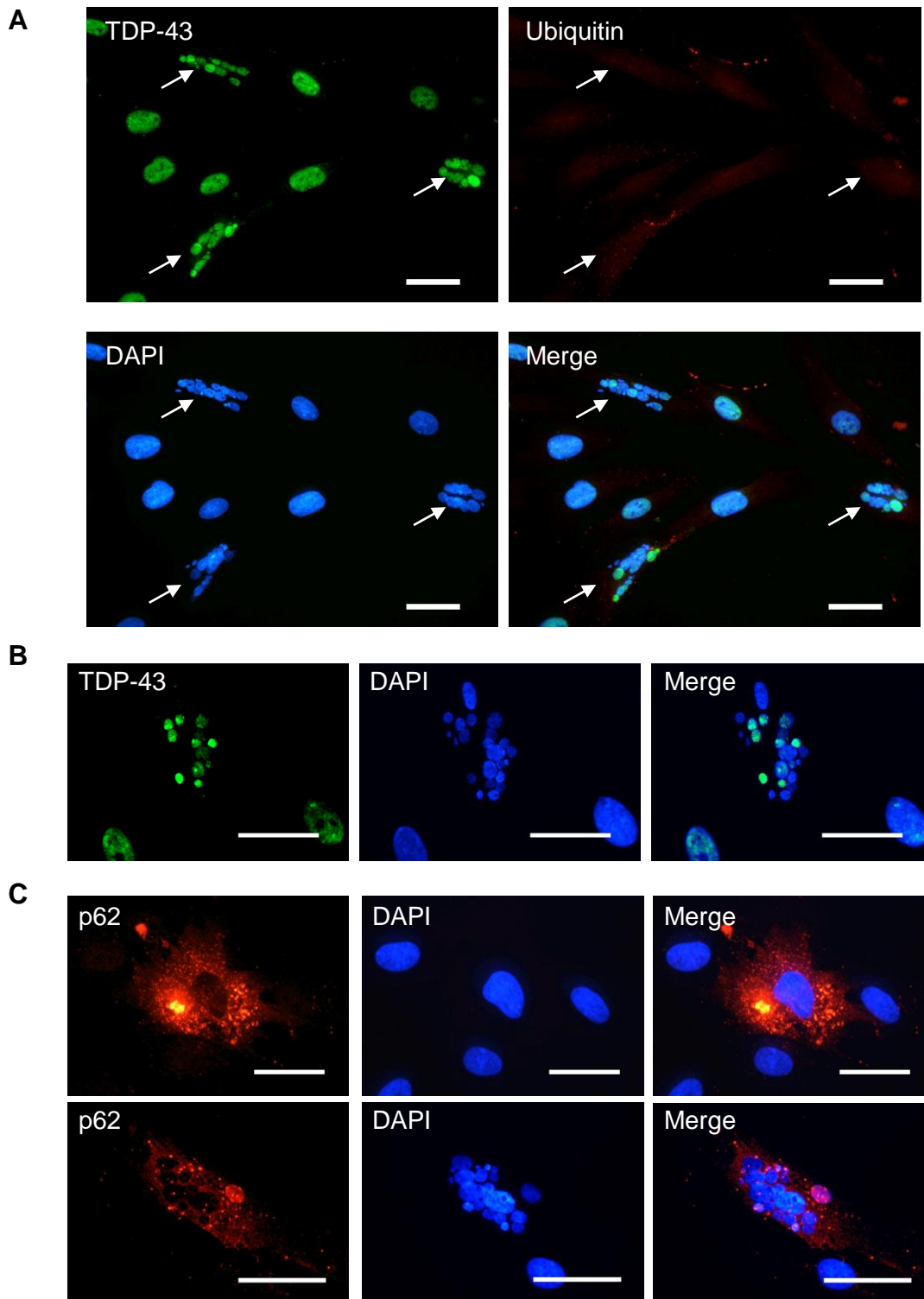


Figure 5.9. Cellular pathology in VCP patient fibroblasts following heat shock
(A) Immunostaining of VCP patient fibroblasts for TDP-43 (green) and ubiquitin (red), co-stained with DAPI (blue). Arrows indicate cells with disrupted nuclei. **(B)** Immunostaining of VCP patient fibroblast showing colocalisation of TDP-43 (green) with multiple micronuclei (blue). **(C)** Immunostaining of VCP patient fibroblasts for p62 (red), co-stained with DAPI (blue). All scale bars represent 20 µm.

As there appeared to be a noticeable increase in the number of micronuclei formed after heat shock, the effect of this stressor on nuclear morphology was assessed next. After a recovery period of 24 hours, control fibroblasts showed a significant increase in the number of cells with disrupted nuclei ($p < 0.001$; two-way ANOVA; **Fig. 5.10 A**). However, there was no difference in the percentage of disrupted nuclei in VCP patient fibroblasts before and after heat shock.

In order to determine whether there was a greater HSR after a shorter recovery period, the effect of heat shock on nuclear morphology was then assessed following a 2-hour recovery period. There was no difference in the percentage of cells with abnormal nuclei in control and patient fibroblasts at 2 hours compared to 24 hours after the induction of heat shock (**Fig. 5.10 B**). Noticeably, immunocytochemistry demonstrated that in VCP patient fibroblast cultures, cells with severely disrupted nuclei showed a lack of HSP70 expression (**Fig. 5.11**).

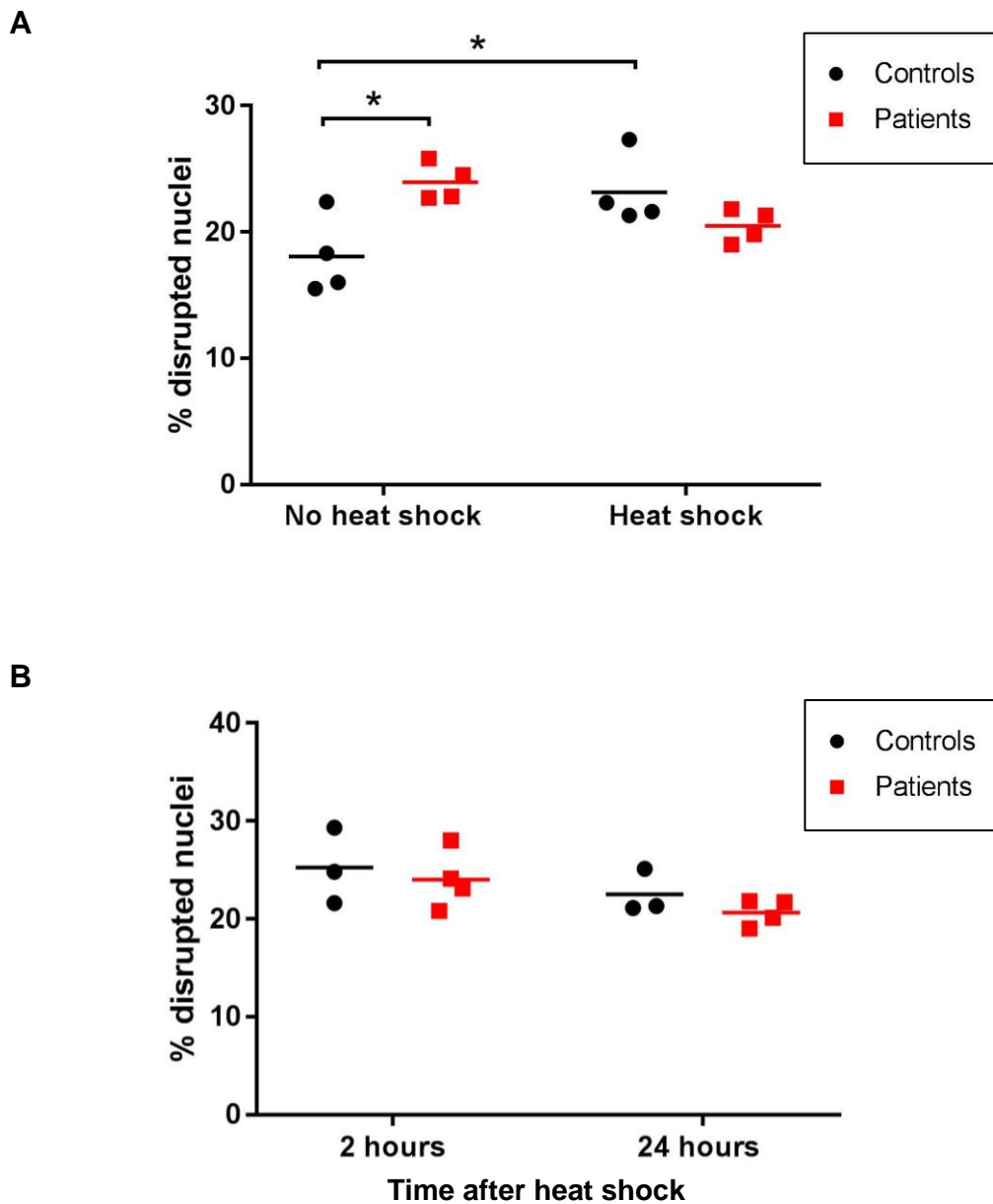


Figure 5.10. Heat shock increases the number of abnormal nuclei in control fibroblasts but has no effect on VCP patient fibroblasts

The graphs show the average percentage of disrupted nuclei in control (black dots) and VCP patient (red squares) fibroblasts **(A)** in the absence of heat shock or 24 hours after induction of heat shock (44°C, 1 hour) and **(B)** 2 hours or 24 hours after induction of heat shock (44°C, 1 hour). Each dot represents the average of three independent cultures for each individual fibroblasts line (i.e. 3 control lines and 4 VCP patient lines; approximately 1500 cells/dot). Centre lines= mean. * $p < 0.05$, ** $p < 0.01$; two-way ANOVA.

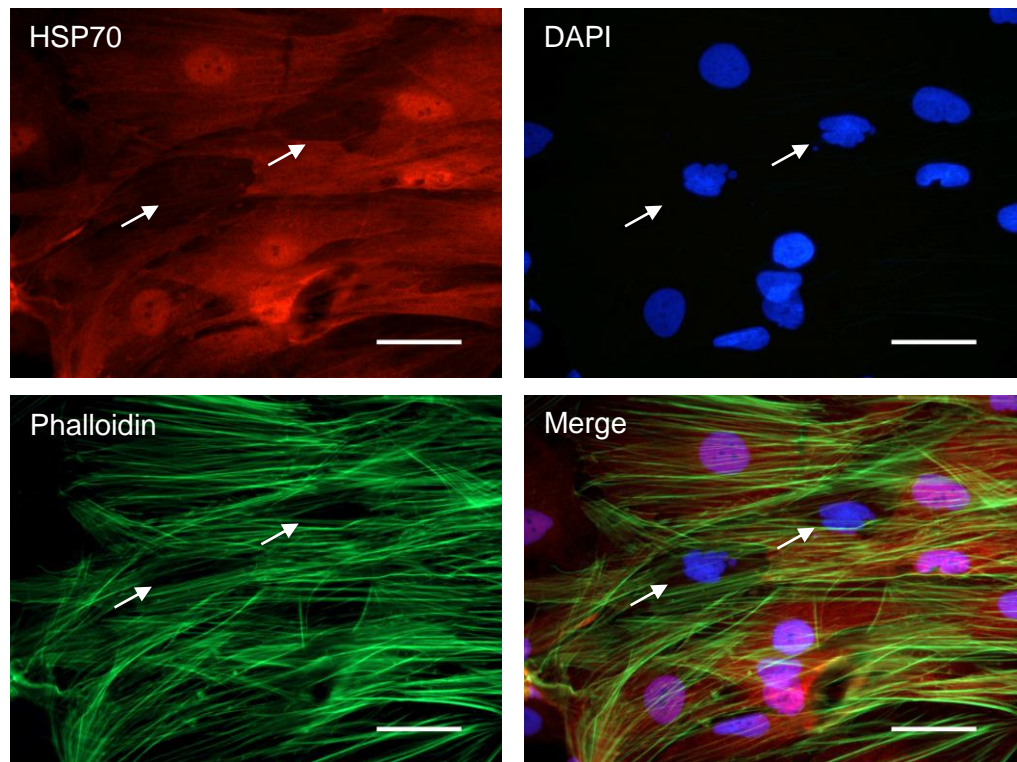


Figure 5.11. VCP patient fibroblasts with severely disrupted nuclei do not express HSP70 after heat shock

Immunostaining of VCP patient fibroblasts after heat shock for HSP70 (red), co-stained with the nuclear marker DAPI (blue) and F-actin-binding Alexa Fluor 488 phalloidin (green). Arrows indicate cells with disrupted nuclei, showing depletion of HSP70. Scale bars represent 20 μm .

5.5. Discussion

Upregulation of the HSR with Arimoclomol has been shown to be beneficial in ameliorating characteristic pathological features and functional deficits in a mutant VCP mouse model of MSP, described in Chapter 3 of this Thesis, which recapitulates the characteristic features of IBM. Furthermore, Arimoclomol is beneficial in ameliorating characteristic pathological features in dermal fibroblasts derived from patients with sporadic IBM, described in Chapter 4. As these models have demonstrated a significant overlap in pathology between IBM and MSP, the aim of this Chapter was to compare the effect of Arimoclomol on fibroblasts obtained from MSP patients with two independent mutations in the *VCP* gene. Three patients had the R155H mutation, the most prevalent MSP-associated mutation, whilst the fourth patient had the R93C mutation.

5.5.1. IBM-relevant pathological features in VCP patient fibroblasts

Since only a limited number of studies have investigated pathological features in VCP patient fibroblasts (Bartolome et al. 2013; Nalbandian, Llewellyn, Gomez et al. 2015; Zhang et al. 2017), this Chapter first aimed to clarify whether the VCP patient fibroblasts obtained for this study displayed characteristic hallmarks of IBM.

5.5.1.1. Aggregation of IBM-associated proteins

Muscle biopsies from MSP patients display sarcoplasmic inclusions of TDP-43, alongside nuclear depletion of the protein in inclusion-bearing fibres (Weihl et al. 2008; Olivé et al. 2009). This cytoplasmic TDP-43 accumulation has also been observed in mutant VCP-expressing cells and the muscle of transgenic mouse models (Gitcho et al. 2009; Ju et al. 2009; Nalbandian et al. 2012; Ahmed et al. 2016), although as previously discussed, the relevance of TDP-43 redistribution in sporadic IBM and MSP remains unclear. Although diffuse cytoplasmic staining was observed in the sporadic IBM fibroblasts described in Chapter 4 of this Thesis, the VCP patient fibroblasts in this study displayed cytoplasmic inclusions of TDP-43, with TDP-43, as normal, restricted to the nuclei in control cells. These cytoplasmic inclusions are more typical of the TDP-43-positive deposits that occur in damaged muscle fibres in MSP and sporadic IBM patients (Weihl et al. 2008).

TDP-43 was retained within the nuclei of VCP patient fibroblasts, even within those cells with cytoplasmic aggregates. However, a number of cells did have nuclear depletion of TDP-43, although these did not necessarily correlate with TDP-43 aggregation. Furthermore, immunostaining revealed that N-terminal TDP-43 was retained within nuclei, including within micronuclei which had pinched off from the main nucleus. No cytoplasmic aggregates were observed with the N-terminal antibody, suggesting that cytoplasmic TDP-43 aggregates were composed of C-terminal fragments, as expected.

Consistent with previous studies, there was also evidence of increased ubiquitin and p62 staining in VCP patient fibroblasts compared to healthy controls. P62-positive rimmed vacuoles were prominent within patient fibroblasts and a smaller number of vacuoles stained positive for ubiquitin, although no colocalisation studies were undertaken. Although cytoplasmic rimmed vacuoles are considered a typical characteristic of MSP, a number of studies have shown that vacuoles are not evident in all cases (Guyant-Marechal et al. 2006; Hübbers et al. 2007; Gidaro et al. 2008; Kimonis, Mehta et al. 2008; Wehl et al. 2009; Evangelista et al. 2016). It is therefore interesting that these vacuoles were so prominent in the VCP patient fibroblasts in this study.

Rimmed vacuoles are thought to be autophagic in nature (Ju et al. 2009). Ubiquitin and p62 both function in aggregate formation and proteolysis. Ubiquitin targets substrates for degradation and p62 directly interacts with ubiquitin and LC3 to act as a shuttle protein, transporting ubiquitinated proteins into the autophagosome or lysosome (Pankiv et al. 2007; Ichimura et al. 2008; Kirkin et al. 2009; Komatsu & Ichimura 2010). Although polyubiquitination is usually required for degradation or aggresome formation, p62 may also function in an ubiquitin-independent manner, for selective autophagic clearance of non-ubiquitinated substrates. Although it is not clear why p62-positive vacuoles were more prominent in VCP patient fibroblasts, it may suggest a build-up of substrates processed independently of ubiquitin or a disruption of p62-dependent autophagic clearance. On the other hand, it may be that the complex substrates have been deubiquitinated and ubiquitin recycled.

5.5.1.2. Mitochondrial morphology in VCP patient fibroblasts

Abnormalities of mitochondrial dynamics have long been considered as a common pathological feature in a number of neurodegenerative and neurological diseases including IBM, although they are less commonly reported in MSP (Weihl et al. 2009; McInnes 2013; Joshi et al. 2014; Gao et al. 2017). No obvious mitochondrial structural defects were observed in VCP patient fibroblasts in this study. Staining for the outer mitochondrial membrane marker TOMM20 revealed evidence of potentially fewer mitochondria in VCP patient fibroblasts harbouring the R93C mutation and some fragmentation. Interestingly, these fibroblasts were obtained from a patient with a more severe phenotype. However, due to time restraints, no quantitative measurements of mitochondrial size, volume and fragmentation, were made in this study. Such measurements of mitochondrial content, alongside examination of mitochondrial membrane potential respiration and mitophagy, would provide a clearer indication of mitochondrial disruption in this model.

Prominent mitochondrial clustering was also evident in the VCP patient fibroblasts in this study and occurred around disrupted nuclei. In comparison, in healthy control fibroblasts and cells with normal nuclear morphology mitochondria were evenly spread. Although perinuclear mitochondrial clustering has been reported in a number of models, discussed below, the mechanism underlying the formation of these mitochondrial clusters and the role they play in disease is unclear.

Mitochondria are highly dynamic organelles that undergo regulated turnover in order to regulate physiological function and adapt to changes in cellular requirements (Detmer & Chan 2007). As mitochondrial number and morphology are tightly regulated by continual fission and fusion events, it has been suggested that alterations in these dynamics may cause abnormal clustering of mitochondria. Expression of hFis1, a mitochondrial protein known to regulate fission in mammalian cells, has been shown to cause rapid fragmentation of the mitochondrial network and dramatic nuclear clustering in HeLa cells (Frieden et al. 2004). Interestingly, these morphological alterations had little impact on mitochondrial function. Furthermore, perinuclear clustering of mitochondria in fibroblasts obtained from patients with sporadic Alzheimer's disease (AD) has

been associated with decreased levels of the mitochondrial fission protein DLP1 (Wang et al. 2008). Again, there was no apparent functional consequence of such mitochondrial redistribution. Abnormal clustering of mitochondria in the cell bodies of spinal cord motor neurons has been also been noted in transgenic mice overexpressing full-length human TDP-43 (Xu et al. 2010). This was associated with abnormal expression of key proteins that regulate mitochondrial fission and fusion. Finally, fission and fusion have been found to be severely impaired in TDP43-overexpressing motor neurons exhibiting abnormal TDP-43 localisation and severe perinuclear aggregation of mitochondria in cell bodies (Wang, et al. 2013). Together, these studies suggest abnormal perinuclear clustering of mitochondrial may be a result of an imbalance of mitochondria fission and fusion events and may be linked to TDP-43 expression.

The removal and degradation of damaged mitochondria occurs via mitophagy. This is the autophagic elimination of mitochondria and is intimately linked to mitochondrial fission and fusion processes (Youle & van der Bliek 2012; Vásquez-Trincado et al. 2016). Interestingly, it has been shown that parkin-mediated degradation of dysfunctional mitochondria by the autophagic pathway results in the recruitment of p62, followed by perinuclear clustering of damaged mitochondria (Narendra et al. 2010; Okatsu et al. 2010; Chan et al. 2011). This suggests that the clustering of mitochondria observed in the VCP patient fibroblasts in the present study could be an attempt of the cell to sequester damaged mitochondria.

Interestingly, in the sporadic IBM patient fibroblasts described in Chapter 4 of this Thesis, morphologically abnormal nuclei were associated with a disrupted actin cytoskeleton. It is therefore possible that mitochondrial clustering may result from a failure of mitochondrial transport and reduced mitochondrial movement due to a disruption in cytoskeletal proteins and microtubules that traffic mitochondria in mammalian cells (Wu et al. 2013; Woods et al. 2016).

Finally, apoptosis-inducing agents have been shown to trigger perinuclear clustering of mitochondria in human NT2 cells (Dewitt et al. 2006). The clustering of mitochondria has been proposed as an initial step in triggering apoptosis and is thought to precede nuclear fragmentation. However,

apoptosis-related transport disruption is unlikely to have caused the mitochondrial clustering in the VCP patient fibroblasts in this study as there was no evidence of apoptosis, as assessed using the TUNEL assay and perinuclear clustering was only observed in cells in which abnormal nuclear morphology was already noticeable.

The cause of mitochondrial clustering around disrupted nuclei in VCP patient fibroblast remains to be determined. However, it would be interesting to assess whether there are any functional mitochondrial deficits associated with the abnormal mitochondrial morphology, as changes in mitochondrial dynamics and bioenergetics have previously been reported in VCP patient fibroblasts (Bartolome et al. 2013; Nalbandian, Llewellyn, Gomez et al. 2015).

5.5.1.3. Disrupted nuclei in VCP patient fibroblasts

An interesting finding in the VCP fibroblasts from MSP patients, as also observed in the sporadic IBM patient fibroblasts, was the increase in the percentage of cells with disrupted nuclei, compared to healthy control fibroblasts. Although only approximately 25% of VCP patient fibroblasts demonstrated abnormal changes in nuclear morphology, this likely reflects the fact that human fibroblasts are heterogeneous cell populations (Tracy et al. 2016; Stunova & Vistejnova 2018).

As discussed in Chapter 4 of this Thesis, changes in nuclear morphologies are associated with a wide range of disease states (Mukherjee et al. 2016). However, the effect of MSP on nuclear morphology has had little attention. Assessment of the integrity of myonuclei surface structures has only been undertaken in a single MSP patient. Using electron micrographs from muscle biopsies, the length of the outer and inner nuclear membranes, as well as the fibrous laminae were markedly decreased in the MSP patient compared to the measurements of the nuclei of seven control muscle biopsies (Matsubara et al. 2016). The findings in this study support abnormal nuclear architecture as a sign of pathology in MSP, in common with IBM cases. VCP is frequently reported to have a role in nuclear envelope reconstruction (Hetzer et al. 2001). However, this has only been demonstrated *in vitro* in *Xenopus* egg extracts and there has been no further investigation into the role of VCP in

nuclear integrity in a mammalian system. It is possible that as the outer nuclear membrane is continuous with the endoplasmic reticulum (ER) membrane, an impaired function of VCP in ER-associated degradation (ERAD) may lead to the early loss of the outer nuclear membrane, or conversely, impairment of the nuclear membrane could impede ERAD (Matsubara et al. 2016). Whether altered nuclear size or shape contributes to disease pathology or is a secondary effect of disease remains to be determined.

5.5.2. Comparison of different VCP mutations on pathological features in patient fibroblasts

Interestingly, aside from some potential alterations in mitochondrial morphology in VCP patient fibroblasts harbouring the R93C mutation, no obvious differences were observed in the extent of pathology between the four patient cell lines examined. Both the R155H and R93C mutations studied in this Chapter reside within the N-domain of the VCP gene. Although the effect of these mutations on VCP function are not well understood, mutations residing within the N-terminal are proposed to be involved in substrate and cofactor association, so it may be that these mutations have similar effects (Watts et al., 2004; Weihl et al., 2009). However, the three MSP patients with the R155H mutation had a mild, muscle-only phenotype compared to the patient with the R93C mutation, who had a more severe disease phenotype, so it is surprising that some difference in pathological features were not observed.

As discussed in Chapter 4 of this Thesis, investigating a greater number of cell lines, including fibroblasts obtained from patients at a more advanced stage of clinical disease, would control for patient variability and provide greater insight into whether the extent of pathology in the fibroblast model correlates with disease severity. It would also be interesting to examine fibroblasts obtained from patients with the A232E VCP mutation, which causes a more severe phenotype and was the mutation described in the *in vivo* mouse model of MSP in Chapter 3. However, due to the rare nature of MSP, it was not possible to obtain fibroblasts from patients harbouring this mutation for the purposes of this study. If a number of patient fibroblasts with different mutations could be obtained, this patient fibroblast model may provide a tool for untangling the different manifestations of various mutations in the VCP gene.

5.5.3. Effect of Arimoclomol on pathological characteristics in VCP patient fibroblasts

The aim of this Chapter was to examine the effects of the HSR co-inducer Arimoclomol *in vitro* in the VCP fibroblast model of MSP. As characteristic histopathological changes were identified in VCP patient fibroblasts under basal culture conditions, the effect of Arimoclomol could be tested in these cells.

Since abnormal nuclear morphology was a prominent feature in the VCP patient fibroblasts, the effect of Arimoclomol was assessed on this key pathological characteristic. A single treatment of Arimoclomol reduced abnormal nuclear morphology after a recovery period of 24 hours. All concentrations were effective, however, there was a significant decrease in the percentage of disrupted nuclei at concentrations above 50 μM . The effect of the highest concentration tested, 400 μM , was no greater than that of 150 μM , suggesting the maximal effect of Arimoclomol was reached at 150 μM . As discussed in Chapter 4 of this Thesis, Arimoclomol did not affect the number of disrupted nuclei in control fibroblasts, most likely because Arimoclomol is a co-inducer of the HSR and thus only acts on cells already under cellular stress.

This beneficial effect of upregulation of the HSR with Arimoclomol in VCP patient fibroblasts, obtained from patients with MSP suggest that these patient fibroblasts are under a cellular stress, most likely due to a disruption of protein homeostasis pathways and the accumulation of damaged proteins. Subsequent elevation of heat shock proteins (HSPs) following treatment with Arimoclomol helps to restore protein homeostasis and improve pathology in these cells. As in the sporadic IBM patient fibroblasts described in Chapter 4, there was no evidence of an increase in HSP70 expression in VCP patient fibroblasts. Again, HSP70 expression in these fibroblasts was assessed 24 hours after the addition of Arimoclomol, so it is possible that the time point in which an Arimoclomol-induced increase in HSP70 occurs may have been missed, or that an increase in the length of Arimoclomol treatment may lead to increase HSP70 expression. Alternatively, it is possible that immunocytochemistry was not sensitive enough to detect a change in HSP70 expression. Immunocytochemistry was only carried out in fibroblasts following treatment with 10 μM concentration of Arimoclomol. As higher concentrations had a greater effect on pathology in VCP

patient fibroblasts, a more obvious increase in HSP70 intensity may be observed with concentrations above 10 μ M. On the other hand, it may be that the threshold for activation of the HSR in untreated patient cells has not been reached and thus, as Arimoclomol only works on cells under stress in which the HSR is already activated, treatment with Arimoclomol would not be expected to further increase HSP70 expression in VCP patient fibroblasts.

5.5.4. VCP mutations and the implications of upregulating the heat shock response

VCP is involved in a variety of cellular functions. A number of studies have identified a role for VCP in protein degradation pathways of the cell and thus in maintaining intracellular protein homeostasis (Ju & Wehl 2010; Nalbandian et al. 2011; Meyer & Wehl 2014). VCP regulates the ubiquitin-dependent degradation of a wide variety of proteins involved in multiple, wide-ranging cellular signalling cascades, binding to ubiquitinated substrates either directly, or indirectly associating through cofactors containing ubiquitin-association domains (Dai et al. 1998; Dai & Li 2001; Wang et al. 2004; Ye 2006; Meyer & Wehl 2014). In this manner, VCP regulates numerous biological processes by the ubiquitin-proteasome system. Indeed, any disruption to VCP due to MSP-causing mutations, particularly in the N-domain, which is involved in ubiquitin binding, can therefore lead to widespread changes in the cellular environment.

Much of the activity of VCP is thought to rely on its 'segregase' activity, disassembling various complexes, including those containing ubiquitinated proteins. Histone deacetylase 6 (HDAC6) is a cytoplasmic deacetylase which interacts with VCP to help determine the fate of misfolded, ubiquitinated proteins (Seigneurin-Berny et al. 2001; Boyault et al. 2007). VCP is able to disassemble HDAC6 from ubiquitinated protein aggregates, which allows them to be degraded via the proteasome. Disruption to the finely tuned equilibrium of HDAC6 and VCP, due to the dysfunction of VCP, can lead to irreversible binding of HDAC6 to polyubiquitin chains and accumulation of ubiquitinated protein aggregates leading to the formation of aggresomes and inclusion body formation (Boyault et al. 2006, Boyault et al. 2007). This suggests a novel mechanism for VCP in preventing the formation of cellular inclusion bodies and acceleration of protein degradation by the proteasome.

Studies have also shown that MSP-causing mutations in *VCP* impair autophagy, via abnormalities of autophagosome maturation, cause defects in ERAD and lead to reduced proteasome activity (Weihl et al. 2006; Ju, et al. 2009; Tresse et al. 2010; Ching et al. 2013; Erzurumlu et al. 2013; Evangelista et al. 2016).

The exact contribution of these defects to the pathogenesis of MSP is unclear and it is possible that not all MSP-causing *VCP* mutations have the same effect. However, it is likely that mutations in the *VCP* gene disrupt the normal function of *VCP*, resulting in the accumulation of ubiquitinated, misfolded proteins that may have deleterious effects and contribute to disease pathogenesis. It is therefore possible that Arimoclomol facilitates the handling and degradation of misfolded cytosolic or ER proteins in *VCP* patient fibroblasts, ultimately reducing signs of pathology and improving the health of the cells.

5.5.5. Effects of heat stress in *VCP* patient fibroblasts

Fibroblasts obtained from patients with *VCP* mutations showed signs of pathological abnormalities under basal culture conditions. To investigate whether the observed cellular phenotypic changes could be exacerbated, this study also investigated the effects of exposure to a mild, short-term heat stress. Acute stress conditions, such as heat shock, can cause many proteins to unfold. Stress-denatured proteins increase the risk of aggregate formation if they exceed the capacity of chaperone systems to handle them (Kakkar et al. 2014). A number of studies, including in the Greensmith lab, have examined the effect of elevated temperature, above the normal body temperature of 37°C, on cellular models of diseases (Rodriguez-Ortiz et al. 2016; Carnemolla et al. 2015; Clarke et al. 2017). However, there is little data on the response of human fibroblasts to heat shock. For this reason, the heat shock conditions of this study first had to be refined.

Heat shock conditions and recovery times in fibroblast studies vary between publications. Temperatures range between 40-45°C for anywhere between 30 minutes to 2 hours (Sato et al. 1996; Paradisi et al. 2005; Rohde et al. 2013; Rodriguez-Ortiz et al. 2016; Lo Bello et al. 2017; San Gil et al. 2017). In this study, cells were subjected to a heat shock of 42°C or 44°C for 1 hour and left

to recover at 37°C for 24 hours. Both control and patient fibroblasts were able to mount a HSR, as evident by an increase in HSP70 expression. HSP70 upregulation was found to be greater at 44°C, therefore this temperature was used for subsequent experiments.

Whether VCP patient fibroblasts are more susceptible to heat stress than control fibroblasts, remains to be established. Some cellular pathologies appeared more evident in patient cells in response to heat shock compared to unstressed cells. Control fibroblasts appeared to have recovered from the stress after 24 hours, as their appearance was similar to control fibroblasts cultured under basal culture conditions. However, there appeared to be greater p62 expression and an increase in micronuclei formation within stressed patient fibroblasts compared to unstressed patient fibroblasts. However, further quantification of these markers is required in order to make a definitive conclusion of the scale of this effect.

As previously discussed in this Thesis, cellular stress invokes a protective HSR in which HSF1 is activated to increase HSP expression. Heat-induced activation of HSF1 is a rapid process, occurring within minutes of heat-shock exposure (Neueder et al. 2017). If the effects of heat shock are less evident in control fibroblasts, this may suggest that protein homeostasis had been restored in these cells following the 24-hour recovery period. If the protein homeostasis network is already disrupted in VCP patient fibroblasts on the other hand, the addition of an extra stressor may overwhelm the cells, making cellular pathology more evident. Interestingly, biochemical analysis of the VCP mutants R155H and A232E demonstrate that these mutants have enhanced ATPase activation in response to elevated temperature, associated with ATP-dependent conformational alterations, which it has been suggested may detrimentally alter VCP function by destabilising VCP-mediated protein interactions and have an impact on protein homeostasis (Halawani et al. 2009).

Although immunocytochemistry suggested that HSP70 expression was increased in patient fibroblasts following heat shock, cells with severely disrupted nuclei, displaying multiple micronuclei, actually showed a lack of HSP70. This may suggest that these cells are not able to mount a HSR and

may consequently undergo cell death. Fragmented nuclei are thought to trigger apoptosis (Negoescu et al. 1998; Cox & Faragher 2007; Utani et al. 2010), although in this study, a TUNEL assay revealed no evidence of apoptosis. This suggests that these micronuclei are either somehow shielded from detection by TUNEL staining or that these fibroblasts are more resistant to apoptosis and the changes in nuclear architecture in these cells may not have reached the threshold limit for activating this cell death pathway.

Surprisingly, there was no difference in the percentage of disrupted nuclei in VCP patient fibroblasts after a heat shock of 44°C for 1 hour. As no effect was found on disrupted nuclei after 24 hours, the effect of heat shock on this outcome measure was also assessed after a shorter recovery period of 2 hours. However, there was no difference in the percentage of disrupted nuclei at 2 hours compared to 24 hours after heat shock. Interestingly, the severity of the disruption to the nuclei appeared much greater, with many cells displaying multiple micronuclei as opposed to herniations of the nuclear envelope. It would therefore be worthwhile to quantify the disrupted nuclei into subgroups, by the degree of disruption. Furthermore, it is possible that cells with severely dysmorphic nuclei died and detached, although this seems unlikely as no freely floating cells were observed within the medium before fixation. As discussed in Chapter 4 (section 4.5.1.3), automated analysis, as opposed to the manual counts undertaken in this study, would potentially provide a more accurate quantitative measure of the degree of nuclear disruption in fibroblasts and would be beneficial for taking into account the range of severities of abnormal nuclear morphologies.

5.6. Conclusion

The results presented in this Chapter suggest that upregulation of the HSR with Arimoclomol is beneficial in attenuating characteristic pathological features in fibroblasts derived from MSP patients presenting with an inclusion body myopathy. This study provided a more extensive investigation of the cytopathology of cultured VCP patient fibroblasts, compared to previously described studies. Under basal culture conditions, these cells displayed characteristic pathological features of MSP and sporadic IBM, including morphologically abnormal nuclei, TDP-43 mislocalisation, increased ubiquitin

expression and p62 aggregation. Moreover, when placed under a mild, short-term heat stress, these cells show evidence of exacerbated pathology. This preclinical model will now be instrumental in gaining a greater understanding of the complex pathomechanisms involved in MSP and will have a vital role for aiding the discovery of other novel therapeutic agents. Furthermore, this model can be used in parallel with fibroblasts obtained from sporadic IBM patients, in order to untangle the differences between sporadic IBM and MSP.

Chapter 6

General discussion

Inclusion body myositis (IBM) is an acquired muscle disease that typically affects adults over the age of 50. Patients develop progressive proximal leg and distal arm weakness, which can lead to severe disability within several years of onset. Muscle biopsies from IBM patients display several pathological features, broadly described as either inflammatory or degenerative, however, the primary pathogenic mechanism remains unclear. At present, there is no effective treatment for IBM.

As most clinical trials targeting the inflammatory component of IBM have been unsuccessful in improving muscle strength or preventing disease progression, attention has turned to targeting non-immune mechanisms, including protein misfolding and aggregation (Kakkar et al. 2014). The endogenous heat shock response (HSR) represents an attractive therapeutic target for IBM, as this stress-induced, cytoprotective mechanism aims to readdress the balance of protein homeostasis, via the rapid and robust expression of molecular chaperones known as heat shock proteins (HSPs).

In this Thesis, the effect of upregulating the HSR on IBM pathology was investigated *in vitro* and *in vivo*. Upregulation of the HSR was achieved using the pharmacological co-inducer Arimoclomol. Arimoclomol was effective in ameliorating disease-relevant pathology and improving muscle function in a mouse model of multisystem proteinopathy (MSP), also referred to as inclusion body myopathy with Paget's disease of bone and frontotemporal dementia (IBMPFD), a disease which has a similar muscle disease phenotype to IBM. Furthermore, Arimoclomol reduced IBM-like pathology in fibroblasts derived from both sporadic IBM patients and patients with MSP, which arguably represent more clinically relevant models. All of these models displayed characteristic pathological features of IBM, including TDP-43 mislocalisation, increased ubiquitin expression, p62 aggregation and mitochondrial disruption, pointing towards a disruption of protein handling networks and therefore making them appropriate models for assessing the effects of Arimoclomol. Together, the results of this Thesis demonstrate that upregulation of the HSR with Arimoclomol may be a useful therapeutic approach for ameliorating protein mishandling in IBM and may therefore be an effective treatment for the disease.

6.1. Replicating the cellular stress response in models of IBM

The regulation of protein homeostasis is vital for maintaining a stable and functional proteome and thus, for cell survival. As many of the proposed pathomechanisms of IBM are known to result in the accumulation of proteinaceous cytoplasmic aggregates, as extensively discussed throughout this Thesis, targeting protein handling mechanisms by harnessing the HSR presents a promising therapeutic strategy.

The HSR is an essential and ubiquitous cellular defence mechanism that is highly conserved, with all living organisms from yeast to man readily upregulating chaperone proteins upon exposure to various types of cellular stress (Richter et al. 2010; Klaips et al. 2018). However, in mammals and more complex organisms, proteostasis networks may differ between diverse cell types and tissues, with some cells of the same tissue displaying variations in the HSR in terms of the speed and magnitude of the response (Blake et al. 1990; Nishimura et al. 1991; Brown & Rush 1999; Kaarniranta et al. 2002; Batulan et al. 2003; Uhlén et al. 2015; Sala et al. 2017). Cell-type specific differences of the HSR may result in a difference in susceptibility of different cell types to the expression of aggregation prone proteins. This may in some respects explain the selective vulnerability of certain tissues affected in diseases such as MSP and the high susceptibility for specific muscle groups to be affected in IBM.

In skeletal muscle, the molecular chaperone HSP70, a typically used marker of the generalised stress response, is rapidly induced in response to both non-damaging and damaging stress stimuli (Senf 2013). Indeed, in the previously described *in vitro* models of IBM (Ahmed et al. 2016), overexpression of β -APP and exposure to inflammatory mediators in cultured rat myocytes results in a significant increase in HSP70 expression, which is further upregulated upon treatment with Arimoclomol. A similar response to Arimoclomol was observed in affected muscle of the IBM mouse model described in Chapter 3 of this Thesis. However, the response of dermal fibroblasts to stress is less well characterised than other cell types. As skin is not characteristically affected in IBM patients, it was not known whether these cells would display key disease features such as protein aggregates, indicative of protein mishandling. The results presented in

Chapters 4 and 5 demonstrate that protein homeostasis is disrupted in fibroblasts derived from both sporadic IBM and MSP patients, with clear evidence of TDP-43 mislocalisation, ubiquitin and p62 aggregation and vacuole formation in these cells. Despite these pathological features, HSP70 was not upregulated in untreated patient fibroblasts. This was also the case in the muscles of untreated mutant VCP mice (Ahmed et al. 2016). This may be due to a reduced ability of these cells and tissues to upregulate the HSR, or may suggest there is higher threshold for the induction of HSP70, Alternatively, other HSPs may be more involved in the response to stress in these cells.

However, it has previously been established that heat shock causes a rapid and transient increase in HSP70 mRNA levels in fibroblasts, which peaks after 1 hour and returns to control levels within 24 hours (Hitraya et al. 1995). The results presented in Chapter 5 of this Thesis confirm this response of control dermal fibroblasts to stress, although in these experiments, HSP70 levels were still elevated 24 hours after heat shock. Surprisingly, although MSP patient fibroblasts displayed signs of cellular stress under basal culture conditions, these cells did not demonstrate an obvious increased vulnerability to cellular stress. An additional heat stress in these cells did not appear to significantly amplify pathology. This may be linked to the increased HSP70 expression that occurred concurrently in these cells upon heat stress, meaning the HSR in these cells was able to prevent further protein aggregation. Although requiring further investigation, this would be physiologically relevant as skin is often exposed to high temperatures and other environmental stresses.

A strength of this study is that multiple models of IBM were characterised. The effect of upregulating the HSR in IBM was investigated both in a clinically relevant human fibroblast *in vitro* model and in a physiologically relevant *in vivo* model, which provided essential data beyond the scope provided by cell culture. Although each individual cell can induce the HSR independently, there may be additional levels of regulation and interactions that exist in multicellular systems. For example, ALS studies have revealed that surrounding astroglia can supply neurons with vital HSPs which are taken up from the extracellular space (Robinson et al. 2005; Gifondorwa et al. 2007; Kalmar & Greensmith 2017). Uncoordinated activation of the HSR in cells could thus cause severe

disturbances of interactions between cells and tissues. Furthermore, in cultured cells, HSF1 has been shown to be stably expressed but expression levels and subcellular localisation in the context of entire animals may vary depending on the tissue and the developmental state (Fiorenza et al. 1995; Vihervaara & Sistonen 2014). This highlights the importance of investigating the effects of upregulation of the HSR both *in vitro* and *in vivo*.

6.2. Cellular chaperones as therapeutic targets

To date there has been little investigation into the effects of targeting the HSR as a therapeutic strategy for IBM. This is in spite of the fact that the accumulation of protein aggregates is a characteristic pathological feature of IBM and studies have found changes in the expression of specific HSPs in IBM and other muscle diseases (Hohlfeld & Engel 1992; Bornman et al. 1995; Banwell & Engel 2000; Askanas et al. 2009; De Paepe et al. 2009; Thakur et al. 2018). Furthermore, numerous studies have also demonstrated that particular HSPs can protect against protein aggregation in disorders such as Huntington's, ALS, and Parkinson's (Wytttenbach & Arrigo 2009).

The results presented in this Thesis demonstrate that targeting the HSR, by upregulating the production of molecular chaperones with Arimoclomol, is a promising therapeutic approach for IBM. Furthermore, this study explores an additional cell type, dermal fibroblasts, in which Arimoclomol is able to prolong the activation of the HSR (Kieran et al. 2004; Kalmar et al. 2008; Kalmar & Greensmith 2009; Kalmar et al. 2012; Malik et al. 2013; Parfitt et al. 2014; Ahmed et al. 2016). Previous attempts at targeting HSP expression in *in vitro* and *in vivo* models of neurodegenerative diseases and ageing have had varying levels of success. These include overexpression of individual HSPs via genetic manipulation and pharmacological modulation, for example with HSP inhibitors (Muchowski & Wacker 2005; Kalmar & Greensmith 2017; Thakur et al. 2018). Arimoclomol has specific and clinically important advantages in that it targets HSF1 and thus results in the coordinated synthesis of multiple HSPs, as opposed to manipulation of a single HSP. Furthermore, Arimoclomol only works in cells under stress in which HSF1 is already activated, thereby reducing the potential for off-target side effects (Hargitai et al. 2003).

6.3. Implications of findings for IBM research

6.3.1. Characterisation of *in vivo* and *in vitro* models of IBM

Well-established and relevant models of disease are vital for examining the efficacy of novel therapeutic compounds and for the translation of successful preclinical research into human trials. Prior to the mutant VCP mouse model, no single animal model had been shown to recapitulate the clinical and pathologic features of IBM. Previously described mouse models of IBM are largely based on the overexpression of β -APP in muscle fibres, as increased amyloid deposits are a characteristic feature in IBM muscle fibres (Fukuchi et al. 1998; Jin et al. 1998; Sugarman et al. 2002; Kitazawa et al. 2006; Moussa et al. 2006). Despite displaying some aspects of the IBM phenotype, including muscle degeneration and weakness, these mouse models do not develop the full spectrum of the disease, for example there is no evidence of rimmed vacuoles, necrosis or inflammation in the muscle fibres of these mice (Fukuchi et al. 1998; Jin et al. 1998; Sugarman et al. 2002; Moussa et al. 2006).

The characterisation of the mutant VCP mouse model described in Chapter 3 of this Thesis, demonstrates that these mice display both inflammatory and degenerative components of IBM in muscle, reminiscent of the pathology seen in patients. This pathology includes TDP-43 mislocalisation, ubiquitinated inclusion formation, fibre hypertrophy and damaged mitochondria, evidence of muscle degeneration, alongside macrophage and inflammatory cell infiltration and upregulated expression of the inflammatory markers MHC-I and phospho-I κ B α . Despite the pathomechanisms of both IBM and MSP being unclear, the overlap between the two diseases suggests that disrupted protein handling plays a key role in the development of both diseases. Thus, the mutant VCP mouse model represents a relevant model and useful tool for examining the effects of HSR upregulation, in order to restore the balance of protein homeostasis in IBM. This model therefore has significant advantages over previously described models.

In addition to characterisation of the *in vivo* mouse model, *in vitro* patient fibroblast models were also characterised. Fibroblasts derived from patients with either sporadic IBM or MSP display histopathological features of IBM, including TDP-43 mislocalisation, ubiquitin and p62 aggregation and disruption

of nuclear membranes and mitochondrial morphology. The patient fibroblast models have a unique advantage over the previously described *in vitro* models of IBM, in which the degenerative and inflammatory components are modelled independently in rat cultured myocytes, either by β -APP-overexpression or exposure to inflammatory mediators (Ahmed et al. 2016). Patient-derived fibroblasts are more clinically relevant and replicate key characteristics such as rimmed vacuole formation, which was not apparent in the previous models.

In combination, the models described in this Thesis are valuable tools in which novel therapeutic compounds can be assessed. Compounds may first be rapidly screened in the *in vitro* fibroblast model, before the effects in the more time-consuming, but physiologically relevant, *in vivo* mouse model are investigated. Furthermore, TDP-43 mislocalisation is observed in rat *in vitro* models of IBM, in an *in vivo* mouse model of MSP, in the human sporadic IBM and MSP fibroblast models, as well as in muscle of IBM patients, suggesting that this is a key pathological feature of the disease. As such, the novel finding of this study that fibroblasts from sporadic IBM patients have this pathology, even under basal culture conditions, in the absence of any induced experimental stress, suggests that TDP-43 mislocalisation in sporadic IBM patient fibroblasts may be used as an outcome measure for high-throughput screening of therapeutic compounds for IBM. The effect of Arimoclomol on this pathology in patient fibroblasts is currently under investigation. As Arimoclomol has been shown to be beneficial in ameliorating both degenerative and inflammatory pathological features simultaneously, this drug can also be used as a standard by which the efficacy of other novel therapeutic compounds can be assessed.

As the exact cause of IBM remains elusive, hindering the search for effective therapeutic treatments, a greater understanding of the cellular pathology of IBM is essential. The observation of key IBM pathological features in these models supports the hypothesis that protein homeostasis is disrupted in IBM and means that these models can be used to further investigate the pathomechanisms underlying IBM. The ultimate aim would be to target a dysfunctional mechanism, alongside upregulation of the endogenous cytoprotective HSR. Furthermore, as the observed cellular phenotypic changes

in MSP patient fibroblasts are similar to those seen in fibroblasts obtained from sporadic IBM patients, there are likely common pathways disrupted between the two diseases, which may be explored in these models.

6.3.2. Clinical trial of Arimoclomol in sporadic IBM patients

IBM remains a disease for which there is no effective treatment to offer patients. The work presented in this Thesis demonstrates that upregulation of the HSR with Arimoclomol ameliorates IBM-like pathology both *in vitro* and *in vivo*. These positive findings in experimental models supported an investigator-led, randomised, double-blind, placebo-controlled, proof of concept trial of Arimoclomol in 24 sporadic IBM patients, jointly led by the MRC Centre for Neuromuscular Diseases at Queen Square and the University of Kansas (Ahmed et al. 2016). This pilot study demonstrated that Arimoclomol is safe and well-tolerated in patients and although there was no statistically significant evidence of efficacy in the patient trial, a trend of a slower decline in muscle strength and physical function was observed in patients receiving Arimoclomol versus placebo. Whether Arimoclomol can ameliorate IBM pathology in patients will be determined by a 20-month study powered for efficacy, enrolling 150 IBM patients. This trial commenced in August 2017 and has an estimated completion date of December 2021. Furthermore, the positive findings presented in this Thesis, in both the mouse model of MSP and MSP patient-derived fibroblasts suggest that Arimoclomol may also be beneficial for patients with this disease, although, as yet, there are no current plans to follow this up with a clinical trial.

Importantly, as already discussed, Arimoclomol only targets cells already under stress, in which the endogenous HSR has already been instigated (Vigh et al. 1997; Hargitai et al. 2003). This is particularly beneficial when it comes to use in patients as widespread activation of the HSR may in fact be harmful (Hargitai et al. 2003; Kieran et al. 2004; Kalmar & Greensmith 2009; Walcott & Heikkila 2010).

6.4. Limitations of this investigation

The effects of upregulation of the HSR in models of IBM have successfully been investigated and described in this Thesis. However, as with any study, there are limitations to the study presented. Animal models have a unique advantage when it comes to investigating human disease, in that they enable studies at the level of the whole organism. However, sporadic diseases, such as IBM, with no known genetic cause, cannot be directly modelled *in vivo* and typically have a more complex pathogenesis. This can make these diseases difficult to model accurately. To overcome this problem in this study, a mouse model of MSP was used. Although the pathophysiological aspects of MSP mimic those seen in IBM patients, the most notable difference between MSP and IBM is the immune-mediated inflammatory component of IBM, which suggests that these diseases share some, but perhaps not all, aspects of the pathogenic cascade. As already discussed, these mice surprisingly did have signs of inflammation in affected muscle but it is still possible that there are different mechanisms involved in the pathogenesis of these two diseases.

Furthermore, IBM, like many complex diseases, is often not diagnosed until long after symptom onset. In this study, treatment of the mutant VCP mice began at 4 months of age, at the first signs of symptom onset. This may not ideally reflect the clinical situation and it would be beneficial to further investigate the effects of Arimoclomol as a late-stage treatment in the mouse model.

Whilst human fibroblasts have a number of advantages as a cellular model due to their inherent availability and robustness, they present with a unique set of challenges. The greatest limitation in this study was the availability of patient-derived fibroblasts. Particularly in the case of rare diseases such as IBM, it can prove difficult to obtain cells from a sufficient number of patients. Thus, in this study, only four patient cell lines were examined for both sporadic IBM and MSP. This may account for the fact that there was not a more obvious difference between the pathology observed among individual patient fibroblasts, despite a seemingly large variation in disease progression. Whilst the sporadic IBM patients were at a more advanced stage of disease when fibroblasts were harvested, with three of the four patients having a decline of 50% or greater on

the IBM Functional Rating Scale (IBMFRS), the MSP patients, from whom the VCP patient fibroblasts were obtained, were mostly reported to have a mild, muscle only phenotype. In addition, one MSP patient had a different mutation and a more severe clinical phenotype, but no difference was seen between the two mutations examined or the degree of pathology within the cultured fibroblasts. Furthermore, it would have also been interesting to examine fibroblasts with the more severe disease-causing A232E VCP mutation, the mutation described in the *in vivo* mouse model, but these were not possible to obtain. With such a small cohort, it was therefore be difficult to investigate the range of clinical variability.

The difficulty in obtaining a sufficient number of patient-derived fibroblasts also extended to control cell lines. Furthermore, information about these controls was limited. As the healthy population are less likely to have skin biopsies taken, it is possible that these samples may come from sources which may not be truly healthy, such as supposedly unaffected relatives or patients with other diseases.

Furthermore, other factors may influence variability, such as differences in seeding density, confluence of the cells and the different phases of the cell cycle. Although every attempt was made to stringently control for these factors in this study, the results had to be replicated a number of times to account for this inherent variability. The time-consuming nature of performing replicates meant that a number of the pathological changes observed in the patient fibroblasts could be not quantified.

In particular, it is important to take into account the population doubling level (PDL) of each fibroblast line, which is a measure of the total number of times a cell population has doubled since the initial isolation *in vitro*. This is in comparison to passage number, which reflects the number of times a particular cell line has been subcultured, rather than the absolute time in culture of that particular cell line. This is important as human fibroblast cultures have a finite number of population doublings before they reach senescence (Hayflick & Moorhead 1961; Chen et al. 1995). In this study, population doublings were kept consistent between control and patient fibroblast lines, although

information on PDL for each line was not available at the point at which fibroblasts were obtained. However, each fibroblast cell line was obtained at a very early passage number and thus this variation in PDL would have been limited.

Finally, as well as lacking physiological, *in vivo* signals, fibroblasts have a short life span meaning the ageing process was not replicated in this model. IBM is a chronic condition which progresses slowly and may be exacerbated by ageing. These limitations were overcome by use of the *in vivo* mouse model alongside the *in vitro* fibroblasts.

6.5. Future work

Whilst the effects of upregulation of the HSR with Arimoclomol in IBM have been explored, there remain a number of unanswered questions. In particular the underlying cause of IBM remains uncertain. The characterisation of IBM-like pathology in the *in vitro* and *in vivo* models described in this Thesis, make them valuable tools for uncovering the pathomechanisms underlying the disease. Common to both models was the cytoplasmic aggregation of a number of proteins (TDP-43, ubiquitin, p62) and the formation of vacuoles, implicating abnormal proteostasis within these models. This suggests that there is either an increase in the amount of misfolded or damaged proteins or there is a dysfunction of either of the two proteolytic degradation systems (Weihl & Pestronk 2010). Although this was beyond the scope of this investigation, these models can be harnessed in the future to investigate the disruption of protein homeostasis in IBM and examine the individual specificity of the aforementioned aggregated proteins in IBM pathology.

Of particular interest for further investigation, is the mitochondrial disruption observed in both the mouse model and patient fibroblasts and the implications of Arimoclomol on this pathology. As discussed in Chapter 5, mitochondrial abnormalities including cytochrome c oxidase (COX)-deficient fibres, succinate dehydrogenase (SDH)-positive fibres and ragged red fibres have been consistently noted in IBM muscle, as well as accumulation of mtDNA deletions, loss of oxidative phosphorylation enzyme activity and abnormal mitophagy (Müller-Höcker 1990; Oldfors et al. 1993; Oldfors et al. 1995; Rifai et al. 1995;

Dahlbom et al. 2002; Oldfors et al. 2006; Lightfoot et al. 2015; Rygiel et al. 2015; Catalan-García et al. 2016). Furthermore, fibroblasts from patients with *VCP* mutations have a reduced mitochondrial membrane potential, uncoupled respiration, reduced oxidative phosphorylation causing decreased ATP production and depletion of cellular ATP (Bartolome et al. 2013; Nalbandian, Llewellyn, Gomez et al. 2015; Zhang et al. 2017). As reported in Chapter 3 of this Thesis, extensive mitochondrial damage was observed in affected muscle of the mutant *VCP* mice, which was dramatically improved with Arimoclomol treatment. Immunofluorescent labelling of mitochondria in IBM and MSP patient-derived fibroblasts also revealed some evidence of fragmented and disrupted mitochondria. Further investigation would thus determine whether there is a link between mitochondrial dysfunction and the pathogenesis of IBM.

Another major uncertainty in IBM is the relative contributions of the degenerative and inflammatory components to the disease. Both sporadic IBM and MSP patient-derived fibroblasts display characteristic pathological features indicative of degeneration, including protein aggregation and the formation of rimmed vacuoles. However, whether the inflammatory component is also modelled in these cells is unclear. By establishing whether inflammatory features are present within sporadic IBM or MSP patient fibroblasts, the exact contribution of the degenerative and inflammatory components can be examined. It would be predicted that sporadic IBM fibroblasts would show an inflammatory component, whilst the MSP fibroblasts would not. If this were the case, the MSP fibroblasts could be exposed to inflammatory mediators such as IL-1 β or TNF α , which have previously been shown to induce IBM-like pathology in cultured rat myocytes (Ahmed et al. 2016). However, the mutant *VCP* mouse model did display inflammatory features in muscle, so this may also be the case in *VCP* patient fibroblasts. Alternatively, fibroblasts from patients with a purely inflammatory muscle disease could be characterised in order to dissect the exact contributions of the degenerative and inflammatory components.

IBM is a disease that occurs later on in life, suggesting that as with other neurodegenerative disorders, age is a primary risk factor. It would therefore be interesting to obtain fibroblasts from younger, healthy subjects and compare them to our age-matched controls and patient-derived fibroblasts, in order to

investigate whether the pathology observed in IBM is an exacerbation of the ageing phenotype, as has been previously suggested (Askanas & Engel 2001; Askanas & Engel 2007). Primary skin fibroblasts are also increasingly being used to develop induced pluripotent stem cells (iPSCs). Recently, several protocols have been described for the successful derivation of skeletal muscle from human iPSCs (Roca et al. 2015; Miyagoe-Suzuki & Takeda 2017). Although there are still major challenges in this area, it may be possible in the future to culture these cells for a prolonged period of time and thus be able to investigate disease pathogenesis in a long-term study, thus incorporating the chronic nature of the disease into an *in vitro* model.

Although Arimoclomol is thought to act by prolonging HSF1 activation, it is unlikely that this is the sole mechanism of action (Vigh et al. 1997; Hargitai et al. 2003). The hydroxylamine class of compounds, of which Arimoclomol belongs, have also been shown to interact with the plasma membrane, particularly lipid rafts which are detergent-resistant membrane regions that have a role in sensing cellular stress. By modifying membrane fluidity in response to heat shock, Arimoclomol may lower the threshold of the HSR, resulting in greater activation of heat shock genes and increased resistance to cellular stress (Torok et al. 2003; Vigh et al. 2007). Further investigation into alternative mechanisms of action of Arimoclomol will be beneficial for the development of novel therapeutic compounds.

Finally, as the *in vivo* mutant VCP mouse model described in this study has a phenotype that also encompasses frontotemporal dementia (FTD) and amyotrophic lateral sclerosis (ALS), further research is being undertaken in this model to examine the effect of Arimoclomol on brain and spinal cord. The histopathology is remarkably similar in all MSP-affected tissues, with the presence of ubiquitin-positive inclusions containing p62, VCP and RNA-binding proteins such as TDP-43. Investigation into these pathologies in different tissues may provide further insight of the pathomechanisms of the disease and explain why these particular tissues are selectively involved in MSP.

6.6. Concluding remarks

This Thesis aimed to investigate the effects of upregulation of the HSR with the pharmacological co-inducer Arimoclomol, in models of IBM, a disease for which there is currently no effective treatment. It can now be concluded that Arimoclomol reduces characteristic pathological features of IBM both *in vivo*, in a mutant VCP mouse model, and *in vitro*, in patient-derived dermal fibroblasts, likely by reducing the effects of protein mishandling and cellular degeneration. Arimoclomol ameliorates features of both the degenerative and inflammatory components of IBM, including TDP-43 mislocalisation, ubiquitin and p62 aggregation and mitochondrial disruption. Furthermore, Arimoclomol improves pathology in fibroblasts obtained from patients with MSP, with an associated inclusion body myopathy. Ultimately the results presented in this Thesis suggest that upregulation of the HSR is a suitable therapeutic strategy for IBM. This possibility is now under study in a multi-centre efficacy trial in IBM patients.

References

- Abrahao, A., Abrahao, A., Abath Neto, O., Kok, F., Zanoteli, E., Santos, B., Pinto, W.B., Barsottini, O.G., Oliveira, A.S. & Pedroso, J.L. 2016. One family, one gene and three phenotypes: A novel VCP (valosin-containing protein) mutation associated with myopathy with rimmed vacuoles, amyotrophic lateral sclerosis and frontotemporal dementia. *Journal of the Neurological Sciences*, 368, pp.352–358.
- Abujarour, R. & Valamehr, B. 2015. Generation of skeletal muscle cells from pluripotent stem cells: advances and challenges. *Frontiers in Cell and Developmental Biology*, 3, p.29.
- Ahmed, M., Machado, P.M., Miller, A., Spicer, C., Herbelin, L., He, J., Noel, J., Wang, Y., McVey, AL., Pasnoor, M., Gallagher, P; Statland, J., Lu, CH., Kalmar, B., Brady, S., Sethi, H., Samandouras, G., Parton, M., Holton, JL., Weston, A., Collinson, L., Taylor, JP., Schiavo, G., Hanna, MG., Barohn, RJ., Dimachkie, MM. & Greensmith, L. 2016. Targeting protein homeostasis in sporadic inclusion body myositis. *Science Translational Medicine*, 8(331), p.331ra41.
- Al-Obeidi, E., Al-Tahan, S., Surampalli, A., Goyal, N., Wang, AK., Hermann, A., Omizo, M., Smith, C., Mozaffar, T. & Kimonis, V. 2018. Genotype-phenotype study in patients with valosin-containing protein mutations associated with multisystem proteinopathy. *Clinical Genetics*, 93(1), pp.119–125.
- Al-Ramahi, I., Panapakkam Giridharan, S.S., Chen, Y.C., Patnaik, S., Safren, N., Hasegawa, J., de Haro, M., Wagner Gee, A.K., Titus, S.A., Jeong, H., Clarke, J., Krainc, D., Zheng, W., Irvine, R.F., Barmada, S., Ferrer, M., Southall, N., Weisman, L.S., Botas, J. & Marugan, J.J. 2017. Inhibition of PIP4Ky ameliorates the pathological effects of mutant huntingtin protein. *eLife*, 6: pii:e29123.
- Al-Tahan, S., Al-Tahan, S., Al-Obeidi, E., Yoshioka, H., Lakatos, A., Weiss, L., Grafe, M., Palmio, J., Wicklund, M., Harati, Y., Omizo, M., Udd, B. & Kimonis, V. 2018. Novel valosin-containing protein mutations associated with multisystem proteinopathy. *Neuromuscular Disorders*. pii: S0960-8966(18)30015-4.
- Al-Zaidy, S.A., Sahenk, Z., Rodino-Klapac, L.R., Kaspar, B. & Mendell J.R. 2015. Follistatin Gene Therapy Improves Ambulation in Becker Muscular Dystrophy. *Journal of Neuromuscular Diseases*, 2(3), pp.185–192.
- Albayda, J., Christopher-Stine, L., Bingham, Iii C.O., Paik, J.J., Tiniakou, E., Billings, S., Uy, O.M. & Burlina, P. 2018. Pattern of muscle involvement in inclusion body myositis: a sonographic study. *Clinical and Experimental Rheumatology*. [Epub ahead of print].
- Alexanderson, H. 2012. Exercise in Inflammatory Myopathies, Including Inclusion Body Myositis. *Current Rheumatology Reports*, 14(3), pp.244–251.
- Alexanderson, H. & Lundberg, I.E. 2012. Exercise as a therapeutic modality in patients with idiopathic inflammatory myopathies. *Current Opinion in Rheumatology*, 24(2), pp.201–207.

- Allen, S.P., Rajan, S, Duffy, L, Mortiboys, H, Higginbottom, A, Grierson, A.J. & Shaw, J. 2014. Superoxide dismutase 1 mutation in a cellular model of amyotrophic lateral sclerosis shifts energy generation from oxidative phosphorylation to glycolysis. *Neurobiology of Aging*, 35(6), pp.1499–1509.
- Altun, M., Besche, H.C., Overkleeft, H.S., Piccirillo, R., Edelmann, M.J., Kessler, B.M., Goldberg, A.L. & Ulfhake, B. 2010. Muscle wasting in aged, sarcopenic rats is associated with enhanced activity of the ubiquitin proteasome pathway. *The Journal of Biological Chemistry*, 285(51), pp.39597–39608.
- Amato, A.A., Badrising, U., Benveniste, O., Needham, M., Chinoy, H., Wu, M., Koumaras, B., de Vera, A., Papanicolaou, D.A. & Hanna, M.G. 2016. A Randomized, Double-Blind, Placebo-Controlled Study of Bimagrumab in Patients with Sporadic Inclusion Body Myositis [abstract]. *Arthritis & Rheumatology*, 68 (suppl 10).
- Amato, A.A. & Barohn, R.J. 2009. Evaluation and treatment of inflammatory myopathies. *Journal of Neurology, Neurosurgery, and Psychiatry*, 80(10), pp.1060–1068.
- Amato, A.A., Barohn, R.J., Jackson, C.E., Pappert, E.J., Sahenk, Z. & Kissel, J.T. 1994. Inclusion body myositis: treatment with intravenous immunoglobulin. *Neurology*, 44(8), pp.1516–1518.
- Amato, A.A., Gronseth, G.S., Jackson, C.E., Wolfe, G.I., Katz, J.S., Bryan, W.W. & Barohn, R.J., 1996. Inclusion body myositis: Clinical and pathological boundaries. *Annals of Neurology*, 40(4), pp.581–586.
- Amato, A.A. & Shebert, R.T. 1998. Inclusion body myositis in twins. *Neurology*, 51(2), pp.598–600.
- Amato, A.A., Sivakumar, K., Goyal, N., David, W.S., Salajegheh, M., Praestgaard, J., Lach-Trifillieff, E., Trendelenburg, A.U., Laurent, D., Glass, D.J., Roubenoff, R., Tseng, B.S. & Greenberg, S.A. 2014. Treatment of sporadic inclusion body myositis with bimagrumab. *Neurology*, 83(24), pp.2239–2246.
- Ambrosi, G., Ghezzi, C., Sepe, S., Milanese, C., Payan-Gomez, C., Bombardieri, C.R., Armentero, M.T., Zangaglia, R., Pacchetti, C., Mastroberardino, P.G. & Blandini, F. 2014. Bioenergetic and proteolytic defects in fibroblasts from patients with sporadic Parkinson's disease. *Biochimica et Biophysica Acta (BBA) - Molecular Basis of Disease*, 1842(9), pp.1385–1394.
- Amici, D.R., Pinal-Fernandez, I., Mázala, DA., Lloyd, T.E., Corse, A.M., Christopher-Stine, L., Mammen, A.L. & Chin E.R. 2017. Calcium dysregulation, functional calpainopathy, and endoplasmic reticulum stress in sporadic inclusion body myositis. *Acta Neuropathologica Communications*, 5(1), p.24.
- Anderson, P. & Kedersha, N. 2002. Stressful initiations. *Journal of Cell Science*, 115(Pt 16), pp.3227–34.

- Anderson, P. & Kedersha, N. 2006. RNA granules. *The Journal of Cell Biology*, 172(6), pp.803–8.
- Aoife, C., Capkun, G., Freitas, R., Vasanthaprasad, V., Ghosh, S. & Needham, M. 2016. Prevalence of Sporadic Inclusion Body Myositis (P1.127). *Neurology*, 86(16 Supplement), p.P1.127.
- Arahata, K. & Engel, A.G. 1984. Monoclonal antibody analysis of mononuclear cells in myopathies. I: Quantitation of subsets according to diagnosis and sites of accumulation and demonstration and counts of muscle fibers invaded by T cells. *Annals of Neurology*, 16(2), pp.193–208.
- Arai, T., Hasegawa, M., Akiyama, H., Ikeda, K., Nonaka, T., Mori, H., Mann, D., Tsuchiya, K., Yoshida, M., Hashizume, Y. & Oda T. 2006. TDP-43 is a component of ubiquitin-positive tau-negative inclusions in frontotemporal lobar degeneration and amyotrophic lateral sclerosis. *Biochemical and Biophysical Research Communications*, 351(3), pp.602–611.
- Area-Gomez, E., del Carmen, M., Castillo, L., Tambini, M.D., Guardia-Laguarta, C., de Groof A.J., Madra, M., Ikenouchi, J., Umeda, M., Bird, T.D., Sturley, S.L. & Scho, E.A. 2012. Upregulated function of mitochondria-associated ER membranes in Alzheimer disease. *The EMBO Journal*, 31(21), pp.4106–4123.
- Arnardottir, S., Alexanderson, H., Lundberg I.E. & Borg, K. 2003. Sporadic inclusion body myositis: pilot study on the effects of a home exercise program on muscle function, histopathology and inflammatory reaction. *Journal of Rehabilitation Medicine*, 35(1), pp.31–35.
- Arnardottir, S., Borg, K. & Ansved, T. 2004. Sporadic inclusion body myositis: morphology, regeneration, and cytoskeletal structure of muscle fibres. *Journal of Neurology, Neurosurgery, and Psychiatry*, 75, pp.917–920.
- Askanas, V. & Engel, W.K. 1993. New advances in inclusion-body myositis. *Current Opinion in Rheumatology*, 5(6), pp.732–741.
- Askanas, V. & Engel, W.K. 1998. Sporadic Inclusion-Body Myositis and Hereditary Inclusion-Body Myopathies. *Archives of Neurology*, 55(7), p.915.
- Askanas, V. & Engel, W.K. 2001. Inclusion-body myositis: newest concepts of pathogenesis and relation to aging and Alzheimer disease. *Journal of Neuropathology and Experimental Neurology*, 60(1), pp.1–14.
- Askanas, V. & Engel, W.K. 2002. Inclusion-body myositis and myopathies: different etiologies, possibly similar pathogenic mechanisms. *Current Opinion in Neurology*, 15(5), pp.525–531.
- Askanas, V. & Engel, W.K. 2005. Molecular pathology and pathogenesis of inclusion-body myositis. *Microscopy Research and Technique*, 67(3–4), pp.114–120.

- Askanas, V. & Engel, W.K. 2007. Inclusion-body myositis, a multifactorial muscle disease associated with aging: current concepts of pathogenesis. *Current Opinion in Rheumatology*, 19(6), pp.550–559.
- Askanas, V. & Engel, W.K. 2008. Inclusion-body myositis: muscle-fiber molecular pathology and possible pathogenic significance of its similarity to Alzheimer's and Parkinson's disease brains. *Acta Neuropathologica*, 116(6), pp.583–95.
- Askanas, V., Engel, W.K. & Nogalska, A. 2009. Inclusion body myositis: a degenerative muscle disease associated with intra-muscle fiber multi-protein aggregates, proteasome inhibition, endoplasmic reticulum stress and decreased lysosomal degradation. *Brain Pathology*, 19(3), pp.493–506.
- Askanas, V., Engel, W.K. & Nogalska, A. 2012. Pathogenic considerations in sporadic inclusion-body myositis, a degenerative muscle disease associated with aging and abnormalities of myoproteostasis. *Journal of Neuropathology and Experimental Neurology*, 71(8), pp.680–693.
- Askanas, V., Engel, W.K. & Nogalska, A. 2015. Sporadic inclusion-body myositis: A degenerative muscle disease associated with aging, impaired muscle protein homeostasis and abnormal mitophagy. *Biochimica et Biophysica Acta*, 1852(4), pp.633–643.
- Askanas, V., Serdaroglu, P., Engel, W.K., Alvarez, R.B. 1991. Immunolocalization of ubiquitin in muscle biopsies of patients with inclusion body myositis and oculopharyngeal muscular dystrophy. *Neuroscience letters*, 130(1), pp.73–76.
- Auburger, G. Klinkenberg, M., Drost, J., Marcus, K., Morales-Gordo, B., Kunz, W.S., Brandt, U., Broccoli, V., Reichmann, H., Gispert, S. & Jendrach, M. 2012. Primary skin fibroblasts as a model of Parkinson's disease. *Molecular Neurobiology*, 46(1), pp.20–27.
- Aulas, A., Stabile, S. & Vande Velde, C. 2012. Endogenous TDP-43, but not FUS, contributes to stress granule assembly via G3BP. *Molecular Neurodegeneration*, 7(1), pp.1.
- Ayala, Y.M., Zago, P., D'Ambrogio, A., Xu, Y.F., Petrucelli, L., Buratti E. & Baralle F.E. 2008. Structural determinants of the cellular localization and shuttling of TDP-43. *Journal of Cell Science*, 121(22), pp.3778–3785.
- Badrising, U.A., Maat-Schieman, M., van Duinen, S.G., Breedveld, F., van Doorn, P., van Engelen, B., van den Hoogen, F., Hoogendijk, J., Höweler, C., de Jager, A., Jennekens, F., Koehler, P., van der Leeuw, H., de Visser, M., Verschuuren, J.J. & Wintzen, A.R. 2000. Epidemiology of inclusion body myositis in the Netherlands: a nationwide study. *Neurology*, 55(9), pp.1385–1387.

- Badrising, U.A., Maat-Schieman, M.L., Ferrari, M.D., Zwinderman, A.H., Wessels, J.A., Breedveld, F.C., van Doorn, P.A., van Engelen, B.G., Hoogendijk, J.E., Höweler, C.J., de Jager, A.E., Jennekens, F.G., Koehler, P.J., de Visser, M., Viddeleer, A., Verschuuren, J.J. & Wintzen, A.R., 2002. Comparison of weakness progression in inclusion body myositis during treatment with methotrexate or placebo. *Annals of Neurology*, 51(3), pp.369–372.
- Badrising, U.A., Maat-Schieman, M.L., van Houwelingen, J.C., van Doorn, P.A., van Duinen, S.G., van Engelen, B.G., Faber, C.G., Hoogendijk, J.E., de Jager, A.E., Koehler, P.J., de Visser, M., Verschuuren, J.J. & Wintzen, A.R. 2005. Inclusion body myositis. Clinical features and clinical course of the disease in 64 patients. *Journal of Neurology*, 252(12), pp.1448–1454.
- Badrising, U.A., Schreuder, G.M., Giphart, M.J., Geleijns, K., Verschuuren, J.J., Wintzen, A.R., Maat-Schieman, M.L., van Doorn, P., van Engelen, B.G., Faber, C.G., Hoogendijk, J.E., de Jager, A.E., Koehler, P.J., de Visser, M., van Duinen, S.G. & Dutch IBM Study Group. 2004. Associations with autoimmune disorders and HLA class I and II antigens in inclusion body myositis. *Neurology*, 63(12), pp.2396–2398.
- Badrising, U.A., Tsonaka, R., Hiller, M., Niks, E.H., Evangelista, T., Lochmüller, H., Verschuuren, J.J., Aartsma-Rus, A. & Spitali, P. 2017. Cytokine Profiling of Serum Allows Monitoring of Disease Progression in Inclusion Body Myositis. *Journal of Neuromuscular Diseases*, 4(4), pp.327–335.
- Baehr, L.M., West, D.W., Marcotte, G., Marshall, A.G., De Sousa, L.G., Baar, K. & Bodine, SC. 2016. Age-related deficits in skeletal muscle recovery following disuse are associated with neuromuscular junction instability and ER stress, not impaired protein synthesis. *Aging*, 8(1), pp.127–46.
- Balch, W.E., Morimoto, R.I., Dillin, A. & Kelly J.W. 2008. Adapting Proteostasis for Disease Intervention. *Science*, 319(5865), pp.916–919.
- Baloh, R.H. 2011. TDP-43: the relationship between protein aggregation and neurodegeneration in amyotrophic lateral sclerosis and frontotemporal lobar degeneration. *FEBS Journal*, 278(19), pp.3539–3549.
- Bandyopadhyay, U. & Cuervo, A.M. 2008. Entering the lysosome through a transient gate by chaperone-mediated autophagy. *Autophagy*, 4(8), pp.1101–3.
- Banwell, B.L. & Engel, A.G. 2000. AlphaB-crystallin immunolocalization yields new insights into inclusion body myositis. *Neurology*, 54(5), pp.1033–41.
- Barmada, S.J., Skibinski, G., Korb, E., Rao, E.J., Wu, J.Y. & Finkbeiner S. 2010. Cytoplasmic Mislocalization of TDP-43 Is Toxic to Neurons and Enhanced by a Mutation Associated with Familial Amyotrophic Lateral Sclerosis. *Journal of Neuroscience*, 30(2), pp.639–649.

- Barohn, R.J., Herbelin, L., Kissel, J.T., King, W., McVey, A.L., Saperstein, D.S. & Mendell, J.R. 2006. Pilot trial of etanercept in the treatment of inclusion-body myositis. *Neurology*, 66(Issue 1, Supplement 1), pp.S123–S124.
- Bartolome, F., Wu, H.C., Burchell, V.S., Preza, E., Wray, S., Mahoney C.J., Fox N.C., Calvo, A., Canosa, A., Moglia, C., Mandrioli, J., Chiò, A., Orrell, R.W., Houlden, H., Hardy, J., Abramov, A.Y., Plun-Favreau, H. 2013. Pathogenic VCP Mutations Induce Mitochondrial Uncoupling and Reduced ATP Levels. *Neuron*, 78(1), pp.57–64.
- Batulan, Z., Shinder, G.A., Minotti, S., He, B.P., Doroudchi, M.M., Nalbantoglu, J., Strong, M.J. & Durham, H.D. 2003. High threshold for induction of the stress response in motor neurons is associated with failure to activate HSF1. *Journal of Neuroscience*, 23(13), pp.5789–5798.
- Bayraktar, O., Oral, O., Kocaturk, N.M., Akkoc, Y., Eberhart, K., Kosar, A. & Gozuacik, D. 2016. IBMPFD disease-causing mutant VCP/p97 proteins are targets of autophagic-lysosomal degradation. *PLOS ONE*, 11(10), p.e0164864.
- Lo Bello, M., Di Fini, F., Notaro, A., Spataro, R., Conforti, F.L. & La Bella, V. 2017. ALS-related mutant FUS protein is mislocalized to cytoplasm and is recruited into stress granules of fibroblasts from asymptomatic FUS P525L mutation carriers. *Neurodegenerative Diseases*, 17(6), pp.292–303.
- Ben-Zvi, A., Miller, E.A. & Morimoto, R.I.. 2009. Collapse of proteostasis represents an early molecular event in *Caenorhabditis elegans* aging. *Proceedings of the National Academy of Sciences of the United States of America*, 106(35), pp.14914–14919.
- Benabdallah, B.F., Bouchentouf, M., Rousseau, J., Bigey, P., Michaud, A., Chapdelaine, P., Scherman, D. & Tremblay, JP. 2008. Inhibiting myostatin with follistatin improves the success of myoblast transplantation in dystrophic mice. *Cell Transplantation*, 17(3), pp.337–50.
- Benatar, M., Wu, J., Andersen, P.M., Atassi, N., David, W., Cudkowicz, M. & Schoenfeld, D. 2018. Randomized, double-blind, placebo-controlled trial of arimoclomol in rapidly progressive *SOD1* ALS. *Neurology*, 90(7), pp.e565-e574.
- Benatar, M., Wu, J., Fernandez, C., Weihl, C.C., Katzen, H., Steele, J., Oskarsson, B. & Taylor, J.P. 2013. Motor neuron involvement in multisystem proteinopathy: implications for ALS. *Neurology*, 80(20), pp.1874–1880.
- Bence, N.F., Sampat, R.M. & Kopito, R.R. 2001. Impairment of the ubiquitin-proteasome system by protein aggregation. *Science*, 292(5521), pp.1552–1555.
- Benveniste, O., Guiguet, M., Freebody, J., Dubourg, O., Squier, W., Maisonobe, T., Stojkovic, T., Leite, M.I., Allenbach, Y., Herson, S., Brady, S., Eymard, B. & Hilton-Jones, D. 2011. Long-term observational study of sporadic inclusion body myositis. *Brain*, 134(Pt 11), pp.3176–3184.

- Benveniste, O. & Hilton-Jones, D. 2010. International Workshop on Inclusion Body Myositis held at the Institute of Myology, Paris, on 29 May 2009. *Neuromuscular Disorders*, 20(6), pp.414–421.
- Le Ber, I. Van Bortel, I., Nicolas G., Bouya-Ahmed, K., Camuzat, A., Wallon, D., De Septenville, A., Latouche, M., Lattante, S., Kabashi, E., Jornea, L., Hannequin, D., Brice, A. & French research Network on FTL/FTLD-ALS. 2014. hnRNPA2B1 and hnRNPA1 mutations are rare in patients with “multisystem proteinopathy” and frontotemporal lobar degeneration phenotypes. *Neurobiology of Aging*, 35(4) pp. 934.e5-6
- Beuron, F., Dreveny, I., Yuan, X., Pye, V.E., McKeown, C., Briggs, L.C., Cliff, M.J., Kaneko, Y., Wallis, R., Isaacson, R.L., Ladbury, J.E., Matthews, S.J., Kondo, H., Zhang, X. & Freemont, P.S., 2006. Conformational changes in the AAA ATPase p97-p47 adaptor complex. *The EMBO Journal*, 25(9), pp.1967–1976.
- Bhattacharyya, S. Yu, H., Mim, C. & Matouschek, A. 2014. Regulated protein turnover: snapshots of the proteasome in action. *Nature reviews. Molecular Cell Biology*, 15(2), pp.122–133.
- Blake, M.J. Fargnoli J., Gershon, D. & Holbrook N.J. 1991. Concomitant decline in heat-induced hyperthermia and HSP70 mRNA expression in aged rats. *American Journal of Physiology*, 260(4 Pt 2), pp.R663-7.
- Blake, M.J., Gershon, D., Fargnoli, J. & Holbrook, N.J., 1990. Discordant expression of heat shock protein mRNAs in tissues of heat-stressed rats. *Journal of Biological Chemistry*, 265(25), pp.15275–9.
- De Bleecker, J.L., De Paepe, B., Vanwalleghem, I.E. & Schröder, J.M. 2002. Differential expression of chemokines in inflammatory myopathies. *Neurology*, 58(12), pp.1779–85.
- Bohnert, K.R., McMillan, J.D. & Kumar, A. 2017. Emerging Roles of ER Stress and Unfolded Protein Response Pathways in Skeletal Muscle Health and Disease. *Journal of Cellular Physiology*, 233(1), pp. 67-78.
- Bornman, L., Polla, B.S., Lotz, B.P. & Gericke, G.S. 1995. Expression of heat-shock/stress proteins in duchenne muscular dystrophy. *Muscle & Nerve*, 18(1), pp.23–31.
- Bossola, M., Pacelli, F., Costelli, P., Tortorelli, A., Rosa, F. & Doglietto, G.B. 2008. Proteasome activities in the rectus abdominis muscle of young and older individuals. *Biogerontology*, 9(4), pp.261–268.
- de Bot, S.T., Schelhaas, H.J., Kamsteeg, E.J. & van de Warrenburg, B.P. 2012. Hereditary spastic paraplegia caused by a mutation in the VCP gene. *Brain*, 135(12), pp.e223–e223.
- Boya, P., Reggiori, F. & Codogno, P. 2013. Emerging regulation and functions of autophagy. *Nature Cell Biology*, 15(7), pp.713–720.

- Boyault, C., Gilquin, B., Zhang, Y., Rybin, V., Garman, E., Meyer-Klaucke, W., Matthias, P., Müller, C.W. & Khochbin, S. 2006. HDAC6-p97/VCP controlled polyubiquitin chain turnover. *The EMBO Journal*, 25(14), pp.3357–3366.
- Boyault, C., Sadoul, K., Pabion, M. & Khochbin S. 2007. HDAC6, at the crossroads between cytoskeleton and cell signaling by acetylation and ubiquitination. *Oncogene*, 26(37), pp.5468–5476.
- Brady, S., Squier, W. & Hilton-Jones, D. 2013. Clinical assessment determines the diagnosis of inclusion body myositis independently of pathological features. *Journal of Neurology, Neurosurgery & Psychiatry*, 84(11), pp.1240–1246.
- Bragoszewski, P., Turek, M. & Chacinska, A. 2017. Control of mitochondrial biogenesis and function by the ubiquitin-proteasome system. *Open Biology*, 7(4), pii. 1700007.
- Brandmeir, N.J., Geser, F., Kwong, L.K., Zimmerman, E., Qian, J., Lee, V.M. & Trojanowski, J.Q. 2007. Severe subcortical TDP-43 pathology in sporadic frontotemporal lobar degeneration with motor neuron disease. *Acta Neuropathologica*, 115(1), pp.123–131.
- Britson, K.A., Yang, S.Y. & Lloyd, T.E. 2018. New Developments in the Genetics of Inclusion Body Myositis. *Current Rheumatology Reports*, 20(5), p.26.
- Broccolini, A., Gidaro, T., Morosetti, R., Gliubizzi, C., Servidei, T., Pescatori, M., Tonali, P.A., Ricci, E. & Mirabella, M. 2006. Neprilysin participates in skeletal muscle regeneration and is accumulated in abnormal muscle fibres of inclusion body myositis. *Journal of Neurochemistry*, 96, pp.777–789.
- Brown, I.R. 2007. Heat shock proteins and protection of the nervous system. *Annals of the New York Academy of Sciences*, 1113(1), pp.147–158.
- Brown, I.R. & Rush, S.J. 1999. Cellular localization of the heat shock transcription factors HSF1 and HSF2 in the rat brain during postnatal development and following hyperthermia. *Brain Research*, 821(2), pp.333–340.
- Brown, M.K. & Naidoo, N. 2012. The endoplasmic reticulum stress response in aging and age-related diseases. *Frontiers in Physiology*, 3, p.263.
- Bucelli, R.C., Arhzaouy K., Pestronk, A., Pittman, S.K., Rojas, L., Sue, C.M., Evilä, A., Hackman, P., Udd, B., Harms, M.B. & Weihl, C.C. 2015. SQSTM1 splice site mutation in distal myopathy with rimmed vacuoles. *Neurology*, 85(8), pp.665–674.
- Buchan, J.R. & Parker, R. 2009. Eukaryotic stress granules: the ins and outs of translation. *Molecular Cell*, 36(6), pp.932–941.
- Buchberger, A., Schindelin, H. & Hänzelmann, P. 2015. Control of p97 function by cofactor binding. *FEBS Letters*, 589(19PartA), pp.2578–2589.

- Bug, M. & Meyer, H. 2012. Expanding into new markets – VCP/p97 in endocytosis and autophagy. *Journal of Structural Biology*, 179(2), pp.78–82.
- Buratti, E. & Baralle, F.E. 2010. The multiple roles of TDP-43 in pre-mRNA processing and gene expression regulation. *RNA Biology*, 7(4), pp.420–429.
- Buratti, E., Brindisi, A., Giombi, M., Tisminetzky, S., Ayala, Y.M. & Baralle, F.E. 2005. TDP-43 binds heterogeneous nuclear ribonucleoprotein A/B through its C-terminal tail: an important region for the inhibition of cystic fibrosis transmembrane conductance regulator exon 9 splicing. *Journal of Biological Chemistry*, 280(45), pp.37572–37584.
- Cacciottolo, M., Nogalska, A., D'Agostino, C., Engel, W.K. & Askanas, V. 2013. Chaperone-mediated autophagy components are upregulated in sporadic inclusion-body myositis muscle fibres. *Neuropathology and Applied Neurobiology*, 39(7), pp.750–761.
- Cadot, B., Gache, V. & Gomes, E.R. 2015. Moving and positioning the nucleus in skeletal muscle - one step at a time. *Nucleus*, 6(5), pp.373–81.
- Cadot, B., Gache, V., Vasyutina, E., Falcone, S., Birchmeier, C. & Gomes, E.R. 2012. Nuclear movement during myotube formation is microtubule and dynein dependent and is regulated by Cdc42, Par6 and Par3. *EMBO Reports*, 13(8), pp.741–749.
- Calabrese, L.H., Mitsumoto, H. & Chou, S.M. 1987. Inclusion body myositis presenting as treatment-resistant polymyositis. *Arthritis and Rheumatism*, 30(4), pp.397–403.
- Callan, A., Capkun, G., Vasanthaprasad, V., Freitas, R. & Needham M. 2017. A Systematic Review and Meta-Analysis of Prevalence Studies of Sporadic Inclusion Body Myositis. *Journal of Neuromuscular Diseases*, 4(2), pp.127–137.
- Calvo, S.E. & Mootha, V.K. 2010. The mitochondrial proteome and human disease. *Annual Review of Genomics and Human Genetics*, 11, pp.25–44.
- de Camargo, L.V., de Carvalho M.S., Shinjo, S.K., de Oliveira, A.S.B. & Zanoteli, E. 2018. Clinical, Histological, and Immunohistochemical Findings in Inclusion Body Myositis. *BioMed Research International*, 2018, p.5069042.
- Carnemolla, A., Lazell, H., Moussaoui, S. & Bates G.P. 2015. In Vivo Profiling Reveals a Competent Heat Shock Response in Adult Neurons: Implications for Neurodegenerative Disorders. *PLoS ONE*, 10(7), p.e0131985.
- Carnio, S., LoVerso, F., Baraibar, M.A., Longa, E., Khan, M.M., Maffei, M., Reischl, M., Canepari, M., Loeffler, S., Kern, H., Blaauw, B., Friguet, B., Bottinelli, R., Rudolf, R. & Sandri, M. 2014. Autophagy impairment in muscle induces neuromuscular junction degeneration and precocious aging. *Cell Reports*, 8(5), pp.1509–1521.
- Carpenter, S., Karpati, G., Heller, I. & Eisen, A. 1978. Inclusion body myositis: a distinct variety of idiopathic inflammatory myopathy. *Neurology*, 28(1), pp.8–17.

- Carstens, P.O. & Schmidt, J. 2014. Diagnosis, pathogenesis and treatment of myositis: recent advances. *Clinical and Experimental Immunology*, 175(3), pp.349–358.
- Catalan-García, M., Garrabou, G., Morén, C., Guitart-Mampel, M., Hernando, A., Díaz-Ramos, À., González-Casacuberta, I., Juárez, D.L., Bañó, M., Enrich-Bengoia, J., Emperador, S., Milisenda, J.C., Moreno, P., Tobías, E., Zorzano, A., Montoya, J., Cardellach, F. and Grau, J.M. 2016. Mitochondrial-DNA disturbances and deregulated expression of OXPHOS and mitochondrial fusion proteins in sporadic inclusion body myositis. *Clinical Science*, 130(19), pp. 1741-51.
- Chacinska, A., Koehler, C.M., Milenkovic, D., Lithgow, T., Pfanner, N. 2009. Importing mitochondrial proteins: machineries and mechanisms. *Cell*, 138(4), pp.628–644.
- Chan, N., Le, C., Shieh, P., Mozaffar, T., Khare, M., Bronstein, J. & Kimonis V. 2012. Valosin-containing protein mutation and Parkinson's disease. *Parkinsonism & Related Disorders*, 18(1), pp.107–109.
- Chan, N.C., Salazar, A.M., Pham, A.H., Sweredoski, M.J., Kolawa, N.J., Graham, R.L., Hess, S. & Chan, DC. 2011. Broad activation of the ubiquitin-proteasome system by Parkin is critical for mitophagy. *Human Molecular Genetics*, 20(9), pp.1726–37.
- Chargé, S.B. & Rudnicki, M.A. 2004. Cellular and Molecular Regulation of Muscle Regeneration. *Physiological Reviews*, 84(1), pp.209–238.
- Chen, B., Co, C. & Ho, C.C. 2015. Cell shape dependent regulation of nuclear morphology. *Biomaterials*, 67, pp.129–136.
- Chen, B., Retzlaff, M., Roos, T. & Frydman J. 2011. Cellular strategies of protein quality control. *Cold Spring Harbor Perspectives in Biology*, 3(8), p.a004374.
- Chen, H.J., Mitchell, J.C., Novoselov, S., Miller, J., Nishimura, A.L., Scotter, E.L., Vance, C.A., Cheetham, M.E. & Shaw, C.E. 2016. The heat shock response plays an important role in TDP-43 clearance: evidence for dysfunction in amyotrophic lateral sclerosis. *Brain*, 139, pp.1417–1432.
- Chen, J.L., Walton, K.L., Winbanks, C.E., Murphy, K.T., Thomson, R.E., Makanji, Y., Qian, H., Lynch, G.S., Harrison, C.A. & Gregorevic, P. 2014. Elevated expression of activins promotes muscle wasting and cachexia. *The FASEB Journal*, 28(4), pp.1711–1723.
- Chen, L. & Liu, B. 2017. Relationships between Stress Granules, Oxidative Stress, and Neurodegenerative Diseases. *Oxidative Medicine and Cellular Longevity*, 2017, pp.1–10.
- Chen, Q., Fischer, Ann., Reagan, J.D., Yan, L-J., Ames, B.N. & Hall, B. 1995. Oxidative DNA damage and senescence of human diploid fibroblast cells. *Proceedings of the National Academy of Sciences of the United States of America*, 92(10), pp.4337-4341.

- Chen, Q., Thorpe, J., Ding, Q., El-Amouri, I.S. & Keller, J.N. 2004. Proteasome synthesis and assembly are required for survival during stationary phase. *Free Radical Biology and Medicine*, 37(6), pp.859–868.
- Chen, Q. Thorpe, J., Dohmen, J.R., Li, F. & Keller, J.N. 2006. Ump1 extends yeast lifespan and enhances viability during oxidative stress: Central role for the proteasome? *Free Radical Biology and Medicine*, 40(1), pp.120–126.
- Cherin, P., Pelletier, S., Teixeira, A., Laforet, P., Simon, A., Herson, S. & Eymard, B. 2002. Intravenous immunoglobulin for dysphagia of inclusion body myositis. *Neurology*, 58(2), p.326.
- Ching, J.K. Elizabeth, S.V., Ju, J.S., Lusk, C., Pittman, S.K. & Weihl, C.C. 2013. mTOR dysfunction contributes to vacuolar pathology and weakness in valosin-containing protein associated inclusion body myopathy. *Human Molecular Genetics*, 22(6), pp.1167–1179.
- Ching, J.K. & Weihl, C.C. 2013. Rapamycin-induced autophagy aggravates pathology and weakness in a mouse model of VCP-associated myopathy. *Autophagy*, 9(5), pp.799–800.
- Chiti, F. & Dobson, C.M. 2006. Protein Misfolding, Functional Amyloid, and Human Disease. *Annual Review of Biochemistry*, 75(1), pp.333–366.
- Choi, S., Wang, W., Ribeiro, A.J.S., Kalinowski, A., Gregg, S.Q., Opresko, P.L., Niedernhofer, L.J., Rohde, G.K. & Dahl, K.N. 2011. Computational image analysis of nuclear morphology associated with various nuclear-specific aging disorders. *Nucleus*. 2(6), pp.570-579.
- Chondrogianni, N. Georgila, K., Kourtis, N., Tavernarakis, N. & Gonos, E.S. 2015. 20S proteasome activation promotes life span extension and resistance to proteotoxicity in *Caenorhabditis elegans*. *The FASEB Journal*, 29(2), pp.611–622.
- Chondrogianni, N. Petropoulos, I., Franceschi, C., Friguet, B. & Gonos, E.S. 2000. Fibroblast cultures from healthy centenarians have an active proteasome. *Experimental Gerontology*, 35(6–7), pp.721–728.
- Chou, C.C., Zhang, Y., Umoh, M.E. Vaughan, S.W., Lorenzini, I., Liu, F., Sayegh, M., Donlin-Asp, P.G., Chen, Y.H., Duong, D.M., Seyfried, N.T., Powers, M.A., Kukar, T., Hales, C.M., Gearing, M., Cairns, N.J., Boylan, K.B., Dickson, D.W., Rademakers, R., Zhang, Y.J., Petrucelli, L., Sattler, R., Zarnescu, D.C., Glass, J.D. & Rossoll W. 2018. TDP-43 pathology disrupts nuclear pore complexes and nucleocytoplasmic transport in ALS/FTD. *Nature Neuroscience*, p.1.
- Ciani, B., Layfield, R., Cavey, J.R., Sheppard, P.W. & Searle, M.S. 2003. Structure of the ubiquitin-associated domain of p62 (SQSTM1) and implications for mutations that cause Paget's disease of bone. *The Journal of Biological Chemistry*, 278(39), pp.37409–37412.

- Clarke, B., Kalmar, B. & Greensmith, L., 2017. Characterisation of the heat shock response in primary and ES-cell derived spinal motor neurons and astrocytes exposed to cellular stress conditions modelling ALS. *Neuromuscular Disorders*, 27, p.S28.
- Clemen, C.S., Marko, M., Strucksberg, K.H., Behrens, J., Wittig, I., Gärtner, L., Winter, L., Chevessier, F., Matthias, J., Türk, M., Tangavelou, K., Schütz, J., Arhzaouy, K., Klopffleisch, K., Hanisch, F.G., Rottbauer, W., Blümcke, I., Just, S., Eichinger, L., Hofmann, A. & Schröder, R. 2015. VCP and PSMF1: Antagonistic regulators of proteasome activity. *Biochemical and Biophysical Research Communications*, 463(4), pp.1210-1217.
- Clerici, A.M., Bono, G., Delodovici, M.L., Azan, G., Cafasso, G. & Micieli, G. 2013. A rare association of early-onset inclusion body myositis, rheumatoid arthritis and autoimmune thyroiditis: a case report and literature review. *Functional Neurology*, 28(2), pp.127–132.
- Cortese, A. Plagnol, V., Brady, S., Simone, R., Lashley, T., Acevedo-Aroza, A., de Silva, R., Greensmith, L., Holton, J., Hanna, M.G., Fisher, E.M. & Fratta P. 2014. Widespread RNA metabolism impairment in sporadic inclusion body myositis TDP43-proteinopathy. *Neurobiology of Aging*, 35(6), pp.1491–1498.
- Couture, P., Malfatti, E., Morau, G., Mathian, A., Cohen-Aubart, F., Nielly, H., Amoura, Z. & Cherin, P. 2018. Inclusion body myositis and human immunodeficiency virus type 1: A new case report and literature review. *Neuromuscular Disorders*, 28(4), pp.334–338.
- Cox, F.M., Reijnierse, M., Reijnierse, M., van Rijswijk, C.S., Wintzen, A.R., Verschuuren, J.J. & Badrising, U.A. 2011. Magnetic resonance imaging of skeletal muscles in sporadic inclusion body myositis. *Rheumatology*, 50(6), pp.1153–1161.
- Cox, F.M., Titulaer, M.J., Titulaer, M.J., Sont, J.K., Wintzen, A.R., Verschuuren, J.J. & Badrising, U.A. 2011. A 12-year follow-up in sporadic inclusion body myositis: an end stage with major disabilities. *Brain*, 134(11), pp.3167–3175.
- Cox, F.M., Verschuuren J.J., Verbist, B.M., Niks, E.H., Wintzen, A.R. & Badrising, U.A. 2009. Detecting dysphagia in inclusion body myositis. *Journal of Neurology*, 256(12), pp.2009–2013.
- Cox, L.S. & Faragher, R.G.A. 2007. From old organisms to new molecules: integrative biology and therapeutic targets in accelerated human ageing. *Cellular and Molecular Life Sciences*, 64(19–20), pp.2620–2641.
- Crist, C. 2017. Emerging new tools to study and treat muscle pathologies: genetics and molecular mechanisms underlying skeletal muscle development, regeneration, and disease. *The Journal of Pathology*, 241(2), pp.264–272.

- Crul, T., Toth, N., Piotto, S., Literati-Nagy, P., Tory, K., Haldimann, P., Kalmar, B., Greensmith, L., Torok, Z., Balogh, G., Gombos, I., Campana, F., Concilio, S., Gallyas, F., Nagy, G., Berente, Z., Gungor, B., Peter, M., Glatz, A., Hunya, A., Literati-Nagy, Z., Vigh, L., Hoogstra-Berends, F., Heeres, A., Kuipers, I., Loen, L., Seerden, J.P., Zhang, D., Meijering, R.A., Henning, R.H., Brundel, B.J., Kampinga, H.H., Koranyi, L., Szilvassy, Z., Mandl, J., Sumegi, B., Febbraio, M.A., Horvath, I., Hooper, P.L., Vigh, L. 2013. Hydroximic acid derivatives: pleiotropic HSP co-inducers restoring homeostasis and robustness. *Current Pharmaceutical Design*, 19(3), pp.309–346.
- Cudkovicz, M.E., Shefner J.M., Simpson, E., Grasso, D., Yu, H., Zhang, H., Shui, A., Schoenfeld, D., Brown, R.H., Wieland, S., Barber, J.R. & Northeast ALS Consortium. 2008. Arimoclomol at dosages up to 300 mg/day is well tolerated and safe in amyotrophic lateral sclerosis. *Muscle & Nerve*, 38(1), pp.837–844.
- Cuervo, A.M. & Dice, J.F. 2000. When lysosomes get old. *Experimental Gerontology*, 35(2), pp.119–131.
- Cuervo, A.M. & Wong, E. 2014. Chaperone-mediated autophagy: roles in disease and aging. *Cell Research*, 24(1), pp.92–104.
- Cupler, E.J., Leon-Monzon, M., Miller, J., Semino-Mora, C., Anderson, T.L. & Dalakas, M.C. 1996. Inclusion body myositis in HIV-1 and HTLV-1 infected patients. *Brain*, 119(Pt6), pp.1887–93.
- Custer, S.K., Neumann, M., Lu, H., Wright, A.C. & Taylor, J.P. 2010. Transgenic mice expressing mutant forms VCP/p97 recapitulate the full spectrum of IBMPFD including degeneration in muscle, brain and bone. *Human Molecular Genetics*, 19(9), pp.1741–1755.
- D'Agostino, C., Nogalska, A., Cacciottolo, M., Engel, W.K. & Askanas, V. 2011. Abnormalities of NBR1, a novel autophagy-associated protein, in muscle fibers of sporadic inclusion-body myositis. *Acta Neuropathologica*, 122(5), pp.627–636.
- D'Angelo, M.A., Raices, M., Panowski, S.H. & Hetzer, M.W. 2009. Age-Dependent Deterioration of Nuclear Pore Complexes Causes a Loss of Nuclear Integrity in Postmitotic Cells. *Cell*, 136(2), pp.284–295.
- Dabby, R., Lange D.J., Trojaborg, W., Hays, A.P., Lovelace, R.E., Brannagan, T.H. & Rowland, L.P. 2001. Inclusion body myositis mimicking motor neuron disease. *Archives of Neurology*, 58(8), p.1253.
- Dahlbom, K., Lindberg, C. & Oldfors, A. 2002. Inclusion body myositis: morphological clues to correct diagnosis. *Neuromuscular Disorders*, 12(9), pp.853–857.
- Dai, R.M., Chen, E., Longo, D.L., Gorbea, C.M. & Li, C.C. 1998. Involvement of valosin-containing protein, an ATPase Co-purified with IkappaBalpha and 26 S proteasome, in ubiquitin-proteasome-mediated degradation of IkappaBalpha. *The Journal of Biological Chemistry*, 273(6), pp.3562–3573.

- Dai, R.M. & Li, C.C. 2001. Valosin-containing protein is a multi-ubiquitin chain-targeting factor required in ubiquitin–proteasome degradation. *Nature Cell Biology*, 3(8), pp.740–744.
- Dalakas, M.C. 1998. Controlled studies with high-dose intravenous immunoglobulin in the treatment of dermatomyositis, inclusion body myositis, and polymyositis. *Neurology*, 51(6 Suppl 5), pp.S37-45.
- Dalakas, M.C. 2006a. Inflammatory, immune, and viral aspects of inclusion-body myositis. *Neurology*, 66(2 Suppl 1), pp.S33-38.
- Dalakas, M.C. 2006b. Sporadic inclusion body myositis--diagnosis, pathogenesis and therapeutic strategies. *Nature Clinical Practice. Neurology*, 2(8), pp.437–447.
- Dalakas, M.C. 2008. Interplay between inflammation and degeneration: Using inclusion body myositis to study “neuroinflammation.” *Annals of Neurology*, 64(1), pp.1–3.
- Dalakas, M.C. 2015. Inflammatory Muscle Diseases. *New England Journal of Medicine*, 372(18), pp.1734–1747.
- Dalakas, M.C. 2016. Polymyositis. In *International Neurology*. Chichester, UK: John Wiley & Sons, Ltd, pp. 497–500.
- Dalakas, M.C., Koffman, B., Fujii, M., Spector, S., Sivakumar, K. & Cupler, E. 2001. A controlled study of intravenous immunoglobulin combined with prednisone in the treatment of IBM. *Neurology*, 56(3), pp.323–327.
- Dalakas, M.C., Rakocevic, G., Schmidt, J., Salajegheh, M., McElroy, B., Harris-Love, M.O., Shrader, J.A., Levy, E.W., Dambrosia, J., Kampen, R.L., Bruno, D.A. & Kirk, A.D. 2009. Effect of Alemtuzumab (CAMPATH 1-H) in patients with inclusion-body myositis. *Brain*, 132(Pt 6), pp.1536–1544.
- Dalakas, M.C., Rakocevic, G., Shatunov, A., Goldfarb, L., Raju, R. & Salajegheh, M. 2007. Inclusion body myositis with human immunodeficiency virus infection: Four cases with clonal expansion of viral-specific T cells. *Annals of Neurology*, 61(5), pp.466–475.
- Dardis, A., Zampieri, S., Canterini, S., Newell, K.L., Stuani, C., Murrell, J.R., Ghetti, B., Fiorenza, M.T., Bembi, B. & Buratti, E. 2016. Altered localization and functionality of TAR DNA Binding Protein 43 (TDP-43) in niemann- pick disease type C. *Acta Neuropathologica Communications*, 4(1), p.52.
- Dastmalchi, M., Grundtman, C., Alexanderson, H., Mavragani, C.P., Einarsdottir, H., Helmers, S.B., Elvin, K., Crow, M.K., Nennesmo, I. & Lundberg, I.E. 2008. A high incidence of disease flares in an open pilot study of infliximab in patients with refractory inflammatory myopathies. *Annals of the Rheumatic Diseases*, 67(12), pp.1670–1677.

- Dasuri, K., Zhang, L., Ebenezer, P., Liu, Y., Fernandez-Kim, S.O. & Kellera, J.N. 2009. Aging and dietary restriction alter proteasome biogenesis and composition in the brain and liver. *Mechanisms of Ageing and Development*, 130(11–12), pp.777–783.
- David, D.C., Ollikainen, N., Trinidad, J.C., Cary, M.P., Burlingame, A.L. & Kenyon, C. 2010. Widespread Protein Aggregation as an Inherent Part of Aging in *C. elegans*. *PLoS Biology*, 8(8), p.e1000450.
- Davidson, Y., Kelley, T., Mackenzie, I.R., Pickering-Brown, S., Du Plessis, D., Neary, D., Snowden, J.S. & Mann DM. 2007. Ubiquitinated pathological lesions in frontotemporal lobar degeneration contain the TAR DNA-binding protein, TDP-43. *Acta Neuropathologica*, 113(5), pp.521–533.
- Dec, E., Ferguson, D., Nalbandian, A., Gargus, M., Katheria, V., Rana, P., Ibrahim, A., Hatch, M, Lan, M., Llewellyn, K.J., Keirstead, H. & Kimonis, V.E. 2014. Disease-specific Induced Pluripotent Stem Cell Modeling: Insights into the Pathophysiology of Valosin Containing Protein (VCP) Disease. *Journal of Stem Cell Research & Therapy*, 4(168).
- Dec, E., Rana, P., Rana, P., Katheria, V., Dec, R., Khare, M., Nalbandian, A., Leu, S.Y., Radom-Aizik, S., Llewellyn, K., BenMohamed, L., Zaldivar, F. & Kimonis, V. 2014. Cytokine profiling in patients with VCP-associated disease. *Clinical and Translational Science*, 7(1), pp.29–32.
- Deerinck, T.J., Bushong, E.A., Thor, A, & Ellisman M.H. 2010. NCMIR methods for 3D EM: a new protocol for preparation of biological specimens for serial block face scanning electron microscopy. *Microscopy*, 6-8.
- Van Deerlin, V.M., Leverenz, J.B., Bekris, L.M., Bird, T.D., Yuan, W., Elman, L.B., Clay, D., Wood, E.M., Chen-Plotkin, A.S., Martinez-Lage, M., Steinbart, E., McCluskey, L., Grossman, M., Neumann, M., Wu, I.L., Yang, W.S., Kalb, R., Galasko, D.R., Montine, T.J., Trojanowski, J.Q., Lee, V.M., Schellenberg, G.D. & Yu, C.E. 2008. TARDBP mutations in amyotrophic lateral sclerosis with TDP-43 neuropathology: a genetic and histopathological analysis. *The Lancet. Neurology*, 7(5), pp.409–416.
- Defenouillere, Q., Yao, Y., Mouaikel, J., Namane, A., Galopier, A., Decourty, L., Doyen, A., Malabat, C., Saveanu, C., Jacquier, A. & Fromont-Racine, M. 2013. Cdc48-associated complex bound to 60S particles is required for the clearance of aberrant translation products. *Proceedings of the National Academy of Sciences*, 110(13), pp.5046–5051.
- DeLaBarre, B. & Brunger, A.T. 2003. Complete structure of p97/valosin-containing protein reveals communication between nucleotide domains. *Nature Structural Biology*, 10(10), pp.856–863.
- Demontis, F. & Perrimon, N. 2010. FOXO/4E-BP Signaling in *Drosophila* Muscles Regulates Organism-wide Proteostasis during Aging. *Cell*, 143(5), pp.813–825.

- Detmer, S.A. & Chan, D.C. 2007. Functions and dysfunctions of mitochondrial dynamics. *Nature Reviews Molecular Cell Biology*, 8(11), pp.870–879.
- Dewitt, D.A., Hurd, J.A., Fox, N., Townsend, B.E., Griffioen, K.J., Ghribi, O. & Savory J. 2006. Peri-nuclear clustering of mitochondria is triggered during aluminum maltolate induced apoptosis. *Journal of Alzheimer's Disease*, 9, pp.195–205.
- Dimachkie, M. & Barohn, R. 2012. Inclusion Body Myositis. *Seminars in Neurology*, 32(03), pp.237–245.
- Dion, E., Cherin P., Payan, C., Fournet, J.C., Papo, T., Maisonobe, T., Auberton, E., Chosidow, O., Godeau, P., Piette, J.C., Herson, S. & Grenier, P. 2002. Magnetic resonance imaging criteria for distinguishing between inclusion body myositis and polymyositis. *The Journal of Rheumatology*, 29(9), pp.1897–906.
- Dobloug, G.C., Antal, E.A, Sveberg, L., Garen, T., Bitter, H., Stjärne, J., Grøvle, L., Gran, J.T. & Molberg, Ø. 2015. High prevalence of inclusion body myositis in Norway; a population-based clinical epidemiology study. *European Journal of Neurology*, 22(4), pp.672-e41.
- Dobloug, G.C., Walle-Hansen, R., Gran, J.T. & Molberg, Ø. 2012. Long-term follow-up of sporadic inclusion body myositis treated with intravenous immunoglobulin: a retrospective study of 16 patients. *Clinical and Experimental Rheumatology*, 30(6), pp.838–842.
- Doran, P., Gannon, J., O'Connell, K. & Ohlendieck, K. 2007. Aging skeletal muscle shows a drastic increase in the small heat shock proteins α B-crystallin/HspB5 and α vHsp/HspB7. *European Journal of Cell Biology*, 86, pp.629–640.
- Dormann, D., Capell ,A., Carlson, A.M., Shankaran, S.S., Rodde, R., Neumann, M., Kremmer, E., Matsuwaki, T., Yamanouchi, K., Nishihara, M. & Haass, C. 2009. Proteolytic processing of TAR DNA binding protein-43 by caspases produces C-terminal fragments with disease defining properties independent of progranulin. *Journal of Neurochemistry*, 110(3), pp.1082–1094.
- Douglas, P.M. & Dillin, A. 2010. Protein homeostasis and aging in neurodegeneration. *The Journal of Cell Biology*, 190(5).
- Dubourg, O., Wanschitz, J., Maisonobe, T., Béhin, A., Allenbach, Y., Herson, S. & Benveniste, O. 2011. Diagnostic value of markers of muscle degeneration in sporadic inclusion body myositis. *Acta Myologica*, 30(2), pp.103–108.
- Duddy, W., Duguez, S., Johnston, H., Cohen, T.V., Phadke, A., Gordish-Dressman, H., Nagaraju, K, Gnocchi, V., Low, S. & Partridge, T. 2015. Muscular dystrophy in the mdx mouse is a severe myopathy compounded by hypotrophy, hypertrophy and hyperplasia. *Skeletal Muscle*, 5, p.16.
- Engel, A.G. & Arahata, K. 1984. Monoclonal antibody analysis of mononuclear cells in myopathies. II: Phenotypes of autoinvasive cells in polymyositis and inclusion body myositis. *Annals of Neurology*, 16(2), pp.209–215.

- Erickson, R.R., Dunning, L.M. & Holtzman, J.L. 2006. The effect of aging on the chaperone concentrations in the hepatic, endoplasmic reticulum of male rats: the possible role of protein misfolding due to the loss of chaperones in the decline in physiological function seen with age. *The Journals of Gerontology. Series A, Biological Sciences and Medical Sciences*, 61(5), pp.435–443.
- Erzurumlu, Y. et al., 2013. A unique IBMPFD-related P97/VCP mutation with differential binding pattern and subcellular localization. *The International Journal of Biochemistry & Cell Biology*, 45(4), pp.773–782.
- Eura, N. Sugie, K., Kinugawa, K., Nanaura, H., Ohara, H., Iwasa, N., Shobatake, R., Kiriya, T., Izumi, T., Kataoka, H. & Ueno, S.I. 2016. Anti-Cytosolic 5'-Nucleotidase 1A (cN1A) Positivity in Muscle is Helpful in the Diagnosis of Sporadic Inclusion Body Myositis: A Study of 35 Japanese Patients. *Journal of Neurobiology and Neuroscience*, 7(5), p.155.
- Evangelista, T., Wehl, C.C., Kimonis, V., Lochmüller, H. & VCP-related diseases Consortium. 2016. 215th ENMC International Workshop VCP-related multi-system proteinopathy (IBMPFD) 13–15 November 2015, Heemskerk, The Netherlands. *Neuromuscular Disorders*, 26(8), pp.535-547.
- Fargnoli, J., Kunisada, T., Fornace, A.J. Jr., Schneider, E.L. & Holbrook, N.J. 1990. Decreased expression of heat shock protein 70 mRNA and protein after heat treatment in cells of aged rats. *Proceedings of the National Academy of Sciences of the United States of America*, 87(2), pp.846–850.
- Felice, K.J. & North, W.A. 2001. Inclusion body myositis in Connecticut: observations in 35 patients during an 8-year period. *Medicine*, 80(5), pp.320–327.
- Fernandez-Estevez, M.A., Casarejos, M.J., López Sendon, J., Garcia Caldentey, J., Ruiz, C., Gomez, A., Perucho, J., de Yébenes, J.G. & Mena, M.A. 2014. Trehalose reverses cell malfunction in fibroblasts from normal and Huntington's disease patients caused by proteasome inhibition. *PLoS ONE*, 9(2), p.e90202.
- Fernández-Sáiz, V. & Buchberger, A. 2010. Imbalances in p97 co-factor interactions in human proteinopathy. *EMBO reports*, 11(6), pp.479–485.
- Ferreira, S.T., Vieira, M.N.N. & De Felice, F.G. 2007. Soluble protein oligomers as emerging toxins in Alzheimer's and other amyloid diseases. *IUBMB Life*, 59(4), pp.332–345.
- Ferrer, I., Martín, B., Castaño, J.G., Lucas, J.J., Moreno, D. & Olivé, M. 2004. Proteasomal expression, induction of immunoproteasome subunits, and local MHC class I presentation in myofibrillar myopathy and inclusion body myositis. *Journal of Neuropathology and Experimental Neurology*, 63(5), pp.484–498.
- Ferrington, D.A., Husom, A.D. & Thompson, L.V. 2005. Altered proteasome structure, function, and oxidation in aged muscle. *The FASEB Journal*, 19(6), pp.644–6.

- Fidzianska, A., Glinka, Z., Kaminska, A. & Niebroj-Dobosz, I. 2008. Altered distribution of lamin and emerin in muscle nuclei of sIBM patients. *Clinical Neuropathology*, 27(6), pp.424–429.
- Figarella-Branger, D., Civatte, M., Bartoli, C. & Pellissier, J.F. 2003. Cytokines, chemokines, and cell adhesion molecules in inflammatory myopathies. *Muscle & Nerve*, 28(6), pp.659–682.
- Figuroa-Bonaparte, S., Hudson, J., Barresi, R., Polvikoski, T., Williams, T., Töpf, A., Harris E., Hilton-Jones D., Petty R., Willis T.A., Longman C., Dougan, C.F., Parton M.J., Hanna, M.G., Quinlivan, R., Farrugia, M.E., Guglieri, M., Bushby, K., Straub, V., Lochmüller, H. & Evangelista, T. 2016. Mutational spectrum and phenotypic variability of VCP-related neurological disease in the UK. *Journal of Neurology, Neurosurgery, and Psychiatry*, 87(6), pp.680–681.
- Fiorenza, M.T., Farkas, T., Dissing, M., Kolding, D. & Zimarino, V. 1995. Complex expression of murine heat shock transcription factors. *Nucleic Acids Research*, 23(3), pp.467–474.
- Folker, E.S. & Baylies, M.K. 2013. Nuclear positioning in muscle development and disease. *Frontiers in Physiology*, 4, p.363.
- Foreman, C., Russo, P., Davies, N., Hissaria, P., Proudman, S., Hughes, T. & Limaye, V. 2017. Use of intravenous immunoglobulin therapy for myositis: an audit in South Australian patients. *Internal Medicine Journal*, 47(1), pp.112–115.
- Forman, M.S., Mackenzie, I.R., Cairns, N.J., Swanson, E., Boyer, P.J., Drachman, D.A., Jhaveri, B.S., Karlawish, J.H., Pestronk, A., Smith, T.W., Tu, P.H., Watts, G.D., Markesbery, W.R., Smith, C.D. & Kimonis, V.E. 2006. Novel ubiquitin neuropathology in frontotemporal dementia with valosin-containing protein gene mutations. *Journal of Neuropathology and Experimental Neurology*, 65(6), pp.571–581.
- Fratta, P., Engel W.K., McFerrin, J., Davies, K.J., Lin, S.W. & Askanas, V. 2005. Proteasome inhibition and aggresome formation in sporadic inclusion-body myositis and in amyloid-beta precursor protein-overexpressing cultured human muscle fibers. *The American Journal of Pathology*, 167(2), pp.517–526.
- Frieden, M., James, D., Castelbou, C., Danckaert, A., Martinou, J.C. & Demarex, N. 2004. Ca²⁺ Homeostasis during Mitochondrial Fragmentation and Perinuclear Clustering Induced by hFis1. *Journal of Biological Chemistry*, 279(21), pp.22704–22714.
- Fukuchi, K., Pham, D., Hart, M., Li, L. & Lindsey, J.R. 1998. Amyloid-beta deposition in skeletal muscle of transgenic mice: possible model of inclusion body myopathy. *The American Journal of Pathology*, 153(6), pp.1687–1693.
- Gang, Q., Bettencourt, C., Houlden, H., Hanna, M.G. & Machado, P.M. 2015. Genetic advances in sporadic inclusion body myositis. *Current Opinion in Rheumatology*, 27(6), pp.586–594.

- Gang, Q., Bettencourt, C., Machado, P.M., Brady, S., Holton, J.L., Pittman, A.M, Hughes, D., Healy, E., Parton, M., Hilton-Jones, D., Shieh, P.B., Needham, M., Liang, C., Zanoteli, E., de Camargo, L.V., De Paepe, B., De Bleecker, J., Shaibani, A., Ripolone, M., Violano, R., Moggio, M., Barohn, R.J., Dimachkie, M.M., Mora, M., Mantegazza, R., Zanotti, S., Singleton, A.B., Hanna, M.G., Houlden, H., & The Muscle Study Group & The International IBM Genetics Consortium, 2016. Rare variants in SQSTM1 and VCP genes and risk of sporadic inclusion body myositis. *Neurobiology of Aging*, 47, p.218.e1-218.e9.
- Gang, Q., Bettencourt, C., Machado, P.M., Fox, Z., Brady, S., Healy, E., Parton, M., Holton, J.L., Hilton-Jones, D., Shieh, P.B., Zanoteli, E., De Paepe, B., De Bleecker, J., Shaibani, A., Ripolone, M., Violano, R., Moggio, M., Barohn, R.J., Dimachkie, M.M., Mora, M., Mantegazza, R., Zanotti, S., Hanna, M.G., Houlden, H.; Muscle Study Group and the International IBM Genetics Consortium. 2015. The effects of an intronic polymorphism in TOMM40 and APOE genotypes in sporadic inclusion body myositis. *Neurobiology of Aging*, 36(4), p.1766.e1-3.
- Gang, Q., Bettencourt, C., Machado, P.M., Hanna, M.G. & Houlden, H. 2014. Sporadic inclusion body myositis: the genetic contributions to the pathogenesis. *Orphanet Journal of Rare Diseases*, 9, p.88.
- Gao, J., Wang, L., Liu, J., Xie, F., Su, B. & Wang X. 2017. Abnormalities of Mitochondrial Dynamics in Neurodegenerative Diseases. *Antioxidants*, 6(2), p.25.
- Garlepp, M.J., Laing, B., Zilko, P.J., Ollier, W. & Mastaglia, F.L. 1994. HLA associations with inclusion body myositis. *Clinical & Experimental Immunology*, 98, pp.40–45.
- Garner, T.P., Long, J., Layfield, R. & Searle MS. 2011. Impact of p62/SQSTM1 UBA Domain Mutations Linked to Paget's Disease of Bone on Ubiquitin Recognition. *Biochemistry*, 50(21), pp.4665–4674.
- Gendron, T.F., Rademakers, R. & Petrucelli, L., 2013. TARDBP mutation analysis in TDP-43 proteinopathies and deciphering the toxicity of mutant TDP-43. *Journal of Alzheimer's Disease : JAD*, 33 Suppl 1, pp.S35-45.
- Gidaro, T., Modoni, A., Sabatelli, M., Tasca, G., Broccolini, A. & Mirabella, M. 2008. An Italian family with inclusion-body myopathy and frontotemporal dementia due to mutation in the VCP gene. *Muscle & Nerve*, 37(1), pp.111–114.
- Gifondorwa, D.J., Robinson, M.B., Hayes, C.D., Taylor, A.R., Prevette, D.M., Oppenheim, R.W., Caress, J. & Milligan, C.E. 2007. Exogenous Delivery of Heat Shock Protein 70 Increases Lifespan in a Mouse Model of Amyotrophic Lateral Sclerosis. *Journal of Neuroscience*, 27(48), pp.13173–13180.
- Girolamo, F., Lia, A., Amati, A., Strippoli, M., Coppola, C., Virgintino, D., Roncali, L., Toscano, A., Serlenga, L. & Trojano, M. 2013. Overexpression of autophagic proteins in the skeletal muscle of sporadic inclusion body myositis. *Neuropathology and Applied Neurobiology*, 39(7), pp.736–749.

- Gispert-Sanchez, S. & Auburger, G. 2006. The role of protein aggregates in neuronal pathology: guilty, innocent, or just trying to help? *Parkinson's Disease and Related Disorders*, pp.111–117.
- Gitcho, M.A., Strider, J., Carter, D., Taylor-Reinwald, L., Forman, M.S., Goate, A.M., Cairns, N.J. 2009. VCP Mutations Causing Frontotemporal Lobar Degeneration Disrupt Localization of TDP-43 and Induce Cell Death. *Journal of Biological Chemistry*, 284(18), pp. 12384-98.
- Gonzalez, M.A., Feely, S.M., Speziani, F., Strickland, A.V., Danzi, M., Bacon, C., Lee, Y., Chou, T.F., Blanton, S.H.1, Weihl, C.C., Zuchner, S. & Shy, M.E. 2014. A novel mutation in VCP causes Charcot-Marie-Tooth Type 2 disease. *Brain*, 137(Pt 11), pp.2897–2902.
- Greenberg, S.A. 2009. Inflammatory myopathies: disease mechanisms. *Current Opinion in Neurology*, 22(5), pp.516–523.
- Greenberg, S.A. 2010. Comment on alemtuzumab and inclusion body myositis. *Brain*, 133(5), pp.e135–e135.
- Greenberg, S.A. 2012. Pathogenesis and therapy of inclusion body myositis. *Current Opinion in Neurology*, 25(5), pp.630–639.
- Greenberg, S.A. 2014. Cytoplasmic 5'-nucleotidase autoantibodies in inclusion body myositis: Isotypes and diagnostic utility. *Muscle & Nerve*, 50(4), pp.488-492.
- Greenberg, S.A. 2017. Unfounded Claims of Improved Functional Outcomes Attributed to Follistatin Gene Therapy in Inclusion Body Myositis. *Molecular Therapy*, 25(10), pp.2235–2237.
- Greenberg, S.A., Pinkus, J.L. & Amato, A.A. 2006. Nuclear membrane proteins are present within rimmed vacuoles in inclusion-body myositis. *Muscle & Nerve*, 34(4), pp.406–416.
- Griggs, R.C., Askanas, V., DiMauro, S., Engel, A., Karpatis, G., Mendell, J.R. & Rowland, L.P. 1995. Inclusion body myositis and myopathies. *Annals of Neurology*, 38(5), pp.705–713.
- Guimaraes, J.B., Zanoteli, E., Link, T.M., de Camargo, L.V., Facchetti, L., Nardo, L. & Fernandes, A.D.R.C. 2017. Sporadic Inclusion Body Myositis: MRI Findings and Correlation With Clinical and Functional Parameters. *American Journal of Roentgenology*, 209(6), pp.1340–1347.
- Gutmann, L., Govindan, S., Riggs, J.E. & Schochet, S. 1985. Inclusion Body Myositis and Sjogren's Syndrome. *Archives of Neurology*, 42(10), pp.1021–1022.

- Güttsches, A.K., Brady, S., Krause, K., Maerkens, A., Uszkoreit, J., Eisenacher, M., Schreiner, A., Galozzi, S., Mertens-Rill, J., Tegenthoff, M., Holton, J.L., Harms, M.B., Lloyd, T.E., Vorgerd, M., Wehl, C.C., Marcus, K. & Kley, R.A. 2016. Proteomics of Rimmed Vacuoles Define New Risk Allele in Inclusion Body Myositis. *American Neurological Association*, 81(2), pp.227-239.
- Guyant-Marechal, L., Laquerrière, A., Duyckaerts, C., Dumanchin, C., Bou, J., Dugny, F., Le Ber, I., Frébourg, T., Hannequin, D. & Campion, D. 2006. Valosin-containing protein gene mutations: Clinical and neuropathologic features. *Neurology*, 67(4), pp.644–651.
- Halawani, D., LeBlanc, A.C., Rouiller, I., Michnick, S.W., Servant, M.J. & Latterich, M. 2009. Hereditary inclusion body myopathy-linked p97/VCP mutations in the NH2 domain and the D1 ring modulate p97/VCP ATPase activity and D2 ring conformation. *Molecular and Cellular Biology*, 29(16), pp.4484–4494.
- Hall, D.M., Xu, L., Drake V.J., Oberley, L.W., Oberley, T.D., Moseley, PL., Kregel, K.C. 2000. Aging reduces adaptive capacity and stress protein expression in the liver after heat stress. *Journal of Applied Physiology*, 89(2), pp.749–759.
- Hara, T., Nakamura, K., Matsui, M., Yamamoto, A., Nakahara, Y., Suzuki-Migishima, R., Yokoyama, M., Mishima, K., Saito, I., Okano, H. & Mizushima, N. 2006. Suppression of basal autophagy in neural cells causes neurodegenerative disease in mice. *Nature*, 441(7095), pp.885–889.
- Hargitai, J., Lewis, H., Boros, I., Rácz, T., Fiser, A., Kurucz, I., Benjamin, I., Vigh, L., Péntzes, Z., Csermely, P., Latchman, D.S., 2003. Bimoclolol, a heat shock protein co-inducer, acts by the prolonged activation of heat shock factor-1. *Biochemical and Biophysical Research Communications*, 307(3), pp.689–695.
- Hartl, F.U. & Hayer-Hartl, M. 2009. Converging concepts of protein folding in vitro and in vivo. *Nature Structural & Molecular Biology*, 16(6), pp.574–581.
- Hatch, E. & Hetzer, M. 2014. Breaching the nuclear envelope in development and disease. *The Journal of Cell Biology*, 205(2), pp.133–141.
- Hayashi, T. & Goto, S. 1998. Age-related changes in the 20S and 26S proteasome activities in the liver of male F344 rats. *Mechanisms of Ageing and Development*, 102(1), pp.55–66.
- Hayflick, L. & Moorhead, P.S. 1961. The serial cultivation of human diploid cell strains. *Experimental Cell Research*, 25(3), pp.585-621.
- Hemion, C., Flammer, J. & Neutzner, A. 2014. Quality control of oxidatively damaged mitochondrial proteins is mediated by p97 and the proteasome. *Free Radical Biology and Medicine*, 75, pp.121–128.

- Heo, J.M., Livnat-Levanon, N., Taylor, E.B., Jones, K.T., Dephoure, N., Ring, J., Xie, J., Brodsky, J.L., Madeo, F., Gygi, S.P., Ashrafi, K., Glickman, M.H. & Rutter, J. 2010. A stress-responsive system for mitochondrial protein degradation. *Molecular Cell*, 40(3), pp.465–480.
- Herbelet, S., De Vlieghere, E., Gonçalves, A., De Paepe, B., Schmidt, K., Nys, E., Weynants, L., Weis, J., Van Peer, G., Vandesompele, J., Schmidt, J., De Wever, O. & De Bleecker, J.L.. 2018. Localization and Expression of Nuclear Factor of Activated T-Cells 5 in Myoblasts Exposed to Pro-inflammatory Cytokines or Hyperosmolar Stress and in Biopsies from Myositis Patients. *Frontiers in Physiology*, 9, p.126.
- Hetzer, M., Meyer, H.H., Walther, T.C., Bilbao-Cortes, D., Warren, G. & Mattaj, I.W. 2001. Distinct AAA-ATPase p97 complexes function in discrete steps of nuclear assembly. *Nature Cell Biology*, 3(12), pp.1086–1091.
- Heydari, A.R., Wu, B., Takahashi, R., Strong, R. & Richardson, A. 1993. Expression of heat shock protein 70 is altered by age and diet at the level of transcription. *Molecular and Cellular Biology*, 13(5), pp.2909–2918.
- Heydari, A.R., You, S., Takahashi, R., Gutschmann-Conrad, A., Sarge, K.D. & Richardson, A. 2000. Age-Related Alterations in the Activation of Heat Shock Transcription Factor 1 in Rat Hepatocytes. *Experimental Cell Research*, 256(1), pp.83–93.
- Hilton-Jones, D., Miller, A., Parton, M., Holton, J., Sewry, C. & Hanna, M.G. 2010. Inclusion body myositis: MRC Centre for Neuromuscular Diseases, IBM workshop, London, 13 June 2008. *Neuromuscular Disorders*, 20(2), pp.142–147.
- Hiniker, A., Daniels, B.H. & Margeta, M. 2016. T-Cell-Mediated Inflammatory Myopathies in HIV-Positive Individuals: A Histologic Study of 19 Cases. *Journal of Neuropathology and Experimental Neurology*, 75(3), pp.239–245.
- Hitraya, E.G., Varga, J. & Jimenez, S.A. 1995. Heat shock of human synovial and dermal fibroblasts induces delayed up-regulation of collagenase-gene expression. *Biochemical Journal*, 308(Pt3), pp.743–747.
- Hohlfeld, R. & Engel, A.G. 1992. Expression of 65-kd heat shock proteins in the inflammatory myopathies. *Annals of Neurology*, 32(6), pp.821–823.
- Holleman, D., Budka, H., Löscher, W.N., Yanagida, G., Fischer, M.B. & Wanschitz, J.V. 2008. Endothelial and Myogenic Differentiation of Hematopoietic Progenitor Cells in Inflammatory Myopathies. *Journal of Neuropathology and Experimental Neurology*, 67(7), pp.711–719.
- Houser, S.M., Calabrese, L.H. & Strome, M. 1998. Dysphagia in patients with inclusion body myositis. *The Laryngoscope*, 108(7), pp.1001–1005.

- del Hoyo, P., García-Redondo, A., de Bustos, F., Molina, J.A., Sayed, Y., Alonso-Navarro, H., Caballero, L., Arenas, J., Agúndez, J.A. & Jiménez-Jiménez, F.J. 2010. Oxidative stress in skin fibroblasts cultures from patients with Parkinson's disease. *BMC Neurology*, 10(1), p.95.
- del Hoyo, P., García-Redondo, A., de Bustos, F., Molina, J.A., Sayed, Y., Alonso-Navarro, H., Caballero, L., Arenas, J. & Jiménez-Jiménez, F.J. 2006. Oxidative Stress in Skin Fibroblasts Cultures of Patients with Huntington's Disease. *Neurochemical Research*, 31(9), pp.1103–1109.
- Hübbers, C.U., Clemen, C.S., Kesper, K., Böddrich, A., Hofmann, A., Kämäräinen, O., Tolksdorf, K., Stumpf, M., Reichelt, J., Roth, U., Krause, S., Watts, G., Kimonis, V., Wattjes, MP., Reimann, J., Thal, D.R., Biermann, K., Evert, B.O., Lochmüller, H., Wanker, E.E., Schoser, B.G., Noegel, A.A. & Schröder, R. 2007. Pathological consequences of VCP mutations on human striated muscle. *Brain*, 130, pp.381–393.
- Hunsucker, S.A., Sychala, J. & Mitchell, B.S. 2001. Human cytosolic 5'-nucleotidase I: characterization and role in nucleoside analog resistance. *The Journal of Biological Chemistry*, 276(13), pp.10498–10504.
- Husom, A.D., Peters, E.A., Kolling, E.A., Fugere, N.A., Thompson, L.V. & Ferrington, D.A. 2004. Altered proteasome function and subunit composition in aged muscle. *Archives of Biochemistry and Biophysics*, 421(1), pp.67–76.
- Hussain, S.G. & Ramaiah, K.V.A. 2007. Reduced eIF2 α phosphorylation and increased proapoptotic proteins in aging. *Biochemical and Biophysical Research Communications*, 355(2), pp.365–370.
- Hwang, J.S., Hwang, J.S., Chang, I. & Kim S. 2007. Age-associated decrease in proteasome content and activities in human dermal fibroblasts: restoration of normal level of proteasome subunits reduces aging markers in fibroblasts from elderly persons. *The Journals of Gerontology. Series A, Biological Sciences and Medical Sciences*, 62(5), pp.490–499.
- Ichimura, Y., Kumanomidou, T., Sou, Y.S., Mizushima, T., Ezaki, J., Ueno, T., Kominami, E., Yamane, T., Tanaka, K. & Komatsu, M. 2008. Structural Basis for Sorting Mechanism of p62 in Selective Autophagy. *Journal of Biological Chemistry*, 283(33), pp.22847–22857.
- Iwasa, K. Nambu, Y., Motozaki, Y., Furukawa, Y., Yoshikawa, H. & Yamada, M. 2014. Increased skeletal muscle expression of the endoplasmic reticulum chaperone GRP78 in patients with myasthenia gravis. *Journal of Neuroimmunology*, 273(1–2), pp.72–76.
- Jackson, C.E., Barohn, R.J., Gronseth, G., Pandya, S., Herbelin, L. & Muscle Study Group. 2008. Inclusion body myositis functional rating scale: A reliable and valid measure of disease severity. *Muscle & Nerve*, 37(4), pp.473–476.

- Jee, H. 2016. Size dependent classification of heat shock proteins: a mini-review. *Journal of Exercise Rehabilitation*, 12(4), pp.255–259.
- Jin, L.W., Hearn, M.G., Ogburn, C.E., Dang, N., Nochlin, D., Ladiges, W.C. & Martin, G.M. 1998. Transgenic mice over-expressing the C-99 fragment of betaPP with an alpha-secretase site mutation develop a myopathy similar to human inclusion body myositis. *The American Journal of Pathology*, 153(6), pp.1679–1686.
- Johari, M., Arumilli, M., Palmio, J., Savarese, M., Tasca, G., Mirabella, M., Sandholm, N., Lohi, H., Hackman, P. & Udd, B. 2017. Association study reveals novel risk loci for sporadic inclusion body myositis. *European Journal of Neurology*, 24(4), pp.572–577.
- Johnson, B.S., Snead, D., Lee, J.J., McCaffery, J.M., Shorter, J. & Gitler, A.D. 2009. TDP-43 is intrinsically aggregation-prone, and amyotrophic lateral sclerosis-linked mutations accelerate aggregation and increase toxicity. *The Journal of Biological Chemistry*, 284(30), pp.20329–20339.
- Johnson, J.O., Mandrioli, J., Benatar, M., Abramzon, Y., Van Deerlin, V.M., Trojanowski, J.Q., Gibbs, J.R., Brunetti, M., Gronka, S., Wu, J., Ding, J., McCluskey, L., Martinez-Lage, M., Falcone, D., Hernandez, D.G., Arepalli, S., Chong, S., Schymick, J.C., Rothstein, J., Landi, F., Wang, Y.D., Calvo, A., Mora, G., Sabatelli, M., Monsurrò, M.R., Battistini, S., Salvi, F., Spataro, R., Sola, P., Borghero, G; ITALSGEN Consortium, Galassi, G., Scholz, S.W., Taylor, J.P., Restagno, G., Chiò, A. & Traynor, B.J. 2010. Exome Sequencing Reveals VCP Mutations as a Cause of Familial ALS. *Neuron*, 68(5), pp.857–864.
- Johnson, L.G., Collier, K.E., Edwards, D.J., Philippe, D.L., Eastwood, P.R., Walters, S.E., Thickbroom, G.W. & Mastaglia, F.L. 2009. Improvement in Aerobic Capacity After an Exercise Program in Sporadic Inclusion Body Myositis. *Journal of Clinical Neuromuscular Disease*, 10(4), pp.178–184.
- Johnson, L.G., Edwards, D.J., Walters, S., Thickbroom, G.W. & Mastaglia, F.L. 2007. The Effectiveness of an Individualized, Home-Based Functional Exercise Program for Patients With Sporadic Inclusion Body Myositis. *Journal of Clinical Neuromuscular Disease*, 8(4), pp.187–194.
- Jørgensen, A., Aagaard, P., Frandsen, U., Boyle, E. & Diederichsen, L.P. 2018. Blood-flow restricted resistance training in patients with sporadic inclusion body myositis: a randomized controlled trial. *Scandinavian Journal of Rheumatology*, pp.1–10.
- Joshi, P.R., Vetterke M., Hauburger, A., Tacik, P., Stoltenburg, G. & Hanisch, F. 2014. Functional relevance of mitochondrial abnormalities in sporadic inclusion body myositis. *Journal of Clinical Neuroscience*, 21, pp.1959–1963.
- Joyce, N.C., Oskarsson, B. & Jin, L-W. 2012. Muscle biopsy evaluation in neuromuscular disorders. *Physical Medicine and Rehabilitation Clinics of North America*. 23(3), pp.609-631.

- Ju, J.S., Fuentealba, R.A., Miller, S.E., Jackson, E., Piwnica-Worms, D., Baloh, R.H. & Weihl, C.C. 2009. Valosin-containing protein (VCP) is required for autophagy and is disrupted in VCP disease. *The Journal of Cell Biology*, 187(6), pp.875–888.
- Ju, J.S., Miller, S.E., Hanson, P.I. & Weihl, C.C. 2008. Impaired Protein Aggregate Handling and Clearance Underlie the Pathogenesis of p97/VCP-associated Disease. *Journal of Biological Chemistry*, 283(44), pp.30289–30299.
- Ju, J.S. & Weihl, C.C. 2010. p97/VCP at the intersection of the autophagy and the ubiquitin proteasome system. *Autophagy*, 6(2), pp.283–285.
- Juhász, G., Erdi, B., Sass, M. & Neufeld, T.P. 2007. Atg7-dependent autophagy promotes neuronal health, stress tolerance, and longevity but is dispensable for metamorphosis in *Drosophila*. *Genes & Development*, 21(23), pp.3061–3066.
- Kaarniranta, K., Oksala, N., Karjalainen, H.M., Suuronen, T., Sistonen, L., Helminen, H.J., Salminen, A. & Lammi, M.J. 2002. Neuronal cells show regulatory differences in the hsp70 gene response. *Molecular Brain Research*, 101(1–2), pp.136–140.
- Kabashi, E., Lin, L., Tradewell, M.L., Dion, P.A., Bercier, V., Bourgouin, P., Rochefort, D., Bel, Hadj, S., Durham, H.D., Vande Velde, C., Rouleau, G.A. & Drapeau, P. 2010. Gain and loss of function of ALS-related mutations of TARDBP (TDP-43) cause motor deficits in vivo. *Human Molecular Genetics*, 19(4), pp.671–683.
- Kakkar, V., Meister-Broekema, M., Minoia, M., Carra, S. & Kampinga, H.H. 2014. Barcoding heat shock proteins to human diseases: looking beyond the heat shock response. *Disease Models & Mechanisms*, 7(4), pp.421–434.
- Kalmar, B. & Greensmith, L. 2009. Activation of the heat shock response in a primary cellular model of motoneuron neurodegeneration-evidence for neuroprotective and neurotoxic effects. *Cellular & Molecular Biology Letters*, 14(2), pp.319–335.
- Kalmar, B. & Greensmith, L. 2017. Cellular Chaperones As Therapeutic Targets in ALS to Restore Protein Homeostasis and Improve Cellular Function. *Frontiers in Molecular Neuroscience*, 10, p.251.
- Kalmar, B., Edet-Amana, E. & Greensmith, L., 2012. Treatment with a coinducer of the heat shock response delays muscle denervation in the SOD1-G93A mouse model of amyotrophic lateral sclerosis. *Amyotrophic Lateral Sclerosis*, 13(4), pp.378–392.
- Kalmar, B., Novoselov, S., Gray, A., Cheetham, M.E., Margulis, B. & Greensmith, L. 2008. Late stage treatment with arimoclomol delays disease progression and prevents protein aggregation in the SOD1 mouse model of ALS. *Journal of Neurochemistry*, 107(2), pp.339–350.
- Karpati, G., Pouliot, Y. & Carpenter, S. 1988. Expression of immunoreactive major histocompatibility complex products in human skeletal muscles. *Annals of Neurology*, 23(1), pp.64–72.

- Kaufman, R.J. 1999. Stress signaling from the lumen of the endoplasmic reticulum: coordination of gene transcriptional and translational controls. *Genes & Development*, 13(10), pp.1211–1233.
- Kedersha, N. & Anderson, P. 2007. Mammalian Stress Granules and Processing Bodies. *Methods in Enzymology*, 431, pp.61–81.
- Keller, C.W., Fokken, C., Turville, S.G., Lünemann, A., Schmidt, J., Münz, C. & Lünemann, J.D. 2011. TNF- α induces macroautophagy and regulates MHC class II expression in human skeletal muscle cells. *The Journal of Biological Chemistry*, 286(5), pp.3970–3980.
- Keller, C.W., Schmitz, M., Münz, C., Lünemann, J.D. & Schmidt, J. 2013. TNF- α upregulates macroautophagic processing of APP/ β -amyloid in a human rhabdomyosarcoma cell line. *Journal of the Neurological Sciences*, 325(1), pp.103–107.
- Keller, J.N., Huang, F.F. & Markesbery, W.R. 2000. Decreased levels of proteasome activity and proteasome expression in aging spinal cord. *Neuroscience*, 98(1), pp.149–156.
- Khraishi, M.M., Jay, V. & Keystone, E.C. 1992. Inclusion body myositis in association with vitamin B12 deficiency and Sjögren's syndrome. *The Journal of Rheumatology*, 19(2), pp.306–309.
- Kieran, D. & Greensmith, L. 2004. Inhibition of calpains, by treatment with leupeptin, improves motoneuron survival and muscle function in models of motoneuron degeneration. *Neuroscience*, 125(2), pp.427–439.
- Kieran, D., Kalmar, B., Dick, J.R., Riddoch-Contreras, J., Burnstock, G. & Greensmith, L. 2004. Treatment with arimoclomol, a coinducer of heat shock proteins, delays disease progression in ALS mice. *Nature Medicine*, 10(4), pp.402–405.
- Kim, H.J., Kim N.C., Wang, Y.D., Scarborough, E.A., Moore, J., Diaz, Z., MacLea, K.S., Freibaum, B., Li, S., Molliex, A., Kanagaraj, A.P., Carter, R., Boylan, K.B., Wojtas, A.M., Rademakers, R., Pinkus, J.L., Greenberg, S.A., Trojanowski, J.Q., Traynor, B.J., Smith, B.N., Topp, S., Gkazi, A.S., Miller, J., Shaw, C.E., Kottlors, M., Kirschner, J., Pestronk, A., Li, Y.R., Ford, A.F., Gitler, A.D., Benatar, M., King, O.D., Kimonis, V.E., Ross, E.D., Weihl, C.C., Shorter, J. & Taylor, J.P. 2013. Mutations in prion-like domains in hnRNPA2B1 and hnRNPA1 cause multisystem proteinopathy and ALS. *Nature*, 495(7442), pp.467–473.
- Kim, H.J. & Taylor, J.P. 2017. Lost in Transportation: Nucleocytoplasmic Transport Defects in ALS and Other Neurodegenerative Diseases. *Neuron*, 96(2), pp.285–297.

- Kim, N.C., Tresse, E., Kolaitis, R.M., Molliex, A., Thomas, R.E., Alami, N.H., Wang, B., Joshi, A., Smith, R.B., Ritson, G.P., Winborn, B.J., Moore, J., Lee, J.Y., Yao, T.P., Pallanck, L., Kundu, M. & Taylor, J.P. 2013. VCP is essential for mitochondrial quality control by PINK1/Parkin and this function is impaired by VCP mutations. *Neuron*, 78(1), pp.65–80.
- Kimonis, V.E., Donkervoort, S. & Watts, G.D. 2011. Inclusion body myopathy with Paget disease of bone and/or frontotemporal dementia. *NCBI Bookshelf, GeneReviews*, 68(6), pp.787–796.
- Kimonis, V.E., Fulchiero, E., Vesa, J. & Watts, G. 2008. VCP disease associated with myopathy, Paget disease of bone and frontotemporal dementia: Review of a unique disorder. *Biochimica et Biophysica Acta (BBA) - Molecular Basis of Disease*, 1782(12), pp.744–748.
- Kimonis, V.E., Mehta, S.G., Fulchiero, E.C., Thomasova, D., Pasquali, M., Boycott, K., Neilan, E.G., Kartashov, A., Forman, M.S., Tucker, S., Kimonis, K., Mumm, S., Whyte, M.P., Smith, C.D. & Watts, G.D. 2008. Clinical studies in familial VCP myopathy associated with Paget disease of bone and frontotemporal dementia. *American Journal of Medical Genetics. Part A*, 146A(6), pp.745–757.
- Kirkegaard, T., Gray, J., Priestman, D.A., Wallom, K.L., Atkins, J., Olsen, O.D., Klein, A., Drndarski, S., Petersen, N.H., Ingemann, L., Smith, D.A., Morris, L., Bornæs, C., Jørgensen, S.H., Williams, I., Hinsby, A., Arenz, C., Begley, D., Jäättelä, M. & Platt, F.M. 2016. Heat shock protein-based therapy as a potential candidate for treating the sphingolipidoses. *Science Translational Medicine*, 8(355), p.355ra118-355ra118.
- Kirkin, V., McEwan, D.G., Novak, I. & Dikic, I. 2009. A role for ubiquitin in selective autophagy. *Molecular Cell*, 34(3), pp.259–269.
- Kisselev, A.F., Kitami, T., Nagahama, M., Tagaya, M., Hori, S., Kakizuka, A., Mizuno, Y. & Hattori, N. 1999. The sizes of peptides generated from protein by mammalian 26 and 20 S proteasomes. Implications for understanding the degradative mechanism and antigen presentation. *The Journal of Biological Chemistry*, 274(6), pp.3363–3371.
- Kitami, M.I., Kitami, T., Nagahama, M., Tagaya, M., Hori, S., Kakizuka, A., Mizuno, Y., Hattori, N. 2006. Dominant-negative effect of mutant valosin-containing protein in aggresome formation. *FEBS Letters*, 580(2), pp.474–478.
- Kitazawa, M., Green, K.N., Caccamo, A. & LaFerla, F.M. 2006. Genetically augmenting Abeta42 levels in skeletal muscle exacerbates inclusion body myositis-like pathology and motor deficits in transgenic mice. *The American Journal of Pathology*, 168(6), pp.1986–1997.
- Klaips, C.L., Jayaraj, G.G. & Hartl, F.U. 2018. Pathways of cellular proteostasis in aging and disease. *The Journal of Cell Biology*, 217(1), pp.51–63.

- Klar, J., Sobol, M., Melberg, A., Mäbert, K., Ameer, A., Johansson, A.C., Feuk, L., Entesarian, M., Orlén, H., Casar-Borota, O. & Dahl, N. 2013. Welander Distal Myopathy Caused by an Ancient Founder Mutation in TIA1 Associated with Perturbed Splicing. *Human Mutation*, 34(4), pp. 572-577.
- Kodaka, Y., Rabu, G. & Asakura, A., 2017. Skeletal Muscle Cell Induction from Pluripotent Stem Cells. *Stem Cells International*, 2017, p.1376151.
- Koffman, B.M., Rugiero, M. & Dalakas, M.C., 1998. Immune-mediated conditions and antibodies associated with sporadic inclusion body myositis. *Muscle & Nerve*, 21(1), pp.115–117.
- Koffman, B.M., Sivakumar, K., Simonis, T., Stroncek, D. & Dalakas, M.C. 1998. HLA allele distribution distinguishes sporadic inclusion body myositis from hereditary inclusion body myopathies. *Journal of Neuroimmunology*, 84(2), pp.139–142.
- Komatsu, M. & Ichimura, Y. 2010. Physiological significance of selective degradation of p62 by autophagy. *FEBS Letters*, 584(7), pp.1374–1378.
- Konrad, C., Kawamata, H., Bredvik, K.G., Arreguin, A.J., Cajamarca, S.A., Hupf, J.C., Ravits, J.M., Miller, T.M., Maragakis, N.J., Hales, C.M., Glass, J.D., Gross, S., Mitsumoto, H. & Manfredi, G. 2017. Fibroblast bioenergetics to classify amyotrophic lateral sclerosis patients. *Molecular Neurodegeneration*, 12(1), p.76.
- Kopito, R.R. & Ron, D. 2000. Conformational disease. *Nature Cell Biology*, 2(11), pp.E207–E207.
- Kosmidis, M.L., Alexopoulos, H., Tzioufas, A.G. & Dalakas, M.C. 2013. The effect of anakinra, an IL1 receptor antagonist, in patients with sporadic inclusion body myositis (sIBM): A small pilot study. *Journal of the Neurological Sciences*, 334, pp.123–125.
- Kota, J., Handy, C.R., Haidet, A.M., Montgomery, C.L., Eagle, A., Rodino-Klapac, L.R., Tucker, D., Shilling, C.J., Therfall, W.R., Walker, C.M., Weisbrode, S.E., Janssen, P.M., Clark, K.R., Sahenk, Z., Mendell, J.R. & Kaspar, B.K. 2009. Follistatin gene delivery enhances muscle growth and strength in nonhuman primates. *Science Translational Medicine*, 1(6), p.6ra15.
- Kovach, M.J., Waggoner, B., Leal, S.M., Gelber, D., Khardori, R., Levenstien, M.A., Shanks, C.A., Gregg, G., Al-Lozi, M.T., Miller, T., Rakowicz, W., Lopate, G., Florence, J., Glosser, G., Simmons, Z., Morris, J.C., Whyte, M.P., Pestronk, A. & Kimonis, V.E. 2001. Clinical delineation and localization to chromosome 9p13.3-p12 of a unique dominant disorder in four families: hereditary inclusion body myopathy, Paget disease of bone, and frontotemporal dementia. *Molecular Genetics and Metabolism*, 74(4), pp.458-475.
- Kriegenburg, F. 2012. Quality control of protein folding: an overview. *The FEBS Journal*, 279(4), p.525.

- Kruegel, U., Robison, B., Dange, T., Kahlert, G., Delaney, J.R., Kotireddy, S., Tsuchiya, M., Tsuchiyama, S., Murakami, C.J., Schleit, J., Sutphin, G., Carr, D., Tar, K., Dittmar, G., Kaeberlein, M., Kennedy, B.K. & Schmidt, M. 2011. Elevated Proteasome Capacity Extends Replicative Lifespan in *Saccharomyces cerevisia*. *PLoS Genetics*, 7(9), p.e1002253.
- Kumamoto, T., Ueyama, H., Tsumura, H., Toyoshima, I. & Tsuda, T. 2004. Expression of lysosome-related proteins and genes in the skeletal muscles of inclusion body myositis. *Acta Neuropathologica*, 107(1), pp.59–65.
- Lach-Trifilieff, E., Minetti, G.C., Sheppard, K., Ibebunjo, C., Feige, J.N., Hartmann, S., Brachat, S., Rivet, H., Koelbing, C., Morvan, F., Hatakeyama, S. & Glass, D.J. 2014. An antibody blocking activin type II receptors induces strong skeletal muscle hypertrophy and protects from atrophy. *Molecular and Cellular Biology*, 34(4), pp.606–618.
- Lampe, J.B., Gossrau, G., Kempe, A., Füssel, M., Schwurack, K., Schröder, R., Krause, S., Kohnen, R., Walter, M.C., Reichmann, H. & Lochmüller, H. 2003. Analysis of HLA class I and II alleles in sporadic inclusion-body myositis. *Journal of Neurology*, 250(11), pp.1313–1317.
- Lanka, V., Wieland, S., Barber, J. & Cudkowicz, M. 2009. Arimoclomol: a potential therapy under development for ALS. *Expert Opinion on Investigational Drugs*, 18(12), pp.1907–1918.
- Larman, H., Salajegheh, M., Nazareno, R., Lam, T., Sauld, J., Steen, H., Kong, S.W., Pinkus, J.L., Amato, A.A., Elledge, S.J. & Greenberg, S.A. 2013. Cytosolic 5'-nucleotidase 1A autoimmunity in sporadic inclusion body myositis. *Annals of Neurology*, 73(3), pp.408–418.
- Lavian, M., Goyal, N. & Mozaffar, T. 2016. Sporadic inclusion body myositis misdiagnosed as idiopathic granulomatous myositis. *Neuromuscular Disorders*, 26(11), pp.741–743.
- Lee, H.S., Daniels, B.H., Salas, E., Bollen, A.W., Debnath, J. & Margeta, M. 2012. Clinical Utility of LC3 and p62 Immunohistochemistry in Diagnosis of Drug-Induced Autophagic Vacuolar Myopathies: A Case-Control Study. *PLoS ONE*, 7(4), p.e36221.
- Leff, R.L., Miller, F.W., Hicks, J., Fraser, D.D. & Plotz, P.H. 1993. The treatment of inclusion body myositis: a retrospective review and a randomized, prospective trial of immunosuppressive therapy. *Medicine*, 72(4), pp.225–35.
- Lefter, S., Hardiman, O. & Ryan, A.M. 2017. A population-based epidemiologic study of adult neuromuscular disease in the Republic of Ireland. *Neurology*, 88(3), pp.304–313.

- Li, L., Zhao, D., Wei, H., Yao, L., Dang, Y., Amjad, A., Xu, J., Liu, J., Guo, L., Li, D., Li, Z., Zuo, D., Zhang, Y., Liu, J., Huang, S., Jia, C., Wang, L., Wang, Y., Xie, Y., Luo, J., Zhang, B., Luo, H., Donehower, L.A., Moses, R.E., Xiao, J., O'Malley, B.W. & Li, X. 2013. REGγ deficiency promotes premature aging via the casein kinase 1 pathway. *Proceedings of the National Academy of Sciences of the United States of America*, 110(27), pp.11005–11010.
- Li, W., Li, J. & Bao, J. 2012. Microautophagy: lesser-known self-eating. *Cellular and Molecular Life Sciences*, 69(7), pp.1125–1136.
- Lightfoot, A.P., McArdle A., Jackson, M.J. & Cooper, R.G. 2015. In the idiopathic inflammatory myopathies (IIM), do reactive oxygen species (ROS) contribute to muscle weakness? *Annals of the Rheumatic Diseases*, 74(7), pp.1340–1346.
- Lilleker, J., Rietveld, A., Badrising, U., Benveniste, O., Gheorghe, K., Hanna, M., Herbert, M., Hilton-Jones, D., Lamb, J., Lecky, B., Lundberg, I., Machado, P., Mariampillai, K., Miller, J., Parton, M., Peeters, M., Pye, S., Roberts, M., Sacconi, S., Saris, C., Cooper, R., Pruijn, G., Chinoy, H., & van Engelen, B. 2016. Anti-cN1A Autoantibody Seropositivity Is Associated with Increased Mortality Risk in Inclusion Body Myositis. *Neurology*, 86(16 Supplement), p.I4.001.
- Lindberg, C., & Oldfors, A. 2012. Prognosis and prognostic factors in sporadic inclusion body myositis. *Acta Neurologica Scandinavica*, 125(5), pp.353–358.
- Lindberg, C., Persson L.I., Björkander, J. & Oldfors, A. 1994. Inclusion body myositis: clinical, morphological, physiological and laboratory findings in 18 cases. *Acta Neurologica Scandinavica*, 89(2), pp.123–131.
- Lindgren, U., Roos, S., Hedberg Oldfors C., Moslemi, A.R., Lindberg, C. & Oldfors, A. 2015. Mitochondrial pathology in inclusion body myositis. *Neuromuscular Disorders*, 25(4), pp.281–288.
- Lipinski, M.M., Zheng, B., Lu, T., Yan, Z., Py, B.F., Ng, A., Xavier, R.J., Li, C., Yankner, B.A., Scherzer, C.R. & Yuan, J. 2010. Genome-wide analysis reveals mechanisms modulating autophagy in normal brain aging and in Alzheimer's disease. *Proceedings of the National Academy of Sciences*, 107(32), pp.14164–14169.
- Liu-Yesucevitz, L., Bilgutay, A., Zhang, Y.J., Vanderweyde, T., Citro, A., Mehta, T., Zaarur, N., McKee, A., Bowser, R., Sherman, M., Petrucelli, L. & Wolozin, B. 2010. Tar DNA Binding Protein-43 (TDP-43) Associates with Stress Granules: Analysis of Cultured Cells and Pathological Brain Tissue. *PLoS ONE*, 5(10), p.e13250.
- Liu, W.C., Liu, T., Liu, Z.H. & Deng, M. 2016. [Detection the mutated protein aggregation and mitochondrial function in fibroblasts from amyotrophic lateral sclerosis patients with SOD1 gene mutations]. *Zhonghua yi xue za zhi*, 96(25), pp.1982–1986.

- Liu, Y., Hei, Y., Shu, Q., Dong, J., Gao, Y., Fu, H., Zheng, X. & Yang, G. 2012. VCP/p97, down-regulated by microRNA-129-5p, could regulate the progression of hepatocellular carcinoma. *PLoS ONE*, 7(4), p.e35800.
- Llewellyn, K.J., Nalbandian, A., Weiss, L.N., Chang, I., Yu, H., Khatib, B., Tan, B., Scarfone, V. & Kimonis, V.E. 2017. Myogenic differentiation of VCP disease-induced pluripotent stem cells: A novel platform for drug discovery. *PLoS ONE*, 12(6), p.e0176919.
- Lloyd, T.E., Mammen, A.L., Amato, A.A., Weiss, M.D., Needham, M. & Greenberg, S.A. 2014. Evaluation and construction of diagnostic criteria for inclusion body myositis. *Neurology*, 83(5), pp.426–433.
- Locke, M. 2000. Heat shock transcription factor activation and hsp72 accumulation in aged skeletal muscle. *Cell Stress & Chaperones*, 5(1), pp.45–51.
- Locke, M. & Tanguay, R.M. 1996. Diminished heat shock response in the aged myocardium. *Cell Stress & Chaperones*, 1(4), pp.251–60.
- Lotz, B.P., Engel, A.G., Nishino, H., Stevens, J.C. & Litchy, W.J. 1989. Inclusion body myositis. Observations in 40 patients. *Brain*, pp.727–747.
- Ludtmann, M.H.R., Arber, C., Bartolome, F., de Vicente, M., Preza, E., Carro, E., Houlden, H., Gandhi, S., Wray, S. & Abramov, A.Y. 2017. Mutations in valosin-containing protein (VCP) decrease ADP/ATP translocation across the mitochondrial membrane and impair energy metabolism in human neurons. *The Journal of Biological Chemistry*, 292(21), pp.8907–8917.
- Machado, P.M., Ahmed, M., Brady, S., Gang, Q., Healy, E., Morrow, J.M., Wallace, A.C., Dewar, L., Ramdharry, G., Parton, M., Holton, J.L., Houlden, H., Greensmith, L. & Hanna, M.G. 2014. Ongoing developments in sporadic inclusion body myositis. *Current Rheumatology Reports*, 16(12), p.477.
- Machado, P.M., Brady, S. & Hanna, M.G. 2013. Update in inclusion body myositis. *Current Opinion in Rheumatology*, 25(6), pp.763–771.
- Magli, A. & Perlingeiro, R.R.C. 2017. Myogenic progenitor specification from pluripotent stem cells. *Seminars in Cell & Developmental Biology*, 72, pp.87–98.
- Majounie, E., Traynor, B.J., Chiò, A., Restagno, G., Mandrioli, J., Benatar, M., Taylor, J.P. & Singleton, A.B. 2012. Mutational analysis of the VCP gene in Parkinson's disease. *Neurobiology of Aging*, 33(1), p.209.e1-2.
- Malik, B., Nirmalanathan, N., Gray, A.L., La Spada, A.R., Hanna, M.G. & Greensmith, L. 2013. Co-induction of the heat shock response ameliorates disease progression in a mouse model of human spinal and bulbar muscular atrophy: implications for therapy. *Brain*, 136(Pt 3), pp.926–943.
- Mammen, A.L. 2017. Which nonautoimmune myopathies are most frequently misdiagnosed as myositis? *Current Opinion in Rheumatology*, 29(6), p.1.

- Manno, A., Noguchi, M., Fukushi, J., Motohashi, Y. & Kakizuka, A. 2010. Enhanced ATPase activities as a primary defect of mutant valosin-containing proteins that cause inclusion body myopathy associated with Paget disease of bone and frontotemporal dementia. *Genes to Cells*, 15(8), pp.911-922.
- Marchina, E., Misasi, S., Bozzato, A., Ferraboli, S., Agosti, C., Rozzini, L., Borsani, G., Barlati, S. & Padovani, A. 2014. Gene expression profile in fibroblasts of Huntington's disease patients and controls. *Journal of the Neurological Sciences*, 337(1-2), pp.42-46.
- Mastaglia, F.L. 2009. Sporadic inclusion body myositis: variability in prevalence and phenotype and influence of the MHC. *Acta Myologica*, 28(2), pp.66-71.
- Mastaglia, F.L., Rojana-udomsart, A., James, I., Needham, M., Day, T.J., Kiers, L., Corbett, J.A., Saunders, A.M., Lutz, M.W., Roses, AD; Alzheimer's Disease Neuroimaging Initiative. 2013. Polymorphism in the TOMM40 gene modifies the risk of developing sporadic inclusion body myositis and the age of onset of symptoms. *Neuromuscular Disorders*, 23(12), pp.969-974.
- Matsubara, S., Kondo, K., Miyamoto, K., Kawata, A., Komori, T. & Nakano, I. 2016. Early disintegration of myonuclear fibrous lamina in inclusion body myositis: Ultrastructural and immunohistochemical studies. *Clinical and Experimental Neuroimmunology*, 7(2), pp.185-196.
- Maziuk, B., Ballance, H.I. & Wolozin, B. 2017. Dysregulation of RNA Binding Protein Aggregation in Neurodegenerative Disorders. *Frontiers in Molecular Neuroscience*, 10, p.89.
- McDonald, K.K., Aulas, A., Destroismaisons, L., Pickles, S., Beleac, E., Camu, W., Rouleau, G.A. & Vande Velde, C. 2011. TAR DNA-binding protein 43 (TDP-43) regulates stress granule dynamics via differential regulation of G3BP and TIA-1. *Human Molecular Genetics*, 20(7), pp.1400-1410.
- McFerrin, J., Engel, W.K. & Askanas, V., 1999. Cultured inclusion-body myositis muscle fibers do not accumulate beta-amyloid precursor protein and can be innervated. *Neurology*, 53(9), pp.2184-2187.
- McInnes, J. 2013. Insights on altered mitochondrial function and dynamics in the pathogenesis of neurodegeneration. *Translational Neurodegeneration*, 2(1), p.12.
- Mehta, S.G., Khare, M., Ramani, R., Watts, G.D., Simon, M., Osann, K.E., Donkervoort, S., Dec, E., Nalbandian, A., Platt, J., Pasquali, M., Wang, A., Mozaffar, T., Smith, C.D. & Kimonis, VE. 2013. Genotype-phenotype studies of VCP-associated inclusion body myopathy with Paget disease of bone and/or frontotemporal dementia. *Clinical Genetics*, 83(5), pp.422-431.
- Meléndez, A., Tallóczy, Z., Seaman, M., Eskelinen, E.L., Hall, D.H. & Levine, B. 2003. Autophagy Genes Are Essential for Dauer Development and Life-Span Extension in *C. elegans*. *Science*, 301(5638), pp.1387-1391.

- Mendell, J.R., Sahenk, Z., Al-Zaidy, S., Rodino-Klapac, L.R., Lowes, L.P., Alfano, L.N., Berry, K., Miller, N., Yalvac, M., Dvorchik, I., Moore-Clingenpeel, M., Flanigan, K.M., Church, K., Shontz, K., Curry, C., Lewis, S., McColly, M., Hogan, M.J. & Kaspar, B.K. 2017. Follistatin Gene Therapy for Sporadic Inclusion Body Myositis Improves Functional Outcomes. *Molecular Therapy*, 25(4), pp.870–879.
- Mertens, J., Paquola, A.C.M., Ku, M., Hatch, E., Böhnke, L., Ladjevardi, S., McGrath, S., Campbell, B., Lee, H.1, Herdy, J.R., Gonçalves, J.T., Toda, T., Kim, Y., Winkler, J., Yao, J., Hetzer, M.W. & Gage, F.H.. 2015. Directly Reprogrammed Human Neurons Retain Aging-Associated Transcriptomic Signatures and Reveal Age-Related Nucleocytoplasmic Defects. *Cell Stem Cell*, 17(6), pp.705–718.
- van der Meulen, M.F., Hoogendijk, J.E., Jansen, G.H., Veldman, H. & Wokke, J.H. 1998. Absence of characteristic features in two patients with inclusion body myositis. *Journal of Neurology, Neurosurgery, and Psychiatry*, 64(3), pp.396–398.
- Meyer, A., Meyer, N., Schaeffer, M., Gottenberg, J.E., Geny, B. & Sibia, J. 2015. Incidence and prevalence of inflammatory myopathies: a systematic review. *Rheumatology*, 54(1), pp.50–63.
- Meyer, H., Bug, M. & Bremer, S. 2012. Emerging functions of the VCP/p97 AAA-ATPase in the ubiquitin system. *Nature Cell Biology*, 14(2), pp.117–123.
- Meyer, H. & Weihl, C.C. 2014. The VCP/p97 system at a glance: connecting cellular function to disease pathogenesis. *Journal of Cell Science*, 127, pp.3877–3883.
- Miller, T.D., Jackson, A.P., Barresi, R., Smart, C.M., Eugenicos, M., Summers, D., Clegg, S., Straub, V. & Stone, J. 2009. Inclusion body myopathy with Paget disease and frontotemporal dementia (IBMPFD): clinical features including sphincter disturbance in a large pedigree. *Journal of Neurology, Neurosurgery & Psychiatry*, 80(5), pp.583–584.
- Misterska-Skóra, M., Sebastian, A., Dzięgiel, P., Sebastian, M. & Wiland, P. 2013. Inclusion body myositis associated with Sjögren's syndrome. *Rheumatology International*, 33(12), pp.3083–3086.
- Miyagoe-Suzuki, Y. & Takeda, S. 2017. Skeletal muscle generated from induced pluripotent stem cells - induction and application. *World Journal of Stem Cells*, 9(6), pp.89–97.
- Mori, K. 2000. Tripartite management of unfolded proteins in the endoplasmic reticulum. *Cell*, 101(5), pp.451–454.
- Mori, F., Tanji, K., Zhang, H.X., Nishihira, Y., Tan, C.F., Takahashi, H. & Wakabayashi, K. 2008. Maturation process of TDP-43-positive neuronal cytoplasmic inclusions in amyotrophic lateral sclerosis with and without dementia. *Acta Neuropathologica*, 116(2), pp.193–203.

- Morosetti, R., Broccolini, A., Sancricca, C., Gliubizzi, C., Gidaro, T., Tonali, P.A., Ricci, E. & Mirabella, M. 2010. Increased aging in primary muscle cultures of sporadic inclusion-body myositis. *Neurobiology of Aging*, 31(7), pp.1205–1214.
- Morosetti, R., Mirabella, M., Gliubizzi, C., Broccolini, A., De Angelis, L., Tagliafico, E., Sampaolesi, M., Gidaro, T., Papacci, M., Roncaglia, E., Rutella, S., Ferrari, S., Tonali, P.A., Ricci, E. & Cossu, G. 2006. MyoD expression restores defective myogenic differentiation of human mesoangioblasts from inclusion-body myositis muscle. *Proceedings of the National Academy of Sciences of the United States of America*, 103(45), pp.16995–17000.
- Morrow, J.M., Sinclair, C.D., Fischmann, A., Machado, P.M., Reilly, M.M., Yousry, T.A., Thornton, J.S. & Hanna, M.G. 2016. MRI biomarker assessment of neuromuscular disease progression: a prospective observational cohort study. *The Lancet. Neurology*, 15(1), pp.65–77.
- Moussa, C.E., Fu, Q., Kumar, P., Shtifman, A., Lopez, J.R., Allen, P.D., LaFerla, F., Weinberg, D., Magrane, J., Aprahamian, T., Walsh, K., Rosen, K.M. & Querfurth, H.W. 2006. Transgenic expression of beta-APP in fast-twitch skeletal muscle leads to calcium dyshomeostasis and IBM-like pathology. *The FASEB Journal*, 20(12), pp.2165–2167.
- Mowzoon, N., Sussman, A. & Bradley, W.G. 2001. Mycophenolate (CellCept) treatment of myasthenia gravis, chronic inflammatory polyneuropathy and inclusion body myositis. *Journal of the Neurological Sciences*, 185(2), pp.119–122.
- Muchowski, P.J. & Wacker, J.L. 2005. Modulation of neurodegeneration by molecular chaperones. *Nature Reviews Neuroscience*, 6(1), pp.11–22.
- Mukherjee, R.N., Chen, P. & Levy, D.L. 2016. Recent advances in understanding nuclear size and shape. *Nucleus*, 7(2), pp.167–186.
- Mulcahy, K.P., Langdon, P.C. & Mastaglia, F. 2012. Dysphagia in Inflammatory Myopathy: Self-report, Incidence, and Prevalence. *Dysphagia*, 27(1), pp.64–69.
- Müller-Höcker, J. 1990. Cytochrome c oxidase deficient fibres in the limb muscle and diaphragm of man without muscular disease: An age-related alteration. *Journal of the Neurological Sciences*, 100(1–2), pp.14–21.
- Müller, J.M.M., Deinhardt, K., Rosewell, I., Warren, G. & Shima, D.T. 2007. Targeted deletion of p97 (VCP/CDC48) in mouse results in early embryonic lethality. *Biochemical and Biophysical Research Communications*, 354(2), pp.459–465.
- Münch, C. & Harper, J.W. 2016. Mitochondrial unfolded protein response controls matrix pre-RNA processing and translation. *Nature*, 534(7609), pp.710–713.
- Musanti, R., Parati, E., Lamperti, E. & Ghiselli, G. 1993. Decreased Cholesterol Biosynthesis in Fibroblasts from Patients with Parkinson Disease. *Biochemical Medicine and Metabolic Biology*, 49(2), pp.133–142.

- Mytilineou, C., Werner, P., Molinari, S., Di Rocco, A., Cohen, G. & Yahr, M.D. 1994. Impaired oxidative decarboxylation of pyruvate in fibroblasts from patients with Parkinson's disease. *Journal of Neural Transmission*, 8(3), pp.223–228.
- Nagaraju, K., Casciola-Rosen, L., Lundberg, I., Rawat, R., Cutting, S., Thapliyal, R., Chang, J., Dwivedi, S., Mitsak, M., Chen, Y.W., Plotz, P., Rosen, A., Hoffman, E. & Raben, N. 2005. Activation of the endoplasmic reticulum stress response in autoimmune myositis: Potential role in muscle fiber damage and dysfunction. *Arthritis & Rheumatism*, 52(6), pp.1824–1835.
- Nah, J., Yuan, J. & Jung, Y.K. 2015. Autophagy in neurodegenerative diseases: from mechanism to therapeutic approach. *Molecules and Cells*, 38(5), pp.381–389.
- Naidoo, N., Ferber, M., Master, M., Zhu, Y. & Pack, A.I. 2008. Aging impairs the unfolded protein response to sleep deprivation and leads to proapoptotic signaling. *Journal of Neuroscience* : 28(26), pp.6539–6548.
- Nakano, S., Shinde, A., Fujita, K., Ito, H. & Kusaka, H. 2008. Histone H1 is released from myonuclei and present in rimmed vacuoles with DNA in inclusion body myositis. *Neuromuscular Disorders*, 18(1), pp.27–33.
- Nakano, S., Shinde, A., Ito, H., Ito, H. & Kusaka, H. 2005. Messenger RNA degradation may be inhibited in sporadic inclusion body myositis. *Neurology*, 65(3), pp.420–425.
- Nakatani, M., Takehara, Y., Sugino, H., Matsumoto, M., Hashimoto, O., Hasegawa, Y., Murakami, T., Uezumi, A., Takeda, S., Noji, S., Sunada, Y. & Tsuchida, K. 2007. Transgenic expression of a myostatin inhibitor derived from follistatin increases skeletal muscle mass and ameliorates dystrophic pathology in mdx mice. *The FASEB Journal*, 22(2), pp.477–487.
- Nalbandian, A., Donkervoort, S., Dec, E., Badadani, M., Katheria, V., Rana, P., Nguyen, C., Mukherjee, J., Caiozzo, V., Martin, B., Watts, G.D., Vesa, J., Smith, C. & Kimonis, V.E. 2011. The multiple faces of valosin-containing protein-associated diseases: inclusion body myopathy with Paget's disease of bone, frontotemporal dementia, and amyotrophic lateral sclerosis. *Journal of Molecular Neuroscience*, 45(3), pp.522–531.
- Nalbandian, A., Llewellyn, K.J., Gomez, A., Walker, N., Su, H., Dunnigan, A., Chwa, M., Vesa, J., Kenney, M.C. & Kimonis, V.E. 2015. In vitro studies in VCP-associated multisystem proteinopathy suggest altered mitochondrial bioenergetics. *Mitochondrion*, 22, pp.1–8.
- Nalbandian, A., Llewellyn, K.J., Kitazawa, M., Yin, H.Z., Badadani, M., Khanlou, N., Edwards, R., Nguyen, C., Mukherjee, J., Mozaffar, T., Watts, G., Weiss, J. & Kimonis, V.E. 2012. The homozygote VCP(R¹⁵⁵H/R¹⁵⁵H) mouse model exhibits accelerated human VCP-associated disease pathology. *PLoS ONE*, 7(9), p.e46308.

- Nalbandian, A., Llewellyn, K.J., Nguyen, C., Yazdi, P.G. & Kimonis, V.E. 2015. Rapamycin and chloroquine: the in vitro and in vivo effects of autophagy-modifying drugs show promising results in valosin containing protein multisystem proteinopathy. *PLoS ONE*, 10(4), p.e0122888.
- Nalbantoglu, J., Karpati, G. & Carpenter, S. 1994. Conspicuous accumulation of a single-stranded DNA binding protein in skeletal muscle fibers in inclusion body myositis. *The American Journal of Pathology*, 144(5), pp.874–882.
- Narendra, D., Kane, L.A., Hauser, D.N., Fearnley, I.M. & Youle, R.J. 2010. p62/SQSTM1 is required for Parkin-induced mitochondrial clustering but not mitophagy; VDAC1 is dispensable for both. *Autophagy*, 6(8), pp.1090–1106.
- Needham, M., Corbett, A., Day, T., Christiansen, F., Fabian, V. & Mastaglia, F.L. 2008. Prevalence of sporadic inclusion body myositis and factors contributing to delayed diagnosis. *Journal of Clinical Neuroscience*, 15(12), pp.1350–1353.
- Needham, M., James, I., Corbett, A., Day, T., Christiansen, F., Phillips, B., Mastaglia, F.L. 2008. Sporadic inclusion body myositis: Phenotypic variability and influence of HLA-DR3 in a cohort of 57 Australian cases. *Journal of Neurology, Neurosurgery & Psychiatry*, 79(9), pp.1056–1060.
- Needham, M., Mastaglia, F.L. & Garlepp, M.J. 2007. Genetics of inclusion-body myositis. *Muscle & Nerve*, 35(5), pp.549–561.
- Negoescu, A., Guillermet, C., Lorimier, P., Brambilla, E. & Labat-Moleur, F. 1998. Importance of DNA fragmentation in apoptosis with regard to TUNEL specificity. *Biomedicine & Pharmacotherapy*, 52(6), pp.252–258.
- Neueder, A., Gipson, T.A., Batterton, S., Lazell H.J., Farshim, P.P., Paganetti, P., Housman, D.E. & Bates, G.P. 2017. HSF1-dependent and -independent regulation of the mammalian in vivo heat shock response and its impairment in Huntington's disease mouse models. *Scientific Reports*, 7(1), p.12556.
- Neumann, M., Mackenzie, I.R., Cairns, N.J., Boyer, P.J., Markesbery, W.R., Smith, C.D., Taylor, J.P., Kretschmar, H.A., Kimonis, V.E. & Forman, M.S. 2007. TDP-43 in the ubiquitin pathology of frontotemporal dementia with VCP gene mutations. *Journal of Neuropathology and Experimental Neurology*, 66(2), pp.152–157.
- Neumann, M., Sampathu, D.M., Kwong, L.K., Truax, A.C., Micsenyi, M.C., Chou, T.T., Bruce, J., Schuck, T., Grossman, M., Clark, C.M., McCluskey, L.F., Miller, B.L., Masliah, E., Mackenzie, I.R., Feldman, H., Feiden, W., Kretschmar, H.A., Trojanowski, J.Q., Lee, VM. 2006. Ubiquitinated TDP-43 in Frontotemporal Lobar Degeneration and Amyotrophic Lateral Sclerosis. *Science*, 314(5796), pp.130–133.
- Nikoletopoulou, V., Papandreou, M.E. & Tavernarakis, N., 2015. Autophagy in the physiology and pathology of the central nervous system. *Cell Death and Differentiation*, 22(3), pp.398–407.

- Nishii, M., Nakano, S., Nakamura, S., Wate, R., Shinde, A., Kaneko, S. & Kusaka, H. 2011. Myonuclear breakdown in sporadic inclusion body myositis is accompanied by DNA double strand breaks. *Neuromuscular Disorders*, 21(5), pp.345–352.
- Nishimura, R.N., Dwyer, B.E., Clegg, K., Cole, R. & de Vellis, J. 1991. Comparison of the heat shock response in cultured cortical neurons and astrocytes. *Molecular Brain Research*, 9(1–2), pp.39–45.
- Niwa, H., Ewens, C.A., Tsang, C., Yeung, H.O., Zhang, X. & Freemont, P.S. 2012. The role of the N-domain in the ATPase activity of the mammalian AAA ATPase p97/VCP. *The Journal of Biological Chemistry*, 287(11), pp.8561–8570.
- Nixon, R.A. 2013. The role of autophagy in neurodegenerative disease. *Nature Medicine*, 19(8), pp.983–997.
- Nogalska, A., D'Agostino, C., Engel, W.K., Cacciottolo, M., Asada, S., Mori, K. & Askanas, V. 2015. Activation of the Unfolded Protein Response in Sporadic Inclusion-Body Myositis but Not in Hereditary *GNE* Inclusion-Body Myopathy. *Journal of Neuropathology & Experimental Neurology*, 74(6), pp.538–546.
- Nogalska, A., D'Agostino, C., Engel, W.K., Klein, W.L & Askanas, V. 2010. Novel demonstration of amyloid- β oligomers in sporadic inclusion-body myositis muscle fibers. *Acta Neuropathologica*, 120(5), pp.661–666.
- Nogalska, A., D'Agostino, C., Terracciano, C. & Engel, W.K. 2010. Impaired autophagy in sporadic inclusion-body myositis and in endoplasmic reticulum stress-provoked cultured human muscle fibers. *The American Journal of Pathology*, 177(3), pp.1377–1387.
- Nogalska, A., Engel, W.K., McFerrin, J., Kokame, K., Komano, H. & Askanas, V. 2006. Homocysteine-induced endoplasmic reticulum protein (Herp) is up-regulated in sporadic inclusion-body myositis and in endoplasmic reticulum stress-induced cultured human muscle fibers. *Journal of Neurochemistry*, 96(5), pp.1491–1499.
- Nogalska, A., Terracciano, C., D'Agostino, C., Engel, W.K & Askanas, V. 2009. p62/SQSTM1 is overexpressed and prominently accumulated in inclusions of sporadic inclusion-body myositis muscle fibers, and can help differentiating it from polymyositis and dermatomyositis. *Acta Neuropathologica*, 118(3), pp.407–413.
- Nutt, L.K., Pataer, A., Pahler, J., Fang, B., Roth, J., McConkey, D.J. & Swisher, S.G. 2002. Bax and Bak promote apoptosis by modulating endoplasmic reticular and mitochondrial Ca^{2+} stores. *The Journal of Biological Chemistry*, 277(11), pp.9219–9225.
- Oddo, S. 2008. The ubiquitin-proteasome system in Alzheimer's disease. *Journal of Cellular and Molecular Medicine*, 12(2), pp.363–373.
- Oflazer, P.S., Deymeer, F. & Parman, Y. 2011. Sporadic-inclusion body myositis (s-IBM) is not so prevalent in Istanbul/Turkey: a muscle biopsy based survey. *Acta Myologica*, 30(1), pp.34–36.

- Ogen-Shtern, N., Ben David, T. & Lederkremer, G.Z. 2016. Protein aggregation and ER stress. *Brain Research*, 1648, pp.658–666.
- Oh, T.H., Brumfield, K.A., Hoskin T.L., Kasperbauer, J.L. & Basford, J.R. 2008. Dysphagia in Inclusion Body Myositis. *American Journal of Physical Medicine & Rehabilitation*, 87(11), pp.883–889.
- Okatsu, K., Saisho, K., Shimanuki, M., Nakada, K., Shitara, H, Sou, Y.S., Kimura, M., Sato, S., Hattori, N., Komatsu, M., Tanaka, K. & Matsuda, N. 2010. p62/SQSTM1 cooperates with Parkin for perinuclear clustering of depolarized mitochondria. *Genes to Cells*, 15(8), p.887-900.
- Oldfors, A., Larsson, N.G., Lindberg, C. & Holme, E. 1993. Mitochondrial DNA deletions in inclusion body myositis. *Brain*, 116 (Pt 2), pp.325–336.
- Oldfors, A., Moslemi, A.R., Fyhr, I.M., Holme, E., Larsson, N.G. & Lindberg C. 1995. Mitochondrial DNA deletions in muscle fibers in inclusion body myositis. *Journal of Neuropathology and Experimental Neurology*, 54(4), pp.581–587.
- Oldfors, A., Moslemi, A.R., Jonasson, L., Ohlsson, M., Kollberg, G. & Lindberg, C. 2006. Mitochondrial abnormalities in inclusion-body myositis. *Neurology*, 66(2 Suppl 1), pp.S49-55.
- Olivé, M., Janué, A., Moreno, D., Gámez, J., Torrejón-Escribano, B. & Ferrer, I. 2009. TAR DNA-Binding Protein 43 Accumulation in Protein Aggregate Myopathies. *Journal of Neuropathology & Experimental Neurology*, 68(3), pp.262–273.
- Olzscha, H., Schermann, S.M., Woerner, A.C., Pinkert, S., Hecht, M.H., Tartaglia, G.G., Vendruscolo, M., Hayer-Hartl, M., Hartl, F.U., Vabulas, R.M. 2011. Amyloid-like aggregates sequester numerous metastable proteins with essential cellular functions. *Cell*, 144(1), pp.67–78.
- Onodera, O., Sugai, A., Konno, T., Tada, M., Koyama, A. & Nishizawa, M; 2013. What is the key player in TDP-43 pathology in ALS: Disappearance from the nucleus or inclusion formation in the cytoplasm? *Neurology and Clinical Neuroscience*, 1(1), pp.11–17.
- Onofre, I., Mendonça N., Lopes, S., Nobre, R., de Melo, J. B., Carreira, I.M., Januário, C., Gonçalves, A.F. & de Almeida, L.P. 2016. Fibroblasts of Machado Joseph Disease patients reveal autophagy impairment. *Scientific Reports*, 6(1), p.28220.
- Osafune, K., Caron, L., Borowiak, M., Martinez, R.J., Fitz-Gerald, C.S., Sato, Y., Cowan, C.A., Chien, K.R. & Melton, D.A. 2008. Marked differences in differentiation propensity among human embryonic stem cell lines. *Nature Biotechnology*, 26(3), pp.313–315.
- Ott, C. König, J., Höhn, A., Jung, T. & Grune, T. 2016. Macroautophagy is impaired in old murine brain tissue as well as in senescent human fibroblasts. *Redox Biology*, 10, pp.266–273.

- De Paepe, B., Creus, K.K., Martin, J.J., Weis, J. & De Bleecker, J.L. 2009. A dual role for HSP90 and HSP70 in the inflammatory myopathies: from muscle fiber protection to active invasion by macrophages. *Annals of the New York Academy of Sciences*, 1173(1), pp.463–469.
- Page, T.J., Sikder, D., Yang, L., Pluta, L., Wolfinger, R.D., Kodadek, T. & Thomas, R.S. 2006. Genome-wide analysis of human HSF1 signaling reveals a transcriptional program linked to cellular adaptation and survival. *Molecular BioSystems*, 2(12), pp.627–639.
- Paillusson, S., Stoica, R., Gomez-Suaga, P., Lau, D.H.W., Mueller, S., Miller, T. & Miller, C.C.J. 2016. There's Something Wrong with my MAM; the ER–Mitochondria Axis and Neurodegenerative Diseases. *Trends in Neurosciences*, 39(3), pp.146–157.
- Palikaras, K. & Tavernarakis, N. 2012. Mitophagy in neurodegeneration and aging. *Frontiers in Genetics*, 3, p.297.
- Paltiel, A.D., Ingvarsson, E., Lee, D.K., Leff, R.L., Nowak, R.J., Petschke, K.D., Richards-Shubik, S., Zhou, A., Shubik, M., O'Connor, K.C. 2015. Demographic and clinical features of inclusion body myositis in north America. *Muscle & Nerve*, 52(4), pp.527–533.
- Pankiv, S., Clausen, T.H., Lamark, T., Brech, A., Bruun, J.A., Outzen, H., Øvervatn, A., Bjørkøy, G. & Johansen, T. 2007. p62/SQSTM1 Binds Directly to Atg8/LC3 to Facilitate Degradation of Ubiquitinated Protein Aggregates by Autophagy. *Journal of Biological Chemistry*, 282(33), pp.24131–24145.
- Papadopoulos, C., Kirchner, P., Bug, M., Grum, D., Koerver, L., Schulze, N., Poehler, R., Dressler, A., Fengler, S., Arhzaouy, K., Lux, V., Ehrmann, M., Wehl, C.C. & Meyer, H. 2017. VCP/p97 cooperates with YOD1, UBXD1 and PLAA to drive clearance of ruptured lysosomes by autophagy. *The EMBO Journal*, 36(2), pp.135–150.
- Paradisi, M., McClintock, D., Boguslavsky, R.L., Pedicelli, C., Worman, H.J. & Djabali, K. 2005. Dermal fibroblasts in Hutchinson-Gilford progeria syndrome with the lamin A G608G mutation have dysmorphic nuclei and are hypersensitive to heat stress. *BMC Cell Biology*, 6(1), p.27.
- Parfitt, D.A., Aguila, M., McCulley, C.H., Bevilacqua, D., Mendes, H.F., Athanasiou, D., Novoselov, S.S., Kanuga, N., Munro, P.M., Coffey, P.J., Kalmar, B., Greensmith, L. & Cheetham, M.E. 2014. The heat-shock response co-inducer arimoclomol protects against retinal degeneration in rhodopsin retinitis pigmentosa. *Cell Death & Disease*, 5(5), p.e1236.
- Pars, K., Garde, N., Skripuletz, T., Pul, R., Dengler, R. & Stangel, M. 2013. Subcutaneous immunoglobulin treatment of inclusion-body myositis stabilizes dysphagia. *Muscle & Nerve*, 48(5), pp.838–839.

- Patwa, H.S., Chaudhry, V., Katzberg, H., Rae-Grant, A.D. & So, Y.T. 2012. Evidence-based guideline: intravenous immunoglobulin in the treatment of neuromuscular disorders: report of the Therapeutics and Technology Assessment Subcommittee of the American Academy of Neurology. *Neurology*, 78(13), pp.1009–1015.
- Paz Gavilán, M., Vela, J., Castaño, A., Ramos, B., del Río, J.C., Vitorica, J. & Ruano, D. 2006. Cellular environment facilitates protein accumulation in aged rat hippocampus. *Neurobiology of Aging*, 27(7), pp.973–982.
- Pellegrino, M.W. & Haynes, C.M. 2015. Mitophagy and the mitochondrial unfolded protein response in neurodegeneration and bacterial infection. *BMC Biology*, 13, p.22.
- Peng, A., Koffman, B.M., Malley, J.D. & Dalakas, M.C. 2000. Disease progression in sporadic inclusion body myositis: Observations in 78 patients. *Neurology*, 55(2), pp.296–298.
- Pérez, M.J., Ponce, D.P., Osorio-Fuentealba, C., Behrens, M.I. & Quintanilla, R.A. 2017. Mitochondrial Bioenergetics Is Altered in Fibroblasts from Patients with Sporadic Alzheimer's Disease. *Frontiers in Neuroscience*, 11, p.553.
- Peverelli, L., Testolin, S., Villa, L., D'Amico, A., Petrini, S., Favero, C., Magri, F., Morandi, L., Mora, M., Mongini, T., Bertini, E., Sciacco, M., Comi, G.P. & Moggio, M. 2015. Histologic muscular history in steroid-treated and untreated patients with Duchenne dystrophy. *Neurology*, 85(21), pp.1886-1893.
- Peyer, A.K., Kinter, J., Hench, J., Frank, S., Fuhr, P., Thomann, S., Fischmann, A., Kneifel, S., Camaño, P., López de Munain, A., Sinnreich, M. & Renaud, S. 2013. Novel valosin containing protein mutation in a Swiss family with hereditary inclusion body myopathy and dementia. *Neuromuscular Disorders*. 23(2), pp.149-154.
- Phillips, B.A., Cala, L.A., Thickbroom, G.W., Melsom, A., Zilko, P.J. & Mastaglia, F.L. 2001. Patterns of muscle involvement in inclusion body myositis: clinical and magnetic resonance imaging study. *Muscle & Nerve*, 24(11), pp.1526–1534.
- Phillips, B.A., Zilko, P.J. & Mastaglia, F.L. 2000. Prevalence of sporadic inclusion body myositis in Western Australia. *Muscle & Nerve*, 23(6), pp.970–972.
- Pickering, A.M., Lehr, M. & Miller, R.A. 2015. Lifespan of mice and primates correlates with immunoproteasome expression. *Journal of Clinical Investigation*, 125(5), pp.2059–2068.
- Pieraggi, M.T., Bouissou, H., Angelier, C., Uhart, D., Magnol, J.P. & Kokolo, J. 1985. [The fibroblast]. *Annales de Pathologie*, 5(2), pp.65–76.
- Pinkus, J.L., Amato, A.A., Taylor, J.P. & Greenberg, S.A. 2014. Abnormal distribution of heterogeneous nuclear ribonucleoproteins in sporadic inclusion body myositis. *Neuromuscular Disorders*, 24(7), pp.611–616.

- Pluk, H., van Hoeve, B.J., van Dooren, S.H., Stammen-Vogelzangs, J., van der Heijden, A., Schelhaas, H.J., Verbeek, M.M., Badrising, U.A., Arnardottir, S., Gheorghe, K., Lundberg, I.E., Boelens, W.C., van Engelen, B.G. & Pruijn, G.J. 2013. Autoantibodies to cytosolic 5'-nucleotidase 1A in inclusion body myositis. *Annals of Neurology*, 73(3), pp.397–407.
- Prause, J., Goswami, A., Katona, I., Roos, A., Schnizler, M., Bushuven, E., Dreier, A., Buchkremer, S., Johann, S., Beyer, C., Deschauer, M., Troost, D. & Weis, J. 2013. Altered localization, abnormal modification and loss of function of Sigma receptor-1 in amyotrophic lateral sclerosis. *Human Molecular Genetics*, 22(8), pp.1581–1600.
- Price, M.A., Barghout, V., Benveniste, O., Christopher-Stine, L., Corbett, A., de Visser, M., Hilton-Jones, D., Kissel, J.T., Lloyd, T.E., Lundberg, I.E., Mastaglia, F., Mozaffar, T., Needham, M., Schmidt, J., Sivakumar, K., DeMuro, C. & Tseng, B.S. 2016. Mortality and Causes of Death in Patients with Sporadic Inclusion Body Myositis: Survey Study Based on the Clinical Experience of Specialists in Australia, Europe and the USA. *Journal of Neuromuscular Diseases*, 3(1), pp.67–75.
- Price, P., Santoso, L., Mastaglia, F., Garlepp, M., Kok, C.C., Allcock, R. & Laing, N. 2004. Two major histocompatibility complex haplotypes influence susceptibility to sporadic inclusion body myositis: critical evaluation of an association with HLA-DR3. *Tissue Antigens*, 64(5), pp.575–580.
- Pyo, J.O., Yoo, S.M., Ahn, H.H., Nah, J., Hong, S.H., Kam, T.I., Jung, S. & Jung, Y.K. 2013. Overexpression of Atg5 in mice activates autophagy and extends lifespan. *Nature Communications*, 4, p.2300.
- Querfurth, H.W., Suhara, T., Rosen, K.M., McPhie, D.L., Fujio, Y., Tejada, G., Neve, R.L., Adelman, L.S. & Walsh, K. 2001. β -Amyloid Peptide Expression Is Sufficient for Myotube Death: Implications for Human Inclusion Body Myopathy. *Molecular and Cellular Neuroscience*, 17(5), pp.793–810.
- Rabek, J.P., Boylston, W.H. & Papaconstantinou, J. 2003. Carbonylation of ER chaperone proteins in aged mouse liver. *Biochemical and Biophysical Research Communications*, 305(3), pp.566–572.
- Radák, Z., Takahashi, R., Kumiyama, A., Nakamoto, H., Ohno, H., Ookawara, T. & Goto, S. 2002. Effect of aging and late onset dietary restriction on antioxidant enzymes and proteasome activities, and protein carbonylation of rat skeletal muscle and tendon. *Experimental Gerontology*, 37(12), pp.1423–1430.
- Raju, R., Vasconcelos, O., Granger, R., Dalakas, M.C. 2003. Expression of IFN-gamma-inducible chemokines in inclusion body myositis. *Journal of Neuroimmunology*, 141(1–2), pp.125–131.

- Raman, R., Allen, S.P., Goodall, E.F., Kramer, S., Ponger, L.L., Heath, P.R., Milo, M., Hollinger, H.C., Walsh, T., Highley, J.R., Olpin, S., McDermott, C.J., Shaw, P.J. & Kirby, J. 2015. Gene expression signatures in motor neurone disease fibroblasts reveal dysregulation of metabolism, hypoxia-response and RNA processing functions. *Neuropathology and Applied Neurobiology*, 41(2), pp.201–226.
- Ranque-Francois, B., Maisonobe, T., Dion, E., Piette, J.C., Chauveheid, M.P., Amoura, Z. & Papo, T. 2005. Familial inflammatory inclusion body myositis. *Annals of the Rheumatic Diseases*, 64(4), pp.634–637.
- Rao, D.V., Watson, K. & Jones, G.L. 1999. Age-related attenuation in the expression of the major heat shock proteins in human peripheral lymphocytes. *Mechanisms of Ageing and Development*, 107(1), pp.105–118.
- Rea, I.M., McNerlan, S. & Pockley, A.G. 2001. Serum heat shock protein and anti-heat shock protein antibody levels in aging. *Experimental gerontology*, 36(2), pp.341–352.
- Recher, M., Sahrbacher, U., Bremer, J., Arndt, B., Steiner, U. & Fontana, A. 2012. Treatment of inclusion body myositis: is low-dose intravenous immunoglobulin the solution? *Rheumatology International*, 32(2), pp.469–472.
- Regensburger, M., Türk, M., Pagenstecher, A., Schröder, R. & Winkler, J. 2017. VCP-related multisystem proteinopathy presenting as early-onset Parkinson disease. *Neurology*, 89(7), pp.746-748.
- Reisz, J.A., Barrett, A.S., Nemkov, T., Hansen, K.C. & D'Alessandro, A. 2018. When nature's robots go rogue: exploring protein homeostasis dysfunction and the implications for understanding human aging disease pathologies. *Expert Review of Proteomics*, 15(4), pp.293–309.
- Reits, E., Griekspoor, A., Neijssen, J., Groothuis, T., Jalink, K., van Veelen, P., Janssen, H., Calafat, J., Drijfhout, J.W. & Neefjes, J. 2003. Peptide diffusion, protection, and degradation in nuclear and cytoplasmic compartments before antigen presentation by MHC class I. *Immunity*, 18(1), pp.97–108.
- Richter, K., Haslbeck, M. & Buchner, J. 2010. The heat shock response: life on the verge of death. *Molecular Cell*, 40(2), pp.253–266.
- Rietveld, A., van den Hoogen, L.L., Bizzaro, N., Blokland, S.L.M., Dährnich, C., Gottenberg, J-E., Houen, G., Johannsen, N., Mandl, T., Meyer, A., Nielsen, C.T., Olsson, P., van Roon, J., Schlumberger, W., van Engelen, B.G.M., Saris, C.G.J. & Pruijn, G.J.M. 2018. Autoantibodies to Cytosolic 5'-Nucleotidase 1A in Primary Sjögren's Syndrome and Systemic Lupus Erythematosus. *Frontiers in Immunology*, 9, pp.1200.
- Rifai, Z., Welle, S., Kamp, C. & Thornton, C.A. 1995. Ragged Red Fibers in Normal Aging and Inflammatory Myopathy. *Annals of Neurology*, 37(1), pp.24–29.

- Ritz, D., Vuk, M., Kirchner, P., Bug, M., Schütz, S., Hayer, A., Bremer, S., Lusk, C., Baloh, R.H., Lee, H., Glatter, T., Gstaiger, M., Aebersold, R., Wehl, C.C. & Meyer, H. 2011. Endolysosomal sorting of ubiquitylated caveolin-1 is regulated by VCP and UBXD1 and impaired by VCP disease mutations. *Nature Cell Biology*, 13(9), pp.1116–1123.
- Robinson, M.B., Tidwell, J.L., Gould, T., Taylor, A.R., Newbern, J.M., Graves, J., Tytell, M. & Milligan, C.E. 2005. Extracellular Heat Shock Protein 70: A Critical Component for Motoneuron Survival. *Journal of Neuroscience*, 25(42), pp.9735–9745.
- Roca, I., Requena, J., Edel, M.J. & Alvarez-Palomo, A.B. 2015. Myogenic Precursors from iPS Cells for Skeletal Muscle Cell Replacement Therapy. *Journal of Clinical Medicine*, 4(2), pp.243–259.
- Rodriguez-Ortiz, C.J., Flores, J.C., Valenzuela, J.A., Rodriguez, G.J., Zumkehr, J., Tran, D.N., Kimonis, V.E. & Kitazawa, M. 2016. The Myoblast C2C12 Transfected with Mutant Valosin-Containing Protein Exhibits Delayed Stress Granule Resolution on Oxidative Stress. *The American Journal of Pathology*, 186(6), pp.1623–1634.
- Rohde, M.C., Corydon, T.J., Hansen, J., Pedersen, C.B., Schmidt, S.P., Gregersen, N. & Banner, J. 2013. Heat stress and sudden infant death syndrome—Stress gene expression after exposure to moderate heat stress. *Forensic Science International*, 232(1–3), pp.16–24.
- Rojana-udomsart, A., James, I., Castley, A., Needham, M., Scott, A., Day, T., Kiers, L., Corbett, A., Sue, C., Witt, C., Martinez, P., Christiansen, F. & Mastaglia, F. 2012. High-resolution HLA-DRB1 genotyping in an Australian inclusion body myositis (s-IBM) cohort: An analysis of disease-associated alleles and diplotypes. *Journal of Neuroimmunology*, 250(1–2), pp.77–82.
- Rojana-udomsart, A., Mitropant, C., James, I., Witt, C., Needham, M., Day, T., Kiers, L., Corbett, A., Martinez, P., Wilton, S.D. & Mastaglia, F.L. 2013. Analysis of HLA-DRB3 alleles and supertypal genotypes in the MHC Class II region in sporadic inclusion body myositis. *Journal of Neuroimmunology*, 254(1–2), pp.174–177.
- Rojana-udomsart, A., Needham, M., Luo, Y.B., Fabian, V., Walters, S., Zilko, P.J. & Mastaglia, F.L. 2011. The association of sporadic inclusion body myositis and Sjögren's syndrome in carriers of HLA-DR3 and the 8.1 MHC ancestral haplotype. *Clinical Neurology and Neurosurgery*, 113(7), pp.559–563.
- Roman, W. & Gomes, E.R. 2017. Nuclear positioning in skeletal muscle. *Seminars in Cell & Developmental Biology*. pii. S1084-9521(17)30428-7.
- Rose, F.F., Mattis V.B., Rindt, H. & Lorson, C.L. 2009. Delivery of recombinant follistatin lessens disease severity in a mouse model of spinal muscular atrophy. *Human Molecular Genetics*, 18(6), pp.997–1005.

- Rose, M.R. & ENMC IBM Working Group, 2013. 188th ENMC International Workshop: Inclusion Body Myositis, 2–4 December 2011, Naarden, The Netherlands. *Neuromuscular Disorders*, 23(12), pp.1044–1055.
- Rose M.R., Jones, K., Leong, K., Walter, C., Miller, J., Dalakas, M.C., Brassington, R. & Griggs, R. 2015. Treatment for inclusion body myositis (Review). *Cochrane Database of Systematic Reviews*, (6).
- Ross, J.M., Olson, L. & Coppotelli, G. 2015. Mitochondrial and Ubiquitin Proteasome System Dysfunction in Ageing and Disease: Two Sides of the Same Coin? *International Journal of Molecular Sciences*, 16(8), pp.19458–19476.
- Rothwell, S., Cooper, R.G., Lundberg, I.E., Gregersen, P.K., Hanna, M.G., Machado, P.M., Herbert, M.K., Pruijn, G.J.M., Lilleker, J.B., Roberts, M., Bowes, J., Seldin, M.F., Vencovsky, J., Danko, K., Limaye, V., Selva-O'Callaghan, A., Platt, H., Molberg, Ø., Benveniste, O., Radstake, T.R.D.J., Doria, A., De Bleecker, J., De Paepe, B., Gieger, C., Meitinger, T., Winkelmann, J., Amos, C.I., Ollier, W.E., Padyukov, L., Lee, A.T., Lamb, J.A., Chinoy, H.; Myositis Genetics Consortium. 2017. Immune-Array Analysis in Sporadic Inclusion Body Myositis Reveals HLA-DRB1 Amino Acid Heterogeneity Across the Myositis Spectrum. *Arthritis & Rheumatology*, 69(5), pp.1090–1099.
- Rothwell, S., Lilleker, J.B. & Lamb, J.A. 2017. Genetics in inclusion body myositis. *Current Opinion in Rheumatology*, 29(6), p.1.
- Ruan, L., Zhou, C., Jin, E., Kucharavy, A., Zhang, Y., Wen, Z., Florens, L. & Li, R. 2017. Cytosolic proteostasis through importing of misfolded proteins into mitochondria. *Nature*, 543(7645), pp.443–446.
- Rubinsztein, D.C., Mariño, G. & Kroemer, G. 2011. Autophagy and Aging. *Cell*, 146(5), pp.682–695.
- Ruggiano, A., Foresti, O. & Carvalho, P. 2014. ER-associated degradation: Protein quality control and beyond. *The Journal of Cell Biology*, 204(6).
- Russ, D.W., Krause, J., Wills, A. & Arreguin, R. 2012. “SR stress” in mixed hindlimb muscles of aging male rats. *Biogerontology*, 13(5), pp.547–555.
- Russ, D.W., Wills, A.M., Boyd, I.M. & Krause, J., 2014. Weakness, SR function and stress in gastrocnemius muscles of aged male rats. *Experimental Gerontology*, 50, pp.40–44.
- Rutherford, N.J., Zhang, Y.J., Baker, M., Gass, J.M., Finch, N.A., Xu, Y.F., Stewart, H., Kelley, B.J., Kuntz, K., Crook, R.J., Sreedharan, J., Vance, C., Sorenson, E., Lippa, C., Bigio, E.H., Geschwind, D.H., Knopman, D.S., Mitsumoto, H., Petersen, R.C., Cashman, N.R., Hutton, M., Shaw, C.E., Boylan, K.B., Boeve, B., Graff-Radford, N.R., Wszolek, Z.K., Caselli, R.J., Dickson, D.W., Mackenzie, I.R., Petrucelli, L. & Rademakers, R.. 2008. Novel mutations in TARDBP (TDP-43) in patients with familial amyotrophic lateral sclerosis. *PLoS Genetics*, 4(9), p.e1000193.

- Rygiel, K.A., Miller, J., Grady, J.P., Rocha, M.C., Taylor, R.W. & Turnbull, D.M., 2015. Mitochondrial and inflammatory changes in sporadic inclusion body myositis. *Neuropathology and Applied Neurobiology*, 41(3), pp.288–303.
- Rygiel, K.A., Tuppen, H.A., Grady, J.P., Vincent, A., Blakely, E.L., Reeve, A.K., Taylor, R.W., Picard, M., Miller, J. & Turnbull, D.M. 2016. Complex mitochondrial DNA rearrangements in individual cells from patients with sporadic inclusion body myositis. *Nucleic Acids Research*, 44(11), pp.5313–5329.
- Sabatelli, M., Zollino, M., Conte, A., Del Grande, A., Marangi, G., Lucchini, M., Mirabella, M., Romano, A., Piacentini, R., Bisogni, G., Lattante, S., Luigetti, M., Rossini, P.M. & Moncada, A. 2015. Primary fibroblasts cultures reveal TDP-43 abnormalities in amyotrophic lateral sclerosis patients with and without SOD1 mutations. *Neurobiology of Aging*, 36(5), p.2005.e5-2005.e13.
- Sakuma, K., Akiho, M., Nakashima, H., Akima, H. & Yasuhara, M. 2008. Age-related reductions in expression of serum response factor and myocardin-related transcription factor A in mouse skeletal muscles. *Biochimica et Biophysica Acta (BBA) - Molecular Basis of Disease*. 1782(7-8), pp.453-461.
- Sala, A.J., Bott, L.C. & Morimoto, R.I. 2017. Shaping proteostasis at the cellular, tissue, and organismal level. *The Journal of Cell Biology*, 216(5), pp.1231–1241.
- Salajegheh, M., Lam, T. & Greenberg, S.A. 2011. Autoantibodies against a 43 KDa Muscle Protein in Inclusion Body Myositis. *PLoS ONE*, 6(5), p.e20266.
- Salajegheh, M., Pinkus, J.L., Taylor, J.P., Amato, A.A., Nazareno, R., Baloh, R.H. & Greenberg, S.A. 2009. Sarcoplasmic redistribution of nuclear TDP-43 in inclusion body myositis. *Muscle & Nerve*, 40(1), pp.19–31.
- Saltychev, M., Mikkelsen, M. & Laimi, K. 2016. Medication of inclusion body myositis: a systematic review. *Acta Neurologica Scandinavica*, 133(2), pp.97–102.
- San Gil, R., Berg, T. & Ecroyd, H. 2017. Using bicistronic constructs to evaluate the chaperone activities of heat shock proteins in cells. *Scientific Reports*, 7(1), p.2387.
- Sato, K., Saito, H. & Matsuki, N. 1996. HSP70 is essential to the neuroprotective effect of heat-shock. *Brain Research*, 740(1–2), pp.117–123.
- Schmidt, J., Barthel, K., Wrede, A., Salajegheh, M., Bähr, M. & Dalakas, M.C. 2008. Interrelation of inflammation and APP in sIBM: IL-1 beta induces accumulation of beta-amyloid in skeletal muscle. *Brain*, 131(Pt 5), pp.1228–1240.
- Schmidt, K., Kleinschnitz, K., Rakocevic, G., Dalakas, M.C. & Schmidt, J. 2016. Molecular treatment effects of alemtuzumab in skeletal muscles of patients with IBM. *BMC Neurology*, 16, pp.48.

- Schröder, R., Watts, G.D., Mehta, S.G., Evert, B.O., Broich, P., Fliessbach, K., Pauls, K., Hans, V.H., Kimonis, V. & Thal, D.R. 2005. Mutant valosin-containing protein causes a novel type of frontotemporal dementia. *Annals of Neurology*, 57(3), pp.457–461.
- Schuberth, C. & Buchberger, A. 2008. UBX domain proteins: major regulators of the AAA ATPase Cdc48/p97. *Cellular and Molecular Life Sciences*, 65(15), pp.2360–2371.
- Schwarz, D.S. & Blower, M.D. 2016. The endoplasmic reticulum: structure, function and response to cellular signaling. *Cellular and Molecular Life Sciences*, 73(1), pp.79–94.
- Schwartz, J.C., Podell, E.R., Han, S.S., Berry, J.D., Eggan, K.C. & Cech, T.R. 2014. FUS is sequestered in nuclear aggregates in ALS patient fibroblasts. *Molecular Biology of the Cell*, 25(17), pp.2571–2578.
- Scola, R.H., Werneck, L.C., Iwamoto, F.M., de Messias, I.T. & Tsuchiya, L.V. 1998. [Immunocytochemical analysis of the inflammatory infiltrate in inclusion body myositis and other neuromuscular disorders with rimmed vacuoles]. *Arquivos de neuro-psiquiatria*, 56(3A), pp.388–397.
- Scorrano, L., Oakes, S.A., Opferman, J.T., Cheng, E.H., Sorcinelli, M.D., Pozzan, T. & Korsmeyer, S.J. 2003. BAX and BAK Regulation of Endoplasmic Reticulum Ca²⁺: A Control Point for Apoptosis. *Science*, 300(5616), pp.135–139.
- Seigneurin-Berny, D., Verdel, A., Curtet, S., Lemercier, C., Garin, J., Rousseaux, S. & Khochbin, S. 2001. Identification of components of the murine histone deacetylase 6 complex: link between acetylation and ubiquitination signaling pathways. *Molecular and Cellular Biology*, 21(23), pp.8035–8044.
- Sekul, E.A. & Dalakas, M.C. 1993. Inclusion Body Myositis: New Concepts. *Seminars in Neurology*, 13(3), pp.256–263.
- Selsby, J.T., Judge, A.R., Yimlamai, T., Leeuwenburgh, C. & Dodd, S.L. 2005. Life long calorie restriction increases heat shock proteins and proteasome activity in soleus muscles of Fisher 344 rats. *Experimental Gerontology*, 40(1), pp.37–42.
- Senf, S.M. 2013. Skeletal muscle heat shock protein 70: diverse functions and therapeutic potential for wasting disorders. *Frontiers in Physiology*, 4, p.330.
- Shi, Z., Hayashi, Y.K., Mitsuhashi, S., Goto, K., Kaneda, D., Choi, Y.C., Toyoda, C., Hieda, S., Kamiyama, T., Sato, H., Wada, M., Noguchi, S., Nonaka, I. & Nishino, I. 2012. Characterization of the Asian myopathy patients with VCP mutations. *European Journal of Neurology*, 19(3), pp.501–509.
- Shirakabe, A., Ikeda, Y., Sciarretta, S., Zablocki, D.K. & Sadoshima, J. 2016. Aging and Autophagy in the Heart. *Circulation Research*, 118(10), pp.1563–1576.

- Shorter, J. & Taylor, J.P. 2013. Disease mutations in the prion-like domains of hnRNPA1 and hnRNPA2/B1 introduce potent steric zippers that drive excess RNP granule assembly. *Rare Diseases*, 1, p.e25200.
- Singh, R., Kølvrå, S., Bross, P., Jensen, U.B., Gregersen, N., Tan, Q., Knudsen, C. & Rattan, S.I.S. 2006. Reduced heat shock response in human mononuclear cells during aging and its association with polymorphisms in HSP70 genes. *Cell Stress & Chaperones*, 11(3), pp.208-215.
- Sirabella, D., De Angelis, L. & Berghella, L. 2013. Sources for skeletal muscle repair: from satellite cells to reprogramming. *Journal of Cachexia, Sarcopenia and Muscle*, 4(2), pp.125–136.
- Sivakumar, K., Semino-Mora, C. & Dalakas, M.C., 1997. An inflammatory, familial, inclusion body myositis with autoimmune features and a phenotype identical to sporadic inclusion body myositis. Studies in three families. *Brain*, pp.653–661.
- Soden, M., Boundy, K., Burrow, D., Blumbergs, P. & Ahern, M. 1994. Inclusion body myositis in association with rheumatoid arthritis. *The Journal of Rheumatology*, 21(2), pp.344–346.
- Solski, J.A., Yang, S., Nicholson, G.A., Luquin, N., Williams, K.L., Fernando, R., Pamphlett, R. & Blair, I.P. 2012. A novel *TARDBP* insertion/deletion mutation in the flail arm variant of amyotrophic lateral sclerosis. *Amyotrophic Lateral Sclerosis*, 13(5), pp.465–470.
- Spector, S.A., Lemmer, J.T., Koffman, B.M., Fleisher, T.A., Feuerstein, I.M., Hurley, B.F. & Dalakas, M.C. 1997. Safety and efficacy of strength training in patients with sporadic inclusion body myositis. *Muscle & Nerve*, 20(10), pp.1242-1248.
- Spina, S., Van Laar, A.D., Murrell, J.R., Hamilton, R.L., Kofler, J.K., Epperson, F., Farlow, M.R., Lopez, O.L., Quinlan, J., DeKosky, S.T. & Ghetti, B. 2013. Phenotypic variability in three families with valosin-containing protein mutation. *European Journal of Neurology*, 20(2), pp.251–258.
- Sridhar, S., Botbol, Y., Macian, F. & Cuervo, A.M. 2012. Autophagy and disease: always two sides to a problem. *The Journal of Pathology*, 226(2), pp.255–273.
- Stirling, P.C., Lundin, V.F. & Leroux, M.R. 2003. Getting a grip on non-native proteins. *EMBO Reports*, 4(6), pp.565–570.
- Stoica, R., De Vos, K.J., Paillusson, S., Mueller, S., Sancho, R.M., Lau, K.F., Vizcay-Barrena, G., Lin, W.L., Xu, Y.F., Lewis, J., Dickson, D.W., Petrucelli, L., Mitchell, J.C., Shaw, C.E. & Miller, C.C. 2014. ER–mitochondria associations are regulated by the VAPB–PTPIP51 interaction and are disrupted by ALS/FTD-associated TDP-43. *Nature Communications*, 5(1), p.3996.

- Straub, I.R., Janer, A., Weraarpachai, W., Zinman, L., Robertson, J., Rogaeva, E. & Shoubridge, E.A. 2018. Loss of CHCHD10–CHCHD2 complexes required for respiration underlies the pathogenicity of a CHCHD10 mutation in ALS. *Human Molecular Genetics*, 27(1), pp.178–189.
- Stunova, A. & Vistejnova, L. 2018. Dermal fibroblasts-A heterogeneous population with regulatory function in wound healing. *Cytokine & Growth Factor Reviews*, 39, pp.37-150.
- Sugarman, M.C., Yamasaki, T.R., Oddo, S., Echegoyen, J.C., Murphy, M.P., Golde, T.E., Jannatipour, M., Leissring, M.A. & LaFerla, F.M. 2002. Inclusion body myositis-like phenotype induced by transgenic overexpression of beta APP in skeletal muscle. *Proceedings of the National Academy of Sciences of the United States of America*, 99(9), pp.6334–6339.
- Suzuki, N., Aoki, M., Mori-Yoshimura, M., Hayashi, Y.K., Nonaka, I. & Nishino, I. 2012. Increase in number of sporadic inclusion body myositis (sIBM) in Japan. *Journal of Neurology*, 259(3), pp.554–556.
- Suzuki, T., Nakagawa, M., Yoshikawa, A., Sasagawa, N., Yoshimori, T., Ohsumi, Y., Nishino, I., Ishiura, S. & Nonaka, I. 2002. The first molecular evidence that autophagy relates rimmed vacuole formation in chloroquine myopathy. *Journal of Biochemistry*, 131, pp.647–651.
- Tabas, I. & Ron, D. 2011. Integrating the mechanisms of apoptosis induced by endoplasmic reticulum stress. *Nature Cell Biology*, 13(3), pp.184–190.
- Tajbakhsh, S., 2009. Skeletal muscle stem cells in developmental versus regenerative myogenesis. *Journal of Internal Medicine*, 266(4), pp.372–389.
- Takayama, K., Yagawa, K., Takahashi, A., Nishio, H. & Sudo, M. 1969. Histopathological study on progressive muscular dystrophy--report of a case with autopsy findings. *Acta Pathologica Japonica*, 19(4), pp.547–562.
- Tan, J.A., Roberts-Thomson, P.J., Blumbergs, P., Hakendorf, P., Cox, S.R. & Limaye, V. 2013. Incidence and prevalence of idiopathic inflammatory myopathies in South Australia: a 30-year epidemiologic study of histology-proven cases. *International Journal of Rheumatic Diseases*, 16(3), pp.331–338.
- Tanaka, A., Cleland, M.M., Xu, S., Narendra, D.P., Suen, D.F., Karbowski, M. & Youle, R.J. 2010. Proteasome and p97 mediate mitophagy and degradation of mitofusins induced by Parkin. *The Journal of Cell Biology*, 191(7), pp.1367–1380.
- Tang, W.K., Li, D., Li, C.C., Esser, L., Dai, R., Guo, L. & Xia, D. 2010. A novel ATP-dependent conformation in p97 N-D1 fragment revealed by crystal structures of disease-related mutants. *The EMBO Journal*, 29(13), pp.2217–2229.
- Tang, W.K. & Xia, D. 2016. Mutations in the Human AAA(+) Chaperone p97 and Related Diseases. *Frontiers in Molecular Biosciences*, 3, p.79.

- Tanida, I., Ueno, T. & Kominami, E. 2008. LC3 and Autophagy. *Methods in Molecular Biology*. 445, pp. 77–88.
- Tasca, G., Monforte, M., De Fino, C., Kley, R.A., Ricci, E. & Mirabella, M.. 2015. Magnetic resonance imaging pattern recognition in sporadic inclusion-body myositis. *Muscle & Nerve*, 52(6), pp.956–962.
- Tateyama, M., Saito, N., Fujihara, K., Shiga, Y., Takeda, A., Narikawa, K., Hasegawa, T., Taguchi, Y., Sakuma, R., Onodera, Y., Ohnuma, A., Tobita, M. & Itoyama, Y. 2003. Familial inclusion body myositis: a report on two Japanese sisters. *Internal Medicine*, 42(10), pp.1035–1038.
- Tawara, N., Yamashita, S., Zhang, X., Korogi, M., Zhang, Z., Doki, T., Matsuo, Y., Nakane, S. Maeda, Y., Sugie, K., Suzuki, N., Aoki, M. & Ando, Y. 2017. Pathomechanisms of anti-cytosolic 5'-nucleotidase 1A autoantibodies in sporadic inclusion body myositis. *Annals of Neurology*. 81 (4), pp.512-525.
- Taylor, J.P. 2015. Multisystem proteinopathy: intersecting genetics in muscle, bone, and brain degeneration. *Neurology*, 85(8), pp.658–660.
- Taylor, R.C. & Dillin, A. 2011. Aging as an Event of Proteostasis Collapse. *Cold Spring Harbor Perspectives in Biology*, 3(5), pp.a004440–a004440.
- Teves, J.M.Y., Bhargava, V., Kirwan, K.R., Corenblum, M.J., Justiniano, R., Wondrak, G.T., Anandhan, A., Flores, A.J., Schipper, D.A., Khalpey, Z., Sligh, J.E., Curiel-Lewandrowski, C., Sherman, S.J. & Madhavan, L. 2017. Parkinson's Disease Skin Fibroblasts Display Signature Alterations in Growth, Redox Homeostasis, Mitochondrial Function, and Autophagy. *Frontiers in Neuroscience*, 11, p.737.
- Tews, D.S. & Goebel, H.H. 1996. Cytokine expression profile in idiopathic inflammatory myopathies. *Journal of Neuropathology and Experimental Neurology*, 55(3), pp.342–347.
- Thakur, S.S., Swiderski, K., Ryall, J.G. & Lynch, G.S. 2018. Therapeutic potential of heat shock protein induction for muscular dystrophy and other muscle wasting conditions. *Philosophical transactions of the Royal Society of London. Series B, Biological Sciences*, 373(1738), p.20160528.
- Tigges, J., Krutmann, J., Fritsche, E., Haendeler, J., Schaal, H., Fischer, J.W., Kalfalah, F., Reinke, H., Reifenberger, G., Stühler, K. Ventura, N., Gundermann, S., Boukamp, P. & Boege, F. 2014. The hallmarks of fibroblast ageing. *Mechanics of Ageing and Development*, 138, pp.26-44.
- Toko, H., Minamino, T. & Komuro, I. 2008. Role of Heat Shock Transcriptional Factor 1 and Heat Shock Proteins in Cardiac Hypertrophy. *Trends in Cardiovascular Medicine*, 18(3), pp.88–93.

- Tomaru, U., Takahashi, S., Ishizu, A., Miyatake, Y., Gohda, A., Suzuki, S., Ono, A., Ohara, J., Baba, T., Murata, S., Tanaka, K. & Kasahara, M. 2012. Decreased proteasomal activity causes age-related phenotypes and promotes the development of metabolic abnormalities. *The American Journal of Pathology*, 180(3), pp.963–972.
- Tonoki, A., Kuranaga, E., Tomioka, T., Hamazaki, J., Murata, S., Tanaka, K. & Miura, M. 2009. Genetic evidence linking age-dependent attenuation of the 26S proteasome with the aging process. *Molecular and Cellular Biology*, 29(4), pp.1095–1106.
- Török, Z., Tsvetkova, N.M., Balogh, G., Horváth, I., Nagy, E., Péntes, Z., Hargitai, J., Bensaude, O., Csermely, P., Crowe, J.H., Maresca, B. & Vigh, L. 2003. Heat shock protein coinducers with no effect on protein denaturation specifically modulate the membrane lipid phase. *Proceedings of the National Academy of Sciences*, 100(6), pp.3131–3136.
- Tracy, L.E., Minasian, R.A. & Caterson, E.J. 2016. Extracellular Matrix and Dermal Fibroblast Function in the Healing Wound. *Advances in Wound Care*, 5(3), pp.119-136.
- Travers, K.J., Patil, C.K., Wodicka, L., Lockhart, D.J., Weissman, J.S. & Walter, P. 2000. Functional and genomic analyses reveal an essential coordination between the unfolded protein response and ER-associated degradation. *Cell*, 101(3), pp.249–258.
- Tresse, E., Salomons, F.A., Vesa, J., Bott, L.C., Kimonis, V., Yao, T.P., Dantuma, N.P. & Taylor, J.P. 2010. VCP/p97 is essential for maturation of ubiquitin-containing autophagosomes and this function is impaired by mutations that cause IBMPFD. *Autophagy*, 6(2), pp.217–227.
- Tsukita, K., Yagita, K., Sakamaki-Tsukita, H. & Suenaga, T. 2018. Sporadic inclusion body myositis: magnetic resonance imaging and ultrasound characteristics. *QJM: An International Journal of Medicine*. [Epub ahead of print]
- Uhlén, M., Fagerberg, L., Hallström, B.M., Lindskog, C., Oksvold, P., Mardinoglu, A., Sivertsson, Å., Kampf, C., Sjöstedt, E., Asplund, A., Olsson, I., Edlund, K., Lundberg, E., Navani, S., Szigartyo, C.A., Odeberg, J., Djureinovic, D., Takanen, J.O., Hober, S., Alm, T., Edqvist, P.H., Berling, H., Tegel, H., Mulder, J., Rockberg, J. Nilsson, P., Schwenk, J.M., Hamsten, M. von Feilitzen, K., Forsberg, M., Persson, L., Johansson, F., Zwahlen, M., von Heijne, G., Nielsen & J., Pontén, F. 2015. Tissue-based map of the human proteome. *Science*, 347(6220), pp.1260419–1260419.
- Utani, K., Kohno, Y., Okamoto, A. & Shimizu, N. 2010. Emergence of Micronuclei and Their Effects on the Fate of Cells under Replication Stress. *PLoS ONE*, 5(4), p.e10089.

- Vásquez-Trincado, C., García-Carvajal, I., Pennanen, C., Parra, V., Hill, J.A., Rothermel, B.A. & Lavadero, S. 2016. Mitochondrial dynamics, mitophagy and cardiovascular disease. *The Journal of Physiology*, 594(3), pp.509–525.
- Vattemi, G., Engel, W.K., McFerrin, J. & Askanas, V. 2004. Endoplasmic reticulum stress and unfolded protein response in inclusion body myositis muscle. *The American Journal of Pathology*, 164(1), pp.1–7.
- Vattemi, G., Nogalska, A., Engel W.K., D'Agostino, C., Checler, F. & Askanas V. 2009. Amyloid-beta42 is preferentially accumulated in muscle fibers of patients with sporadic inclusion-body myositis. *Acta Neuropathologica*, 117(5), pp.569–574.
- Verma, R., Oania, R.S., Kolawa, N.J. & Deshaies, R.J. 2013. Cdc48/p97 promotes degradation of aberrant nascent polypeptides bound to the ribosome. *eLife*, 2, p.e00308.
- Vernace, V.A., Arnaud, L., Schmidt-Glenewinkel, T. & Figueiredo-Pereira, M.E. 2007. Aging perturbs 26S proteasome assembly in *Drosophila melanogaster*. *The FASEB Journal*, 21(11), pp.2672–2682.
- Vesa, J., Su, H., Watts, G.D., Krause, S., Walter, M.C., Martin, B., Smith, C., Wallace, D.C. & Kimonis, V.E. 2009. Valosin containing protein associated inclusion body myopathy: abnormal vacuolization, autophagy and cell fusion in myoblasts. *Neuromuscular Disorders*, 19(11), pp.766–772.
- Vígh, L., Horváth, I., Maresca, B. & Harwood, J.L. 2007. Can the stress protein response be controlled by 'membrane-lipid therapy'? *Trends in Biochemical Sciences*, 32(8), pp.357–363.
- Vígh, L., Literáti, P.N., Horváth, I., Török, Z., Balogh, G., Glatz, A., Kovács, E., Boros, I., Ferdinándy, P., Parkas, B., Jaszlits, L., Jednákovits, A., Korányi, L. & Maresca, B. 1997. Bimoclomol: A nontoxic, hydroxylamine derivative with stress protein-inducing activity and cytoprotective effects. *Nature Medicine*, 3(10), pp.1150-1154.
- Vihervaara, A. & Sistonen, L. 2014. HSF1 at a glance. *Journal of Cell Science*, 127(Pt 2), pp.261–266.
- Vilchez, D., Morantte, I., Liu, Z., Douglas, P.M., Merkwirth, C., Rodrigues, A.P., Manning, G. & Dillin, A. 2012. RPN-6 determines *C. elegans* longevity under proteotoxic stress conditions. *Nature*, 489(7415), pp.263–268.
- Vordenbäumen, S., Neuen-Jacob, E., Richter, J. & Schneider, M. 2010. Inclusion body myositis in a patient with long standing rheumatoid arthritis treated with anti-TNF α and rituximab. *Clinical Rheumatology*, 29(5), pp.555–558.
- Walcott, S.E. & Heikkila, J.J. 2010. Celastrol can inhibit proteasome activity and upregulate the expression of heat shock protein genes, hsp30 and hsp70, in *Xenopus laevis* A6 cells. *Comparative Biochemistry and Physiology Part A: Molecular & Integrative Physiology*, 156(2), pp.285–293.

- Waldera-Lupa, D.M., Kalfalah, F., Florea, A.M., Sass, S., Kruse, F., Rieder, V., Tigges, J., Fritsche, E., Krutmann, J., Busch, H., Boerries, M., Meyer, H.E., Boege, F., Theis, F., Reifenberger, G. & Stühler, K. 2014. Proteome-wide analysis reveals an age-associated cellular phenotype of in situ aged human fibroblasts. *Aging*, 6(10), pp.856–872.
- Walter, M.C., Lochmüller, H., Toepfer, M., Schlotter, B., Reilich, P., Schröder, M., Müller-Felber, W. & Pongratz, D. 2000. High-dose immunoglobulin therapy in sporadic inclusion body myositis: a double-blind, placebo-controlled study. *Journal of Neurology*, 247(1), pp.22–28.
- Wang, Q., Song, C. & Li, C.C.H. 2004. Molecular perspectives on p97–VCP: progress in understanding its structure and diverse biological functions. *Journal of Structural Biology*, 146(1–2), pp.44–57.
- Wang, W., Arakawa, H., Wang, L., Okolo, O., Siedlak, S.L., Jiang, Y., Gao, J., Xie, F., Petersen, R.B. & Wang, X.. 2017. Motor-Coordination and Cognitive Dysfunction Caused by Mutant TDP-43 Could Be Reversed by Inhibiting Its Mitochondrial Localization. *Molecular Therapy*, 25(1), pp.127–139.
- Wang, W., Li, L., Lin, W.L., Dickson, D.W., Petrucelli, L., Zhang, T. & Wang, X. 2013. The ALS disease-associated mutant TDP-43 impairs mitochondrial dynamics and function in motor neurons. *Human Molecular Genetics*, 22(23), pp.4706–4719.
- Wang, W., Wang, L., Lu, J., Siedlak, S.L., Fujioka, H., Liang, J., Jiang, S., Ma, X., Jiang, Z., da Rocha, E.L., Sheng, M., Choi, H., Lerou, P.H., Li, H. & Wang, X. 2016. The inhibition of TDP-43 mitochondrial localization blocks its neuronal toxicity. *Nature Medicine*, 22(8), pp.869–878.
- Wang, X., Su, B., Fujioka, H. & Zhu, X. 2008. Dynamin-like protein 1 reduction underlies mitochondrial morphology and distribution abnormalities in fibroblasts from sporadic Alzheimer's disease patients. *The American Journal of Pathology*, 173(2), pp.470–482.
- Wanschitz, J.V., Dubourg, O., Lacene, E., Fischer, M.B., Höftberger, R., Budka, H., Romero, N.B., Eymard, B., Herson, S., Butler-Browne, G.S., Voit, T. & Benveniste, O. 2013. Expression of myogenic regulatory factors and myo-endothelial remodeling in sporadic inclusion body myositis. *Neuromuscular Disorders*, 23(1), pp.75–83.
- Watts, G., Thomasova, D., Ramdeen, S.K., Fulchiero, E.C., Mehta, S.G., Drachman, D.A., Weihl, C.C., Jamrozik, Z., Kwiecinski, H., Kaminska, A. & Kimonis, V.E. 2007. Novel VCP mutations in inclusion body myopathy associated with Paget disease of bone and frontotemporal dementia. *Clinical Genetics*, 72(5), pp.420–426.
- Watts, G.D., Wymer, J., Kovach, M.J., Mehta, S.G., Mumm, S., Darvish, D., Pestronk, A., Whyte, M.P. & Kimonis, V.E. 2004. Inclusion body myopathy associated with Paget disease of bone and frontotemporal dementia is caused by mutant valosin-containing protein. *Nature Genetics*, 36(4), pp.377–381.

- Webster, C.P., Smith, E.F., Shaw, P.J. & De Vos, K.J. 2017. Protein Homeostasis in Amyotrophic Lateral Sclerosis: Therapeutic Opportunities? *Frontiers in Molecular Neuroscience*, 10, p.123.
- Webster, M., Witkin, K.L. & Cohen-Fix, O. 2009. Sizing up the nucleus: nuclear shape, size and nuclear-envelope assembly. *Journal of Cell Science*, 122(Pt 10), pp.1477–1486.
- Wegorzewska, I., Bell, S., Cairns, N.J., Miller, T.M. & Baloh, R.H. 2009. TDP-43 mutant transgenic mice develop features of ALS and frontotemporal lobar degeneration. *Proceedings of the National Academy of Sciences*, 106(44), pp.18809–18814.
- Weihl, C.C. 2011. Valosin containing protein associated fronto-temporal lobar degeneration: clinical presentation, pathologic features and pathogenesis. *Current Alzheimer Research*, 8(3), pp.252–260.
- Weihl, C.C., Baloh, R.H., Lee, Y., Chou, T.F., Pittman, S.K., Lopate, G., Allred, P., Jockel-Balsarotti, J., Pestronk, A. & Harms, M.B. 2015. Targeted sequencing and identification of genetic variants in sporadic inclusion body myositis. *Neuromuscular Disorders*, 25(4), pp.289–296.
- Weihl, C.C., Dalal, S., Pestronk, A. & Hanson, P.I. 2006. Inclusion body myopathy-associated mutations in p97/VCP impair endoplasmic reticulum-associated degradation. *Human Molecular Genetics*, 15(2), pp.189–199.
- Weihl, C.C. & Pestronk, A. 2010. Sporadic inclusion body myositis: possible pathogenesis inferred from biomarkers. *Current Opinion in Neurology*, 23(5), pp.482–488.
- Weihl, C.C., Pestronk, A. & Kimonis, V.E. 2009. Valosin-containing protein disease: Inclusion body myopathy with Paget's disease of the bone and fronto-temporal dementia. *Neuromuscular Disorders*, 19(5), pp.308–315.
- Weihl, C.C., Temiz, P., Miller, S.E., Watts, G., Smith, C., Forman, M., Hanson, P.I., Kimonis, V. & Pestronk, A. 2008. TDP-43 accumulation in inclusion body myopathy muscle suggests a common pathogenic mechanism with frontotemporal dementia. *Journal of Neurology, Neurosurgery, and Psychiatry*, 79(10), pp.1186–1189.
- Wiedemann, F.R., Winkler, K., Lins, H., Wallesch, C.W. & Kunz, W.S.1999. Detection of Respiratory Chain Defects in Cultivated Skin Fibroblasts and Skeletal Muscle of Patients with Parkinson's Disease. *Annals of the New York Academy of Sciences*, 893, pp.426–429.
- Williams, K.L., Warraich, S.T., Yang, S., Solski, J.A., Fernando, R., Rouleau, G.A., Nicholson, G.A. & Blair, I.P. 2012. UBQLN2/ubiquilin 2 mutation and pathology in familial amyotrophic lateral sclerosis. *Neurobiology of Aging*, 33(10), p.2527.e3-2527.e10.

- Wilson, F.C., Ytterberg, S.R., St Sauver, J.L. & Reed, A.M. 2008. Epidemiology of sporadic inclusion body myositis and polymyositis in Olmsted County, Minnesota. *The Journal of Rheumatology*, 35(3), pp.445–447.
- Winbanks, C.E., Weeks K.L., Thomson, R.E., Sepulveda, P.V., Beyer, C., Qian, H., Chen, J.L., Allen, J.M., Lancaster, G.I., Febbraio, M.A., Harrison, C.A., McMullen, J.R., Chamberlain, J.S. & Gregorevic, P. 2012. Follistatin-mediated skeletal muscle hypertrophy is regulated by Smad3 and mTOR independently of myostatin. *The Journal of Cell Biology*, 197(7), pp.997–1008.
- Winter, A. & Bornemann, A. 1999. NCAM, vimentin and neonatal myosin heavy chain expression in human muscle diseases. *Neuropathology and Applied Neurobiology*, 25(5), pp.417–424.
- Winton, M.J., Igaz, L.M., Wong, M.M., Kwong, L.K., Trojanowski, J.Q. & Lee, V.M. 2008. Disturbance of nuclear and cytoplasmic TAR DNA-binding protein (TDP-43) induces disease-like redistribution, sequestration, and aggregate formation. *Journal of Biological Chemistry*, 283(19), pp.13302–13309.
- Woerner, A.C., Frottin, F., Hornburg, D., Feng, L.R., Meissner, F., Patra, M., Tatzelt, J., Mann, M., Winklhofer, K.F., Hartl, F.U., & Hipp, M.S. 2016. Cytoplasmic protein aggregates interfere with nucleocytoplasmic transport of protein and RNA. *Science*, 351(6269), pp.173–176.
- Wolff, S., Weissman, J.S. & Dillin, A. 2014. Differential Scales of Protein Quality Control. *Cell*, 157(1), pp.52–64.
- Wolozin, B. 2012. Regulated protein aggregation: stress granules and neurodegeneration. *Molecular Neurodegeneration*, 7(1), p.56.
- Woods, L.C., Berbusse, G.W. & Naylor, K. 2016. Microtubules Are Essential for Mitochondrial Dynamics-Fission, Fusion, and Motility-in Dictyostelium discoideum. *Frontiers in Cell and Developmental Biology*, 4, p.19.
- Wu, J. & Kaufman, R.J. 2006. From acute ER stress to physiological roles of the Unfolded Protein Response. *Cell Death and Differentiation*, 13(3), pp.374–384.
- Wu, M., Kalyanasundaram, A. & Zhu, J. 2013. Structural and biomechanical basis of mitochondrial movement in eukaryotic cells. *International Journal of Nanomedicine*, 8, p.4033.
- Wytenbach, A. & Arrigo, A.P. 2009. The Role of Heat Shock Proteins during Neurodegeneration in Alzheimer's, Parkinson's and Huntington's Disease. In *Heat Shock Proteins in Neural Cells*. New York, NY: Springer New York, pp. 81–99.
- Xia, D., Tang, W.K. & Ye, Y. 2016. Structure and function of the AAA+ ATPase p97/Cdc48p. *Gene*, 583(1), pp.64–77.

- Xu, S., Peng, G., Wang, Y., Fang, S. & Karbowski, M. 2011 The AAA-ATPase p97 is essential for outer mitochondrial membrane protein turnover. *Molecular Biology of the Cell*, 22(3), pp.291–300.
- Xu, Y.F., Gendron, T.F., Zhang, Y.J., Lin, W.L., D'Alton, S., Sheng, H., Casey, M.C., Tong, J., Knight, J., Yu, X., Rademakers, R., Boylan, K., Hutton, M., McGowan, E., Dickson, D.W., Lewis, J. & Petrucelli, L. 2010. Wild-type human TDP-43 expression causes TDP-43 phosphorylation, mitochondrial aggregation, motor deficits, and early mortality in transgenic mice. *Journal of Neuroscience*, 30(32), pp.10851–10859.
- Xu, Z.S. 2012. Does a loss of TDP-43 function cause neurodegeneration? *Molecular Neurodegeneration*, 7(1), p.27.
- Yang, F., Chu, X., Yin, M., Liu, X., Yuan, H., Niu, Y. & Fu, L.. 2014. mTOR and autophagy in normal brain aging and caloric restriction ameliorating age-related cognition deficits. *Behavioural Brain Research*, 264, pp.82–90.
- Yang, S., Zhang, K.Y., Kariawasam, R., Bax, M., Fifita, J.A., Ooi, L., Yerbury, J.J., Nicholson, G.A. & Blair, I.P. 2015. Evaluation of Skin Fibroblasts from Amyotrophic Lateral Sclerosis Patients for the Rapid Study of Pathological Features. *Neurotoxicity Research*, 28(2), pp.138–146.
- Yang, Z. & Klionsky, D.J. 2010. Eaten alive: a history of macroautophagy. *Nature Cell Biology*, 12(9), pp.814–822.
- Ye, Y. 2006. Diverse functions with a common regulator: Ubiquitin takes command of an AAA ATPase. *Journal of Structural Biology*, 156(1), pp.29–40.
- Yeo, B.K. & Yu, S.W. 2016. Valosin-containing protein (VCP): structure, functions, and implications in neurodegenerative diseases. *Animal Cells and Systems*, 20(6), pp.303–309.
- Yerbury, J.J., Ooi, L., Dillin, A., Saunders, D.N., Hatters, D.M., Beart, P.M., Cashman, N.R., Wilson, M.R. & Ecroyd, H. 2016. Walking the tightrope: proteostasis and neurodegenerative disease. *Journal of Neurochemistry*, 137(4), pp.489–505.
- Yeung, H.O., Kloppsteck, P., Niwa, H., Isaacson, R.L., Matthews, S., Zhang, X. & Freemont, P.S. 2008. Insights into adaptor binding to the AAA protein p97. *Biochemical Society Transactions*, 36(1), pp.62–67.
- Youle, R.J. & van der Bliek, A.M. 2012. Mitochondrial Fission, Fusion, and Stress. *Science*, 337(6098), pp.1062–1065.
- Young, J.C., Agashe, V.R., Siegers, K. & Hartl, F.U. 2004. Pathways of chaperone-mediated protein folding in the cytosol. *Nature Reviews Molecular Cell Biology*, 5(10), pp.781–791.

- Zetterberg, H., Jacobsson, J., Rosengren, L., Blennow, K. & Andersen, P.M. 2007. Cerebrospinal fluid neurofilament light levels in amyotrophic lateral sclerosis: impact of SOD1 genotype. *European Journal of Neurology*, 14(12), pp.1329–1333.
- Zhang, C. & Cuervo, A.M. 2008. Restoration of chaperone-mediated autophagy in aging liver improves cellular maintenance and hepatic function. *Nature Medicine*, 14(9), pp.959–965.
- Zhang, K. & Kaufman, R.J. 2008. From endoplasmic-reticulum stress to the inflammatory response. *Nature*, 454(7203), pp.455–462.
- Zhang, T., Mishra, P., Hay, B.A., Chan, D. & Guo, M. 2017. Valosin-containing protein (VCP/p97) inhibitors relieve Mitofusin-dependent mitochondrial defects due to VCP disease mutants. *eLife*, 6, pii.e17834.
- Zhang, X., Gui, L., Zhang, X., Bulfer, S.L., Sanghez, V., Wong, D.E., Lee, Y., Lehmann, L., Lee, J.S., Shih, P.Y., Lin, H.J., Iacovino, M., Weihl, C.C., Arkin, M.R., Wang, Y. & Chou, T.F.. 2015. Altered cofactor regulation with disease-associated p97/VCP mutations. *Proceedings of the National Academy of Sciences of the United States of America*, 112(14), pp.E1705–1714.
- Zhang, Y.J., Xu, Y.F., Cook, C., Gendron, T.F., Roettges, P., Link, C.D., Lin, W.L., Tong, J., Castanedes-Casey, M., Ash, P., Gass, J., Rangachari, V., Buratti, E., Baralle, F., Golde, T.E., Dickson, D.W. & Petrucelli, L. 2009. Aberrant cleavage of TDP-43 enhances aggregation and cellular toxicity. *Proceedings of the National Academy of Sciences of the United States of America*, 106(18), pp.7607–7612.
- Zong, M., Dorph, C., Dastmalchi, M., Alexanderson, H., Pieper, J., Amoudruz, P., Barbasso Helmers, S., Nennesmo, I., Malmström, V. & Lundberg, I.E. 2014. Anakinra treatment in patients with refractory inflammatory myopathies and possible predictive response biomarkers: a mechanistic study with 12 months follow-up. *Annals of the Rheumatic Diseases*, 73(5), pp.913–920.